



WPI

Open-Source Desktop CNC Mini-Mill

A Major Qualifying Project
submitted to the Faculty of
WORCESTER POLYTECHNIC INSTITUTE
in partial fulfillments for the
degree of Bachelor of Science

Submitted By:
Echo Baumer (ME & PH)
Rafael Caballero (ME)
James Carroll (ME)
Camren Chraplak (RBE & CS)
Michael Doucette (ME)
Perrin Kristoff (ECE)
Andrew Petro (ME)
Daniel Petro (ME)
Michael Primavera (RBE)
JR Thaiprayoon (ME)
Dante Uccello (ME)

Date: May 7th 2025

Approved By:
Professors Pradeep Radhakrishnan (MME/RBE)
Snehalata Kadam (PH)
Joshua Cuneo (CS)

This report represents the work of one or more WPI undergraduate students submitted to the faculty as evidence of completion of a degree requirement. WPI routinely publishes these reports on the web without editorial or peer review.

Acknowledgments

The completion of this project would not have been possible without the unwavering support and contributions of the following people:

Barbara Furhman, Mechanical & Materials Engineering Administrative Assistant VI

Professor Pradeep Radhakrishnan (MME), Project Advisor

Professor Snehalata Kadam (PH), Project Advisor

Professor Joshua Cuneo (CS), Project Advisor

Professor Robert Daniello (MME), Instructional Lab Engineer in Washburn Labs

Peter Hefti, MME Laboratory Manager

Don Greilick, Owner of Rapidchange ATC

Andrew Lapin & Sam Gervasi, MME Teaching Lab Managers

Abstract

This project explores the development of an open-source desktop Computer Numerical Control (CNC) milling machine, including the integration of an improved control architecture and sensor suite, with the intention being to address the lack of accessible desktop-machining options for students and hobbyists. Industrial CNC machines cost over \$30,000, and these machines' individualized software creates obstacles for their users. The base-model machine, priced at \$2,800, provides users with an intuitive graphical interface for controlling the machine and the additional functionality; the design also gives users the ability to manufacture the machine with minimal outsourcing. The modular base-model supports a coolant system, automatic tool changer, 4th-axis, and mechanical bed leveling. User friendly and open-source software were used and customized to expand the capabilities of the previous three axis system. The machine additionally included many electrical safety systems for regular use in classroom settings. Furthermore, various sensors were utilized during the development, producing data that validated the effectiveness of all its functionalities. The machine produced repeatability within 0.005", acceleration within ± 0.03 g, safe motor temperatures. The final result was an affordable CNC mill that allows users to become familiarized with the basics of machining in a safe environment.

Table of Contents

Acknowledgments.....	
Abstract.....	
Table of Contents.....	
List of Figures.....	
List of Tables.....	
Authorship Table.....	
1.0 Introduction.....	1
1.1 Introduction to Commercial Desktop CNC Machines.....	3
1.2 Introduction to Open-Source Desktop CNC Machines.....	6
2.0 Review of the 2023-2024 Desktop CNC MQP (Brown et al., 2024).....	9
2.1 Analysis of the 2023-2024 Desktop CNC MQP Report.....	9
2.2 Review of the 2023-2024 Desktop CNC Mill MQP's Machine Enclosure and Chip Evacuation.....	13
2.3 Enclosure Concerns from the 2023-2024 MQP.....	16
2.4 Inconsistencies with the Previous CAD Assembly.....	18
2.5 Vibration Damping of the 2023-2024 MQP.....	19
2.6 Noise Reduction of the 2023-2024 MQP.....	21
2.7 Rigidity Testing of the 2023-2024 Gantry.....	21
2.8 Machining Capabilities.....	22
2.8.1 2023-2024 Machining Testing.....	22
2.8.2 2024-2025 Machining Testing.....	27
2.9 Control Software for 2023-2024 CNC Mill.....	30
3.0 Goals for this MQP.....	32
3.1 Tool Changer.....	32
3.2 4th-Axis.....	32
3.3 User-Friendly and Open-Source Software.....	33
3.4 Bed Leveling.....	33
3.5 Upgraded Enclosure.....	34
3.6 Chip Evacuation.....	35
3.7 Tolerance.....	35
3.8 Safety.....	35
3.9 Summary of Goals and Specifications.....	36
4.0 Project Timeline.....	38
5.0 Methodology.....	40
5.1 Inter-Team Dependencies.....	40
5.2 Design.....	40

5.3 Testing.....	42
5.4 Implementation.....	42
5.5 Verification.....	43
6.0 Literature Review.....	45
6.1 CNC Enclosures.....	45
6.2 Vacuum System.....	47
6.3 Coolant System.....	49
6.4 Vibration in CNC Milling.....	51
6.5 CNC Automatic Tool Changer.....	54
6.6 4th-Axis.....	61
6.7 Bed Leveling.....	66
6.8 CNC Control System.....	70
6.9 Control Hardware.....	70
6.9.1 Mach3.....	71
6.9.2 grbl & grblHAL.....	71
6.10 Control Software.....	72
6.10.1 Mach 3 Software.....	74
6.10.2 LinuxCNC Software.....	75
6.10.3 CNCJS Software.....	76
6.10.4 bCNC Software.....	77
6.10.5 UGS Software.....	77
6.10.6 Previous MQP's Software Selection.....	78
6.11 Electrical and Safety Systems.....	79
7.0 Mechanical Design Updates.....	81
7.1 Vacuum System.....	81
7.2 Automatic Tool Changer Design.....	89
7.3 4th-Axis Functionality.....	110
7.4 Bed Leveling Functionality.....	118
7.5 Work Area Plates.....	127
7.6 Enclosure Design.....	133
7.6.1 Enclosure Guarding.....	133
7.6.2 Filament Selection.....	134
7.6.3 New Enclosure.....	136
7.7 Coolant Design.....	141
7.8 Lockout-Tagout.....	141
8.0 Electronics and Software Updates.....	143
8.1 Final Control System.....	143
8.1.1 Control System Criteria.....	143

8.1.2 Final Control System Evaluation.....	148
8.1.1 grblHAL.....	150
8.1.2 UGS.....	150
8.2 Sensor Integration.....	151
8.2.1 Inertial Measurement Units.....	152
8.2.2 Temperature Sensors.....	153
8.2.3 Sensor Data Collection.....	155
8.2.4 EMI Effect on Sensors.....	156
8.2.4.1 Inertial Measurement Units.....	157
8.2.5 Strain Gauges.....	158
8.2.6 Spindle Speed.....	162
8.3 Control Board Circuit.....	164
8.3.1 Door Switch.....	165
8.3.2 Stack Light.....	165
8.3.3 Limit Switches.....	167
8.3.4 Spindle.....	168
8.4 EMI Analysis.....	171
8.5 Software Work.....	174
8.6 grblHAL.....	176
8.6.1 Custom Plugins.....	177
8.7 UGS.....	179
8.8 Tool Changer Module.....	182
8.9 Electrical Box.....	184
9.0 Testing of Mechanical Improvements.....	186
9.1 Enclosure Testing.....	186
9.1.1 Enclosure Durability Testing.....	186
9.1.2 Enclosure Coolant Testing.....	189
9.1.2.1 Base Leak Test.....	190
9.1.2.2 Entire Enclosure Leak Test.....	190
9.1.3 Vacuum Test.....	191
9.2 4th-Axis.....	191
9.3 Tool Changer.....	192
9.4 Bed leveling.....	192
9.5 Lockout-Tagout.....	195
10.0 Testing of Electronics and Software.....	196
10.1 Safety Systems.....	196
10.1.1 E-stop.....	196
10.1.2 Limit Switches.....	196

10.1.3 Stack light.....	198
10.1.4 Door Switch.....	198
10.2 Control Board.....	198
10.2.1 Motors.....	199
10.2.2 Spindle.....	200
10.3 Software.....	201
10.3.1 grblHAL plugins.....	201
10.3.2 UGS Plugins.....	202
10.4 Sensors.....	203
10.5 Electrical Box.....	204
11.0 Physical Implementation.....	205
11.1 3D Printing Information.....	205
11.2 Overall System Construction.....	206
11.2.1 Electrical Connections.....	207
11.2.2 Tool Changer.....	214
11.3 Tests Carried Out.....	219
11.3.1 Physics Analysis of the Initial Machine.....	219
11.3.2 Additional Physics Testing.....	221
11.4 Bed Leveling.....	222
11.5 4th-Axis.....	225
11.6 Work Area Plates.....	227
12.0 Results.....	231
12.1 Machining Tolerances Verification.....	231
12.2 Enclosure Verification.....	234
12.2.1 Enclosure Durability Testing Results.....	234
12.2.2 Base Leak Test Results.....	236
12.2.3 Fully Assembled Enclosure Leak Test Results.....	236
12.2.3.1 Fully Assembled Enclosure Leak Test 1 Results.....	236
12.2.3.2 Fully Assembled Enclosure Leak Test 2 Results.....	238
12.3 Vacuum Test Results.....	239
12.4 Physics Initial Testing Results.....	241
12.4.1 Motor Temperatures.....	242
12.4.2 Acceleration Data.....	245
12.4.2.1 Softwood Testing.....	246
12.4.2.2 Teflon Tests.....	254
12.5 Physics Testing After Controller Updates.....	261
12.6 Comparison Test of Softwood.....	264
12.7 Teflon Testing Following All Updates.....	269

12.8 First Aluminum Testing.....	272
12.9 Optimized Softwood Testing.....	274
12.10 Overall Results of Physics Testing.....	279
12.11 Bed Leveling Results.....	280
13.0 Discussion.....	281
13.1 Affordability.....	281
13.2 Accuracy.....	283
13.3 4th Axis.....	283
13.4 Chip Evacuation.....	284
13.5 Tool Changer.....	284
13.6 Bed Leveling.....	285
13.7 Enclosure.....	285
13.8 Safety.....	286
13.9 Ease of Manufacturing.....	286
13.10 Control System.....	287
13.11 Vibration.....	287
13.12 Broader Impacts.....	288
14.0 Conclusion.....	289
14.1 Recommendations for Future Work.....	290
14.1.1 Minor Recommendations.....	290
14.1.1.1 Vacuum System Recommendation.....	290
14.1.1.2 4th-axis Recommendation.....	291
14.1.1.3 Strain Gauge Recommendation.....	291
14.1.1.4 Wire Management Recommendation.....	292
14.1.1.5 Automatic Bed Leveling and Tool Probing Functionality.....	293
14.1.1.6 Sensor Recommendation.....	294
14.1.2 Major Recommendations.....	294
14.1.2.1 Coolant System Recommendation.....	294
14.1.2.2 Tool Changer Code.....	295
14.1.2.3 Expanded Specialized Tool Library.....	296
14.1.2.4 IRB and Student Testing.....	296
14.1.2.5 EMI.....	297
14.1.3 Testing and Data Analysis Recommendations.....	297
14.2 Personal Reflections.....	298
References.....	303
Appendices.....	317
Appendix A: Github Links.....	317
Appendix B: Assembly document for Electrical.....	318

Appendix C: Assembly document for Machine Assembly.....	319
Appendix D: Software Installation.....	320
Appendix E: Assembly Document for Bed Leveling.....	321
Appendix F: Software Testing.....	322
Appendix G: Other relevant info.....	323
Contact Info.....	324

List of Figures

Figure 1.1: Nomad 3 - Desktop CNC Mill.....	4
Figure 1.2: Bantam Tools Desktop CNC Milling Machine (AS100010-01).....	5
Figure 1.3: PrintNC V4 DIY CNC Router.....	7
Figure 2.1: 45 mm 80-20 T-rail.....	14
Figure 2.2: 2023-2024 Enclosure.....	15
Figure 2.3: Coolant System of the CNC Machine.....	16
Figure 2.4: Caulk Used to Seal the Top and Bottom of the T-Rail.....	17
Figure 2.5: The Cracked Panel.....	17
Figure 2.6: Master Sketch of 2023-2024 CAD Assembly.....	19
Figure 2.7: Part Drawing of 2023-2024 Test Part.....	23
Figure 2.8: Finalized UHMW Machined Part.....	23
Figure 2.9: Machining Test of Stainless Steel.....	25
Figure 2.10: Failed UHMW Operation (left) and Recutting of UHMW (right).....	26
Figure 2.11: UHMW Wedgelets for Clyde Robot.....	26
Figure 2.12: Aluminum Wheel Hubs for Clyde Robot.....	27
Figure 2.13: Solidworks Drawing of 2024-2025 Test Part.....	28
Figure 2.14: Example of Machined Part Subject to Heat Generation.....	30
Figure 2.15: Main Mach3 User Interface with Loaded G-code File.....	31
Figure 5.1: Machinable Area.....	41
Figure 6.1: Venturi Pump Schematic.....	48
Figure 6.2: Cyclonic Separator.....	49
Figure 6.3: RapidChange ATC Four Tool Slot Model.....	55
Figure 6.4: Spindle Coming Down on the Collet Nut in the RapidChange ATC at 2,000 RPM.....	56
Figure 6.5: Spindle Stalling After Attaching to the Collet Nut.....	56
Figure 6.6: Collet Nut and End Mill Attached to the Spindle After the Tool Change.....	57
Figure 6.7: Spindle Coming Down to Unload the Tool into the Rapidchange ATC.....	58
Figure 6.8: Collet Nut Makes Contact with the Ball Bearings to Unload the Tool.....	58
Figure 6.9: Collet Nut Falls Deeper into the Pocket Twisting Off of the Spindle.....	59
Figure 6.10: Spindle Comes Back up Which the Nut stays in the Pocket Attached to the Ball Bearings.....	59
Figure 6.11: NEMA 17 Stepper Motor used in RapidChange ATC.....	60
Figure 6.12: Picture of Rapidchange ATC with Vinyl Dust Cover.....	61
Figure 6.13: Picture of Carvera 4th-axis Module.....	62
Figure 6.14: Picture of Carvera 4th-axis Module in the Makera Shop.....	63
Figure 6.15: Picture of Genmitsu 4th-axis Rotary Module Kit.....	64

Figure 6.16: Picture of Changzhou Rattm 4th-axis Kit.....	66
Figure 6.17: Image of Industrial CNC Mill with the Leveling Mechanism Exposed.....	68
Figure 6.18: Mechanical Brass Leveling Shims.....	69
Figure 6.19: Hobbyist CNC Mill with Aluminum Spacers.....	70
Figure 6.20: Sample 4th-axis Part.....	73
Figure 6.21: Main Mach3 User Interface with Loaded G-code File.....	74
Figure 6.22: Main LinuxCNC User Interface with Loaded G-code File.....	75
Figure 6.23: Main CNCJS User Interface.....	76
Figure 6.24: Main bCNC User Interface with Loaded G-code File.....	77
Figure 6.25: Main UGS User Interface with Loaded G-code File.....	78
Figure 7.1: First Iteration of Vacuum System.....	82
Figure 7.2: Vacuum Hose Setup.....	83
Figure 7.3: The Aluminum Chips Collected by the Vacuum System.....	84
Figure 7.4: Final CAD Iteration of the 3D Printed Dust-Boo.....	86
Figure 7.5: 3D Printed Dust-Boot with Dust-Skirt.....	87
Figure 7.6: The Vacuum System with the Dust-Boot and Skirt.....	88
Figure 7.7: First CAD Assembly of the Tool Changer.....	90
Figure 7.8: First CAD Model of the Tri Clips That Hold the Collet Nut.....	90
Figure 7.9: Top View of Clips Showing Ball Bearing Pocket as 0.039”.....	91
Figure 7.10: First CAD Model of the Base of Tool Changer.....	92
Figure 7.11: Base Part of the Rapidchange at 8.54”.....	92
Figure 7.12: CAD Assembly of Clips Inside Pockets of Base Part for Tool Changer.....	93
Figure 7.13: First CAD Model of the Top Layer of Tool Changer.....	94
Figure 7.14: First CAD Model of the Side Part of Tool Changer.....	95
Figure 7.15: CAD Model of the Lever of Tool Changer.....	96
Figure 7.16: CAD Model of the Pin of Tool Changer.....	96
Figure 7.17: First CAD Model of the Dust Cover Rod of Tool Changer.....	97
Figure 7.18: Adjusted CAD of Clip with 3/16” Ball Bearings of Tool Changer.....	98
Figure 7.19: Adjusted Base with New Holes for Clip.....	98
Figure 7.20: CAD Assembly 2nd Iteration of Tool Changer.....	99
Figure 7.21: Showing the New Dimensions of the Base.....	100
Figure 7.22: New Design of the Dust Cover.....	101
Figure 7.23: Dimensions Showing the Delta X of the Dust Cover.....	101
Figure 7.24: Right Side Part of the Mechanism with the Additions.....	102
Figure 7.25: Wire Cover Attached to the Back.....	102
Figure 7.26: Side Part with the Angle Showing the Holes of the Wire Cover.....	103
Figure 7.27: Final Iteration of the Tool Changer.....	104
Figure 7.28: Tool Changer in the Gantry.....	105

Figure 7.29: Left Side Part with Laser Receiver Slot Length.....	106
Figure 7.30: Right Side Part with Laser Sensor Slot Length.....	107
Figure 7.31: Clip Design with Cavity.....	108
Figure 7.32: Servo Coupler Showing the Micro Servo Side with Measurements.....	109
Figure 7.33: Left Servo Motor Cover with the Pico Board Mount, New Holes and Micro Servo Motor Mount.....	110
Figure 7.34: CAD Model of First Iteration of the 4th-axis Base Plate Design.....	111
Figure 7.35: Example of T-Slotting.....	112
Figure 7.36: CAD Model of First Iteration of 4th-axis Baseplate with Installed Kit.....	112
Figure 7.37: CAD Model of Second Iteration of 4th-axis Base Plate Design.....	113
Figure 7.38: CAD Model of Second Iteration of 4th-axis Base Plate Design.....	114
Figure 7.39: CAD Model of Third Iteration 4th-axis Base Plate.....	115
Figure 7.40: CAD Model of 4th-axis Base Plate with Kit Assembly.....	115
Figure 7.41: Top View of the Machine's Assembly with 4th-axis Integration.....	116
Figure 7.42: CAM Tool Path View of 4th-axis Base Plate Using Mastercam.....	117
Figure 7.43: Refitting of Holes on 4th-axis Base Plate to Align the Holes with the Chuck Piece....	118
Figure 7.44: The Location of Each of the Five Set Screws Centered Within the Four Mounting Flat-Head Mounting Screws.....	119
Figure 7.45: Image of a Threaded Set Screw Hole.....	120
Figure 7.46: Image the Set Screw Stainless Steel Plate Location.....	121
Figure 7.47: Image the Oval-Tipped Set Screws Used.....	122
Figure 7.48: Image of the Stainless-Steel Set Screws Used for Bed Leveling.....	123
Figure 7.49: Image Chart for Determining Tensile Strength of a Heli-Coil Assembly.....	125
Figure 7.50: Image of Performing a Proof-of-Concept Test on the Set Screw.....	127
Figure 7.51: Initial Design of the Work Area Plate with Bed Leveling Helicoils.....	129
Figure 7.52: Work Area Plate Design with Holes for Initial 4th-axis Base Plate Design.....	129
Figure 7.53: Image of Wilton 4" Machining Vise.....	130
Figure 7.54: Image Showing Contact of the 4" Wilton Vise with the Door.....	131
Figure 7.55: Final CAD for Option 1 of the Work Area Plate.....	132
Figure 7.56: Final CAD for Option 2 of the Work Area Plate.....	132
Figure 7.57: Full Enclosure Early Design.....	136
Figure 7.58: Triangle Bracket for Enclosure Frame.....	137
Figure 7.59: Angle Bracket for Enclosure Door Frame.....	137
Figure 7.60: T-rail with Panel Cross Section.....	138
Figure 7.61: Coolant Ramp.....	139
Figure 7.62: Ramp Standoff Cross Section.....	140
Figure 7.63: Lockout Box Containing Both Plugs.....	142
Figure 8.1: Sensor Placement on the Machine.....	152

Figure 8.2: Erroneous Spindle Temperature Data.....	154
Figure 8.3: Custom Sensor Interface Board.....	156
Figure 8.4: I2C Read Error.....	157
Figure 8.5: Drift Data Collected from Reading Resistors.....	159
Figure 8.6: Resistor Placed on Breadboard with Pins that are too Small to be Secured.....	160
Figure 8.7: Back and Front of Perfboard that was Soldered.....	161
Figure 8.8: Original Soldered Custom PCB.....	162
Figure 8.9: Laser Spindle Speed System.....	164
Figure 8.10: Stack Light Wiring Diagram.....	166
Figure 8.11: Limit Switch Mount Render.....	167
Figure 8.12: Intended grblHAL Spindle Wiring.....	169
Figure 8.13: Three-Wire and Machine Spindle Wiring.....	170
Figure 8.14: Image of the 13.7 mVAC Noticed on the Spindle Casing.....	172
Figure 8.15: Image of the Ground Wire Installation Point.....	173
Figure 8.16: Image of the Reduction in Voltage Leakage Down to 3.1 mVAC.....	174
Figure 8.17: Error with UGS Logger Plugin.....	180
Figure 8.18: UGS Tool Changer Plugin.....	181
Figure 8.19: Tool Changer Module Wiring Diagram.....	183
Figure 8.20: Tool Changer Module Implementation.....	184
Figure 8.21: Electrical Box Render.....	185
Figure 9.1: Experiment Setup.....	187
Figure 9.2: Setup of Dial Indicator.....	188
Figure 9.3: Testing of Forces Pulling on the Enclosure.....	189
Figure 9.4: Initial Coolant Ramp Testing.....	190
Figure 9.5: Image of the Starting Point of the Flat-Head Screws and Set Screws for Bed Leveling	193
Figure 9.6: Bed Leveling Testing.....	194
Figure 9.7: Bed Leveling Adjustment.....	194
Figure 10.1: Chips Stuck in Limit Switch.....	197
Figure 10.2: Default Measured Motor Curve without Linearization Compensation.....	201
Figure 10.3: Printed Electrical Box.....	204
Figure 11.1: Limit Switch Implementation.....	208
Figure 11.2: Limit Switch Schematic.....	209
Figure 11.3: DHT Sensor Mount.....	210
Figure 11.4: Mounted Sensor Board.....	211
Figure 11.5: Implemented Door Switch.....	212
Figure 11.6: Physical E-stop and Schematic.....	213
Figure 11.7: Physical Stack Light and Schematic.....	213

Figure 11.8: Completed Tool Changer in the Machine.....	214
Figure 11.9: Nylon Clip with Ball Bearings Inside.....	215
Figure 11.10: 1.18" Spring Placed Underneath the Clip.....	216
Figure 11.11: Side Part with all Components Attached to each other using #6 Zinc Screws.....	217
Figure 11.12: Top view of Tool Changer with M6 .787" Black Screws and the M6 2.56" Grey Screws.....	218
Figure 11.13: Left Side part with Pico Board, and Laser Sensor Inside Mounts.....	218
Figure 11.14: Image of the Bed with the Helicoils and Set Screws Installed, in the Center of Each of the Five Mounting Points.....	223
Figure 11.15: Image of the Set Screw Plates Installed Between the Bed and the Aluminum Mount Blocks for the Bed.....	224
Figure 11.16: Image of Adjusting the Set Screw while the Flat-Head Screws are Loose.....	224
Figure 11.17: 4th-axis Baseplate From SendCutSend.....	225
Figure 11.18: 4th-axis Base Plate Mounted to Work Area Plate.....	226
Figure 11.19: 4th-axis Assembly in Current Machine.....	227
Figure 11.20: Milled Work Area Plate Design 2.....	228
Figure 11.21: Work Area Plate 1 in Current Machine.....	229
Figure 11.22: Work Area Plate 2 in Current Machine.....	229
Figure 12.1: Vectorized Aluminum Part Machined on 2023-2024 Mini-Mill.....	234
Figure 12.2: Force vs. Displacement for Enclosure Pushing Test.....	235
Figure 12.3: Force vs. Displacement for Enclosure Pulling Test.....	235
Figure 12.4: Front Face of T-Rails where the Coolant is Leaking From.....	237
Figure 12.5: Bolt Holes.....	239
Figure 12.6: The Work Area After Milling Wood with Vacuum System.....	240
Figure 12.7: The Work Area After Milling Wood without Vacuum System.....	241
Figure 12.8: Softwood_1 Motor Temperatures.....	243
Figure 12.9: Softwood_2 Motor Temperatures.....	243
Figure 12.10: Teflon_1 Motor Temperatures.....	244
Figure 12.11: Teflon_2 Motor Temperatures.....	244
Figure 12.12: Zeroed and Smoothed Acceleration Data from the Bed of Softwood_1.....	246
Figure 12.13: Zeroed and Smoothed Acceleration Data from the Bed of Softwood_2.....	247
Figure 12.14: Zeroed and Smoothed Acceleration on the Spindle Housing during Softwood_1 Testing.....	248
Figure 12.15: Zeroed and Smoothed Acceleration on the Spindle Plate during Softwood_1 Testing.....	249
Figure 12.16: Zeroed and Smoothed Acceleration on the Spindle Housing during Softwood_2 Testing.....	250
Figure 12.17: Zeroed and Smoothed Acceleration on the Spindle Plate during Softwood_2 Testing.....	251

Figure 12.18: Zeroed and Smoothed Enclosure Acceleration for Softwood_1.....	252
Figure 12.19: Zeroed and Smoothed Table Acceleration for Softwood_1.....	252
Figure 12.20: Zeroed and Smoothed Enclosure Acceleration for Softwood_2.....	253
Figure 12.21: Zeroed and Smoothed Table Acceleration for Softwood_2.....	254
Figure 12.22: Teflon_1 Bed Acceleration Zeroed and Smoothed.....	255
Figure 12.23: Teflon_2 Bed Acceleration Zeroed and Smoothed.....	255
Figure 12.24: Teflon_1 Spindle Housing Acceleration Zeroed and Smoothed.....	256
Figure 12.25: Teflon_2 Spindle Housing Acceleration Zeroed and Smoothed.....	257
Figure 12.26: Teflon_1 Spindle Plate Acceleration Zeroed and Smoothed.....	258
Figure 12.27: Teflon_2 Spindle Plate Acceleration Zeroed and Smoothed.....	258
Figure 12.28: Teflon_1 Enclosure Acceleration Zeroed and Smoothed.....	259
Figure 12.29: Teflon_2 Enclosure Acceleration Zeroed and Smoothed.....	260
Figure 12.30: Teflon_1 Table Acceleration Zeroed and Smoothed.....	260
Figure 12.31: Teflon_2 Table Acceleration Zeroed and Smoothed.....	261
Figure 12.32: Softwood Temperature After February Updates.....	262
Figure 12.33: Softwood Bed Acceleration After February Updates Before Sensor Failure, Zeroed and Smoothed.....	263
Figure 12.34: Softwood Spindle Plate Acceleration After February Updates Zeroed and Smoothed.....	264
Figure 12.35: Softwood Comparison Test Temperature Data.....	266
Figure 12.36: Softwood Comparison Test Bed Acceleration Data Zeroed and Smoothed.....	267
Figure 12.37: Softwood Comparison Test Spindle Housing Acceleration Zeroed and Smoothed....	268
Figure 12.38: Softwood Comparison Test Spindle Plate Acceleration Zeroed and Smoothed... ..	269
Figure 12.39: Teflon Bed Acceleration After All Updates, Zeroed and Smoothed.....	270
Figure 12.40: Teflon Spindle Plate Acceleration After All Updates, Zeroed and Smoothed.....	271
Figure 12.41: Teflon Enclosure Acceleration After All Updates, Zeroed and Smoothed.....	272
Figure 12.42: Aluminum Test Temperature Data.....	273
Figure 12.43: Aluminum Enclosure Acceleration Zeroed and Smoothed.....	274
Figure 12.44: Motor Temperatures for Optimized Softwood Process.....	275
Figure 12.45: Bed Acceleration for Optimized Softwood Process Zeroed and Smoothed.....	276
Figure 12.46: Spindle Housing Acceleration for Optimized Softwood Process Zeroed and Smoothed.....	277
Figure 12.47: Table Acceleration for Optimized Softwood Process Zeroed and Smoothed.....	278
Figure 12.48: Enclosure Acceleration for Optimized Softwood Process Zeroed and Smoothed	279
Figure 14.1: Custom PCB Render, with Strain Gauge Section Highlighted.....	292

List of Tables

Table 2.1: Tolerances of Machined Test Parts.....	29
Table 3.1: Goals and Measurable Targets.....	36
Table 4.1: Gantt Chart.....	39
Table 6.1: Decision Matrix for 4th-axis Add-on Kits.....	64
Table 7.1: Cost Breakdown of Tool Changer.....	89
Table 7.2: Values Used for Determining the Optimal Material for the Bed Material.....	124
Table 7.3: Work Area Plate Decision Matrix Value.....	128
Table 7.4: Work Area Plate Decision Matrix Final Score.....	128
Table 7.5: Machines 1 & 2 Hole Sizes for Work Area Plates.....	133
Table 7.6: Filament Material Properties.....	135
Table 7.7: Filament Design Matrix (PLA & PETG).....	135
Table 7.8: Filament Design Matrix (TPU, PC, Nylon).....	135
Table 8.1: Control Software Decision Matrix Criteria.....	144
Table 8.2: Control Software Decision Matrix for Mach3, LinuxCNC, and bCNC.....	145
Table 8.3: Control Software Decision Matrix for CNCJS and UGS.....	146
Table 8.4: Control Board Decision Matrix Criteria.....	147
Table 8.5: Control Board Decision Matrix for Boards Supporting LinuxCNC.....	148
Table 8.6: Control Board Decision Matrix for Boards Supporting grblHAL, grbl, and Mach3.	148
Table 8.7: Final Decision Matrix for Software Control Systems.....	149
Table 11.1: Machining Parameters Used for Initial Machine Testing.....	220
Table 11.2: Machining Parameters Used for Testing Softwood_FEB26 After Electrical and Software Updates.....	221
Table 11.3: Machining Parameters Verified for Optimal Machine Performance.....	222
Table 12.1: Wood Test Part Tolerance Verification.....	231
Table 12.2: Teflon (PTFE) Test Part Tolerance Verification.....	232
Table 12.3: Aluminum Test Part Tolerance Verification.....	233
Table 13.1: Price Breakdown of Base Model.....	282
Table 13.2: Price Breakdown of Add-on Features.....	282

Authorship Table

Section	Author(s)	Editor(s)
Acknowledgements	Andrew	Andrew, Rafael
Abstract	Andrew, Camren, Michael P.	Michael P., Andrew
1. Introduction	Michael D., Daniel, JR, Dante	Andrew, Echo, Daniel, Rafael
2. Review of the 2023-2024 Desktop CNC MQP	Andrew, Camren, Echo, JR, Michael D., Michael P., James	Andrew, Daniel
3. Goals for this MQP	Andrew, Camren, Daniel, Dante, Michael P., Rafael	Andrew, Daniel
4. Project Timeline	Daniel	Andrew
5. Methodology	Camren, Daniel, Dante, Michael P., Rafael	Andrew, Rafael
6. Literature Review	Andrew, Camren, Dante, Echo, JR, Michael P., Perrin, Rafael	Andrew, Daniel, Perrin
7. Mechanical Design Updates	Daniel, Dante, James, JR, Michael D., Michael P., Perrin, Rafael	Andrew, James, JR
8. Electronics and Software	Camren, Michael P., Perrin, Echo	Andrew, JR
9. Testing of Mechanical Improvements	Daniel, Dante, JR, Rafael, Michael P.	Andrew, Perrin, James
10. Testing of Electronics and Software	Camren, Perrin	Andrew, Rafael
11. Physical Implementation	Dante, Echo, James, Michael P. Perrin, Rafael	Andrew, Daniel, JR
12. Results	Andrew, Daniel, Dante, Echo, JR, Michael P.	Andrew, JR, Rafael

Section	Author(s)	Editor(s)
13. Discussion	Everyone	Andrew, JR
14. Conclusion	Andrew, Dante, James, JR, Michael D. Perrin	Andrew, Daniel, Rafael

1.0 Introduction

CNC (computer numerical control) machining is a type of manufacturing process that uses pre-programmed code to move either the workpiece or the tool to produce a product (Astro Machine Works, 2021). The process first starts in the development of a product using a computer-aided design (CAD) software. This design is then put in a computer-aided machining (CAM) program to create G-code (geometry-code) and M-code (miscellaneous-code) that the machine tool can interpret into feeds, speeds, and movement along the axes. This type of programming language allows for specific inputs for a multitude of cutting parameters to create a precise part out of a variety of different materials. It reduces the amount of human interaction needed with the cutting tool, thus lessening the amount of error and increasing production quantity and quality (Goodwin University, 2024). For these reasons, three-axis lathes and mills have most commonly utilized this type of machining process, however both plasma and laser cutters implement this as well (Universal Technical Institute, 2020).

These benefits have also prompted the usage of CNC machining in several fields such as the aerospace, maritime, automotive, and medical industries. These industries take advantage of the CNC's repeatable movements to automate the production of high precision parts (Pickens Technical College, 2024). The process of CNC machining adheres to several industry standards such as ISO 9001, ensuring that all parts produced meet customer and regulatory requirements (Ye, 2024). Machining interest falls well beyond the scope of work settings. Many machine hobbyists enjoy the trade through a mix of personal CNC milling machines.

Despite the popularity of CNC machining, there has been a significant decline in CNC machinists. Research and studies have shown the manufacturing industry could have over two million vacant jobs by 2030, and that nearly 50% of manufacturing executives have declined business opportunities due to lack of qualified machinists (MacFab, 2024). This fact is concerning upon realizing the profession is vital to the machining process; as it performs set-ups, implements programming, and maintains the performance of the CNC machine during operation (Thomas, 2022). The shortage of qualified machinists stems from a large age gap between retiring workers and those newly joining the field. As stigmas surrounding this field pushed more students towards a college-driven path, many training programs were shut down. This “insufficient training infrastructure” (Free, 2023) has resulted in educational training programs not maintaining applicant completion rates to keep up with the growing industry (Castro, 2024).

In understanding what has caused this shortage, companies and organizations have taken measures to address these issues. CNC manufacturing companies have begun investing in more extensive training programs, while also adopting semi-automated processes with the use of automated robot systems. These training programs partner with vocational high schools and community colleges to give students the essential knowledge and experience needed for success in the industry; not only working with the CNC machine tools, but also opening up avenues for those who are interested in the automation of manufacturing processes through robotics (Castro, 2024). This, coupled with apprenticeship programs, has given students the ability to become qualified machinists through gaining insight and exposure to the field.

Desktop CNC milling machines have thus become a pivotal tool for allowing students to gain hands-on experience with a CNC machine. While industrial machines can be burdensome, both financially and physically (in terms of their size), desktop CNC mills offer an effective alternative. These mills, as the name suggests, take up a significantly smaller amount of space, all while maintaining a relatively low cost. It offers users the opportunity to experience all the steps required in operating a full-sized machine: producing a CAD model, using CAM to create the G and M-code, and setting up the tools and workpiece for machining. They have become a readily accessible product perfect for learning and for hobbyist use (Fowle, 2024).

1.1 Introduction to Commercial Desktop CNC Machines

There are currently many different commercial desktop CNC machines on the market. Their price can range anywhere from around \$2,000 to \$7,000. These desktop CNC machines are a good alternative compared to industrial CNC mills for both hobbyist and educational usage as previously referenced.

For example, the Nomad 3 - Desktop CNC Mill by Carbide 3D (Figure 1.1) offers a price point of \$2,800. This desktop CNC machine comes with a 130 W spindle with a maximum of 24,000 RPM, work probe, linear rails on the z-axis, safety door interlock and switches. The machine is 17.5" x 19" x 17" in size, and there is 8" x 8" x 3" of workable area. The Nomad 3 is capable of cutting wood, plastics (e.g., ABS, Acrylic, Polycarbonate, Delrin, HDPE, PEEK, PVC), and metals (e.g., Aluminum, Brass, Copper). To cut these materials, it uses $\frac{1}{8}$ " end mills and ER-11 collets (Carbide 3D, n.d.).

Figure 1.1: *Nomad 3 - Desktop CNC Mill*



Note. This image shows the Nomad 3 - Desktop CNC Mill by Carbide 3D (reproduced as is from (Carbide 3D, n.d.)).

Another machine currently on the market is the Bantam Tools Desktop CNC Milling Machine (Figure 1.2) that costs \$6,999. This machine comes with a 28,000 RPM spindle, ER-11 collets and $\frac{1}{4}$ " end mills, clamps, and other hand tools. The machine is $19.8'' \times 20.9'' \times 19.4''$ in size, and it has a build volume of $7'' \times 9'' \times 3.3''$ while also being forth-axis compatible. It is capable of cutting metals such as aluminum 6061, brass, copper, plastics and more with a material removal rate (MMR) of 0.4 cubic in/min with a repeatability of +/- 0.001" (*Bantam Tools ExplorerTM CNC Milling Machine*, n.d.).

Figure 1.2: Bantam Tools Desktop CNC Milling Machine (AS100010-01)



Note. Reproduced as is from (*Bantam Tools Explorer™ CNC Milling Machine*, n.d.).

While these machines are expensive, there are several benefits to buying pre-built desktop CNC machines. Since these machines are pre-built, the buyer does not need any technical knowledge or time to build one by themselves. Furthermore, they come with free softwares that are designed specifically for the machine by their respective companies. The Nomad 3 includes a MeshCAM License that generates a G-code for STL files without needing other CAM software. The Bantam Tools Desktop CNC Milling Machine comes with their software that include things such as G-code integration, SVG support, automatic material and plan probing, speed and feed rate override, and more. With these included softwares, the buyer does not need to manually create a program to run the machine. Additionally, the buyer can contact customer support and ask questions if they run into any issues with the machines.

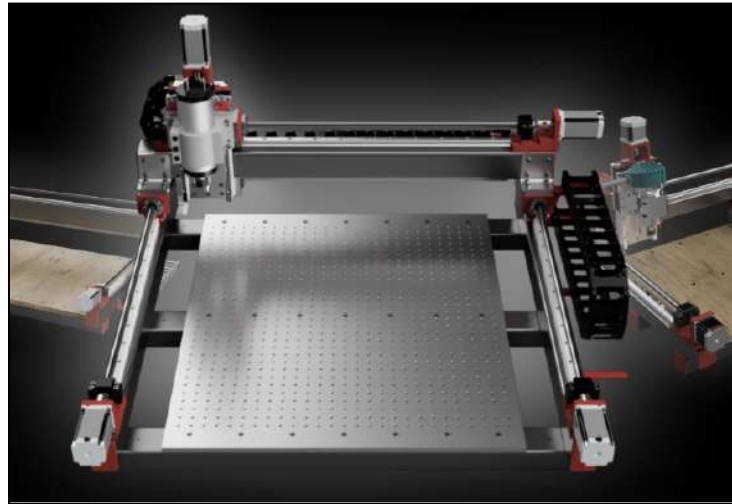
With both the open-source and commercial desktop CNC machines in mind, it is important for the buyer to weigh the pros and cons for both types of desktop CNC machines. An open-source desktop CNC machine is better for hobbyists and students as they are more cost-friendly, however they take a significant amount of time to build.

1.2 Introduction to Open-Source Desktop CNC Machines

Unlike commercial desktop CNC machines, open-source machines are built using freely available plans and design files found online. As mentioned previously, these types of CNC machines are geared towards hobbyists and students because of their cost effective nature. They also allow for increased modifications that the user could decide to add-on to their machine. An overwhelming majority of open source desktop machines rely on community supported designs that are constantly updated and various social media platforms exist such as Discord for users to utilize for troubleshooting problems with their machine.

An example of an open-source desktop CNC machine is the PrintNC V4 (Figure 1.3) (logan2225, 2025). Design documents, a bill of materials, and assembly instructions can be found on its website along with its associated Discord with over 11,000 members. The machine is designed using Fusion360 and is highly customisable to allow for users to build their machine to their own specification requirements. Because of this, prices can range from \$1,500 to \$3,500 based on size and on how many add-on features the user includes. The machine is constructed through parts sourced online, 3D printed components, and HGR20 linear rails and ball screws on all axes.

Figure 1.3: PrintNC V4 DIY CNC Router



Note. Reproduced as is from (logan2225, 2025).

A major draw of open-sourced desktop CNC machines is their relatively cost-effective price and high customization. This allows for users new to CNC machining to get experience with milling without making a large financial commitment like with commercial desktop CNC machines. The build process for open-sourced machines also does not require advanced tools or parts to construct, allowing for novice users or those without access to advanced tools to construct their own machines.

However, downsides do exist to open-sourced machines. Build time and construction does increase time that many users might not have. Furthermore, the majority of open-source CNC machines available on the internet are in the form of routers, not mills. Limiting the number of quality options for those interested in milling and do not have the budget for commercial options. A commercial desktop CNC machine would be better for someone who does not have the knowledge or a lot of time to invest in building the machine, although it will cost more.

This report is organized as follows: Chapter 2 outlines the review of the 2023-2024 team's design and work; Chapters 3, 4, and 5 lay out the 2024-2025 team's goals, timeline, and methodology; Chapters 6, 7, and 8 describe the background research and subsequent designs; Chapters 9 and 10 describes the testing of respective designs; Chapters 11 illustrates the implementation of the designs; Chapter 12 and 13 provide the results and discussions pertaining to the systems and goals; the report concludes with Chapter 14 with the authors' recommendations for future work.

2.0 Review of the 2023-2024 Desktop CNC MQP (Brown et al., 2024)

This chapter will discuss the first iteration of the open-source desktop CNC Mini-Mill developed by Alex Brown, Gabriel Brown, Brian English, Abigail Hodges, Luke Hoy, and Jacob Schools as the 2023-2024 MQP team (Brown et al., 2024). The following sections analyze their MQP report and the work conducted during the 2023-2024 WPI academic year, in addition to the testing and observations of the machine performed by the 2024-2025 MQP team.

2.1 Analysis of the 2023-2024 Desktop CNC MQP Report

The previous work of the 2023-2024 Desktop CNC Mini-Mill initiated as a response to the lack of accessible machining opportunities at WPI. Their report notes the extensive training required to access the machines, in addition to the delayed responses of Washburn Lab, a direct result of staff shortages from the pandemic, as a reason to "discourage individuals" who want or need to use the machines. Adversely, students who wish to engage in hands-on machining cannot purchase industrial-size machinery and do not possess a large, designated area for the machinery. This often leads to students and hobbyists outsourcing their products to external vendors, furthering the disparity in machining knowledge and experience of the younger generation. With this in mind, the 2023-2024 research team pursued a solution to this problem, creating an open-source CNC mini-mill that is capable of being "recreated by anyone with the desire to build and operate their own machine."

To measure their success for the 2023-2024 WPI academic year, the team created measurable goals that aligned with the scope of the project. Highlighted in Chapter 2 of their MQP report, seven goals were set in place:

1. Affordable - Cost under \$1,500
2. Compact - Maximum machine volume 2 ft x 2 ft x 3 ft
3. Safe - Safe enclosure, E-stop, load readings provided
4. Easy to Manufacture - Only basic hand tools, a drill press, a bandsaw, and a 3D printer
5. Accurate - Overall tolerance of +/- 0.0015". Repeatability within 0.0007"
6. Fast - Material removal rate of 0.3 in³/min for 6061 aluminum
7. Powerful - Capable of machining plastics, aluminum, and mild steel

These goals were based on products within the existing mini-mill market. Their research found that the average price point of six different mini-mills was \$3,048. The overall volume was based on the area of a desk, thus making the 2 ft depth a critical dimension. To make the machine as user-friendly and open-source to assemble, only basic hand tools and shop equipment were assumed to be used. The team evaluated the existing Haas Mini-Mills removal rate in Washburn Labs to create a measurable goal for the material removal rate.

With these clear targets in place, the team successfully developed a machine that met the performance and accessibility goals outlined at the project's outset. To begin, a fully assembled machine was produced using the limited machinery and tools outlined in the easy-to-manufacture and open-source nature of the project. Furthermore, the team tested various materials and parts on their desktop CNC mini-mill to measure the machine's

dimensional accuracy, and measures of the targeted feeds, speeds, and material removal rate were all achieved. An ultra high molecular weight polyethylene (UHMW) 2" x 2" x 3/8" piece of stock was machined. The workpiece featured three different geometries that would be measured to evaluate the linear and interpolating motion of the machine (Brown et al., 2024, p. 83). Their measurements confirmed an acceptable replicated tolerance of 0.005". As for metals, the team tested both 6061 aluminum and steel. When milling aluminum, a removal rate of 4.4 in³/min was used, using 0.375" depth of cut, 0.160" stepover, and a feed rate of 70 IPM. However, steel posed a problem for the machine, resulting in a broken end mill, sparks, and visible burnt marks. With this machine, the team successfully made UHMW wedgelets for the 3 lb combat robot, Clyde, in addition to aluminum wheel hubs for the robot.

Concerning the safety of the machine, the The National Institute for Occupational Safety and Health (NIOSH) app was used for noise level monitoring. The machine produced a decibel level well within the maximum limit. Moreover, the team noted that the machine was "able to successfully power all of these components by using our 24 V 25 A AC/DC power converter and supplying the proper amount of amps to each component" (Brown et al., 2024, pp. 90-91).

Upon completing all previous tasks, the team proposed a series of recommendations to further enhance the machine and its capabilities. The primary recommendation proposed was to determine a method to ensure perpendicularity between the x- and y-axes. Due to the manual assembly process with minimal machine tools, verifying proper alignment of these two axes was rather labor intensive and not entirely conclusive. In establishing a set

procedure that guarantees the correct alignment of the axes, the tolerancing of machined parts can significantly improve.

It was also suggested to modify the workable area (the maximum machinable area of the spindle) so the bed can be machined flat. In machining, it is often considered good practice to machine the workable area; this allows for users to make certain that the workable area is completely perpendicular to the z-axis. In doing so, any part or vise placed on this surface will now be perpendicular to the z-axis, and ensures a flat cut during the machining process. The team's machine did not have this capability, as the work area plate¹ was roughly 2" too large in both the x- and y-directions. Reducing the size of the work area plate or increasing the machining area would result in complete perpendicularity of the cutting tool to the work piece.

In the scope of minimizing the overall price of purchased parts, it was proposed to modify the square tubing with angle iron. The manufacturing and assembly of the square tubing attached to the base of the machine was a difficult process for the team. With the drill press not entirely vertical and the tubing requiring the drilling of multiple walls, drills would often walk during the manufacturing process. This resulted in the misalignment of screws during assembly becoming a recurring issue. As such, angle iron was suggested as a replacement due to it only needing to be drilled through one wall allowing for an easier assembly process.

Referencing the power and electrical aspect of the machine, the team advised for future iterations of the project to verify that power requirements were met for their selected components. Components such as the stepper motors, main control board, and spindle, can pose serious issues to machine safety if they receive an insufficient amount of power.

¹ Machine bed where all functionality is fastened including vises, 4th axis, and tool changer

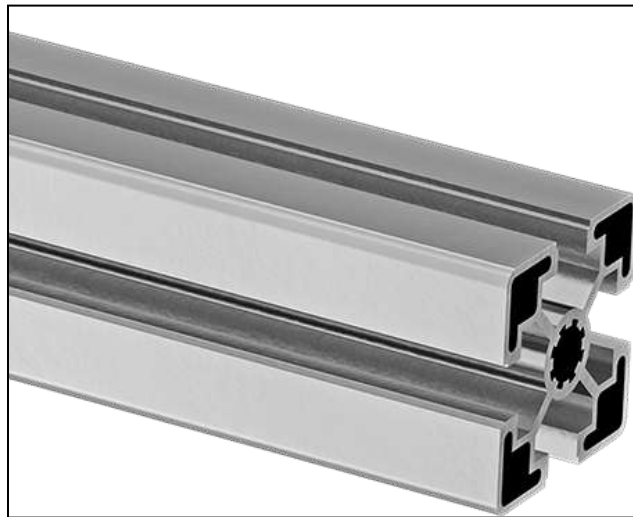
Improper power supply has the ability to result in a drop in torque of the motors, or loss of positioning due to a control board failure. With this, the team has noted the importance of testing to ensure proper power supply for all components.

The team's final recommendation was one pertaining to the enclosure and its leaking. It was noted that the grooves in the t-rail and the manner in which the panels were attached did not provide an easily sealed area. Coolant leakage during operation is not only an inconvenience, but also creates a hazard for the work area and the electrical components. Therefore, a well-constructed redesign of the enclosure that considers solutions for the usage of watertight gaskets and smoother sealing boundaries.

2.2 Review of the 2023-2024 Desktop CNC Mill MQP's Machine Enclosure and Chip Evacuation

With a reduced budget in mind, the previous MQP team decided to use a material that was easily available to them for framing the enclosure. The material that they decided to use was the 45 mm 80-20 t-rail (Figure 2.1) found in Higgins Lab of WPI.

Figure 2.1: 45 mm 80-20 T-rail



Note. Reproduced as is from (*McMaster-Carr*, n.d.).

According to last year's MQP's report, they chose to use the t-rails because it was a cost-effective alternative to other aluminum extrusion and required less manufacturing than bent plate construction. The team ultimately decided to use this material due to its accessibility at WPI, thus reducing the incurred costs of the project (Brown et al., 2024).

As for the guarding, they used polycarbonate sheets and secured it to the outside of the enclosure by screwing it into the t-rails. These panels are $\frac{1}{8}$ " in thickness, and are 2' x 2' in length and width. Polycarbonate was chosen due to its impressive mechanical properties and cost-effectiveness. To open the enclosure, there was a panel in the front between two t-rails with an aluminum piece at the bottom that could be lifted up. The entire enclosure was also bolted down to a table, as seen in Figure 2.2.

Figure 2.2: 2023-2024 Enclosure



For chip evacuation, previous year's team utilized a water based coolant with a rating of 13 gallons per minute. In their setup, there is one coolant hose connecting the submersible pump inside the bucket to the spray nozzle next to the spindle. The second hose is attached to a drainage hole on the table. The used coolant would enter the hole, and then flow down into the filter funnel on the bucket (Figure 2.3). It would then be recycled repeatedly using the pump during machining.

Figure 2.3: Coolant System of the CNC Machine



Note. The hoses are connected from the bucket to the machine through a hole in the table.

Although the enclosure was a reliable design that was able to contain chips from milling operations. The enclosure created several complications, such as frame stability, panel mounting, and coolant leakages. These problems will be discussed in the next section.

2.3 Enclosure Concerns from the 2023-2024 MQP

The enclosure was a reliable design that was able to contain chips from milling operations, however posed issues pertaining to coolant leakage and proper operator access to the work area. The coolant leakage stemmed from the overall placement of the panels to the t-rail. When the machine was first built, the scope of the project did not include a coolant system, hence the rationale behind securing the panels to the outside of the enclosure. With the addition of a coolant system after having already built the enclosure, the easiest solution was to apply caulk to seal the gap where the panel touched the t-rail inside

the enclosure. This was successful for the top part of the t-rail (Figure 2.4), but the bottom part faced severe leakage when the bottom panel between the enclosure and table cracked.

Cracking, as seen in Figure 2.5, was a result of drilling through both the table and the bottom panel to secure the enclosure to the table.

Figure 2.4: Caulk Used to Seal the Top and Bottom of the T-Rail



Figure 2.5: The Cracked Panel



Note. The panel is located between the bottom of the enclosure and the table.

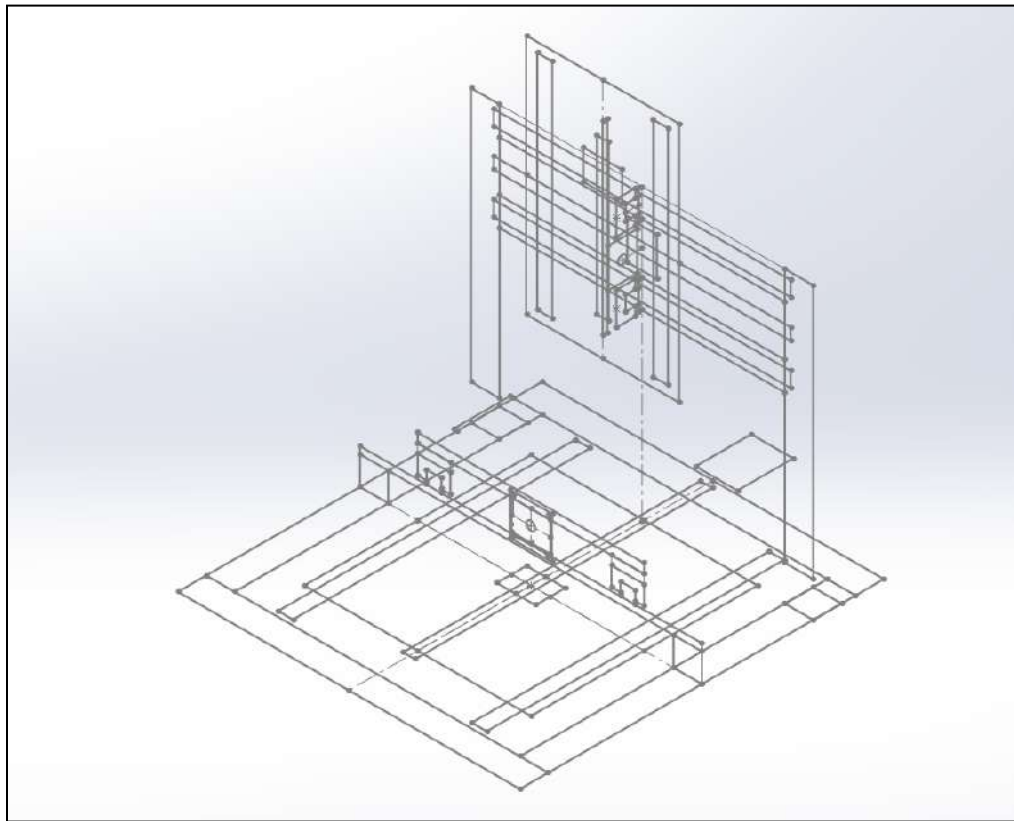
2.4 Inconsistencies with the Previous CAD Assembly

The Solidworks CAD assembly from the previous team was obtained through their GitHub link. Due to the discontinuation of the GrabCAD workbench (Valle, 2022), GitHub offered another solution for storing the assembly and part repository, while maintaining the nature of an open-source project. However, traversing the GitHub repository was challenging and not user-friendly. For this reason, Camren Chraplak of the 2024-2025 MQP team created a GitHub user guide that allowed the entire team to properly navigate the website and merge files without concern (reference Appendix H).

When analyzing the CAD of the 2023-2024 MQP team, it was evident that the team used a top-down assembly approach. A top-down assembly method designs parts or features in reference to a “layout sketch or the geometry of another part” (*Top-Down Design - 2021 - SOLIDWORKS Help*, 2021). Upon opening the 2023-2024 CAD assembly, a *Master Sketch* (Figure 2.6) outlined the gantry² and its surrounding components. The team designed the square tubing, baseplate, brackets, and other gantry parts around this *Master Sketch*. While this top-down method allowed the team to outline the gantry size and formulate parts around it, it offered a unique challenge to recreate the assembly and limited the open-source aspect of the assembly. With parts dependent on the geometry of the *Master Sketch*, the assembly was unable to be modified without changing the sketch.

² Consists of all steel square tubing parts and brackets, and the x-, y-, z-axes linear traversal components

Figure 2.6: Master Sketch of 2023-2024 CAD Assembly



2.5 Vibration Damping of the 2023-2024 MQP

The previous MQP team had completed some research relating to vibration damping for machining, specifically referencing Eberhard Bamberg's thesis, '*Principles of rapid machine design*' which contains a section about vibration damping and some testing performed. In the 2023-2024 MQP it is covered that as the teeth of an end mill engage and disengage with the workpiece it leads to vibrations in the system. However, vibrations are not solely attributed to cutting, but moreover any processes related to movement; as all processes that occur in the machine can cause vibrations. As addressed by the previous project team and confirmed by additional research: vibrations lead to worse finishes and

inaccuracies in the final workpiece. Additionally, vibrations can cause issues by accelerating normal tool wear and deteriorating overall machine health.

A process researched during the previous MQP but not implemented on the actual machine was constrained layer damping which involves inserting a damping material between structural layers. The specific low-cost application of this in small-scale machines involves filling hollow structural tubing with sand or concrete. Research conducted and reported by Bamberg discussed various methods of damping. The research found that forms of constrained layer damping with concrete performed the best, but it was determined that for a student or hobbyist machine due to the great weight of concrete and sand would prove appropriate (Bamberg, 2000).

The structural design and assembly of the machine and gantry did integrate methods that would aid in vibration damping. The gantry was made of steel instead of aluminum adding weight to the structure, as such heavier structures are better suited to damp structures. The previous MQP team did explore using aluminum extrusion for the machine structure but ultimately decided to use steel square tubing to provide rigid structure and reduce vibrations. Additionally, the machine components were fastened using bolts rather than welds. Bolted joints experience friction which dissipates energy, providing a damping effect, which increases with the number of joints (Bamberg, 2000).

It is imperative that a structure is rigid in order to reduce vibrations. The previous MQP team considered welding the structure but ultimately decided that welding the machine would be unfeasible. They addressed creating rigid connections in relation to mounting the spindle using modified spacers to ensure the connection of the spindle is carried through to the linear rails.

The 2023-2024 MQP did use methods to reduce vibrations including using steel instead of aluminum for the frame, using bolted joints in the gantry construction, and using spacers to form a rigid connection between the spindle and the linear rails. The machine was not optimized for vibration damping as when choosing axis motors, stepper motors were chosen despite having a lower efficiency due to vibrations than other DC motors. The team did not test or collect quantitative data about machine vibrations which is something that was included in this 2024-2025 MQP. Overall, the 2023-2024 MQP had good foundations of basic vibration damping for machines of its type while achieving goals of being relatively lightweight and simple for a hobbyist to construct.

2.6 Noise Reduction of the 2023-2024 MQP

The previous MQP discussed noise reduction in deciding between lead screws and ball screws for the axes. The team chose to use ball screws despite lead screws being quieter; ball screws have many benefits over lead screws making it understandable why they were chosen. The machine was tested by the team and it did pass OSHA noise regulations with “the TWA well below the maximum of 85dBA and the LCPeak below the maximum of 135dB before hearing implementation” (Brown et al., 2024, p 87). The levels were measured during feeds and speeds testing using the mobile app NIOSH SLM.

2.7 Rigidity Testing of the 2023-2024 Gantry

It was noted that the existing CNC machine had some level of spindle displacement, so testing was done to confirm the exact level of displacement. For each test, a dial indicator rested on the mount for the clamping system. An initial measurement was taken, then the respective axis was jogged away so the dial indicator was no longer touching the mount. The machine was then jogged back to the exact location and an additional measurement was

taken from the dial indicator. A displacement of up to +/- 0.002" was noted on the dial indicator for the x-axis, +/- 0.003" for the y-axis, and +/- 0.003" for the z-axis. These findings confirmed that there was existing spindle displacement which indicated that the frame of the gantry could not support the torque and speed of the motors.

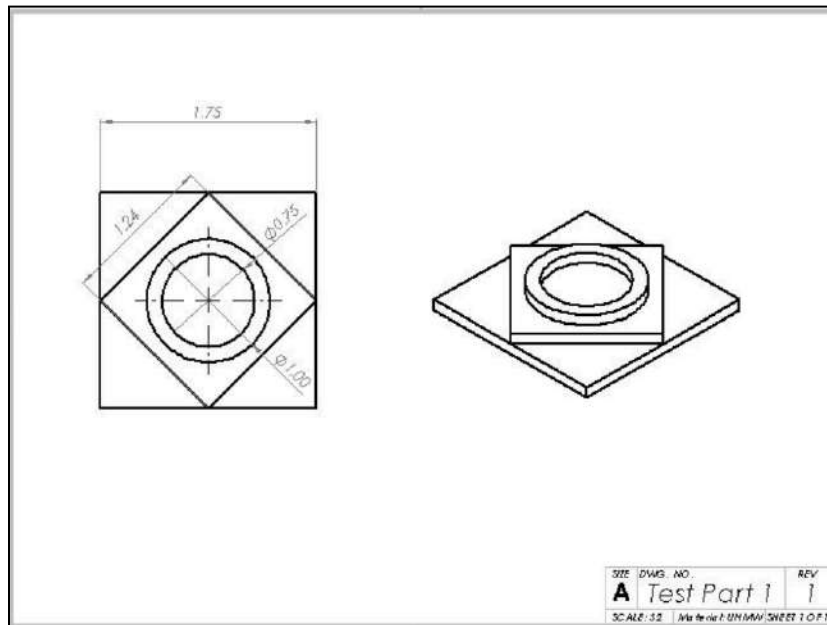
2.8 Machining Capabilities

The following section outlines the tolerancing and machining capability of the mini-mill tested and found by both the 2023-2024 and 2024-2025 teams.

2.8.1 2023-2024 Machining Testing

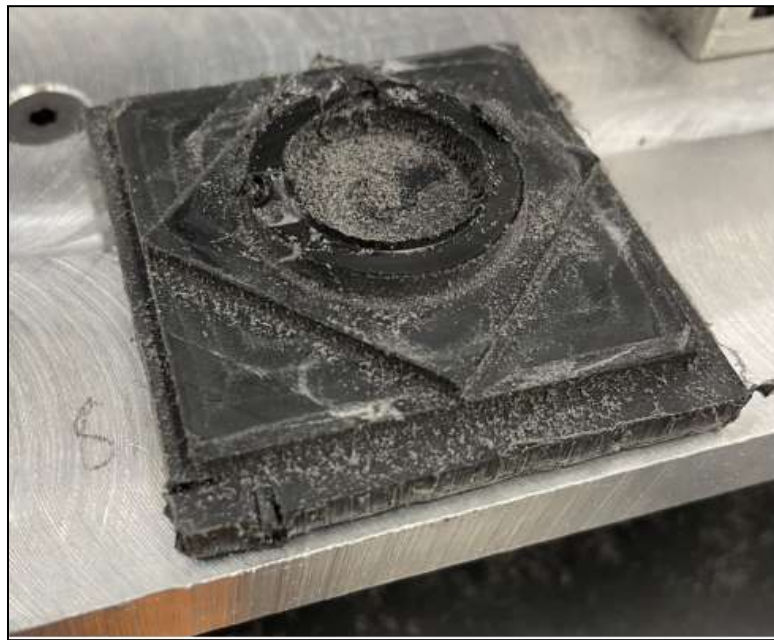
The machine was documented to have the ability to machine UHMW, aluminum, and stainless steel. A standardized test part was created to evaluate the dimensional accuracy of the machine in machining different materials. The part features a circular extrusion with both an outer-diameter (OD) and inner diameter (ID), along with a square rotated 90° from the x-axis (see Figure 2.7). This test part was machined from UHMW, and was able to produce the two squares within 0.001" off nominal, and the circular bore to be 0.005" undersized. It was also noted that the burrs on the part created some difficulty with measuring (Figure 2.8). Nonetheless, this part created a baseline understanding of the machine's capabilities.

Figure 2.7: Part Drawing of 2023-2024 Test Part



Note. Reproduced as is from (Brown et al., 2024).

Figure 2.8: Finalized UHMW Machined Part

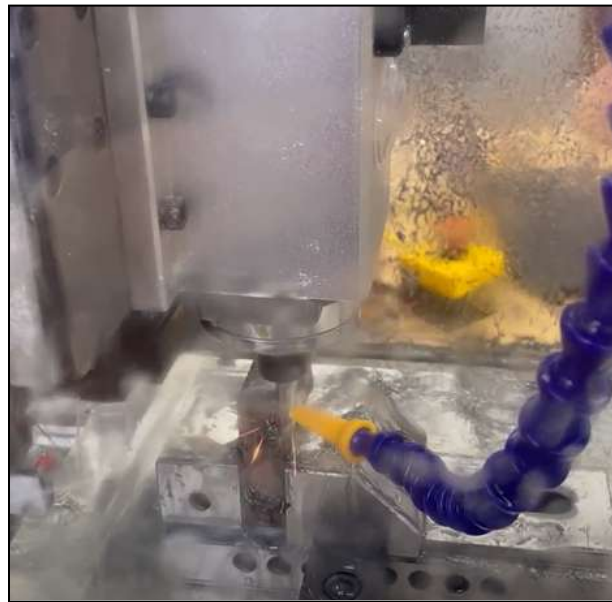


Note. Reproduced as is from (Brown et al., 2024).

Upon verifying the machine's ability to manufacture parts, several tests were carried out to evaluate the maximum cutting parameters for aluminum. These tests used a $\frac{1}{4}$ " four flute flat end mill with a maximum spindle speed of 6,000 RPM. Coolant was not used in its entirety during operation due to leakages from the enclosure. At a maximum material removal rate (MMR) of 4.4 in^3 per minute, 0.375" depth of cut (DOC), 0.16" stepover, and a feed rate of 70 IPM the team noticed a poor surface on the part.

Similar testing was carried out for the machining of stainless steel. Using the same style of end mill as in the aluminum testing and spindle speed, the team was able to determine an MMR of 0.09 in^3 per minute, with a 0.375" DOC, 0.02" stepover, and a feed rate of 12 IPM. The operation was noted to have created a large amount of heat generation, as evidenced by sparking and noticeable burn marks on the stock and the cutting tool, shown in Figure 2.9. This testing ultimately ended due to a broken end mill.

Figure 2.9: Machining Test of Stainless Steel



Note. Reproduced as is from (Brown et al., 2024).

Practical application parts were produced on the machine to further explore its capabilities. The machine was utilized as a router for the production of three UHMW wedgelets for the Clyde combat robot. The stock was held down to the base plate utilizing toe clamps, and after working through an initial problem with the Mach3 software (Figure 2.10), the parts were successfully run and implemented onto the robot as shown in Figure 2.11 (Brown et al., 2024, p. 88). Another component successfully machined were aluminum wheel hubs for the robot. The stock was fixtured in a screwless vise, faced on multiple sides, and incorporated a tool change to a drill. As with the wedgelets, the wheel hubs were effectively fitted and used by the robot during competition as seen in Figure 2.12 below (Brown et al., 2024, p. 89).

Figure 2.10: Failed UHMW Operation (left) and Recutting of UHMW (right)



Note. Image of poor finish quality, indicating a problem with either machine rigidity, motor repeatability, or software malfunction. Reproduced as is from (Brown et al., 2024).

Figure 2.11: UHMW Wedgelets for Clyde Robot



Note. Reproduced as is from (Brown et al., 2024).

Figure 2.12: Aluminum Wheel Hubs for Clyde Robot

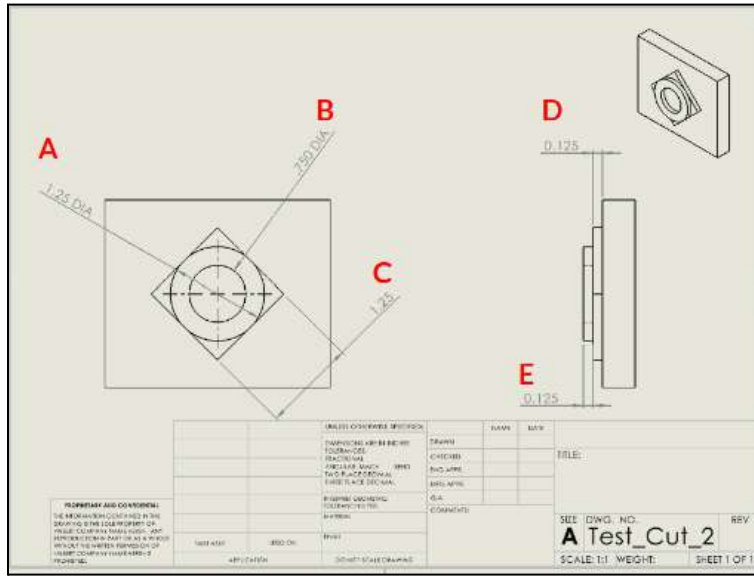


Note. Reproduced as is from (Brown et al., 2024).

2.8.2 2024-2025 Machining Testing

To further understand the machining capability, the 2024-2025 team redesigned the previously established standardized test part. As shown in Figure 2.13, the part possesses both a circular and square extrusion. As with the previous test part, the square extrusion is rotated 90° from the horizontal, with each of its four sides tangent to the circular extrusion. Utilizing Fusion360, a toolpath and CAM file were made for this part, and would only vary based on the speeds and feeds required for machining the stock material. Thus allowing for an accurate measurement of machine repeatability and tolerancing for varying materials.

Figure 2.13: Solidworks Drawing of 2024-2025 Test Part



The team was able to complete test parts machining wood, teflon, and aluminum.

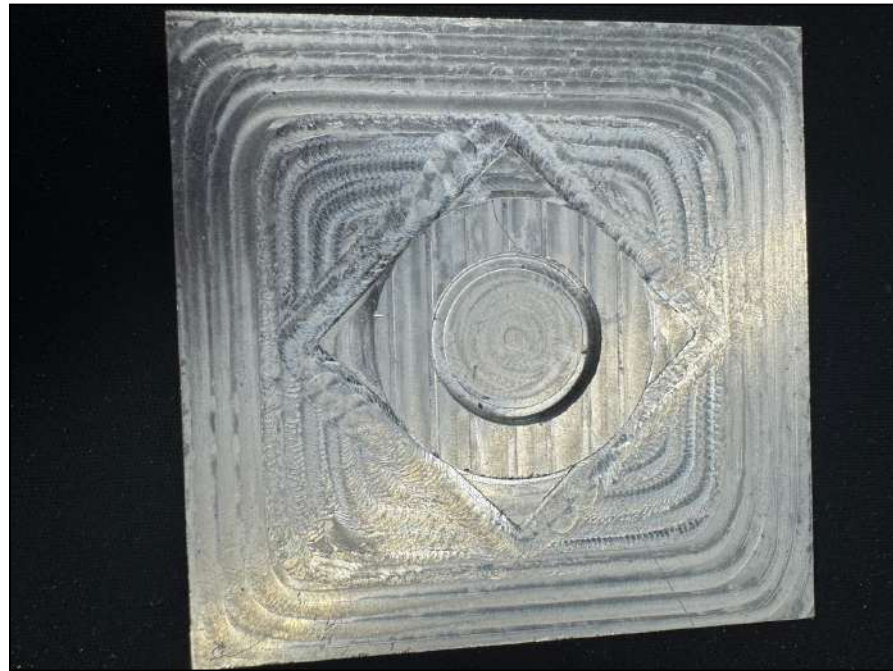
Upon completion of each part, measurements were taken and recorded into a table, as shown in Table 2.1, with all respective spindle speeds, feeds, and depths of cut. The table also provides the values of the measured dimensions and reports them as a result from the nominal desired dimension; A represents the OD of the circular extrusion, B is the ID of the circular extrusion, C is the desired value for each side of the square extrusion, while D and E are the heights for the square and circular extrusions respectively. All parts struggled to attain the desired tolerancing ($\pm 0.005"$) for the outer diameter of the circular extrusion. Nevertheless, the measured values for the other dimensions were relatively close to nominal or just outside of the tolerancing goal. Both the wood and teflon parts finished their respective operations with no issues; however the team noted the large chip buildup and subsequent cleanup to ensure no debris found its way into the linear rails or ball screws.

Table 2.1: Tolerances of Machined Test Parts

Material	Spindle Speed (RPM)	Feed (IPM)	Depth of Cut	A (From Nominal)	B (From Nominal)	C (From Nominal)	D (From Nominal)	E (From Nominal)
Wood	11460	458.4	0.010	-0.013	0.005	-0.005	0.000	-0.003
Teflon	7640	192.528	0.010	-0.017	0.010	-0.005	-0.001	-0.002
Aluminum	17572	351.44	0.005	-0.015	0.000	-0.006	-0.001	-0.001
Aluminum	17572	351.44	0.010	Failed	Failed	Failed	Failed	Failed
Aluminum	17572	351.44	0.005	-0.013	0.002	-0.001	0.005	0.003

The aluminum part runs offered the largest challenge in terms of machining. With an acceptable first run of aluminum, the team decided to increase the depth of cut from 0.005" to 0.010". After initial facing passes, the vibration and sound from the work area required the team to stop the test. The team decided to run the test again, but a lack of coolant and increased tool temperatures resulted in chips welding to the end mill. Although the part met tolerancing standards, the wavy and poor finish made it evident that heat generation can prove to be an issue (Figure 2.14).

Figure 2.14: Example of Machined Part Subject to Heat Generation



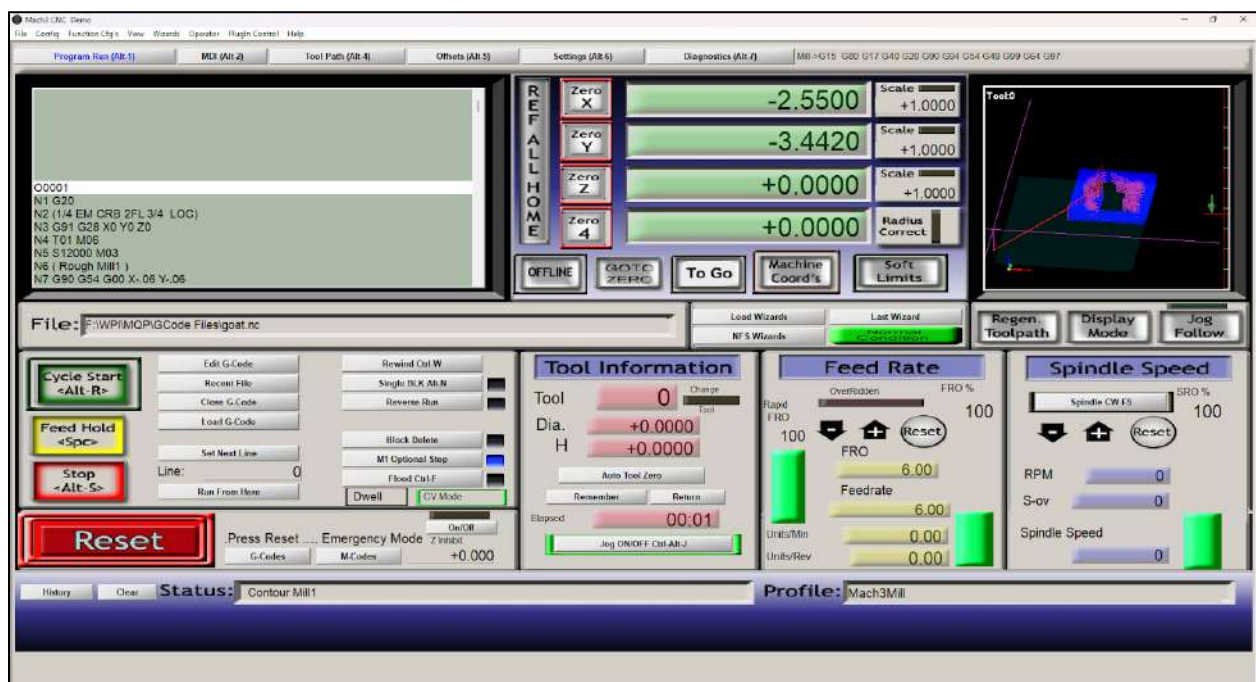
Note. Poor finish noted on the final pass located just outside of the square extrusion.

2.9 Control Software for 2023-2024 CNC Mill

The 2023-2024 MQP team used Mach3 in order to run the machine. This was their software of choice as it was “the cheapest license to purchase” and compatible with the CNC control board that was purchased (Brown et al., 2024, p. 77). Mach3 is a \$175 control software that is used by many machinists and hobbyists (*Mach Mach3*, n.d.). Last year’s team used the software on a Windows 10 laptop, connecting to the control board through a USB connection. This enabled the machine to actuate all three axes, receive input from axes limit switches, and configure setup for operating G-code files. With the software being created in 2001, the user interface (Figure 2.15) of the software had not been updated to today’s standards for UI (*Mach About Us*, n.d.). The 2024-2025 team had experience using this machining software, allowing for a seamless transition for a rather challenging software.

However, it was noted that the software should be changed as the various tabs and programming issues delayed their progress in regards to machine testing (Brown et al., 2024, p. 77). In addition to the concerns with an outdated and complex interface, Mach3 runs into errors when a program is stopped and then started again as discussed in the issues when the team machined UHMW wedgelets (Brown et al., 2024, p. 88).

Figure 2.15: Main Mach3 User Interface with Loaded G-code File



This chapter explored the previous work of the 2023-2024 Desktop CNC Mini-Mill team. It highlighted and discussed key points within their report, as well as addressing their future recommendations. In addition, this chapter reviewed the previous design of the enclosure, the CAD assembly, their software selection, and their efforts to limit vibration and noise. Lastly, it discussed testing of the 2023-2024 machine conducted by the 2024-2025 team in regards to machining capabilities and rigidity of the gantry.

3.0 Goals for this MQP

The higher-order goals of this project were to further expand on a previously built desktop milling machine and incorporate a tool changer, 4th-axis functionality, open-source software, bed leveling, chip evacuation, and a leak-proof enclosure. Additionally, this project aimed to initiate the process of becoming a part of the WPI manufacturing engineering course curriculum and be available in the MME MQP Workspace.

3.1 Tool Changer

One of the project's additions was the implementation of an automatic tool changer. Implementing a tool changer would significantly boost the number of tools usable on one part and enhance mechanical efficiency during milling by eliminating the need to frequently switch parts. With the current spindle in the machine, the tool changer needs to be torque-based to perform a tool change. This also means that a solution to prevent the collet nut from spinning had to be found that would be compact, occupying the least amount of work area possible, while also being strong enough to withstand the force of a spindle turning at approximately 2,000 RPM. The development of a tool changer significantly decreases the time spent not milling and allows the user to switch freely between different end mills. In addition to a tool changer, a dust cover, and a misalignment laser sensor are installed to protect the tools from debris and ensure the nut is tightened correctly onto the spindle.

3.2 4th-Axis

With implementation of add-on functionality in mind, another goal was the addition of a 4th-axis. As it stands, the rudimentary 3-axis machine is capable of only machining a

certain range of parts as a result of its spindle reach. Implementation of a 4th-axis system with 360 degree of rotation allows for more complex, and rounded, geometries not capable within the standard 3-axis machine. With this in mind, the goal was to provide an assembly that was both user friendly and cost efficient. System integration, like all other added functionality for this project, needed to contain the ability for novice users to understand and go through the installation process.

3.3 User-Friendly and Open-Source Software

Another goal of the project was to implement user-friendly and open-source software. This means that a new or novice user to CNC mills should be able to easily and quickly run a part once they have the G-code file from their choice of CAM and CAD software. The control software and firmware should also be open-source to align with the spirit of the project. An advantage of having open-source UI control software and hardware firmware is that the software can be modified as needed to suit every goal of the project. This allows the machine to have features common to the control software/firmware, but to also add custom features such as an automatic tool changer, a 4th-axis, and almost any other feature imaginable. The chosen software should be more user friendly than last year's software solution, while still providing the same essential features with none of the cost.

3.4 Bed Leveling

Fixturing a part such that it is perpendicular to the machine's x-, y-, and z-axes is critical to ensuring that a CNC mill can machine a part within acceptable tolerances. Furthermore, the other additional functionalities being added to the machine must also be perpendicular to the x-, y-, and z-axes to ensure they function properly. For example, the

4th-axis must rotate the part in such a way that after a 180° turn, milling two opposing flats result in parallel planes. Additionally, the tool changer must hold the tools normal to the x-y plane, such that the tool and collet nut will engage properly. Because of these requirements, it was determined that the ability to level the bed must be added to the machine.

The acceptable degree to which the bed must be level is determined by the goal of milling a piece within 0.005". If the difference in height (the z-direction) of the bed surface from one limit switch to the other in both the x- and y-directions were under 0.005", then the machine would theoretically be able to maintain the goal for repeatability when milling a flat surface with respect to the z-direction. Therefore, the goal for bed leveling was to be able to adjust the plate at each corner with an accuracy of +/- 0.0025", allowing for a maximum variance of 0.005" in the z-direction for a part that is the size of the reachable work area.

3.5 Upgraded Enclosure

Ensuring user safety during the machining process is of the utmost importance. Per OSHA regulated safety standards, milling machines require guarding that prevents any area of contact between the work area and the user during operation. Thus, it was critical that all guarding for the enclosure would be able to withstand any impact from a projectile, and the framing to endure any forces from an external source. This also required the enclosure to effectively retain all chips produced during machining as they can be high-speed projectiles. Furthermore, the enclosure must have the capability to withstand any type of spraying from a coolant system as to not damage electronics or create hazardous work conditions.

3.6 Chip Evacuation

Maintaining a clean work area is vital to maintaining dimensional tolerances and smooth surface finishes. Excess chips in the work area can be recut, causing an increase in chip load experienced by the cutting tool. This worsens the tool wear causing dimensional inaccuracies and heightens the chance for the tool to break. Uncleaned chips and dust can find its way into the ball screws, stepper motors, and linear slides; which can create wear and poor dimensional tolerancing. Therefore, this machine must allow for the implementation of a vacuum and coolant system. The vacuum system must not interfere with the machining process, but have the capability to efficiently remove chips from the work area. The coolant system must not only be able to remove chips, but also effectively limit the tool from reaching high temperatures.

3.7 Tolerance

A tolerancing value of $+/- 0.005"$ was determined to be the achievable standard. This value was chosen based upon a comparison of Desktop CNC Milling machines on the market and general machining standards explored in previous sections. This tolerancing ensures that the machine can repeatedly produce parts with proper sizing, allowing the manufactured parts to function in the way they were designed in CAD.

3.8 Safety

The machine must be able to abide by both WPI and the Occupational Safety and Health Administration (OSHA)'s safety standards. Safety features such as a door latch should be implemented to reinforce the concept of maintaining a barrier between the operator and cutting tool. This coincides with the usage of a functional E-stop button, allowing the user to completely stop the machine in unsafe or uncertain conditions. The

implementation of functional limit switches must be used to guarantee the cutting tool does not travel outside the machine's capabilities. A lighting indication system must provide users a quick visual cue of the operating status of the machine. Ultimately, incorporating a safety procedure that ensures risk-free maintenance conditions with electrical components such as a lockout-tagout (LOTO).

3.9 Summary of Goals and Specifications

The table below highlights the measurable goals described in the text above. These goals placed quantitative values on specific tasks set at the beginning of the academic year.

Table 3.1: Goals and Measurable Targets

Goal	Measurable Target
Affordability	Provide a base model price under \$2500 and \$4500 with all add-ons
Accuracy	Maintain a machine tolerance +/- 0.005" for plastic parts and +/- 0.010" for metals
4th-axis	Develop a user-friendly model utilizing a rotary 4th-axis kit with 360° rotation
Chip Evacuation	Reduce chip buildup in the work area and cutting tool path
Tool Changer	Allow for 3-tool active rotation with automatic z-axis probing
Bed Leveling	Develop work-plate leveling within 0.0025"
Enclosure	Maintain a safe barrier between operator and work area while ensuring chips and coolant remain in the enclosure
Safety	Implement features such as an E-stop button, stack light, and a door latch and sensor to ensure user safety during operation
Ease of Manufacture	Create the machine with the use of only a 3D printer, drill press, bandsaw, and hand tools
Control	Support custom features, free and open-source software, OS compatible

Goal	Measurable Target
System	software, and integrate with previous control electronics
Vibration	Reduce the amplitude of static vibrations from the initial mill to the improved mill by a minimum of 25%

This chapter explored the goals set by the 2024-2025 team pertaining to additional functionality, improving the enclosure, maintaining precision during machining, and ensuring user safety during operation.

4.0 Project Timeline

Upon finalizing the project goals the team determined to utilize a Gantt chart to map out the tasks and respective due dates. This chart takes into consideration the four-term system used by WPI. The project was broken down into four main aspects, as described in Chapter 5. The majority of design and testing work was to be completed in the first quarter of the year. The second and third quarters were to be dedicated to the overall manufacturing and production of the mini-mill. This resulted in the testing and verification of the machine and its subsystems to be completed during the last quarter.

Table 4.1: Gantt Chart

Main Task	Sub Task	A Term					B Term								C Term								D Term								
		1	2	3	4	5	1	2	3	4	5	6	7	8	1	2	3	4	5	6	7	8	1	2	3	4	5	6	7	8	
Background Research																															
Read the previous MQP report																															
Complete all user and safety trainings																															
Specify measurable goals																															
Research similar products/projects																															
- Framing/Guarding/Vacuum/Coolant																															
- Vibrations/Softwares/Electrical																															
- Work-area/tool changer																															
Health and safety																															
- OSHA Regulations																															
- WPI health and safety																															
Literature Review																															
- Read other documentation																															
- Assess what was done last year																															
Design and Mathematical Validation																															
Come up with a list of safety precautions																															
- Pertaining to each design for each team																															
Risk Analysis / FMEA																															
Budget components																															
Finalize Bed Leveling Design & Components																															
Fix CAD Assembly																															
Finalize Coolant Method																															
Model Ideas in CAD (New parts)																															
- Coolant System																															
- Vacuum System																															
- Enclosure/Guarding																															
- Electronics																															
- Bed System																															
- Tool Change System																															
- 4th axis																															
Come up with a list of sensors/components																															
Determine CNC Software																															
Vibration simulation/calculation																															
Vacuum System Design																															
Enclosure and Guarding Design																															
Finalize Integrated CAD Design																															
- Combine different CADs																															
Conduct Design Review																															
Manufacturing and Assembly																															
Have First Machine Modified/Built																															
Have Second Machine Built																															
Testing and Validation																															
Electrical Test Validation																															
Test ease of use of software with other team members																															
Testing Machine 1																															
Testing Machine 2																															
WPI Student Testing																															

The content within this chapter provided an insight into the team's timeline for completing the required goals.

5.0 Methodology

The content in this section outlines the team's plan to complete the project goals set out at the beginning of the 2024-2025 WPI Academic Year.

5.1 Inter-Team Dependencies

During the course of the project, the work was divided between 11 individuals working on separate subsections of the project. Subteam 1 was composed of James C., Andrew P., Daniel P., and JR T.. The primary objectives of this team were to redesign the enclosure to properly function with a chip evacuation system and satisfy OSHA and WPI EHS safety protocol. Subteam 2 was composed of Echo B., Camren C., Perrin K., and Michael P.. Their primary tasks were to analyze the CNC mills, implement user-friendly software, integrate electrical safety systems, append new sensors, and design mechanical bed leveling. Subteam 3 was composed of Rafael C., Michael D., and Dante U.. Their primary tasks were to implement the additional functionalities of the 4th-axis, tool changer, and milling of the new work area plate.

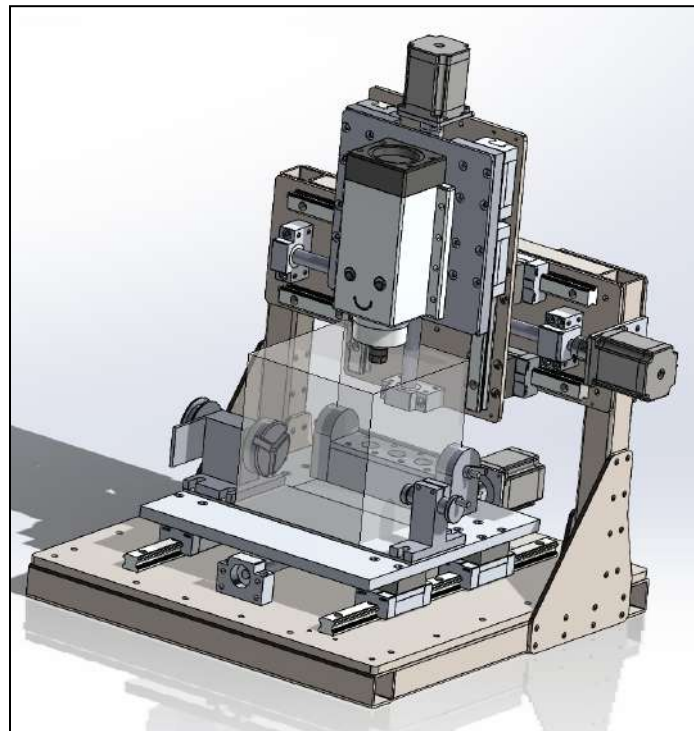
5.2 Design

To ensure a seamless transition between CAD modeling and physical assembly, a significant amount of time was allotted to the design of the mechanical components. The team had overhauled the reworking of the previous CAD assembly to accurately represent the machine's current configuration. In doing so, the team had effectively established a base for which all future iterations and design changes can branch from. With this, it became possible to work through design iterations for the enclosure, manual bed leveling, 4th-axis, and tool changer that all built upon the original assembly. All components pertaining to the

work area expanded upon the work area plate, taking into consideration the maximum machinable area. Moreover, the fasteners would need to be standardized to all have the same thread size, because this would reduce unneeded complexity in the design. As such, the enclosure area was accurately gauged and thus properly built around the work area.

This process of creating a visual of the reachable work area within CAD was critical to ensure that all the fixturing components, tool changer, and 4th-axis could be integrated together properly within the allowable space (Figure 5.1). This step was also imperative to successfully place the mounting holes on the bed where those components would be installed. The process of producing the mounting hole locations is discussed further in Section 7.6.

Figure 5.1: *Machinable Area*



Note. Image showing a transparent box that the tool can reach.

In order to evaluate the continuous state of the machine, a sensor suite was designed to measure pertinent information. This would save the machine status for later analysis and verification. To get the machine to work with the new intended features, the software was designed to extend the base functionality while adding new proposed features. Further details regarding the design of the machine and both mechanical and electrical subsystems can be found in Chapters 6, 7, and 8.

5.3 Testing

Determining a set of procedures to examine the capabilities and operating conditions of the previous team's design was of high importance. It was critical to gather data relating to the motor temperature, vibrations within the system, and the overall tolerancing of machined components. In doing this, baseline values were obtained to then use as a comparison after any changes had been implemented. To verify that any changes to the machine were beneficial, the numbers obtained during testing were required to be of similar or better standing. Testing procedures for mechanical, electrical, and software components can be found in Chapters 9 and 10 respectively.

5.4 Implementation

Upon creating an accurate CAD model and establishing the current standing of the machine, modifications and changes were made. In the scope of satisfying the project requirements, Subteams 1 and 3 had allocated large amounts of time to manually manufacturing and assembling components pertaining to the gantry, enclosure, 4th-axis, and tool changer. Due to the team's dedication to a comprehensive CAD design, implementation was completed with minimal obstacles and subsequent iterations. For the electrical systems, the control system had to be swapped out and troubleshooted, since no team members had

previous experience with the system. New and unexpected issues came up continuously through use, but were solved shortly afterwards. An in depth explanation of the electrical, mechanical and safety feature implementation can be found in Chapter 11.

5.5 Verification

All additional components were subjected to verification testing for functionality. The enclosure was tested to ensure its capability to provide a barrier between the operator and the work area. It was also evaluated on its ability to contain chips and coolant during machining operations. The chip evacuation system used surface finish as a gauge on its overall effectiveness during operation. The gantry was also tested to ensure forces acting until it did not cause inaccuracy in spindle location.

To verify the machine electrically, each safety system was tested under multiple conditions to ensure they functioned properly. During rigorous use and extreme circumstances, the system was deemed to be safe and would not work if any of the critical safety systems failed. To verify the machine through software, the systems were simulated and debugged as much as possible before implementing and iterating them into the physical machines. After running multiple parts, the machine state during the operations was analyzed and compared against the initial state of the machine, indicating areas of improvements and areas that still need work.

This chapter discussed the methodology used by the 2024-2025 MQP team to achieve the goals stated in Chapter 3.0. Chapter 5 lays the groundwork for how tasks were distributed throughout the group, referencing the inter-team dependencies. Furthermore, it discussed the step-by-step method taken by the team. Starting with a CAD assembly, the modified components were designed. Next, procedures were created to evaluate the

operating conditions of the previous machine, allowing a comparison of results after the new mini-mills were built. Following this, implementation of the modified features were applied and verified to compare against the status of the 2023-2024 machine. Results and in-depth analysis for the verification of changes can be found Chapters 12 and 13 respectively.

6.0 Literature Review

The content in this section outlines research done by the 2024-2025 MQP team before modifying the initial CNC machine.

6.1 CNC Enclosures

The purpose of the enclosure around a CNC milling machine is for chips/dust containment, coolant leaks prevention, and noise abatement. It is important that the chips from the machining process and the coolant being sprayed on the end mill stay within the enclosure per OSHA regulations (*1910.212 - General Requirements for All Machines*. | *Occupational Safety and Health Administration*, n.d.). As for the noise during the milling operation, OSHA states that a hearing conservation program is required if the noise level is over 85 dBA over an eight hour workday (*Occupational Noise Exposure - Overview* | *Occupational Safety and Health Administration*, n.d.). Thus, many small desktop CNC machines in the market come with a pre-built enclosure around the work area.

Both of the two desktop CNC machines mentioned previously in Section 1.1 have enclosures made specifically for the machine with transportation and a compact footprint in mind. However, that also means the cost of these machines are fairly high; the Bantam Tools Desktop CNC Milling Machine costs \$6,999 while the Nomad 3 costs \$2,800. While it would have been ideal to have an enclosure similar to other desktop CNC machines, the goal of the make a machine with a budget of \$2,500, so making an enclosure similar in design to the other machines in the market was impossible. For example, the Bantam Tools CNC has a fully enclosed enclosure made of powder-coated steel frame with safety interlocks (*Bantam Tools Desktop CNC Milling Machine*, n.d.).

Although the previous enclosure design had some issues, the utilization of t-slotted extrusion was a major success (reference Section 7.7). These cost-effective components were used to frame the entirety of the enclosure. They are coated aluminum extrusions typically used for structural designs in the construction industry (*8020 Aluminum Extrusions - Buy 80/20 Aluminum at Zetwerk*, n.d.). The cross-sectional design of t-rails allows it the benefit of being modular in the ways that it can be assembled. Its utility allows it to be compatible with panels, doors, hinges, linear movements, and handles, allowing it to be used for a multitude of enclosure applications (*8020 Aluminum Extrusions - Buy 80/20 Aluminum at Zetwerk*, n.d.). To ensure strength and security with the design of an enclosure, it can be used with brackets, corner cubes, and gaskets for slot sealings. These extrusions have high thermal conductivity, high mechanical properties, and strength (*8020 Aluminum Extrusions - Buy 80/20 Aluminum at Zetwerk*, n.d.). It also has high corrosion resistance, extremely important because coolant will be used inside the new enclosure (*Advantages of T Slot Aluminum Extrusions*, n.d.). A t-rail can have between one and four slots in the extrusion. The name of the t-rail depends on the width and height, so a 45 mm t-rail signifies it is 45 mm x 45 mm, and when ordering from a manufacturing website, extrusion length is determined by the customer (Figure 2.1). The structural and mechanical advantages, plus the corrosion resistance made the team confident in their selection of using t-slotted framing.

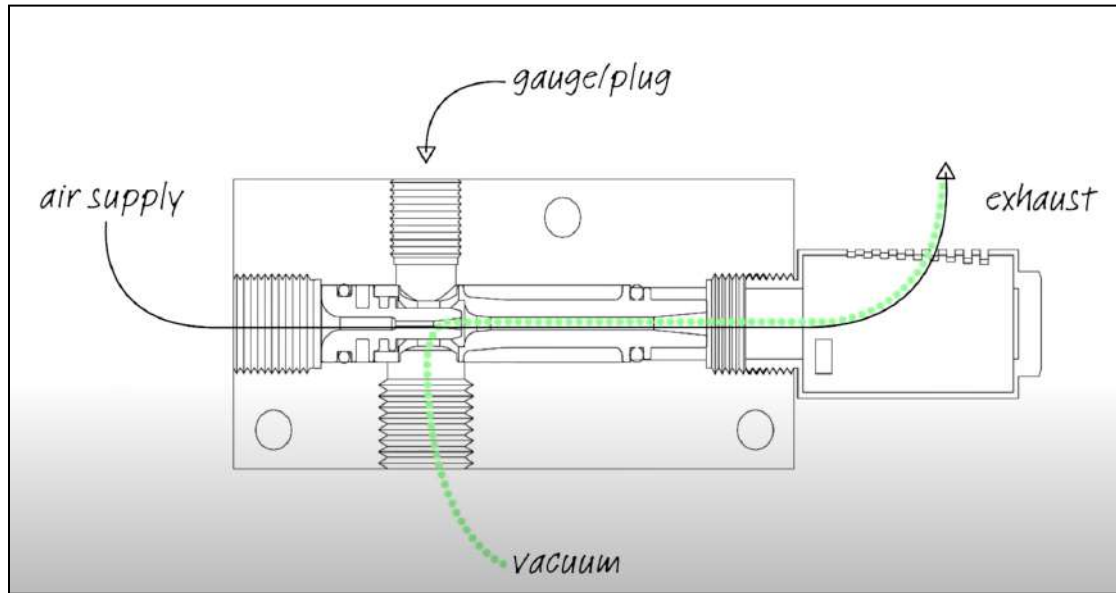
As for the guarding of the machine, when comparing polycarbonate that last year's team used to glass and other plastics, it has a notably high impact strength, transparency, and resistance to corrosion (British Plastics Federation, n.d.). Its high transparency, low weight, and impact resistance make this type of plastic a common solution to safety guarding. With these advantages, there was no reason to switch to another type of guarding material.

6.2 Vacuum System

Chips are a common byproduct of CNC machining. During the machining process, the end mill of the machine shears off the excess material from the workpiece to create a desired shape. Although these chips are contained within the enclosure of the milling machine, they can sometimes be difficult to remove after the milling operation. It is important to at least remove them from the work area after each operation to avoid them getting in the linear rails or stepper motors, as well as reduce the chip load on the cutting tool. The easiest way to remove chips from the work area would be to use a vacuum or a dust blower. The size of the vacuum hose is not an issue with many large commercial CNC machines due to their size, but poses a unique obstacle for the current desktop machine. With limited space around the gantry of the machine such as the sides, back, and under the bed plate, these gaps would make it difficult to remove chips from these areas afterward.

The initial vacuum system design based on our research was to utilize a venturi pump that was connected to a cyclonic separator. A venturi pump is a type of pump where compressed air flows through the venturi nozzle, causing the accelerated air inside the pump to spread, creating a vacuum (*Venturi Pump*, n.d.). Air from the surrounding is then drawn in through the vacuum port of the pump, which escapes through the exhaust port afterwards (Figure 6.1).

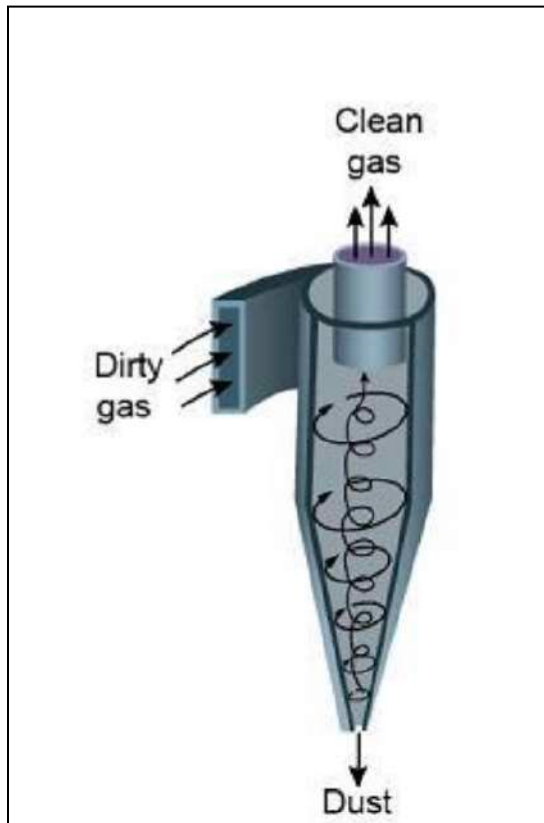
Figure 6.1: Venturi Pump Schematic



Note. Reproduced as is from IMI Bimba (IMI Bimba, 2019).

The next vacuum design researched by the 2024-2025 MQP team was a cyclonic separator. Cyclonic separators, according to *Design and Fabrication of Cyclone Separator* written by Kashan Bahir, are centrifugal separators consisting of an upper cylindrical part referred to as the barrel and lower conical part referred to as the cone (Figure 6.2). It was explained that the separator works by transforming the inertia force of gas particle flows to centrifugal force by the vortex generated in the body of the separator. The increase in velocity in the outer vortex results in a centrifugal force acting on the particles, which separates them from the air steam entering through the inlet. Once the air reaches the bottom of the cone, the clean air radially flows inwards and out the top of the cone, while the particles/dust falls to the collection bin at the bottom (Bashir, 2015). After this research, the team conducted testing with this design (reference Section 7.1).

Figure 6.2: Cyclonic Separator



Note. Reproduced as is from (*Cyclonic Pressure Drop.Pdf*, n.d.).

6.3 Coolant System

Cooling is a vital part of modern CNC practices that enhances cutting tool life, part surface finish, and accuracy (Reddy et al., 2020). As suggested by the name, the cooling liquid reduces the temperature of the cutting tool to normalized temperatures to allow for a greater controlled process. In order to prevent melting the workpiece or damaging the cutting tool, coolant must be added to most turning and milling processes.

According to Secotools, typical successful metal cutting operations see 10% of heat flow through the workpiece, 10% through the tool, and the remaining 80% flow through the chips (*Managing Thermal Loads in Milling Processes | Secotools.Com*, n.d.). To ensure that

the majority of heat flows through the chips and not to the workpiece or cutting tool, proper coolant must be applied. There are various ways in which coolant can be applied, and it does not always have to be in a liquid form. Depending on which material is being cut and what the cutting tool is, different coolant applications are applicable. According to an article published in 2017 there are roughly eight lubrication and cooling systems, with the ones closest in relevance to this project being flood, gaseous cooling (compressed air), and mist (Benedicto et al., 2017). These are the four coolant systems in contention for this project.

Flood cooling involves providing the work area with continuous fluid. This system needs a number of components to operate, such as filters and recirculation systems (Benedicto E. et al., 2017). Additionally, this process uses a large amount of fluid and requires a clean-up time post operation. However, this is the best system for significantly increasing material removal rate (Irani et al., 2005).

Compressed air is a prime example of compressed cooling (Benedicto E. et al., 2017). This system requires a source of compressed air, such as an air compressor or a shop air line. While this system does not reduce temperatures at the rate of flood coolant, it does require the least amount of post processing clean-up.

Mist coolant, or minimum quantity lubrication, includes introducing air to a stream of coolant to apply a fine mist to the work area (Wayken Rapid Manufacturing, 2021). Albeit this system is efficient at cooling down the cutting tool, it introduces significant individual health and safety ramifications if not operated properly. According to OSHA guidelines, “one way to reduce employee exposure to MWF aerosols is to install an exhaust ventilation system to prevent the accumulation or recirculation of airborne contaminants in the workplace” (*Metalworking Fluids - Metalworking Fluids: Safety and Health Best*

Practices Manual | Occupational Safety and Health Administration, n.d.). Adding a ventilation system would greatly increase the anticipated budget of this project and is something not aligned with the goals of this project.

Initially the team wanted to use both air and flood cooling for the machine. Coupling air cooling with a vacuum system will provide significant clean-up reduction and increase chip clearout when flood coolant is not needed. However, with the limited time and budget that were given, it was only possible to implement air coolant in the current machine. Thus, in order to greatly increase our flood coolant system, design changes were made to maximize coolant retention in the machine (reference Section 7.7.3).

6.4 Vibration in CNC Milling

Many aspects related to CNC milling machine design play into machine vibration, including weight and structure which were briefly covered in Section 2.5. The most prevalent area of machine vibration is when it comes to chatter, which is the main form of destructive vibration in the machining process. Chatter is self-excited vibrations brought about by the machine and tool resonance, it is also highly dependent on the machining parameters used for the given workpiece materials and tools (González & Ferreira, 2016). Chatter is destructive to the machine and the workpiece as it reduces tool life and reduces the quality of the final part as it can decrease the precision and lead to rough surface finishes (Kasprowiak et al., 2022).

The conducted literature review explored closed and open frame designs for CNC milling machines for structural rigidity. The frame refers to the gantry structure and how the spindle is supported and mounted. Open frame milling machines are often seen in small scale machines however their asymmetrical design involving an overhung spindle creates

undesired bending. Closed frame CNC milling machines involve a structural loop and are symmetric. This requires more material but this makes the machine more structurally stable, increases stiffness, and therefore reduces deflections (Wei, 2013; Rastvorova & Klyucherev, 2021).

The material making up the machine components is also key, for structural components materials with high rigidity should be used. Additionally, using a heavy material for the frame will help to reduce vibrations as higher mass items vibrate at lower frequencies. A method that can be used to increase machine weight as a way to passively damp vibrations with machine structure is to fill cavities of the machine with sand or concrete. This method was discussed in Section 2.5 as it was explored by the 2023-2024 MQP team as part of the literature review. The machine is being designed for small scale operations, therefore increasing the machine weight by filling cavities is not reasonable.

There are two main methods of damping vibrations in CNC machining: passive damping and active damping. Both passive damping and active damping methods were explored for application into the machine design however passive damping was the most feasible for these machines and with the scale of the project. Passive solutions do not generate force and there is no control system that changes the operating parameters; built in vibration dampers on cutting tools are often proposed as a solution for passively damping vibrations (Kasprowiak et al., 2022). Tuned mass dampers can be implemented with cutting tools, these devices are tuned to resonate out of phase with the unwanted vibrations (Groll, 2018). Although mass dampers are effective at reducing unwanted vibrations, to remain in line with overall project goals implementing a mass damper was not a feasible solution for this machine.

Active damping is the most effective form of damping involving real time monitoring, feedback, and active control to adjust machining to avoid undesirable effects (Kasprowiak et al., 2022). Some methods include input shaping control, which uses data collected through sensors and a program to update the operation so that vibrations are addressed as they are created. Active damping solutions are most common in the laboratory sphere as advancements are being made with adaptive algorithms, artificial intelligence, and digital filters. These applications are much more customizable than passive damping and can achieve excellent results but active damping is entirely unfeasible for this project (Kasprowiak et al., 2022).

Damping solutions implemented by increasing the weight and the rigidity of the machine in the area of design, were done well with the machine design of the previous MQP as discussed in Section 2.5. These implements were not changed with the gantry design. Some vibration damping methods can be used during individual machining processes and adjusted by the operator to reduce vibrations. Vibration damping is individual to the machine and processes, for an individual machine a series of testing can be done to determine parameters known as stability lobes. This involves testing cutting parameters and completing calculations to find the specific parameters that allow for a high material removal rate without creating chatter. Feed, speed, and depth of cut are all parameters tested using different tools and materials to determine what produces the best result possible (González & Ferreira, 2016). Once the stability lobe parameters are found they can be implemented into the CAM.

6.5 CNC Automatic Tool Changer

Tool changers are designed to shorten production times while maintaining the precision and quality of milled parts. Automatic Tool Changers (ATCs) facilitate the swapping of an end mill in a CNC spindle without any manual handling by the user. An ATC typically includes a tool magazine, base, clamping arm, and carrier arm (ShopSabre, 2021). To initiate a tool change, the machine receives a command from a computer. The tool designated for change remains in a fixed position to allow the end mills to swap. The spindle moves to retrieve the tool, and the z-axis shifts towards the carrier arm for the pickup. During this process, the spindle either opens or closes the chuck to replace the tool before reverting to its initial state (Obreja et al., 2013).

Various models of tool changers exist: carousel ATCs, linear ATCs, robotic arm ATCs, and chain track ATCs (TAICNC, 2023). Automatic tool changers require specific CNC spindles that utilize compressed air for tool switching. The spindle model used in this machine, the HLTNC 110 Volt Spindle Motor, does not operate with compressed air. Instead, the user must manually tighten the collet nut to attach an end mill. Automatic attachment of a new tool to the spindle is only feasible through torque. Although ATCs are rare for spindles not utilizing compressed air, one variant, the RapidChange ATC (Figure 6.3), has been developed (RapidChange ATC, n.d.).

Figure 6.3: RapidChange ATC Four Tool Slot Model



Note. RapidChange ATC with four tool slots (reproduced as is from *Speeds and Feeds – RapidChange ATC*, n.d.).

RapidChange ATC is a tool changer that leverages the spindle motor's rotational motion and torque for changing tools. The process is similar to that of conventional tool changers: initially, the spindle moves to the x-axis where the tool slot is, followed by plunging into the pocket at approximately 2,000 RPM (Figure 6.4), engaging with a collet nut and end mill. Inside the pocket, a clip holds three 3/16" ball bearings that act as stoppers for the nut, preventing it from rotating during unloading or while securing a tool. When the spindle touches the nut's threads, the nut begins to rotate at the spindle's RPM. After making contact, the motor stalls (Figure 6.5), enabling the nut to tighten against the spindle through its motion. Once secured, the spindle rotates in reverse, lifting the tool upward (Figure 6.6).

Figure 6.4: Spindle Coming Down on the Collet Nut in the RapidChange ATC at 2,000

RPM



Note. Reproduced as if from (*Speeds and Feeds – RapidChange ATC*, n.d.).

Figure 6.5: Spindle Stalling After Attaching to the Collet Nut



Note. Reproduced as is from (*Speeds and Feeds – RapidChange ATC*, n.d.).

Figure 6.6: Collet Nut and End Mill Attached to the Spindle After the Tool Change



Note. Reproduced as is from (*Speeds and Feeds – RapidChange ATC*, n.d.).

To unload the tool, the spindle plunges back into the pocket at around 2,000 RPM (Figure 6.7), contacting the ball bearings, which allows the nut to engage them and stop spinning (Figure 6.8). Once the nut connects with the ball bearings and halts (Figure 6.9), the spindle ascends while still rotating at 2,000 RPM, effectively unloading the tool (Figure 6.10).

Figure 6.7: Spindle Coming Down to Unload the Tool into the Rapidchange ATC



Note. Reproduced as is from (*Speeds and Feeds – RapidChange ATC*, n.d.).

Figure 6.8: Collet Nut Makes Contact with the Ball Bearings to Unload the Tool



Note. reproduced as is from (*Speeds and Feeds – RapidChange ATC*, n.d.).

Figure 6.9: Collet Nut Falls Deeper into the Pocket Twisting Off of the Spindle



Note. Reproduced as is from (*Speeds and Feeds – RapidChange ATC*, n.d.).

Figure 6.10: Spindle Comes Back up Which the Nut stays in the Pocket Attached to the Ball Bearings



Note. Reproduced as is from (*Speeds and Feeds – RapidChange ATC*, n.d.).

With this design concept in view, the team contacted Don Greilick, the owner of RapidChange ATC, to gather insights about each component and the specific elements. Majority of the product is made from Acrylonitrile Butadiene Styrene (ABS) plastic, with the main body constructed from High-Density Polyethylene (HDPE). Along with the materials, a spring is located beneath the clip, enabling it to return to its original position after tool changes. In addition to understanding the tool-changing functions, the team gained insights into the dust cover mechanism. Crafted from clear vinyl (Figure 6.12), it is designed to cover the tool changer and is operated by two NEMA 17 stepper motors (Figure 6.11), which open during tool changes and close when not in use. Moreover, the RapidChange ATC includes a breaker beam that employs Infrared Proximity Sensors to ensure the nut is securely fastened to the spindle.

Figure 6.11: *NEMA 17 Stepper Motor used in RapidChange ATC*



Note. Reproduced as is from (*Amazon.Com: STEPPERONLINE Short Body Nema 17 Bipolar Stepper Motor*, n.d.).

Figure 6.12: Picture of Rapidchange ATC with Vinyl Dust Cover



Note. Reproduced as is from (RapidChange ATC, n.d.).

While the RapidChange ATC system was an easy plug-and-go system, the team wished to modify the system by making it smaller, more cost-effective, and redesigning the dust cover to be more rigid.

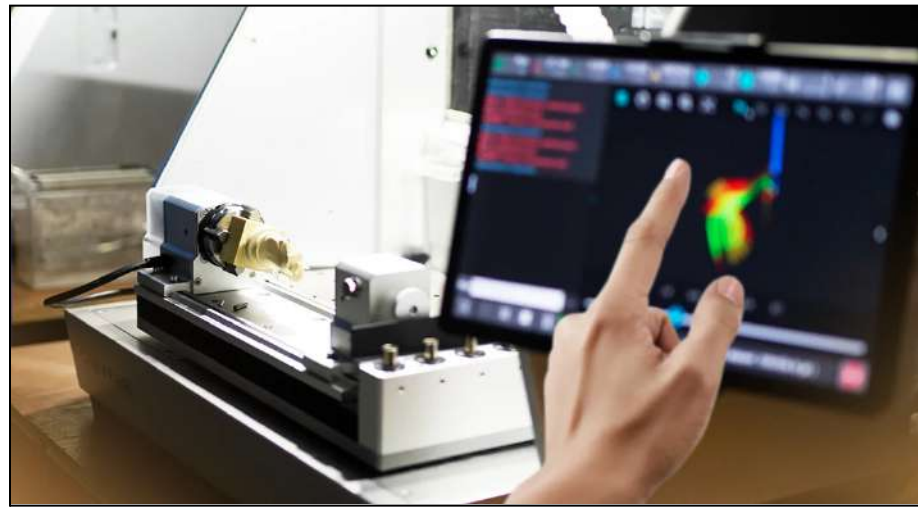
6.6 4th-Axis

Traditional CNC milling machines, many times, have the ability to integrate a 4th-axis add-on. These systems take the place of a vise as the main form of clamping for the milled stock. Similar to a lathe, 4th-axis kits often contain a chuck and tailstock piece. Rounded pieces of stock are clamped into the chuck assembly, which drives the rotation of the part depending on the G and M code. Depending on the length of stock, a tailstock piece may be used on the side opposite the side clamped into the chuck to provide extra stability.

With the idea of open-source in mind, as well as ease of use, implementing a pre-built rotary kit was chosen as the best option moving forward for the 4th axis design.

One of the most popular cost-friendly desktop cnc machines, the Carvera, is known for its ability to incorporate add-on functionality (Figure 6.13). The base design of the machine, capable of 3-axis simple routing operations, utilizes add-on features to provide users the ability to mill more advanced parts.

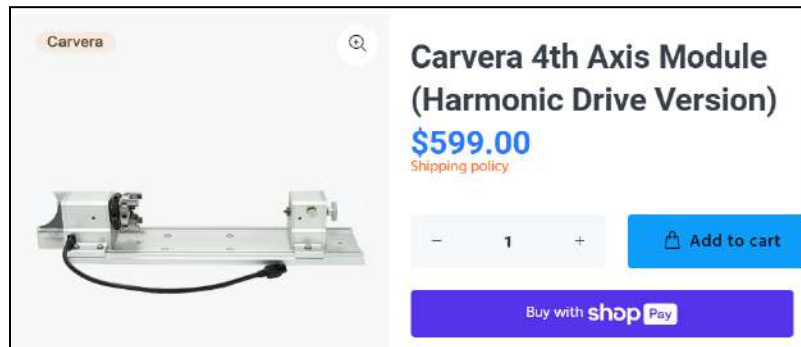
Figure 6.13: Picture of Carvera 4th-axis Module



Note. Reproduced as is from (*Carvera 4th Axis Module (Harmonic Drive Version)*, n.d.).

Although these kits can be robust and allow for much more complex milling operations, prices for these prebuilt kits can be very expensive. The 4th-axis module for the Carvera mini mill, as seen in Figure 6.14, can cost users over \$500.

Figure 6.14: Picture of Carvera 4th-axis Module in the Makera Shop



Note. reproduced as is from (*Carvera 4th Axis Module (Harmonic Drive Version)*, n.d.).

Similar add-on kits however can be purchased online through platforms like Amazon. Like their milling machine 4th-axis counterparts, the desktop cnc machine 4th-axis modules by and large contain a chuck driven by a motor and a support tailstock piece. Driven by a stepper motor (Figure 6.15), many of these systems offer users easy integration with current desktop CNC milling machines on the market.

Figure 6.15: Picture of Genmitsu 4th-axis Rotary Module Kit



Note. Reproduced as is from (Genmitsu 4th Axis Rotary Module for 4040 and 3030 Series CNC Machines with Planetary Geared Stepper Motor, 4 Jaw Chuck, Clamped Range 10-200mm - Amazon.Com, n.d.).

Table 6.1: Decision Matrix for 4th-axis Add-on Kits

	Weight (1-5)	Option 1	OP1 Weighted	Option 2	OP 2 Weighted	Option 3	OP3 Weighted
Compatibility							
Software Integration	4	3	12	3	12	3	12
Performance							
Speed Reducing Ratio	3	5	15	1	3	3	9
Motor Torque	2	1	2	1	2	3	6
Axis Travel Range	3	3	9	3	9	3	9
Ease of Use							
Setup Time	3	4	12	5	15	4	12
Cost							
Unit Price	5	4	20	3	15	3	15
Additional Costs	3	3	9	5	15	3	9
Flexibility							
Workspace Size	5	5	25	5	25	3	15
Safety							
Operator Safety	3	3	9	5	15	5	15
Leadtime							
Availability	1	5	5	4	4	5	5
TOTALS			118		115		107

With many kits available on the internet, a list was created with various 4th-axis kits. Many factors were taken into account such as price, overall size, motor type, wiring, and weight. After narrowing the list down to three options, a decision matrix, represented in Table 6.1, was used to decide the best fit for the project. Several factors were considered when considering the three kit options. The most important aspects of the desired kit were a low price, large clamping OD, and easy software integration. Using grading and aspect weights, the first option was chosen.

The chosen kit, referenced in Figure 6.16, contains a chuck and tailstock piece, set cables, as well as two wrenches to open and close the chuck jaws. The system in total with all components weighs approximately 5.33 lbs. Powered by a NEMA 17 2 phase stepper motor, the 3-jaw chuck attachment can rotate at 64 oz-in with a step angle of 1.8 degrees. The internal clamping diameter can hold a piece of stock anywhere between 0.0394" and 1.9685", reaching much of the spindle's workable area.

Figure 6.16: Picture of Changzhou Rattm 4th-axis Kit



Note. Reproduced as is from (CNC Milling Machine Rotational Axis CNC Router Rotary Table Rotary a Axis 4th Axis 65mm 3 Jaw Chuck Dividing Head w/ Nema17 Stepper Motor w/ 54mm Tailstock Reducing Ratio 4:1 for CNC Engraving Machine - Amazon.Com, n.d.).

With these aspects in mind, the next step is to identify a design that allows the kit to fasten to the work area plate, and eventually integrate into the machine.

6.7 Bed Leveling

The literature for bed leveling was primarily based on research of current technologies used in industry. The two options considered for bed leveling were manual and automatic. The following research determined the optimal bed-leveling method to use.

It was discovered that for both industrial and hobbyist CNC mills, the only automatic leveling used was strictly software based, and this method was found only in routing machines. The method involved first running a cycle that would probe the part, then the software would map the z-coordinates of the part and alter the height of the tool paths

accordingly (Giliam de Carpentier, 2018). The problem with attempting this approach with a mill is that it does not accommodate for the necessity of the part being parallel to the end mill's bottom edge in order to mill a flat without steps; this is critical for maintaining the goal finishing tolerances. Therefore, software leveling would not suffice, as the part itself needs to be parallel to the bottom of the end mill held in the collet.

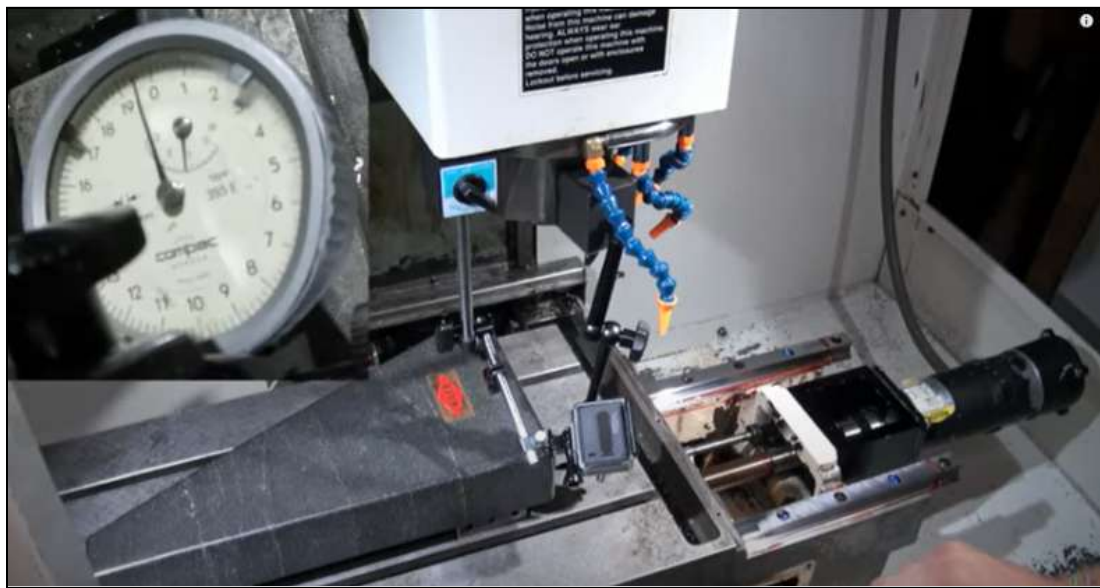
After further research, it was concluded that in general there are no CNC milling machines that incorporate automatic bed leveling. The reason for this is twofold. The first issue is the difficulty in maintaining tolerances, as the components that can automatically move the bed must simultaneously be rigid enough to not move more than 0.005" under loads of up to 20 lbs (Brown et al., 2024, pp. 32-33). For example, automatic leveling would require a motor, and that motor would need to hold constant under the cutting forces. This would require either a motor that would take up substantial space relative to the area available, or gearing that would need to be sealed off from the debris.

This leads to the second problem, which is that the electronics would need to be in an environment consisting of continuous fluid exposure, as well as dust and debris from manufacturing parts. Adding automatic bed leveling components would also include that additional designing and materials required to seal off of the electronics and gears. This would not be an impossible task, but it would require a substantial R&D phase, which was determined to be beyond the scope of what could be done with the resources of the current year's project. Based on these discoveries, the decision was made to implement manual bed leveling with the option of software leveling for router parts.

The most prevalent way CNC mills are mechanically leveled is by adjusting spacers that are located at the rails of the machine. Figures 6.17, 6.18, and 6.19 show examples of

both an industrial and hobbyist mill and their bed leveling mechanisms. The decision was made to implement a similar design in the mini-mill. This method would also be cost-effective, potentially requiring minimal financial resources. Furthermore, leveling could be done during the initial setup of the machine, then subsequently only as often as necessary—this is estimated to be on the order of every 100 hours of use, due to mechanical bed leveling allowing for far more rigidity over an automatic leveling system.

Figure 6.17: *Image of Industrial CNC Mill with the Leveling Mechanism Exposed*



Note. Exposed leveling mechanism is in the bottom right of the image. Reproduced as is from (At-Man Unlimited Machining, 2016)

Figure 6.18: Mechanical Brass Leveling Shims



Note. Zoomed-in image of Figure 6.17 showing the mechanical brass leveling shims on the rail guides. Reproduced as is from (At-Man Unlimited Machining, 2016)

Figure 6.19: Hobbyist CNC Mill with Aluminum Spacers



Note. Image of a hobbyist CNC mill that uses aluminum spacers with screws that mechanically adjust the height of the bed where it attaches to the rails. Reproduced as is from (9Volt Projects, 2024).

6.8 CNC Control System

In determining a software and hardware control system for a CNC machine, there are many considerations that need to be kept in mind. Control software is only intended to work with certain control hardware and vice versa. Additionally, each control system has features that may not be available in other control systems.

6.9 Control Hardware

When determining the hardware to choose for a CNC control system, hardware interactivity needs to be taken into account. These considerations include power levels for

the board, power needed for connected electronics, communication interfaces for components, communication with the computer, and many more. With these considerations in mind, there are four prominent hardware control systems that can be used to control CNC machines. These hardware interfaces include Mach3 (*Mach Mach3*, n.d.), LinuxCNC (*LinuxCNC*, n.d.), grbl (*Grbl Home*, n.d.), and grblHAL (*GrblHAL Home*, 2021).

6.9.1 Mach3

Mach3 control cards can be connected to a computer either through a USB connection or through a parallel port connection. Through Mach3, it sends signals to the control card, which then translates the inputs into electrical signals that then control hardware such as motors, spindles, etc (*Mach3 Mill Install Config*, 2008). LinuxCNC control cards are much different to Mach3 control cards. With LinuxCNC cards, instead of using the dedicated card to provide the real-time calculations and signals, like Mach3, LinuxCNC cards require the Operating System(OS) to do this. The OS does all the real-time calculations and then the card executes those instructions, requiring the OS to have a real-time kernel to produce instructions (*LinuxCNC System Requirements*, 2024). This means that LinuxCNC cards cannot connect to laptops or through USB since they are not designed for real-time communication (*LinuxCNC Hardware Requirements*, 2019) (*LinuxCNC Hardware Interface*, 2024).

6.9.2 grbl & grblHAL

grbl and grblHAL hardware uses off the shelf microcontrollers to control CNC machines. grbl is intended to work on virtually any microcontroller and hence is simple as a result. In contrast, grblHAL requires that the microcontrollers used be at least 32-bit,

making it more capable. With grbl's intended simplicity, it is limited to features such as only being able to run 3-axis machines, having no tool change, and other lacking features (*grbl Home*, 2023). grblHAL attempts to expand upon this by requiring more powerful microcontrollers that can add features that grbl does not have and allow for plugins at the hardware level for custom features (*grblHAL Home*, 2021).

6.10 Control Software

For each of the control hardware systems (Mach3, LinuxCNC, grbl, and grblHAL), they need compatible software controllers to control the hardware. Softwares to consider are Mach3 (Mach3), LinuxCNC (LinuxCNC), CNCJS (grbl), bCNC (grbl and grblHAL), and Universal Gcode Sender (grbl and grblHAL). Each of these softwares allow the user to use them for CNC milling and are designed to work with their associated hardware system. An important consideration to make when choosing software is whether it is open-source or not. If a software is open-source, then it is free and available to download and improvements can be made to the base software (Perens, 2008).

Some features to consider when choosing softwares are support for a 4th-axis, tool changing, custom modules, software bed leveling, and system requirements. If a control system supports a 4th-axis, it can allow the machine to make much more complex parts, such as those in Figure 6.20, and can reduce the amount of times an operator would need to flip the piece around to finish it. For tool changing, it can allow the machine to make more complex parts (ie. add threads, chamfers, drill holes, etc.). Tool changing can come in forms of manual switch (user swaps tool), touch off (tool is calibrated afterwards), and automatic tool change (machine swaps tool autonomously) (*GrblHAL Tool Change*, 2024). Custom modules allow the ability to add UI and functionality that may not be common but useful

(ie. temperature monitoring, vibration readings, etc.). Software bed leveling has the software analyze the shape of the bed to make parts more uniform since even flat plates can have a significant amount of deformation, affecting the part. The system requirements, (ie. OS, CPU, RAM, etc.) should also be taken into effect since this can limit what users need to be able to run the machine.

Figure 6.20: Sample 4th-axis Part

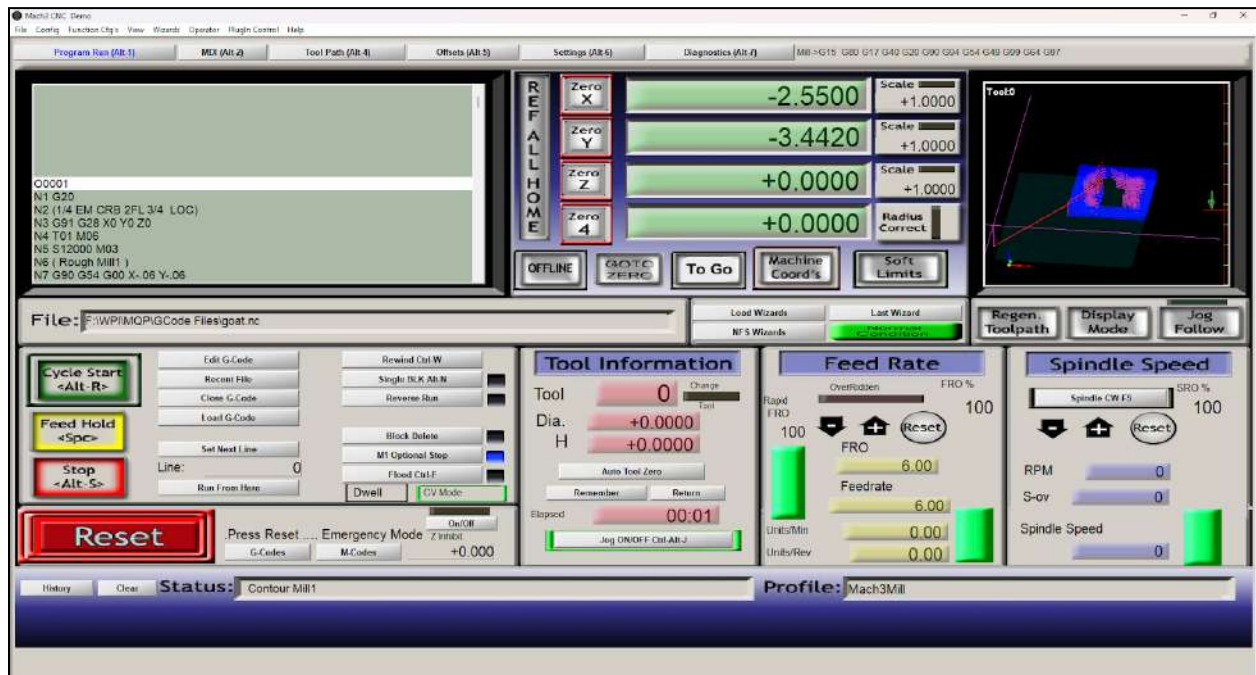


Note. Reproduced as is from (23517973 | Detroit Diesel Series 50/Series 60 Impeller, n.d.).

6.10.1 Mach 3 Software

The Mach3 software is designed only to work with USB motion cards that support Mach3 commands or with parallel port break out boards (BoB). In addition, it is only compatible with Windows OS, making it restrictive for users with other OS's. Additionally, the Windows OS requires more expensive system resources than top Linux distributions. A factor that limit's users' accessibility to the software is that Mach3 costs \$175 for a license, where the other CNC control software are open-source and free (*Newfangled Solutions Mach3*, 2024). Mach3's interface is intended to be run as a program on an existing Windows machine, allowing the machine to be used for other tasks if so desired (Figure 6.20). This software supports a 4th-axis, full tool changing support, custom modules, and more.

Figure 6.21: Main Mach3 User Interface with Loaded G-code File

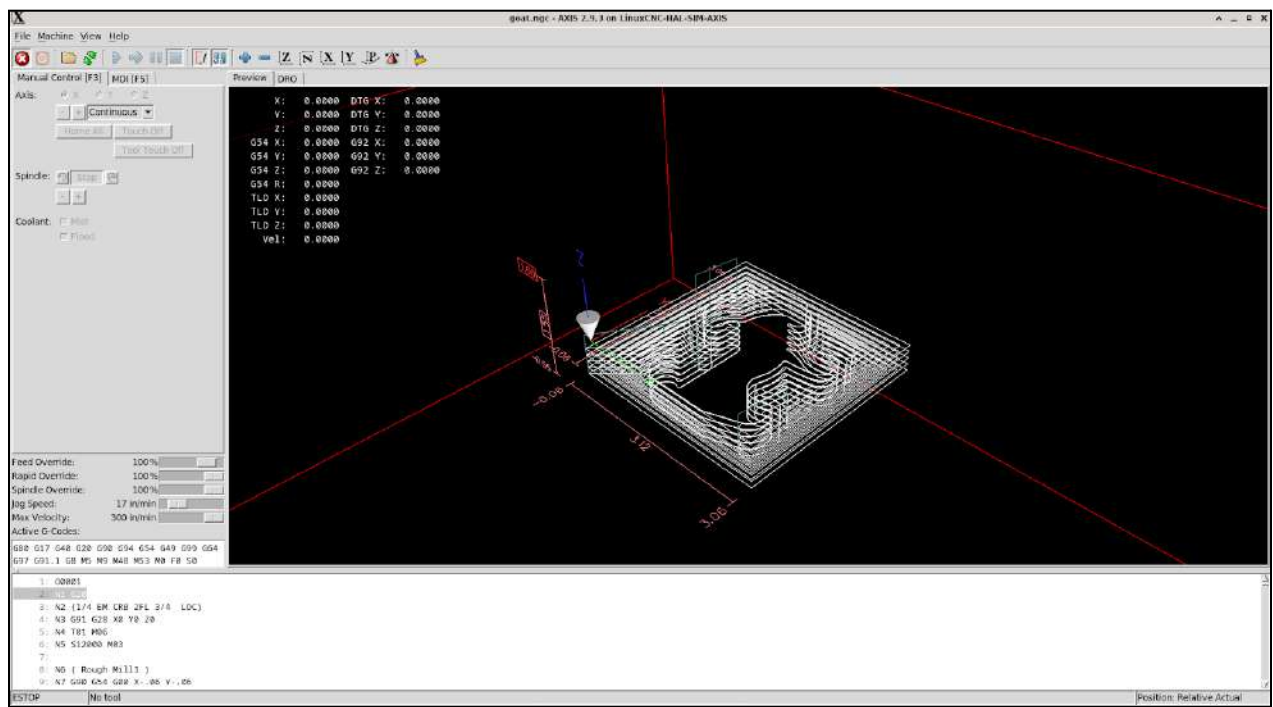


6.10.2 LinuxCNC Software

The LinuxCNC control software is much different than any of the other software.

While the other software is intended to run on commonly run operating systems, LinuxCNC requires installing a Linux OS that comes pre-installed with LinuxCNC. This means that any user would, most likely, need to learn a new OS and CNC interface to use the CNC machine (Figure 6.21). Additionally, because of the real-time kernel mentioned earlier, a user would need a desktop computer with parallel port support. This software supports a 4th-axis, full tool change support, custom modules, and more.

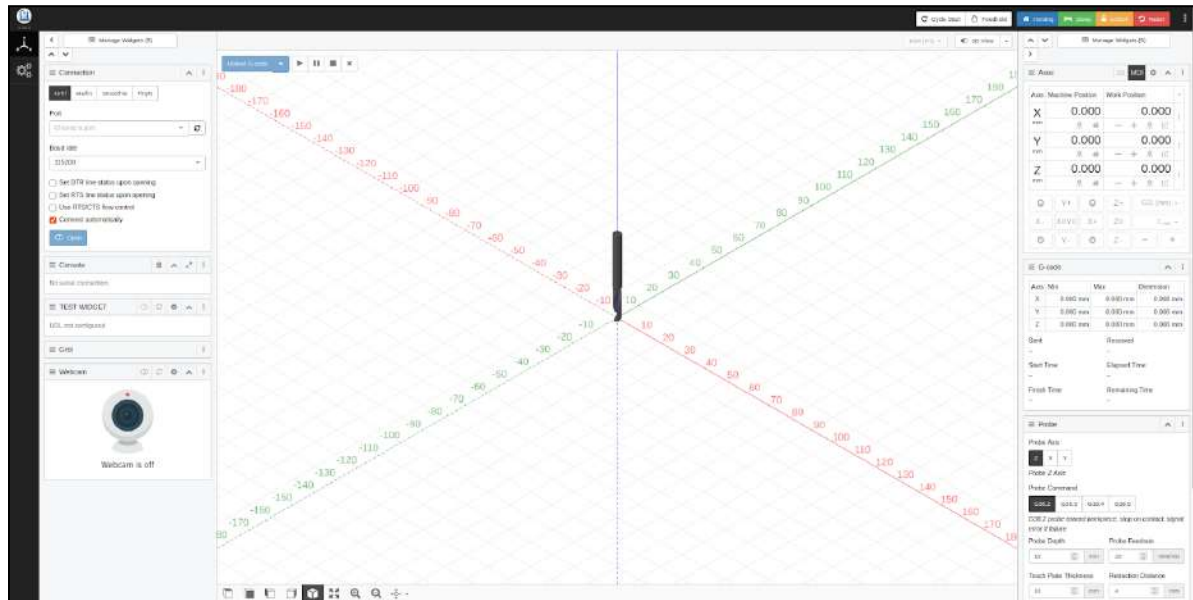
Figure 6.22: Main LinuxCNC User Interface with Loaded G-code File



6.10.3 CNCJS Software

A unique feature of CNCJS that none of the other software control systems has is that it runs entirely in a user's web browser (Figure 6.22). This makes the software extremely compatible with operating systems since every computer has a browser, with most major browsers being supported. This software only supports grbl and not grblHAL, since it is not designed to work with grblHAL systems. This means that features exclusive to grblHAL might not work or if they do, it would not be user friendly to use compared to other software. This software supports custom modules and many other features common to CNC systems. CNCJS does have some limitations with having no support for a 4th-axis (due to grbl's simplicity) and has no tool change support.

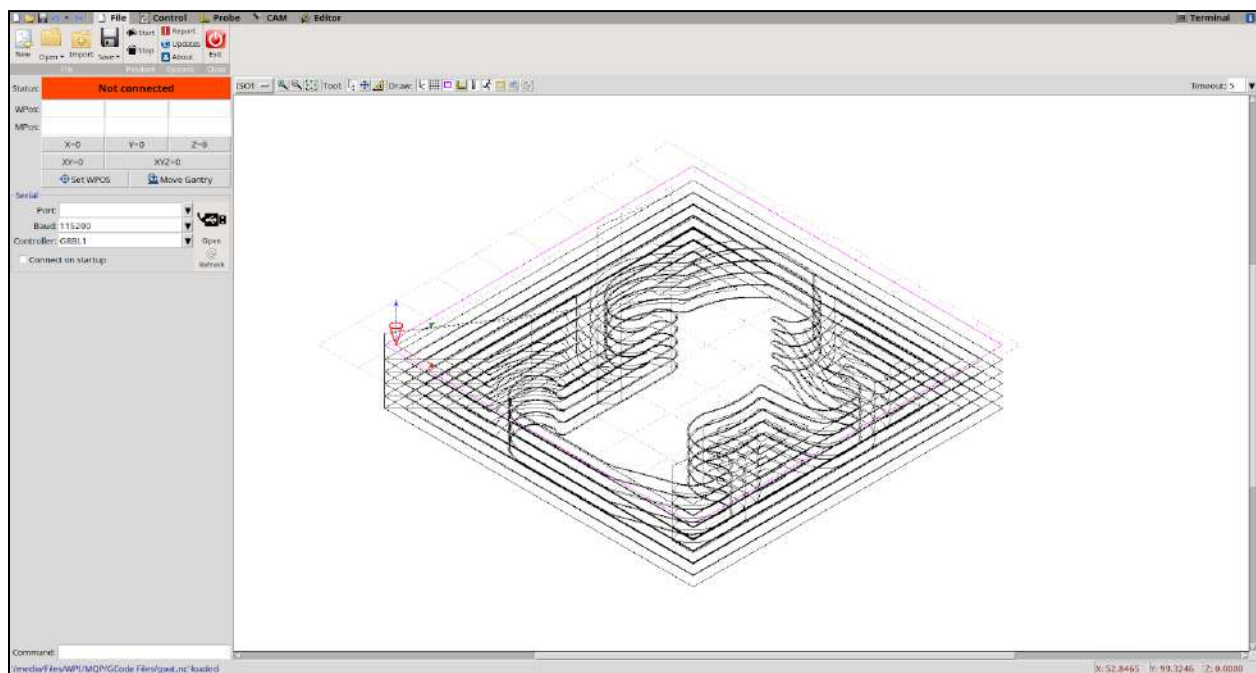
Figure 6.23: Main CNCJS User Interface



6.10.4 bCNC Software

bCNC runs as a standalone program that is available for most operations systems, which includes Windows, Mac, and Linux. It is laid out as a standard program with different tabs that correspond to different features of the software, such as CAM editing, probing, etc (Figure 6.23). bCNC supports a 4th-axis, custom modules, and many other features. It does not, however, have full support for tool changing, limited to touch off without custom plugins that add tool changing support.

Figure 6.24: Main bCNC User Interface with Loaded G-code File

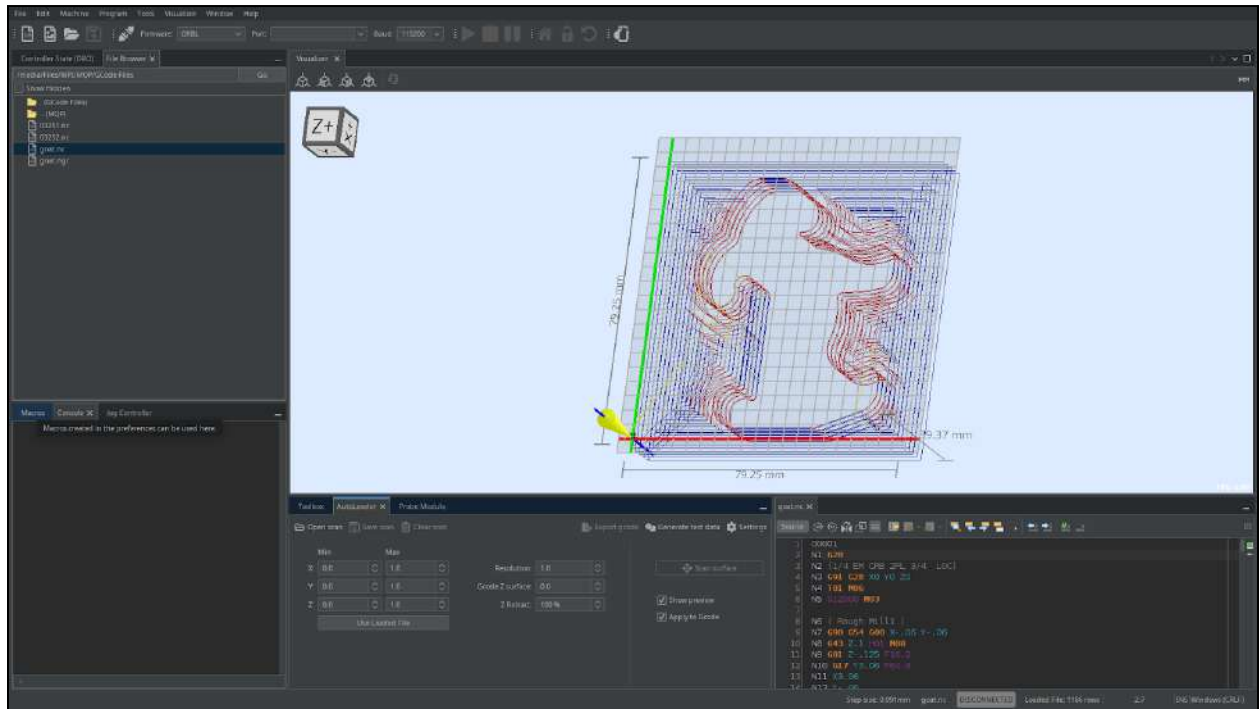


6.10.5 UGS Software

UGS also runs as a standalone program on most operating systems. It is very similar to bCNC in terms of features except that instead of features being laid out in tabs, they are in boxes that can be moved, resized, and hidden. This makes the UI of UGS the most customizable out of all of the control softwares mentioned while having most features that

would be wanted in a CNC mill (Figure 6.24). This software supports 4th-axis, custom modules, software bed leveling, and more. It is limited to touch off tool changing without custom modules being designed for it.

Figure 6.25: Main UGS User Interface with Loaded G-code File



6.10.6 Previous MQP's Software Selection

Last year's MQP team used Mach3 and a USB control card for their CNC control system. This means that any users would be forced to buy Mach3 in order to use the machine without extensive modifications (Hoy et al., 2024). However, the possibilities brought by LinuxCNC, CNCJS, bCNC, and UGS, allow for a more user friendly interface, an open-source software to add custom features, and more supported operating systems.

6.11 Electrical and Safety Systems

Several electrical changes were needed to update the safety of the machine. As discussed in Section 3.8, a safe CNC milling machine must include a functional door latch, an E-stop button that cuts power when pressed, limit switches that cut power when triggered, a stack light to indicate the status of the machine, and a lockout-tagout system to regulate who is able to access and operate the machine.

Last year's system had no way of detecting when the door was opened, which is a large danger to the user. It is imperative for the team to develop some sensor system to detect this change and immediately cut power when the enclosure is opened, similar to the E-stop. However, this pause would not back out of the program in an emergency situation that the E-stop functionality is designed for. It is also important to make sure the E-stop properly cuts power to the spindle when triggered, as last machine's E-stop only cut power to the axes.

Limit switches are located on each end of all three axes, and are used in two main ways in CNC machining. The first is to provide a barrier to prevent the machine from moving beyond its physical limitations and damaging the tool, workpiece, or any component of the overall machine. The second is to provide a reference point for the machine's homing capabilities, as the machine can "zero" itself by calibrating with these switches (Scienc Labs).

Stack lights are a standard addition to professional and hobbyist CNC machines alike, and since the previous machine did not have one, a control system was added to control a new stack light on the machine. Stack lights are important to have as an obvious indication of the state of the machine, improving the surrounding people's awareness of the

situation, and giving the machinist an easy way to tell what is going on with the machine (Bacidore).

Last year's machine was missing any kind of lockout-tagout system (LOTO), which is the name of a set of systems put in place to prevent unauthorized access to the machine. According to OSHA Standard 1910.147, proper CNC milling machine lockout-tagout systems must include some kind of energy isolation device with a physical lock, clear warning labels indicating that the machine should not be used, proper training for any users of the machine, periodic inspections of the energy isolation device and procedures, and verification that the isolation techniques work. To ensure the safety of the end user, a robust LOTO system that follows these guidelines is a must.

A large amount of literature review was needed to prepare the team for such an interdisciplinary project. Every major represented in the team was necessary to provide unique knowledge on every aspect of the machine.

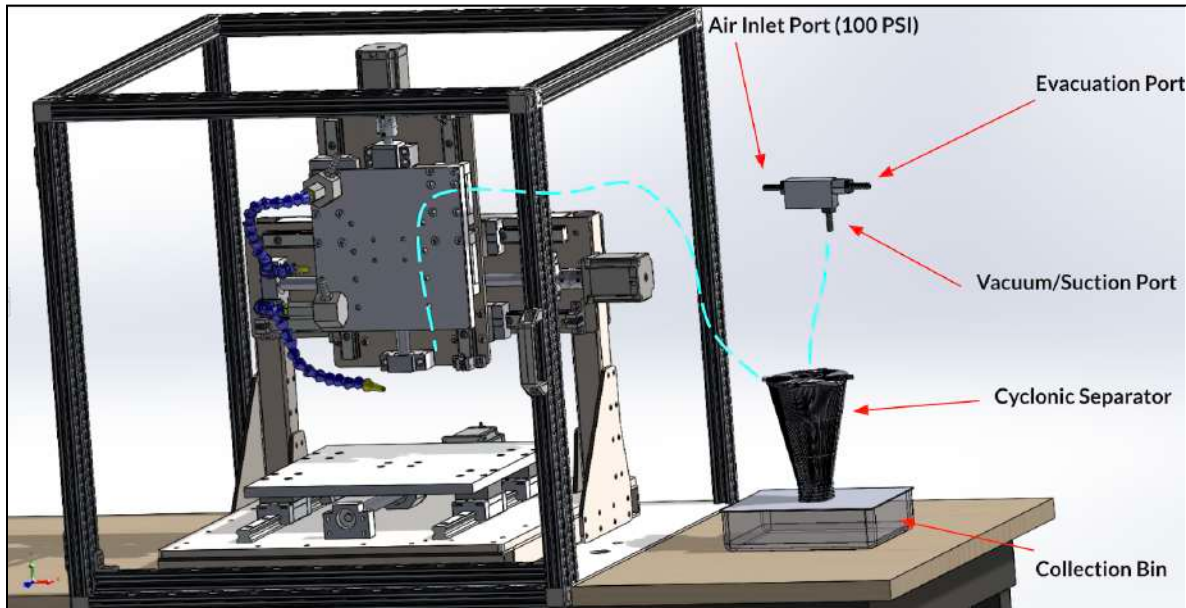
7.0 Mechanical Design Updates

The following sections discuss the mechanical design updates and the additional functionalities to the current CNC machine by the 2024-2025 MQP team.

7.1 Vacuum System

Based on prior research (reference Section 6.2), a vacuum system setup that utilized a venturi pump and cyclonic separator was proposed. For this setup, there would be one hose that connects the vacuum port of the venturi pump to the top port of the cyclonic separator, and then a second hose that connects the side port of the separator to the work area. The separator would then separate the chips from air, and then the air would then exit through the top of the separator into the venturi pump. The process would start once air is supplied to the air supply port of the venturi pump. Figure 7.1 below was the first iteration of vacuum system setup using CAD.

Figure 7.1: First Iteration of Vacuum System



Note. This iteration utilizes a venturi pump and cyclonic separator.

With an idea for the vacuum system finalized, the venturi pump and fittings were purchased, and the cyclonic separator was 3D printed. This cyclonic separator came from the youtuber “Nikodem Bartnik”, and there were STL (stereolithography) files freely available on his channel (Bartnik, 2019). Using this cyclonic separator would save the time needed to design and test it before using it in the vacuum system. There was also an air inlet port where the CNC machine was located that can supply roughly 100 psi of shop pressure to the venturi pump. Based on calculations, approximately 91.4325 kPa of pressure was needed to pull in chips from the work area into the cyclonic separator. The shop pressure would be able to supply more than enough pressure for the vacuum system to work.

Once all the components arrived, testing was conducted based on a previously created procedure document (reference Section 9.1.3 for testing related information). The setup is very similar to Figure 7.1. The only difference was the hose that was supposed to

connect the side port of the separator to the spindle (blue dotted line on the left) is placed next to chips that were created as a result of an earlier milling operation (Figure 7.2). With everything set up and the air inlet port turned on, testing was conducted to vacuum chips into the hose, and the results were unsatisfactory.

Figure 7.2: Vacuum Hose Setup



There were a multitude of issues with this iteration of the vacuum system. The first major issue of the set up was that the shop pressure made a considerable amount of noise while it was running. The second major issue was the minimal suction of the chips. More specifically, the hose needed to be directly next to the chips to be able to vacuum the chips into the hose, which would not be possible during machine operation. Based on earlier research done before conducting this test, it was theorized that since venturi pumps are typically used in pressure applications, it may not produce a volumetric flow rate high

enough to evacuate the chips. The team thought that 100 psi of shop pressure would be enough pressure to create a high flow rate, but that was not the case. Figure 7.3, shows the result of the testing after turning the shop pressure on for over two minutes, and moving the hose around the machine to evacuate the chips.

Figure 7.3: *The Aluminum Chips Collected by the Vacuum System*

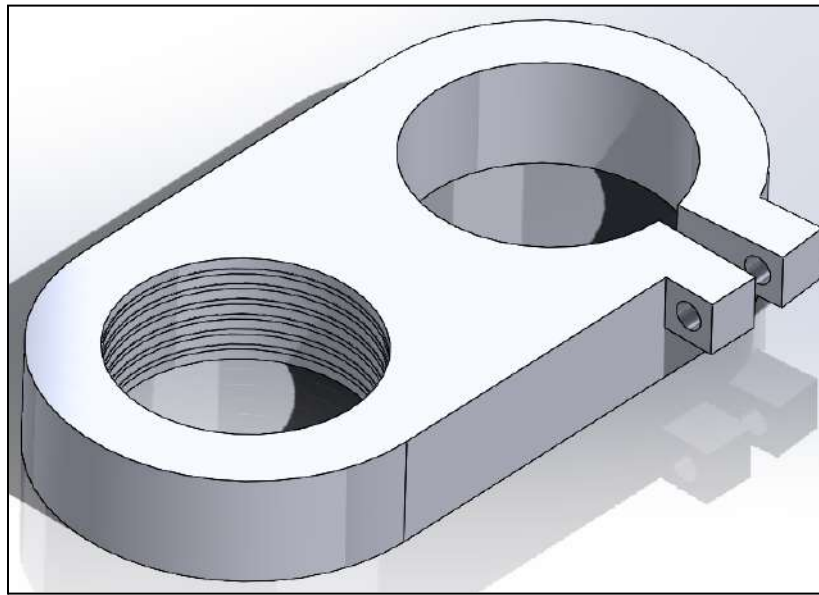


After some considerations, it was decided that while using the cyclonic separator to separate the chips was viable, using the venturi pump for suction pressure was not. More research was done on alternatives for the venturi pump, and the team found that a shop-vac of 5 HP would have sufficient volumetric airflow for 91.4325 kPa needed for the vacuum system. Another subject of research was how to attach the vacuum hose to the spindle. The spindle would always be moving during the entire milling operation, so the hose needed to be both close to the spindle and always moving along with it.

The team later referenced a CNC chip vacuum system made by the youtuber “rctestflight”, and it was a shop-vac vacuum system with a dust boot attachment (rctestflight, 2021). In this video, the vacuum system was similar to the team’s initial design, with the exception of using a “shop-vac” vacuum instead of a venturi valve. The dust-boot that he used not only moved with the spindle at all times, but was able to restrict the air flow and direct the chips to the vacuum hose due to the bristles. The initial plan was to purchase a dust boot that fits the current spindle on Amazon, however, after seeing the cost of commercial dust-boots, it was believed that this would not be worth the price with the project’s limited budget.

It was decided that instead of purchasing a dust-boot, the group would design and 3D print it with PLA (polylactic acid) instead. The 3D printed dust-boot would not only be significantly cost-effective, but also be easy to rapidly modify the sizes to work within the size constraints of our machine. The 3D printed “dust-boot” has two holes. The left hole is where the vacuum house will attach to, and the right hole is where the dust boot will attach to the spindle. The square extrusions on the right is where a screw and nut are used to secure the dust-boot to the spindle. The figure below is the final iteration of the 3D printed dust-boot (Figure 7.4).

Figure 7.4: Final CAD Iteration of the 3D Printed Dust-Boo



There were various iterations of the 3D printed dust-boot before our final design above. The previous iterations were similar in design, but the main difference was the different width or thickness of the dust-boot. There were issues with the old iterations being too large to fit. If the width was too large, the dust boot would collide with the end block of the z-axis linear ballscrew during operation. If the thickness was too large, it could collide with the vise on the bed. Eventually, the final design, featuring a width of 3" and a thickness of 1" was able to solve both issues.

For the bristles of the dust-boot, it was possible to 3D print each bristle individually with TPU and attach it to the dust boot. However, the method of attachment was the main cause of concern. There would have to be holes for them on the dust boot, and they would be attached with super glue. The team was not confident if the glue would be strong enough to prevent the bristles from detaching from the dust-boot if the shop-vac was turned on. After some discussion, instead of 3D printing each bristle individually, the team ended up

3D printing what is called a dust skirt. Figure 7.5 below shows the dust-boot with the dust-skirt attached using hot glue.

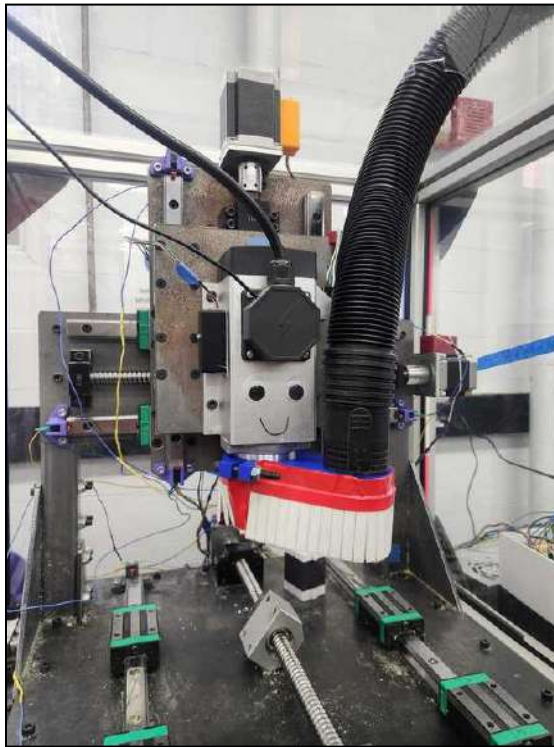
Figure 7.5: 3D Printed Dust-Boot with Dust-Skirt



This skirt was made of TPU, and it was attached around the perimeter of the dust-boot with glue. The flaps of the skirt were thin and flexible enough that when they collided with the workpiece or vise, they bend instead of breaking.

With the final dust-boot and skirt designed, there needed to be a way to get the shop-vac hose inside of the enclosure so that it can attach to the dust-boot. The best method for this was to drill a hole in the top panel of the enclosure. Once the hole was drilled, the vacuum set up was complete. See Figure 7.6 below for the final set up.

Figure 7.6: The Vacuum System with the Dust-Boot and Skirt



Due to the way the dust boot is attached to the spindle, it is not practical to run both the vacuum system and the coolant system at the same time. The shop-vac and the spindle running simultaneously during machine operation resulted in the system being too loud for safe operating conditions. Testing was done on the noise level of the shop-vac and it exceeded the OSHA noise level limit of 85 dBA (*Occupational Noise Exposure - Overview | Occupational Safety and Health Administration*, n.d.). Thus, ear plugs need to be worn when using the “shop-vac” chip evacuation system. Refer to Section 9.1.3 for testing on the final iteration of the vacuum system.

7.2 Automatic Tool Changer Design

After looking over the total cost of the machine, a pre-built model by Rapidchange ATC was \$500 (*ER11-6 Premium – RapidChange ATC*, n.d.) while assembling it with the same components would have cost \$353 (Table 7.1).

Table 7.1: Cost Breakdown of Tool Changer

Part	Link	Cost	Quantity
Infared Sensor	https://www.amazon.co	18.88	1
Stepper Motor	https://www.amazon.co	11.99	2
Infared Photoelectric Sensor	https://www.amazon.co	9.98	1
Stepper Driver	https://www.amazon.co	28.99	1
Collet Nuts	https://www.cncfraises.com	38.92	1
Ball Bearings	https://www.amazon.co	7.25	1
Arduino Uno	https://www.amazon.co	27.6	1
Pneumatic Guide Rails	https://www.amazon.co	72.09	2
Vinyl 20 gauge	https://www.amazon.co	12.99	1
Steel Rod	https://www.homedepot.com	2.93	1
Photoelectric Sensors	https://www.amazon.co	19.99	1
Springs	https://www.amazon.co	17.61	1
Total =		353.3	

The team, however, intended to further reduce costs beyond those of RapidChange ATC. Additionally, they aimed to develop a more compact tool changer that would integrate with our machinery while enhancing its durability. As the model was constructed, the overall expense of the tool changer decreased significantly, totaling \$46.67 instead.

During the initial design iterations (Figure 7.7), the model bore a close resemblance to the RapidChange ATC. It comprised seven components: a base part, a top layer, side parts, a dust cover pin, levers, tri-clips, and a dust cover rod. While the model appeared similar, several modifications were made, notably a reduction in size from 2.36" (60 mm) in

length by 10.83" in width with four holes to a three-hole configuration measuring 2.35" in length and 9.05" in width. Furthermore, the clips (Figure 7.8) within the pockets of the tool changer were of a different shape and employed 0.039" ball bearings (Figure 7.9) as opposed to those measuring 3/16".

Figure 7.7: First CAD Assembly of the Tool Changer

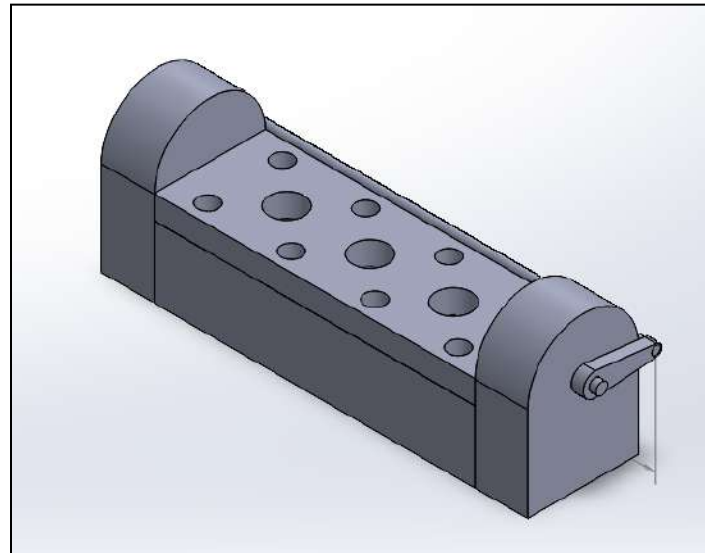


Figure 7.8: First CAD Model of the Tri Clips That Hold the Collet Nut

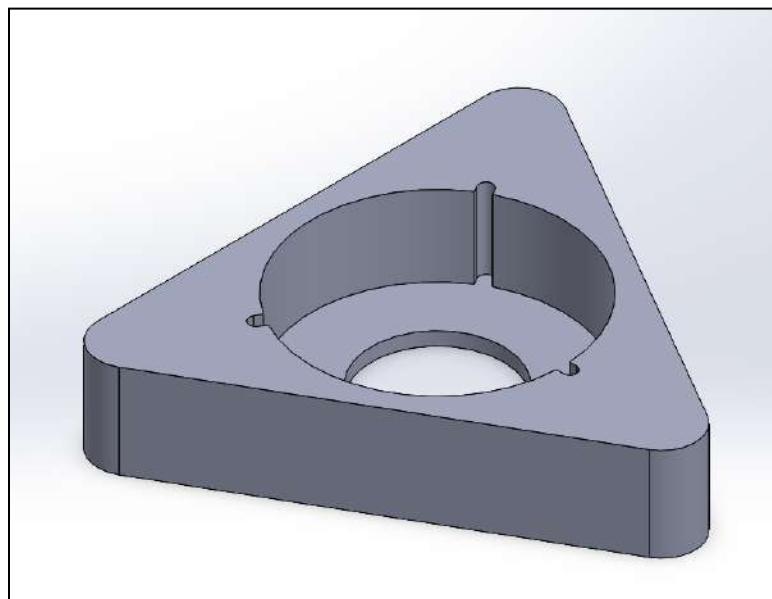
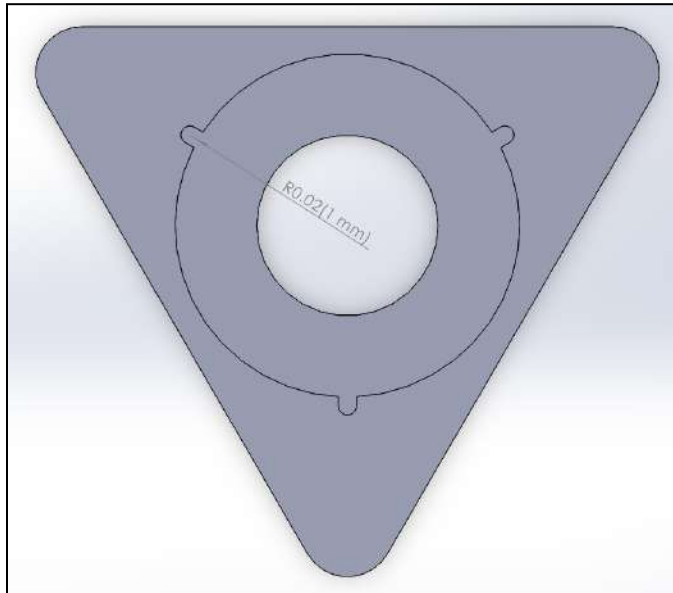


Figure 7.9: Top View of Clips Showing Ball Bearing Pocket as 0.039”



The clips are retained within the base (Figure 7.10) of the tool changer, functioning as the primary mechanism for securing the collet nut. The pockets in the base are sized to correspond with the clips (Figure 7.12), thereby ensuring that the nuts fit securely to prevent misalignment with the spindle and ineffective tightening. In comparison to the Rapidchange, this model maintains the same width and height of 2.36" and 1.52" (Figure 7.11), respectively, while the length is approximately 1.73" shorter, measuring 6.81".

Figure 7.10: First CAD Model of the Base of Tool Changer

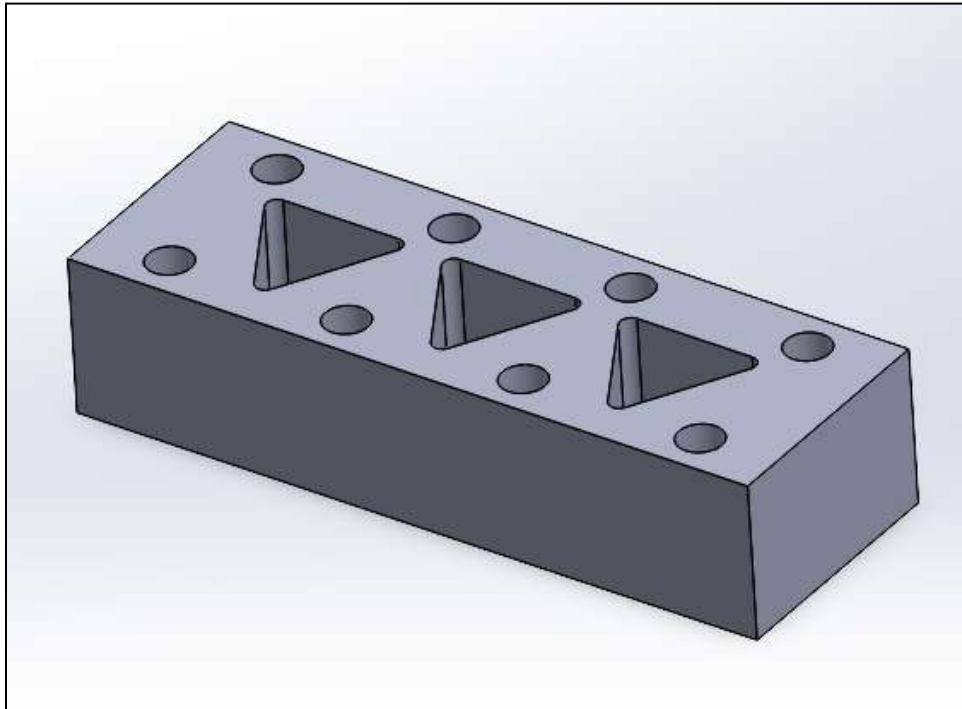


Figure 7.11: Base Part of the Rapidchange at 8.54"

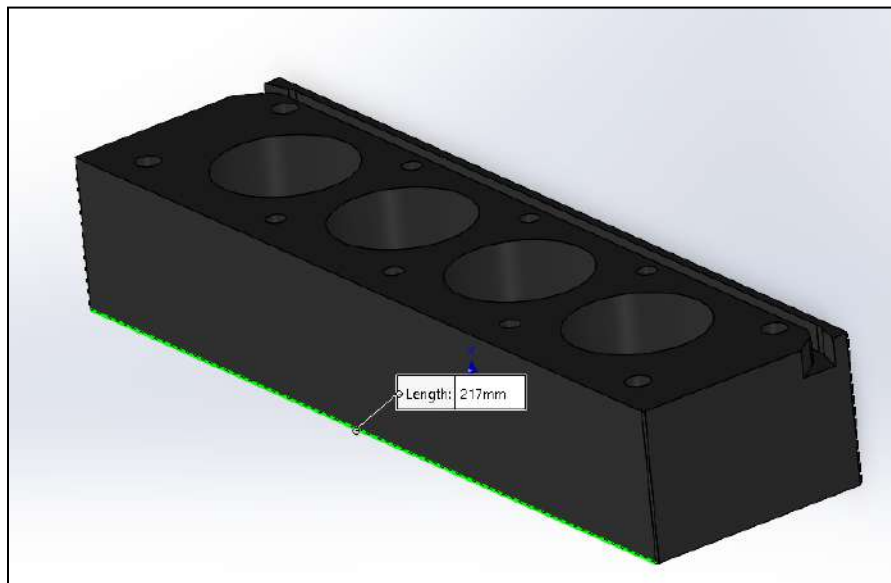
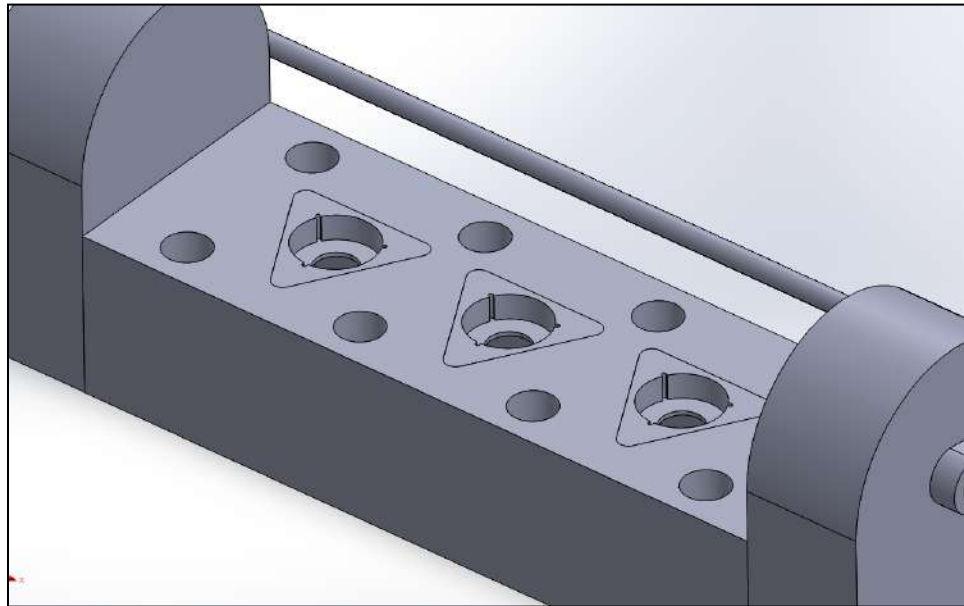
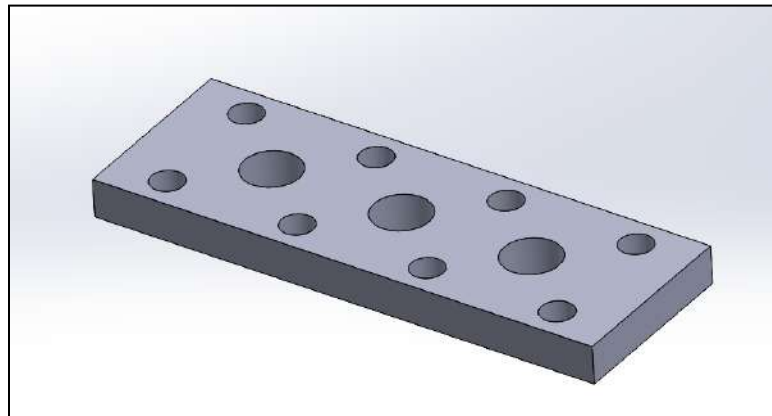


Figure 7.12: CAD Assembly of Clips Inside Pockets of Base Part for Tool Changer



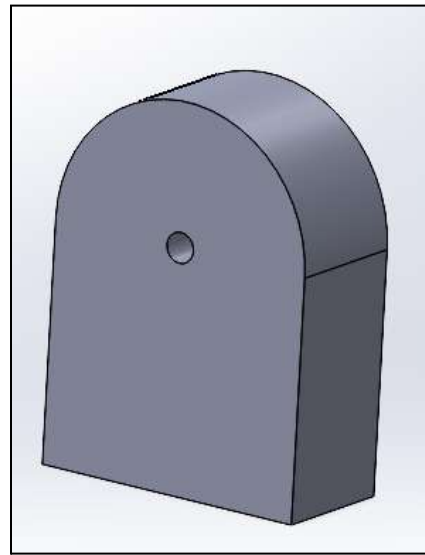
The top layer acts as the main mechanism for securing the clips and preventing their detachment from the tool changer (Figure 7.13). The springs beneath the clips, which have a maximum length of 1.18", generate enough force to lift the clips to the upper section of the base, where they contact the top layer. This effectively retains the clip in place while ensuring that the nut stays within the tool changer. The overall dimensions match those of the Rapidchange, with the same length and width as the base, and a height of 0.5".

Figure 7.13: First CAD Model of the Top Layer of Tool Changer



The lateral sections (Figure 7.14) serve as the compartments responsible for housing the stepper motors within the tool changer, while also accommodating the infrared photoelectric sensor. This particular component is identical in model to the Rapidchange, measuring approximately 2.36" in length, 1.12" in width, and 3.17" in height.

Figure 7.14: First CAD Model of the Side Part of Tool Changer



The final elements of the first model were the levers (Figure 7.15), dust cover pins (Figure 7.16), and dust cover rod (Figure 7.17). The levers provide the main link between the stepper motor and the rod. The pins serve as a reference for the stepper motor, while the rod moves the vinyl over the tool changer to prevent debris. The rod spanned the entire length of the tool changer, measuring 9.05" with a diameter of 3/16".

Figure 7.15: CAD Model of the Lever of Tool Changer

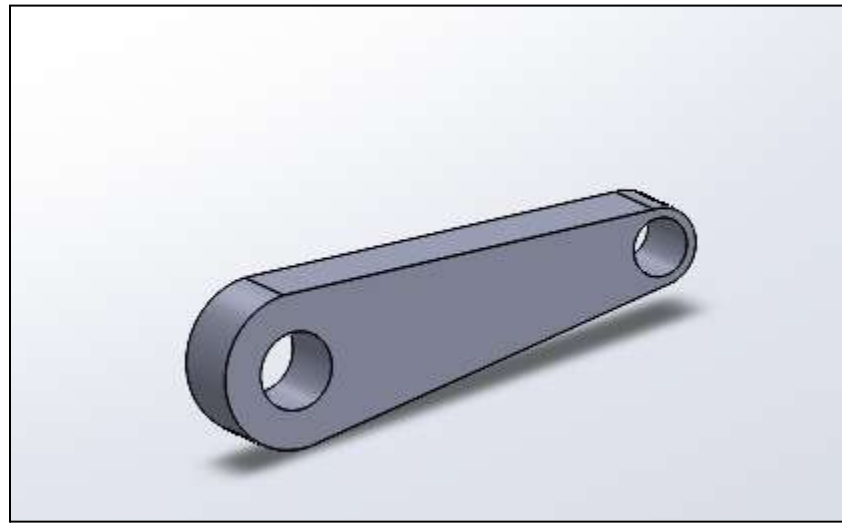
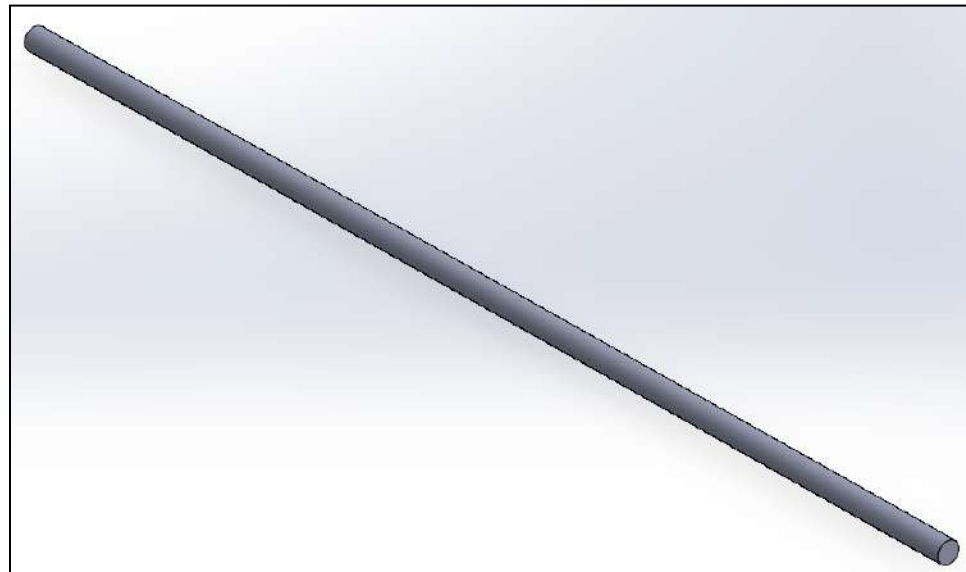


Figure 7.16: CAD Model of the Pin of Tool Changer



Figure 7.17: First CAD Model of the Dust Cover Rod of Tool Changer



Although this was the initial model, several changes were necessary. The triangular clip design occupied excessive space in the base, making it less compact lengthwise than it could be. This initiated the notifications phase for the tool changer.

To initiate the modifications, revisions to the clip to facilitate a more compact design, thereby reducing the space occupied by the clips. Each corner of the clip was modified to incorporate a radius of 0.3" (Figure 7.18). The adjustments made to the clip enhanced the base, allowing for the accommodation of larger holes, specifically enabling the holes to fully adapt to M6 specifications (Figure 7.19). Furthermore, in addition to the modified holes, the clip now utilizes 3/16" ball bearings to provide enhanced grip on the collet nut (Figure 7.18).

Figure 7.18: Adjusted CAD of Clip with 3/16" Ball Bearings of Tool Changer

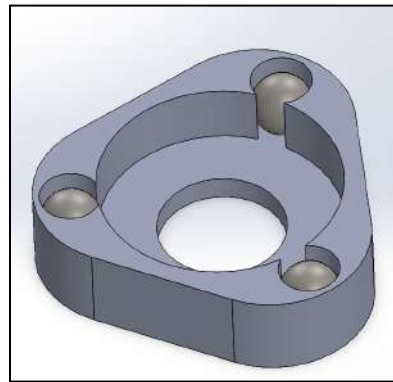
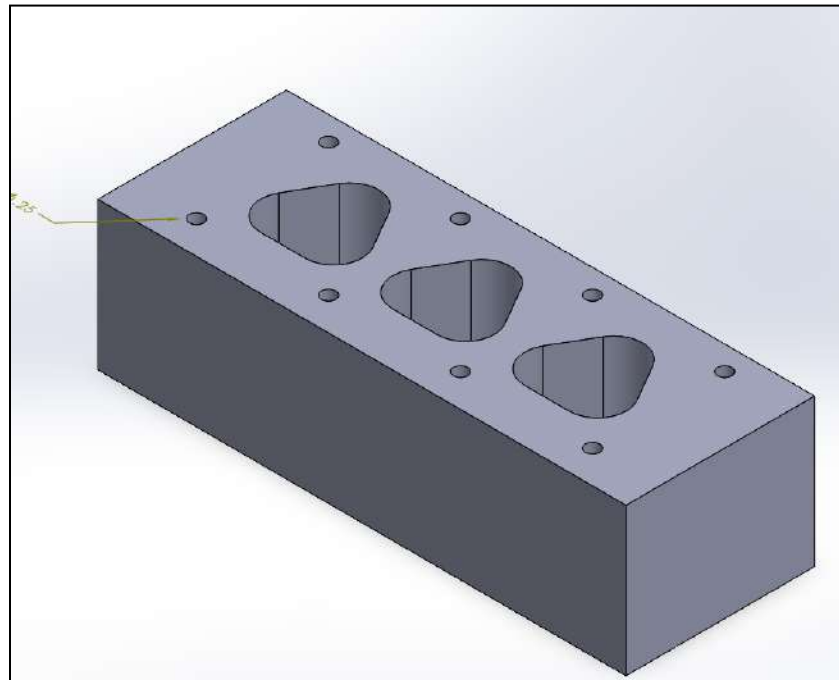


Figure 7.19: Adjusted Base with New Holes for Clip



After completing these adjustments, the changes mainly focused on the dust cover and its new design. The goal for the dust cover was to create a more durable design that relied less on stepper motors to enhance cost-effectiveness. Initially, the aim was to implement a hinge design allowing the cover to lift via a rod, with motors placed on either side. Since the rod would be relatively short, it was determined that two micro servo motors

would suffice for the cover's effective opening. It was crucial that the cover did not touch the gantry to ensure proper functioning. A rectangular shape for the dust cover was developed, leading to modifications in several components of the tool changer, resulting in the second iteration of the tool changer.

In the second interaction, a new dust cover was added, and laser sensor mounts were installed on the side sections (Figure 7.20). Moreover, a wire cover became part of the design. The tool changer's dimensions were revised to emphasize size reduction, altering from 9.05" by 2.35" by 3.17" to 7.25" by 1.97" by 2.79" (Figure 7.21). Additionally, minor changes included converting the holes in the top layer and base from counterbore to countersunk and transitioning from #6 standard holes to M6 holes.

Figure 7.20: CAD Assembly 2nd Iteration of Tool Changer

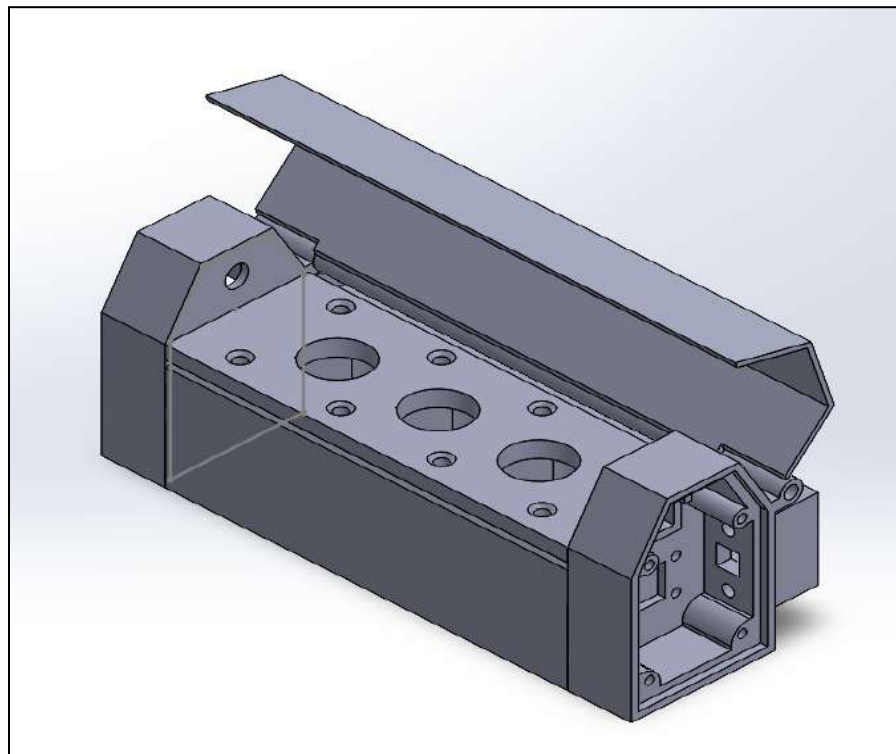
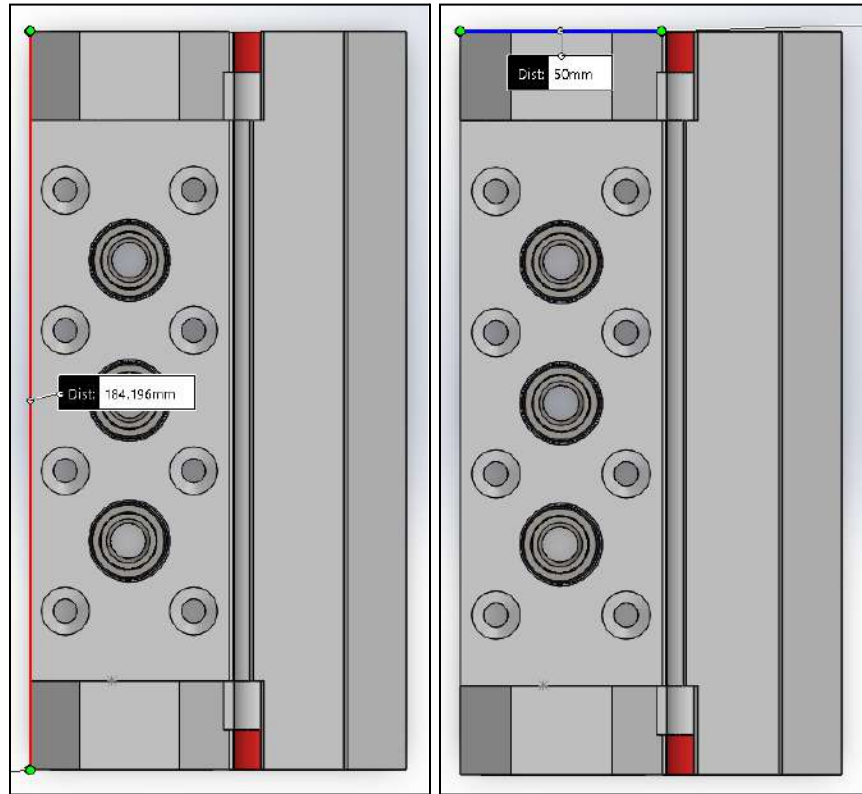


Figure 7.21: Showing the New Dimensions of the Base



Utilizing the dust cover, a trapezoid structure (Figure 7.22) that encompassed the entire base without obstructing the gantry during its ascent. This resulted in a total width of 2.44" (Figure 7.23), allowing it to fit precisely beneath the gantry. Furthermore, the dust cover extended over the full mechanism, including the lateral components.

Figure 7.22: New Design of the Dust Cover

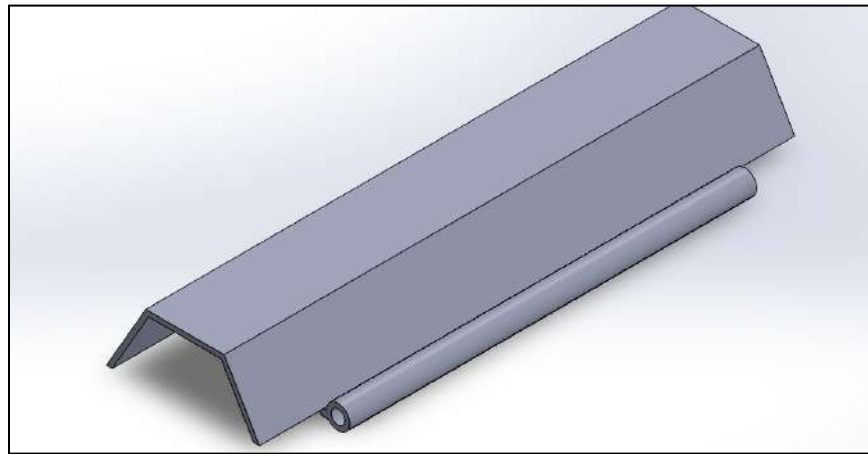
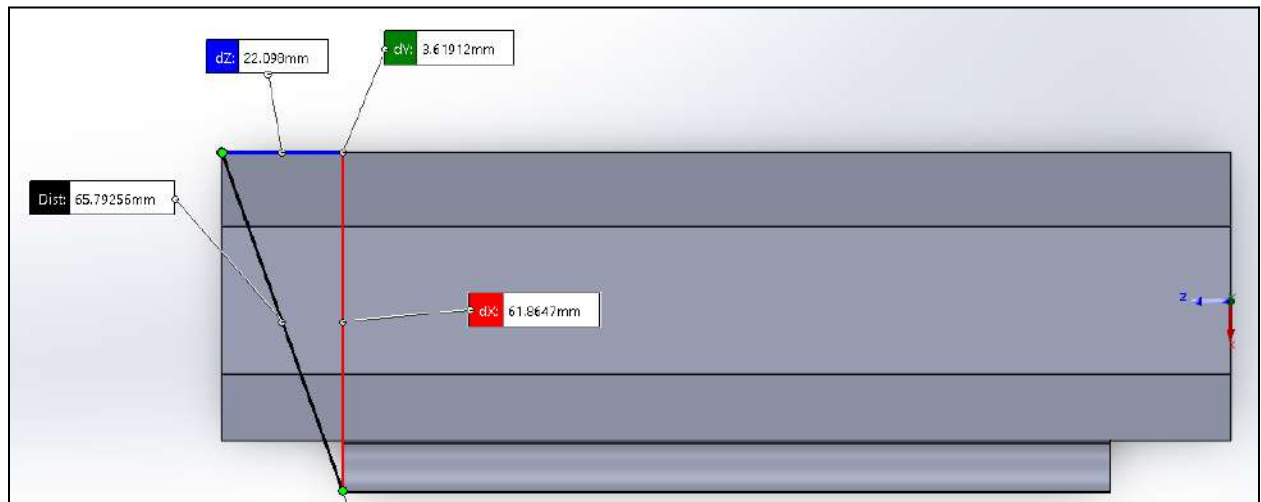
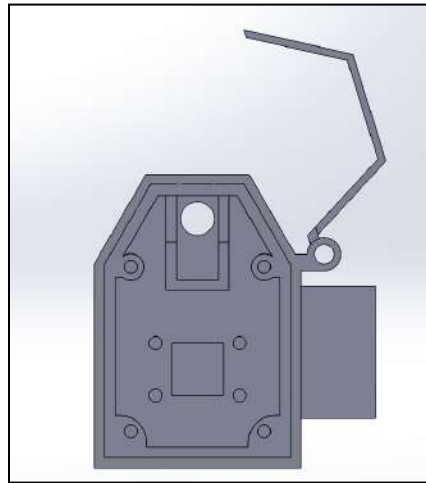


Figure 7.23: Dimensions Showing the Delta X of the Dust Cover



To accommodate the dust cover's fit over the side parts, modifications were necessary. The design was altered to include 0.75" deep holes at each corner for attaching the cover securely, along with a lip to keep it in place. Additionally, holes were created for attachment to the base. Furthermore, each side was equipped with a laser sensor mount to hold the planned laser sensors, which would maximize space efficiency (Figure 7.24).

Figure 7.24: Right Side Part of the Mechanism with the Additions



The final enhancement was the installation of a wire cover to protect the wires from coolant corrosion. To address this issue, a wire cover was positioned at the back of the mechanism since this area did not restrict the machine's workspace. The wire cover extended across the entire rear side of the mechanism (Figure 7.25) and was secured with #6 screws using 0.75" holes on the side (Figure 7.26).

Figure 7.25: Wire Cover Attached to the Back

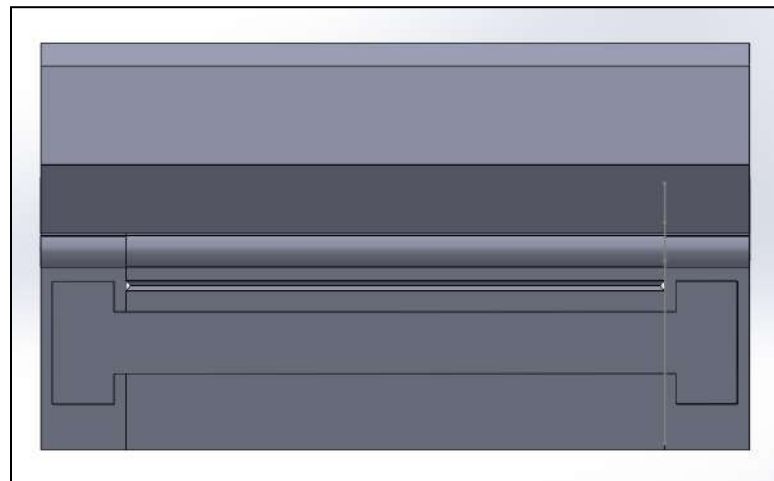
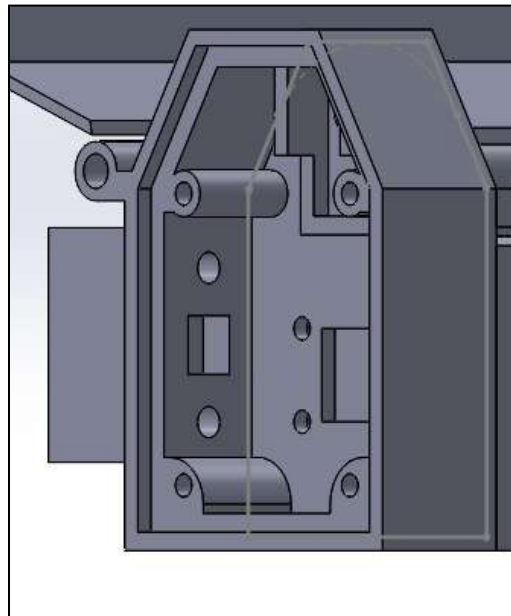


Figure 7.26: Side Part with the Angle Showing the Holes of the Wire Cover



After creating the wire cover, the next focus was on developing the micro servo motor system for the tool changer's dust cover. This system had to secure the servo motors while ensuring they were shielded from coolant exposure. This led to the third and final iteration of the tool changer.

The final version featured three new components: the left and right servo covers, and the servo coupler. Several parts underwent redesigns, including the side pieces, clip, and wire cover. The complete system now measures 249.2" in length (Figure 7.27), which is longer than the previous version but occupies only 1.47" of the workspace, minimizing intrusion (Figure 7.28).

Figure 7.27: Final Iteration of the Tool Changer

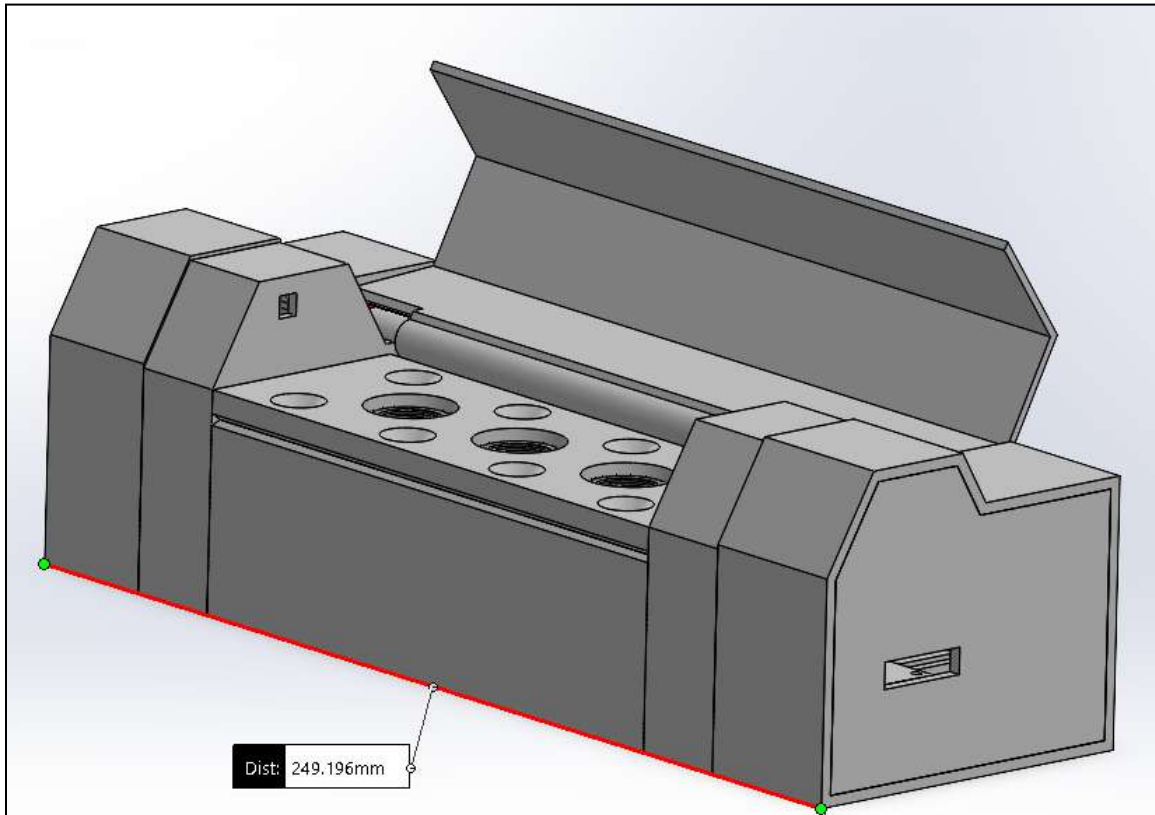
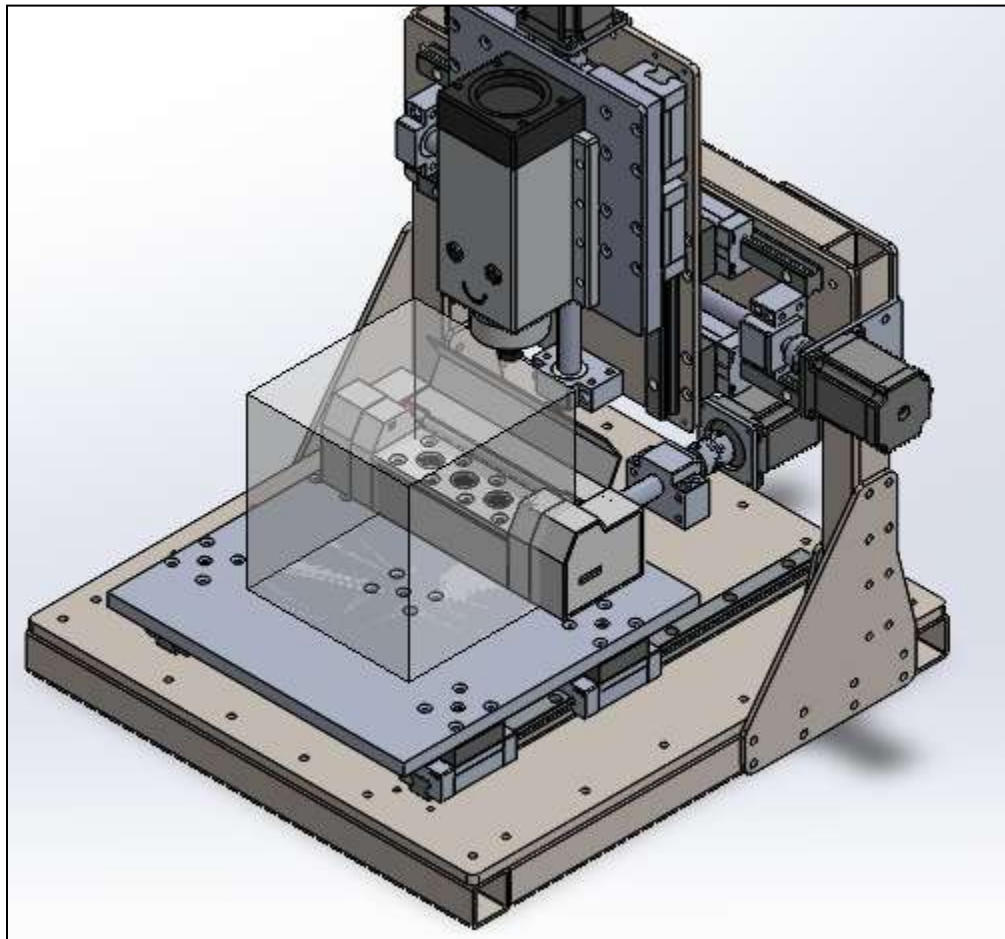


Figure 7.28: Tool Changer in the Gantry



Note. This image shows the minimum amount of space the tool changer requires.

Regarding the modifications to components, one of the most notable changes involved the side parts. The mechanism transitioned from infrared photoelectric sensors to conventional laser sensors, as the tool's height could vary during probing. The previous photoelectric sensors had a fixed z-axis height, which was not suitable for different tool heights. Consequently, the mounts and holes of the side parts were modified. The laser sensor now mounts into the side part by sliding into a 0.052" slot (Figure 7.30), while the laser receiver fits into a 0.07" slot (Figure 7.29). Furthermore, the configuration now

includes only three holes to attach the servo cover to the side part with a #6 screw, and the cover lip has been removed.

Figure 7.29: Left Side Part with Laser Receiver Slot Length

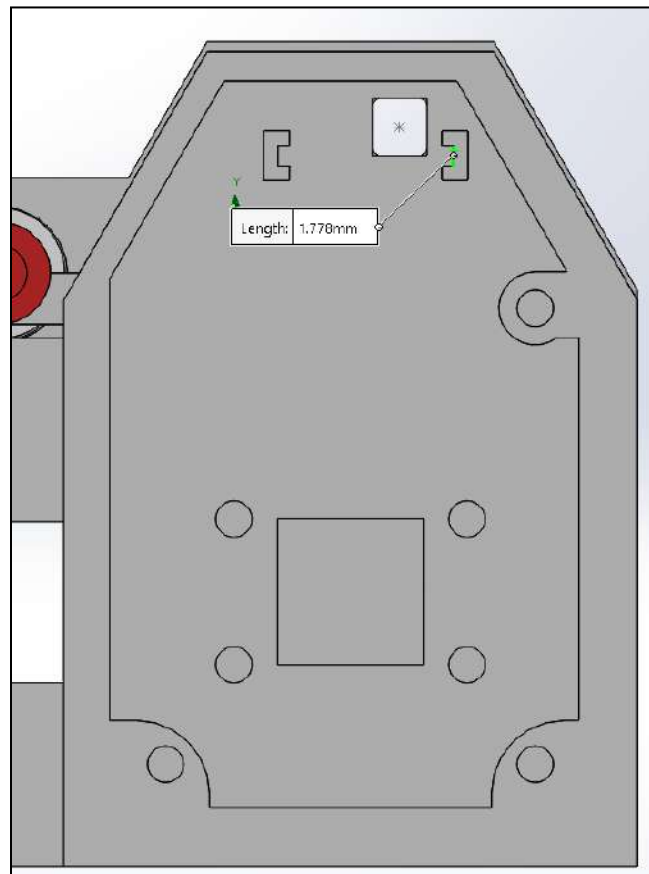
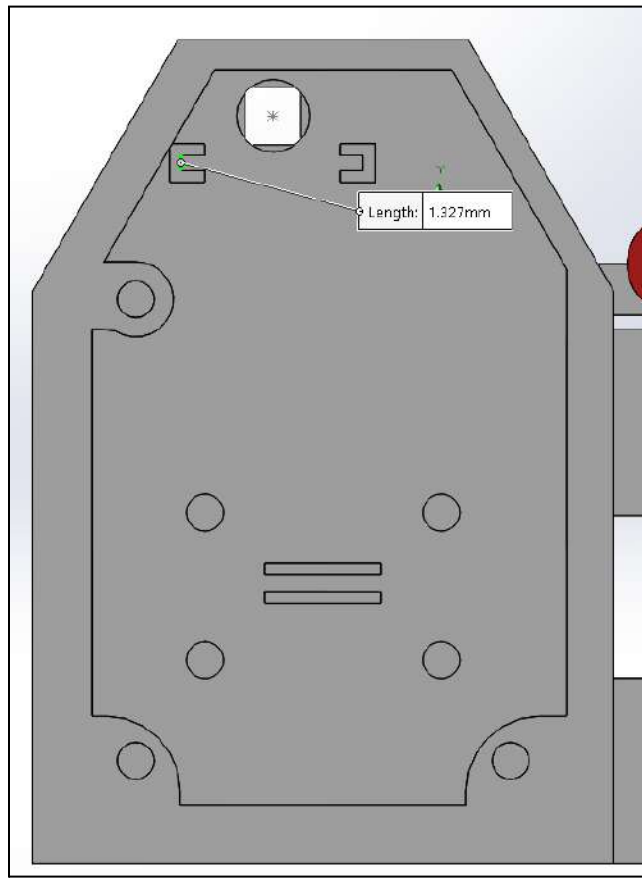
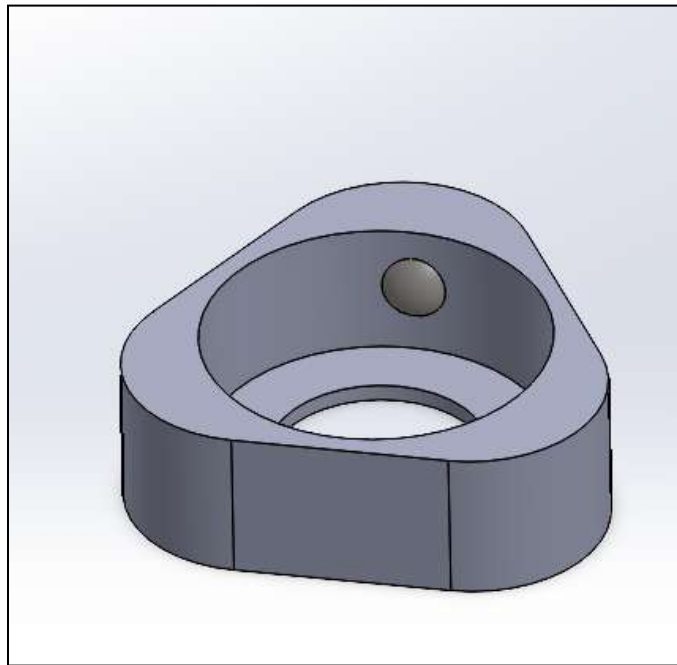


Figure 7.30: Right Side Part with Laser Sensor Slot Length



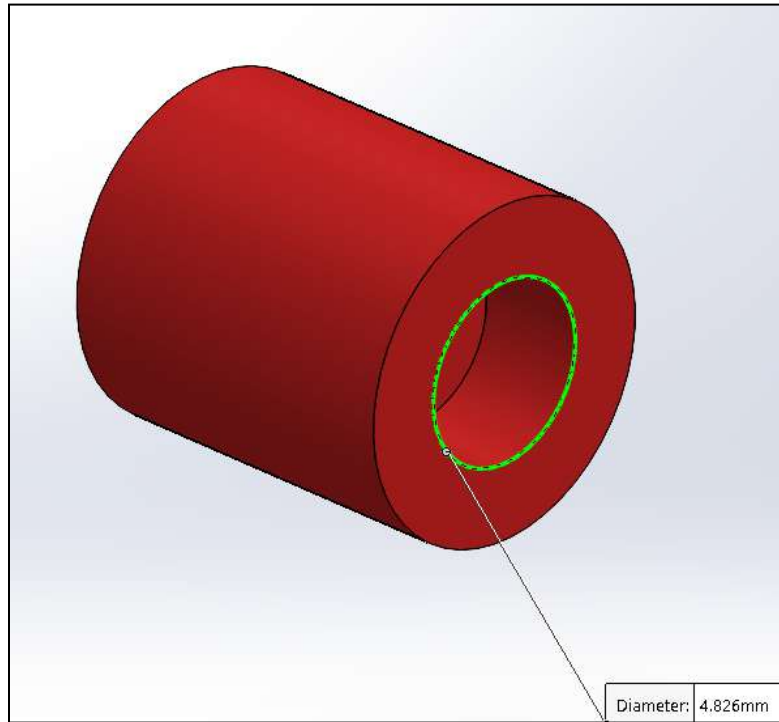
When adjusting the clip, a concern with the ball bearings coming out of the print was developed with how the ball bearings were attached. In order to make the ball bearings more secure, a cavity was created in the assembly that fits the 3/16" ball bearing perfectly. Additionally, covering the top of the clip allows for the ball bearing only to be placed in that cavity through force making it stuck in the cavity (Figure 7.31).

Figure 7.31: Clip Design with Cavity



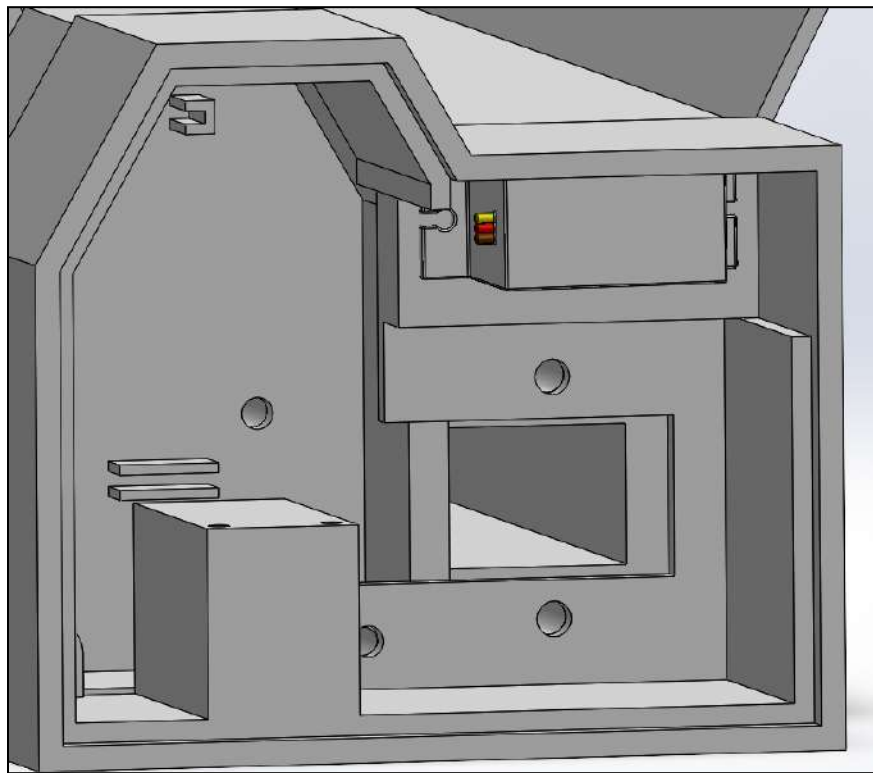
While moving the rod with micro servo motors is possible, finding a way to move the rod with the motors was a challenger. However, a 0.39" servo coupler was used to solve that issue having one side fit the micro servo motor at 0.19" with a depth of 0.118" while the other side fit the rod at 0.19" with a depth of 0.24". This coupler allowed the micro servo motors to grip the rod and turn the dust cover along with it (Figure 7.32).

Figure 7.32: Servo Coupler Showing the Micro Servo Side with Measurements



Lastly, the development of the servo motor covers were the most crucial part of the model. When creating the model, the realization that the servo motors did not have a place to mount or stay produced the creation of the covers. The cover follows the same design concept as the side part while also extending back behind the tool changer. When creating the covers, a pocket was made for the micro servo motors to click into the part while also having a hole for the motor to inch out and attach to the servo coupler. In the servo cover, there are five screw holes, these holes are used to connect the wire cover and the side part together. Lastly, in the left servo cover, a stand to hold the Raspberry Pi Pico was added as well as a slot in the left side part. Adding the side parts and making the wire cover connect to the servo covers finished off all modifications (Figure 7.33).

Figure 7.33: Left Servo Motor Cover with the Pico Board Mount, New Holes and Micro Servo Motor Mount



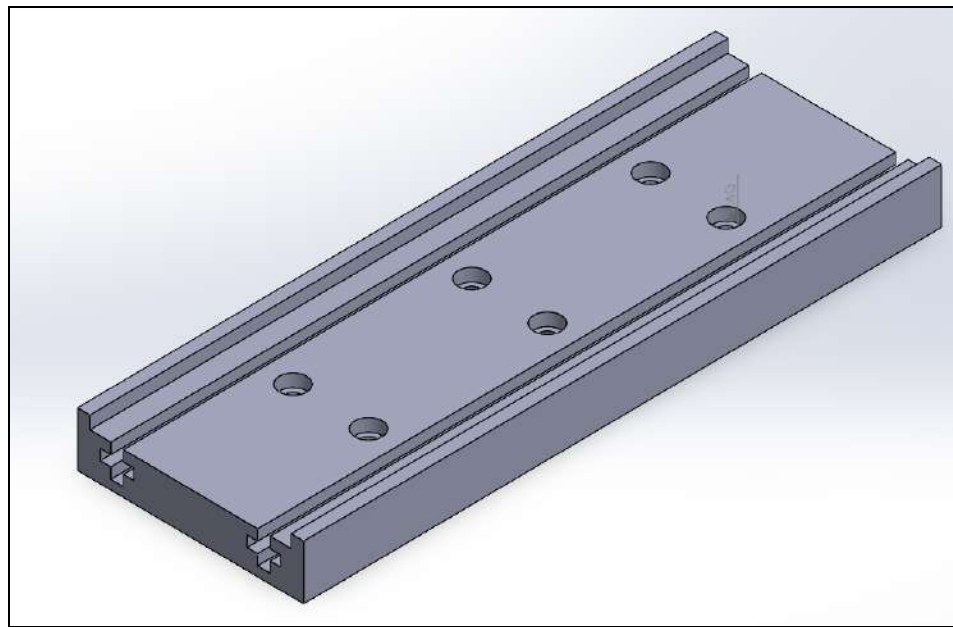
7.3 4th-Axis Functionality

After determining that the team would purchase a 4th-axis kit and integrate its functionality into the current machine's design, the next step was to design a way to fit it to the work area plate. Like many other CNC machines, the original idea was to fasten both the chuck and tailstock pieces to the bed of the machine. Although a design of that capacity was perceived as user friendly, the idea raised questions on its stability, especially with the forces and vibration the pieces would receive from the spindle.

After consideration, the next step was to design a base plate for both pieces to mount to. Doing so would not only provide more support for the 4th-axis pieces, but ensure that both components were aligned and square with the work area plate.

The first design shown in 7.34, of the baseplate, incorporated a slotting design similar to traditional CNC machine fastening methods. Using hammer nuts that would move along the slot, the 4th-axis pieces would be able to slide back and forth to account for a change in a stock's size. This baseplate, using the six holes in the middle, would align with the six holes on the work area plate, and have the ability to be fastened down.

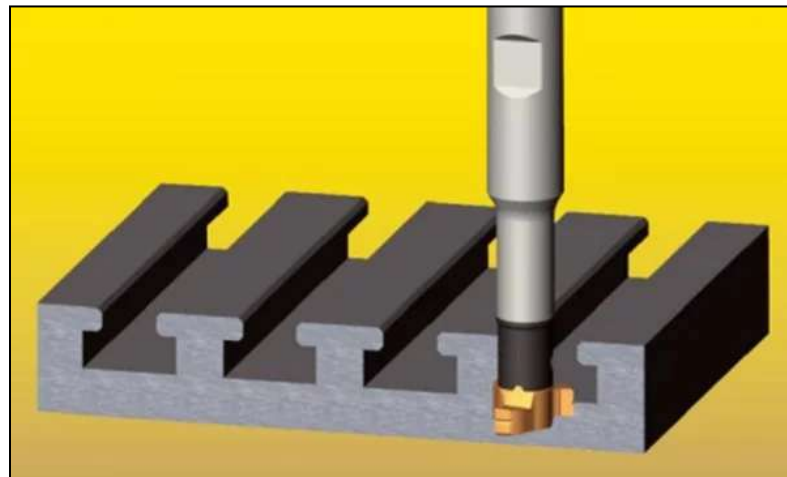
Figure 7.34: CAD Model of First Iteration of the 4th-axis Base Plate Design



The issues with the design came in reference to the manufacturing of the plate. Keeping in mind the open-source nature of the project, concern was raised for the difficulty from milling a slot in at-home CNC machines. To mill a T-slot, which would be required for the design, a special T-slot cutting tool would be required, as shown in Figure 7.35 (Wayken Rapid Manufacturing, 2023). Not only is the process of this milling operation more

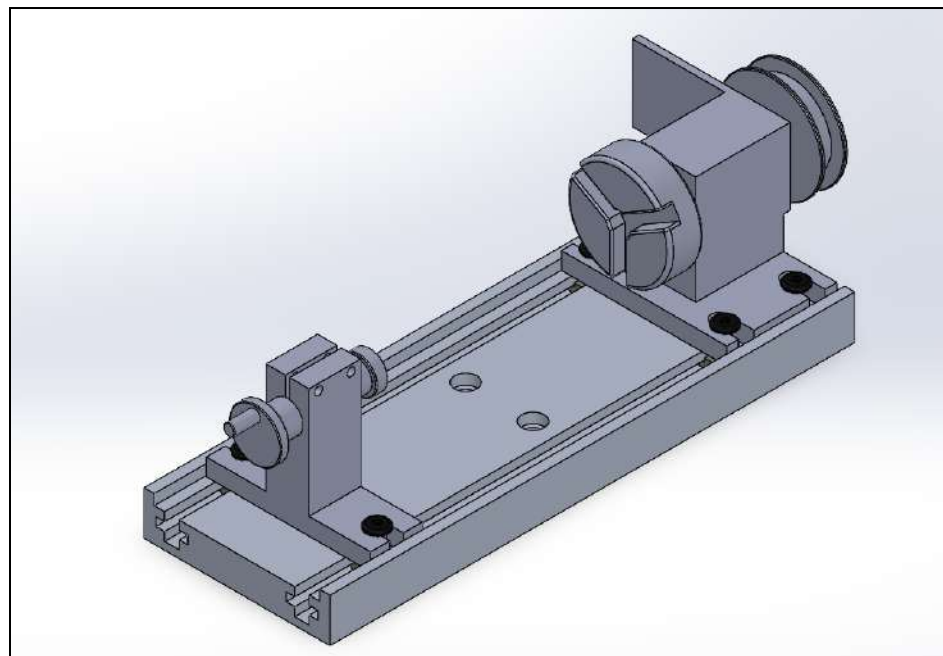
complex, but many machinists lack the resources necessary to complete such an operation. As a result, a new design was developed using holes rather than slots.

Figure 7.35: Example of T-Slotting



Note. Reproduced as is from (Wayken Rapid Manufacturing, 2023).

Figure 7.36: CAD Model of First Iteration of 4th-axis Baseplate with Installed Kit



Unlike the first design, the new iteration would not allow for either the tailstock or chuck pieces to be able to adjust their positions throughout the plate. The array of holes however, as represented in Figures 7.37 and 7.38, allow the tailstock piece to be placed on the plate depending on the length of the stock. This design however, although incorporating a stronger way to fasten all of the components down, was still very bulky.

Figure 7.37: CAD Model of Second Iteration of 4th-axis Base Plate Design

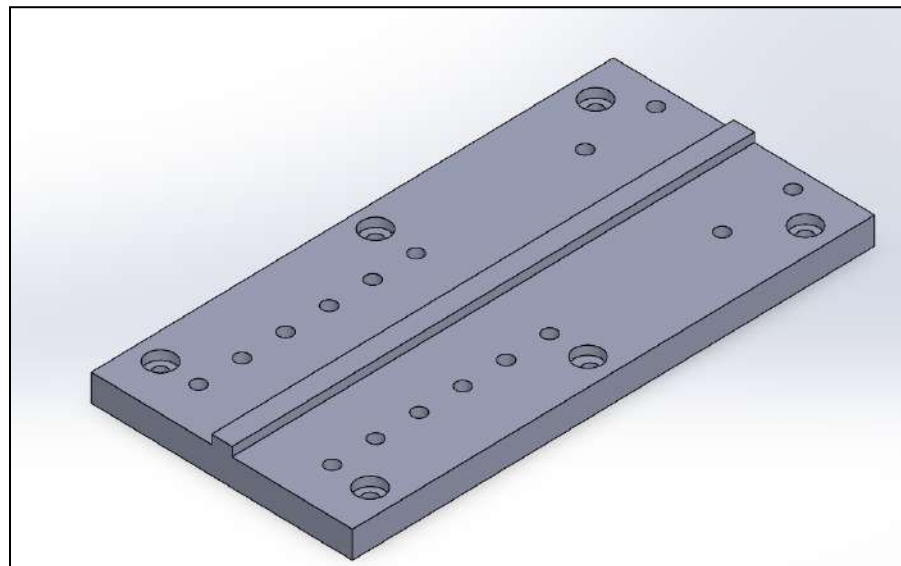
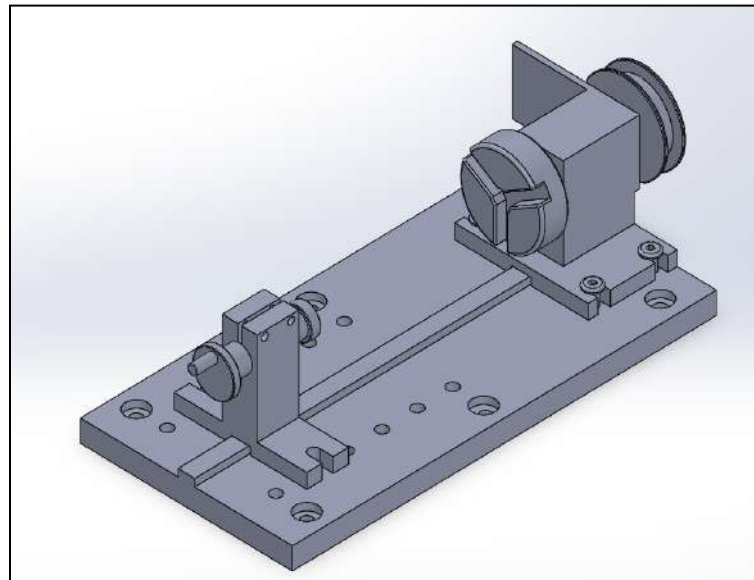


Figure 7.38: CAD Model of Second Iteration of 4th-axis Base Plate Design



When the 4th-axis functionality was being used in the machine, it was assumed that it would act as the primary part clamping down the stock. In doing so, the 4th-axis seemingly replaced itself with the standard clamping vise. With that being said, the additions of the tool changer and bed leveling meant the design needed to be as compact as possible to avoid collision in any way. As represented in Figures 7.39 and 7.40, the width of the plate was shrunk down 33% from 6" to 4". In doing so, it gave the tool changer more flexibility on where its placement would be. The reduction in the width of the plate meant however that the mounting holes for the baseplate to fasten to the work area plate needed to move inwards towards the center.

Figure 7.39: CAD Model of Third Iteration 4th-axis Base Plate

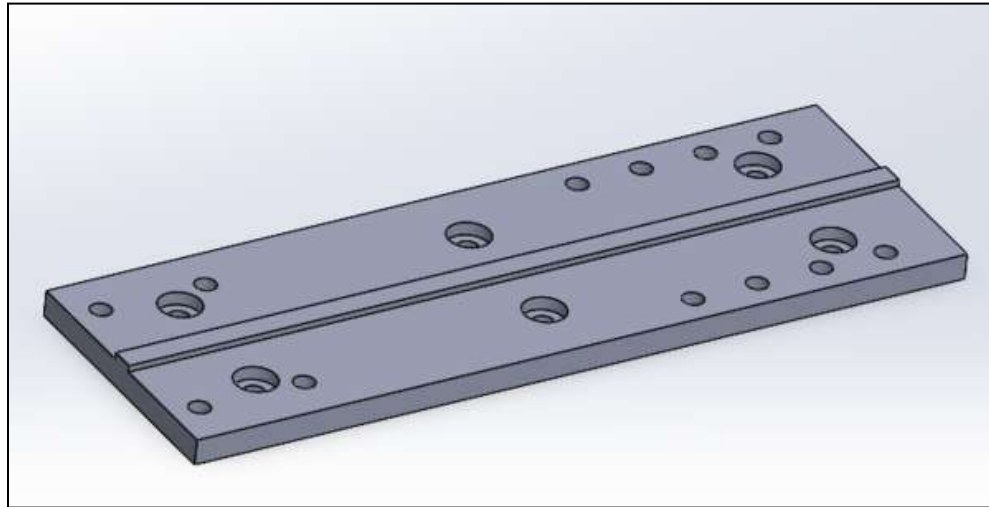
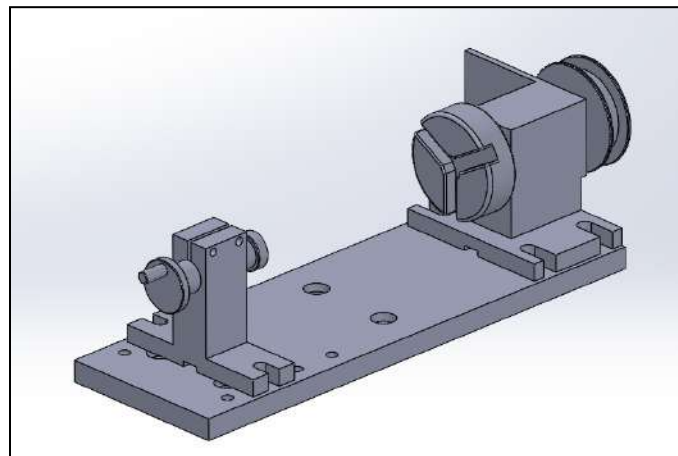
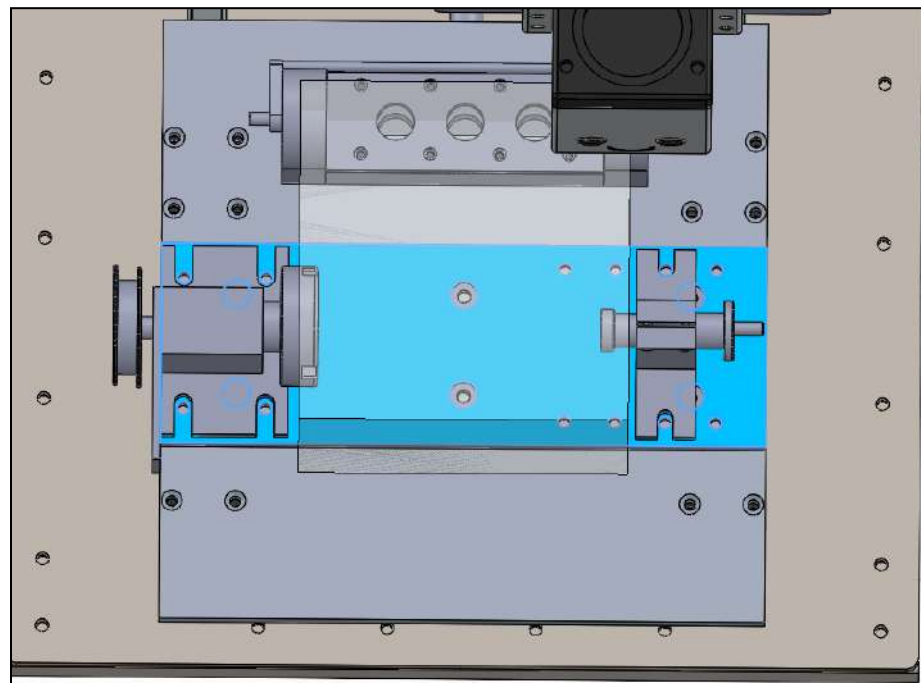


Figure 7.40: CAD Model of 4th-axis Base Plate with Kit Assembly



As shown in Figure 7.41, the decrease in width allows for a comfortable fit of both the 4th-axis and the tool changer in the machine when both are integrated. The rotary piece, located on the left side of the work area plate, sits at the negative-most position in the x-axis of the spindle's workable area. In doing so, when a piece is clamped into the chuck jaws, very little of the workable area is lost as a result, maximizing the 4th-axis' workable area in the x-axis.

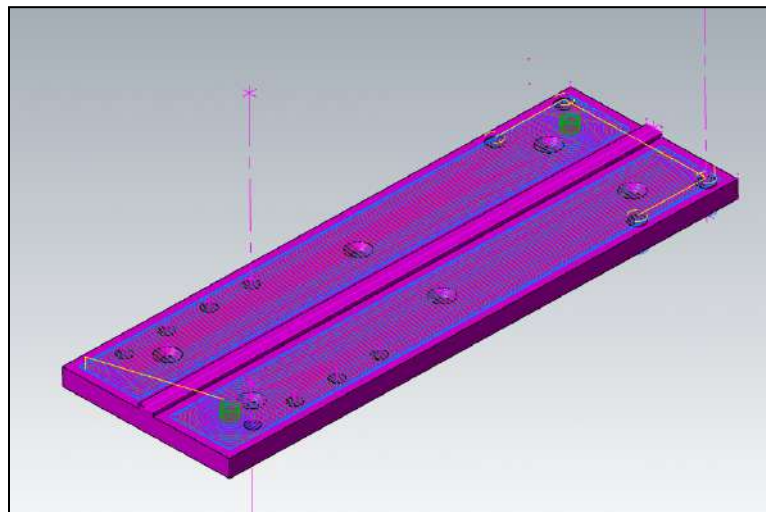
Figure 7.41: Top View of the Machine's Assembly with 4th-axis Integration



The next step in the process was to set up the CAM (Deans, 2021), or Computer Aided Manufacturing for the part. Once a Solidworks file is uploaded to its desired CAM software, toolpaths can be created, and speeds and feeds can be set to set up a cnc machine to complete the operation. The CAM, in essence, creates a line of code detailing what the machine must do to ensure the part comes out exactly like the CAD model.

Using MasterCAM (Deans, 2021), the CAM for base plate was produced as shown in Figure 7.42. The first operation involved a facing operation, roughing out two slots to the right and left of the rail. Some CNC milling machines, like the one in Washburn Shops at WPI, only have a spindle work area of roughly one foot. For a piece of stock required to be at least 12" like the 4th-axis baseplate, it is important to consider how that stock will be mounted to the plate before it is put into the machine.

Figure 7.42: CAM Tool Path View of 4th-axis Base Plate Using Mastercam



The second operation involves drilling, involves the cutting of the holes for all of the baseplates fixturing. Since each of the holes are clearance holes, no extra operations were required other than the peck drill and slot drill for each of the holes. To make sure the 4th-axis system keeps square with the machine's work area plate, it is important that the holes on the 4th-axis baseplate align with the holes on the work area plate. If the 4th-axis is off by even a marginal angle, all parts milled on the 4th-axis will be inaccurate and out of tolerance.

Using SendCutSend, the finalized CAD for the baseplate part was sent off and waterjet cut out. When the part was received, there was an issue with the spacing of the holes on the baseplate for the mounting of the chuck piece. Since the four holes were too close to the center, a screw could not fit into the holes of the chuck piece and go through the baseplate. This meant new holes were required to be able to fasten everything down. With the thinnest machinable wall thickness of aluminum being 0.02" (Ye, 2024), the holes were

adjusted and placed to ensure the chuck piece still could clamp effectively (Figure 7.43).

With this adjustment to the plate, the system was complete and ready to be assembled for testing.

Figure 7.43: Refitting of Holes on 4th-axis Base Plate to Align the Holes with the Chuck Piece



7.4 Bed Leveling Functionality

The design of the bed leveling was intended to be as simplistic as possible, while meeting the goal of maintaining a height variance of <0.005" in the z-direction when moving from limit switch to limit switch along the x- and y-axes. The general approach was to enable each corner to be lifted up independently, and done so with a high level of

accuracy. The method used to align a C02 engraving laser was determined to be the optimal option (Epilog Laser, 2013).

Set screws are used to fine-tune the reflective mirrors in laser engravers, which generally have tolerances within 0.0001". However, they do not sustain any forces, so a way to lock in the accuracy after making an adjustment needed to be implemented. Since the bed was already mounted down at five positions, these locations would be the optimal for placing the adjustment set screws: after a height adjustment, the surrounding flat-head screws could tighten the plate into the adjusted position. The set screws were therefore placed centered within each of the four flat head screws at each of the five mounting points shown in Figures 7.44 and 7.45 below.

Figure 7.44: *The Location of Each of the Five Set Screws Centered Within the Four Mounting Flat-Head Mounting Screws*

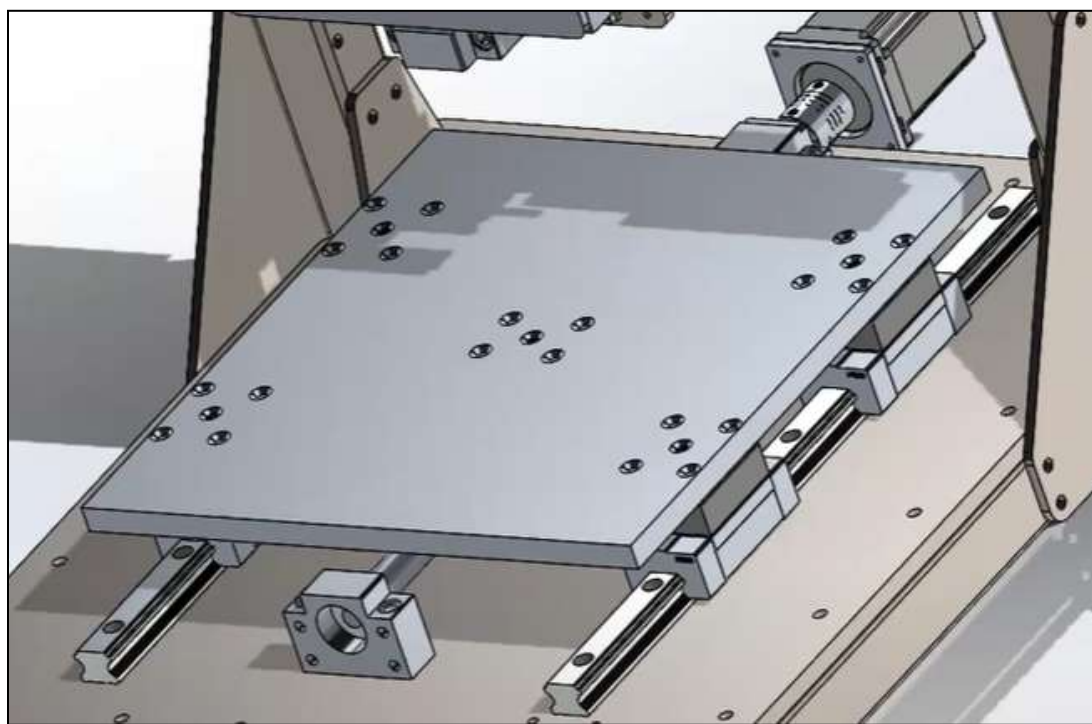
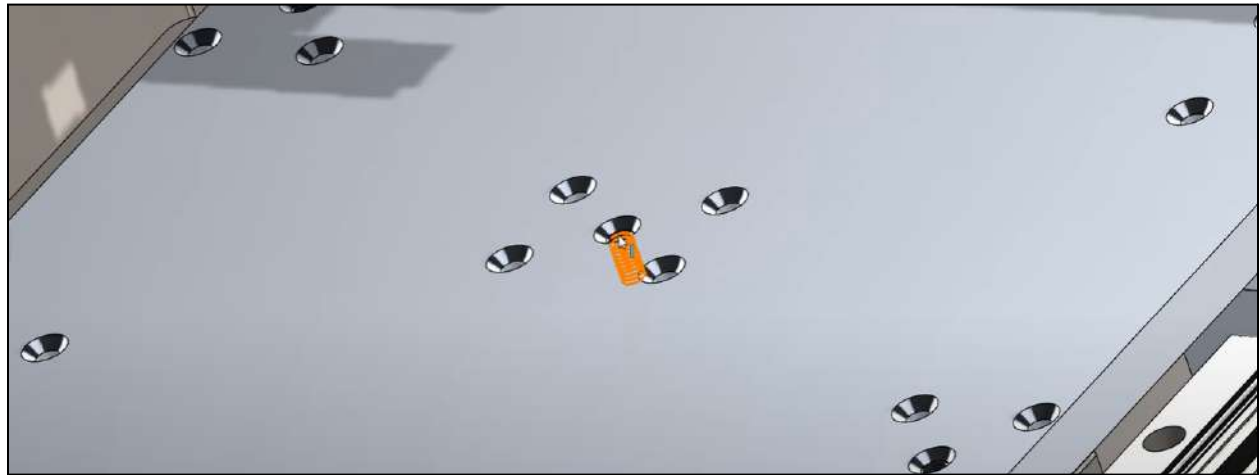


Figure 7.45: Image of a Threaded Set Screw Hole



To ensure that the set screw did not dig into the aluminum mounting blocks that the mounting bolts thread into, the decision was made to install a stainless-steel plate for the set screw to press into (Figure 7.46). This increase in material strength ensured that the set screw would keep the plate lifted up by the amount of adjustment when the flat-head screws are tightened back down. Furthermore, oval-tipped set screws (Figure 7.47) were used to ensure a smooth contact surface between the set screw and the plate, aiding in preventing gouging of the stainless-steel set-screw plate.

Figure 7.46: Image the Set Screw Stainless Steel Plate Location

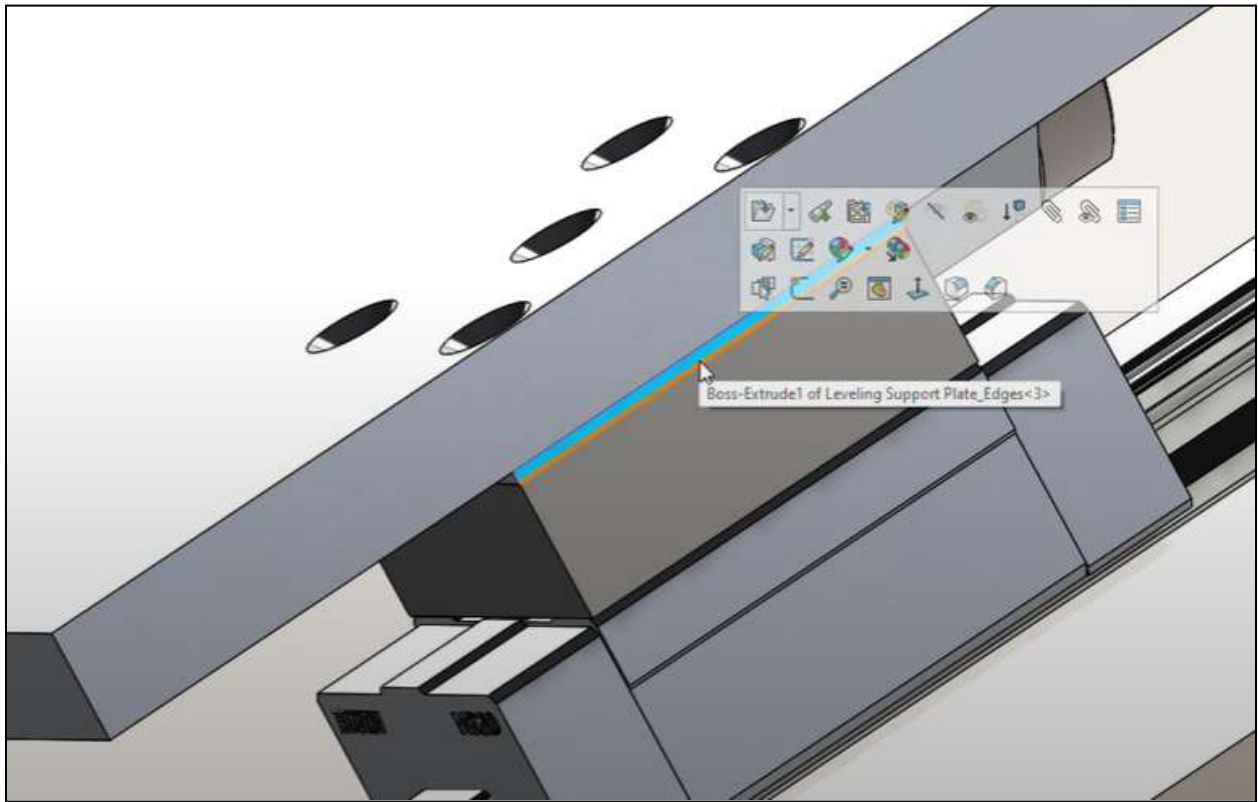
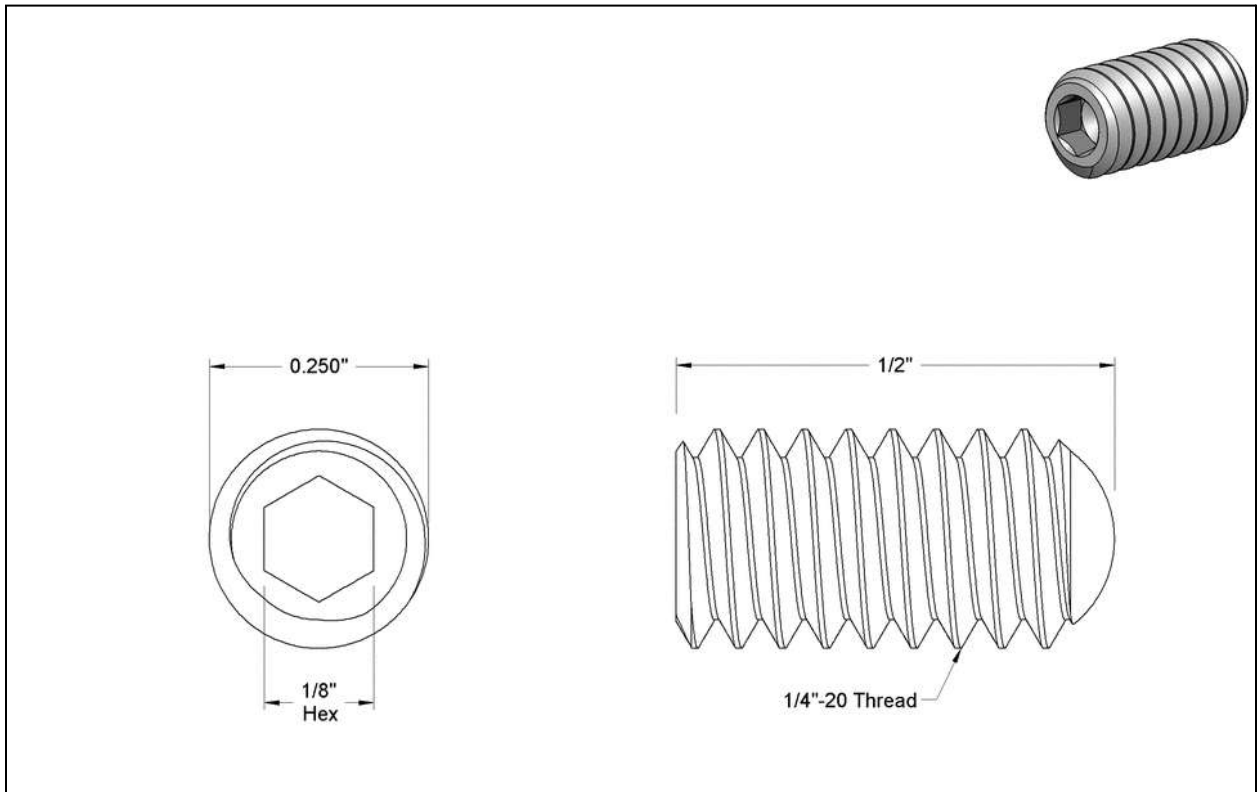


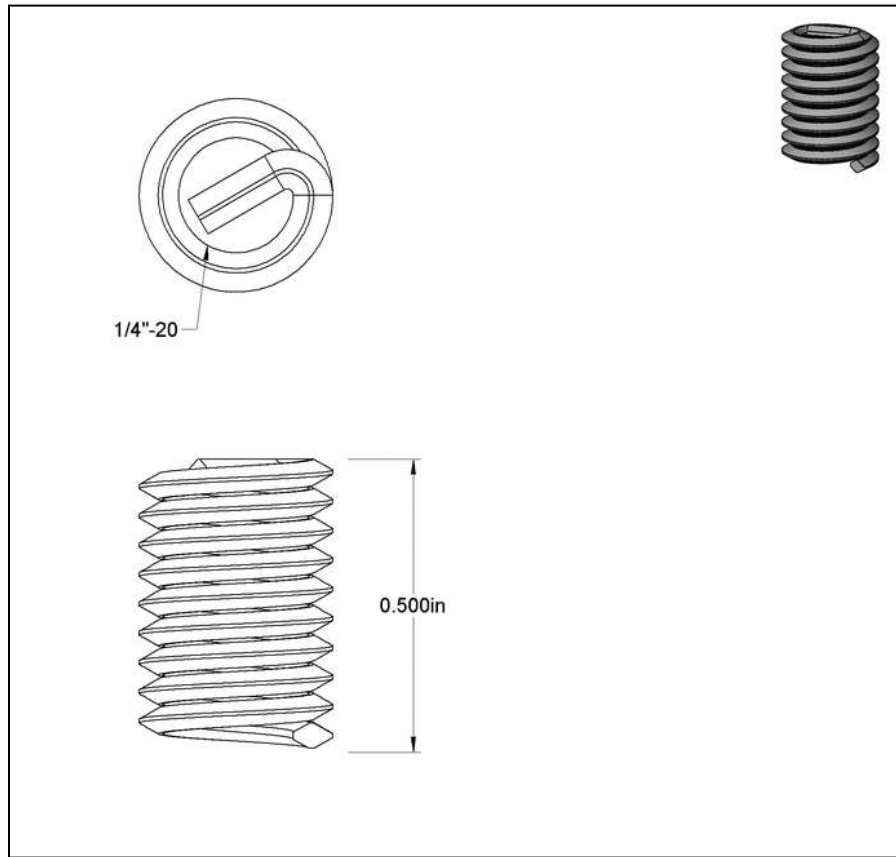
Figure 7.47: Image the Oval-Tipped Set Screws Used



Note. Reproduced as is from (McMaster-Carr, 2019).

The largest diameter set screws available were $\frac{1}{4}$ ". To increase the amount of surface area engagement of threading in the aluminum bed, stainless steel helicoils were used (Figure 7.48). With greater-surface area engagement, a higher amount of torsion could be applied to the set screw threads. In addition, the stainless-steel material of the helicoil would reduce friction against the rotating set screw, thereby reducing galling of the threading against the stainless-steel set screw in subsequent bed leveling after the initial setup.

Figure 7.48: Image of the Stainless-Steel Set Screws Used for Bed Leveling



Note. Reproduced as is from (McMaster-Carr, 2019).

To ensure that the plate would be held down properly and also not strip out the helicoil, the respective calculations were considered. The first step was to determine the tensile strength of the 6061-aluminum work-area bed, since this is where the threading would fail due to 6061 aluminum's Young's modulus of 69 GPa being weaker than stainless steel's value of 200 GPa (Table 7.2).

Table 7.2: Values Used for Determining the Optimal Material for the Bed Material

Factors			
Benefit	6061 Aluminum	2024 Aluminum	304 Stainless Steel
Yield Strength (psi)	35000	47000	40000
Young's Modulus (GPa)	69	73	200
Price	\$62.03	\$298.20	\$519.99
Machinability	Excellent	Excellent	Poor
Flatness	Poor	0.005"	0.005"

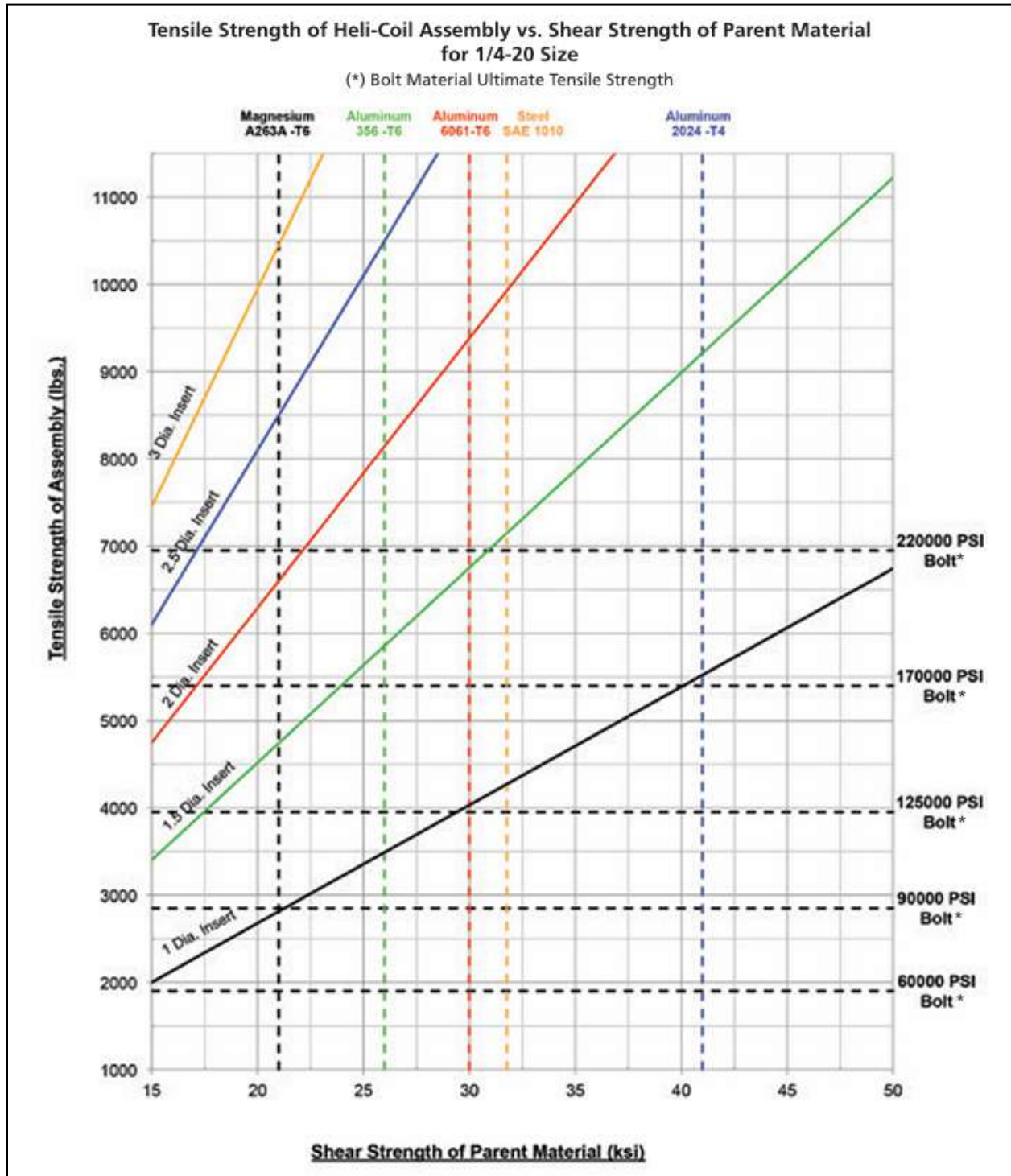
Note. Source for values (The Engineering ToolBox, 2003).

To determine the tensile strength of a $\frac{1}{4}$ "-20 helicoil with a length of the entire thickness of the bed, which is $\frac{1}{2}$ ", the chart in Figure 7.49 was used. The intersection of the red line of the parent material (6061 aluminum on the independent axis) with the length of the helicoil shows the tensile strength that the threading in the bed can withstand. The length of the helicoil was calculated using the following basic formula:

$$\left(\frac{1}{2}''\right) / \left(\frac{1}{4}''\right) = 2$$

Therefore, the helicoil insert can withstand a tensile strength of over 9000 lbs before stripping out of the aluminum bed. This value was then reduced down to 6700 lbs, to be on the safe side—any force up to 6700 lbs should theoretically hold without any risk of failure.

Figure 7.49: Image Chart for Determining Tensile Strength of a Heli-Coil Assembly



Note: Reproduced as is from (Stanley, 2025).

To determine the torque that could be applied to the set screw, the following formula was used ((The Engineering Toolbox), 2003):

$$\text{torque in.- lb} = k * \text{axial force} * \text{diameter} * \left(1 - \frac{\text{lubrication factor}}{100}\right)$$

This formula and the values for each variable were entered into MATLAB, to allow for flexibility if future torque calculations for threading were needed (see Appendix A). The output result was that the set screw could withstand over 335 in.-lbs of torque. This value was then reduced to 200 in.-lbs, again to minimize the risk of failure to near zero. The 200 in.-lbs value was then divided by four to determine that a torque of 50 in.-lbs could be safely applied to each flat-head screw. This would ensure that the set screw would not strip out, and the bed would be mounted with:

$$200 \text{ in.- lb} * 5 = 1000 \text{ in.- lb}$$

This combined torque of 1000 in.-lbs is sufficient to withstand the milling forces of 20 lbs (Brown et al., 2024, pp. 32-33). These values were tested using a torque wrench, prior to going through with manufacturing the design (Figure 7.50). The test involved installing a $\frac{1}{4}$ "-20 x 0.5" set screw and helicoil in a block of aluminum, as well as threading an additional $\frac{1}{4}$ "-20 x 0.5" helicoil on each side of the set screw. The set screw was threaded into the center helicoil such that its tip protruded above the surface by approximately 0.125". Then a 0.375" x 1" x 6" aluminum bar had two through holes drilled into it; the bar was positioned above the set screw, and two bolts were installed through it and into the helicoils on each side of the set screw. A 0.090" thick stainless steel washer was placed between the set screw and the aluminum bar, to simulate the set screw plate. The bolts were tightened to 100 in.-lbs each, and the bar bent until the torque wrench clicked at 100 in.-lbs. The test showed that when applying 100 in.-lbs to two bolts, the set screw bent the

aluminum and did not have its threads damaged at all: the set screw easily threaded out and back in after the test. This test indicated that the design was sufficient to move forward to the implementation phase as a potential solution for manual bed leveling.

Figure 7.50: *Image of Performing a Proof-of-Concept Test on the Set Screw*



Note. A $\frac{1}{4}$ "-20 set screw and helicoil withstanding enough force to bend a 0.375" x 1" 6061 aluminum length under 200 in.-lbs of force.

7.5 Work Area Plates

The material chosen for the work area plates was 2024 aluminum and this was determined based on five pieces of criteria. Those being yield strength, Young's Modulus, price, machinability, and flatness. A decision matrix was made comparing 6061 Aluminum, 2024 Aluminum, and 305 Stainless Steel on these pieces of criteria (Table 7.3 and Table 7.4).

Table 7.3: Work Area Plate Decision Matrix Value

Value (Scaled to range of 1-10, with 10 being best)			
Benefit	6061 Aluminum	2024 Aluminum	304 Stainless Steel
Yield Strength (psi)	3.5	4.7	4
Young's Modulus (GPa)	3.45	3.65	10
Price	8.06	1.68	0.96
Machinability	10	10	3
Flatness	3	9	9

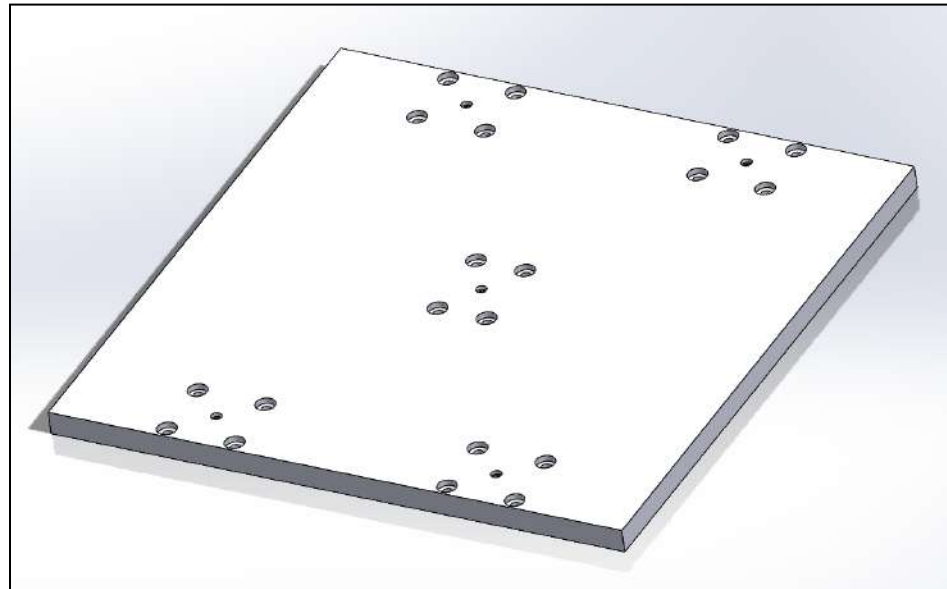
Table 7.4: Work Area Plate Decision Matrix Final Score

Final Score ((Value * Weight of Benefit), with the larger the value the better)			
Benefit	6061 Aluminum	2024 Aluminum	304 Stainless Steel
Yield Strength (psi)	10.5	14.1	12
Young's Modulus (GPa)	24.15	25.55	70
Price	48.36	10.06	5.77
Machinability	80	80	24
Flatness	27	81	81
Total	190.013695	210.7103622	192.7693417

Based on the decision matrix, 2024 aluminum was chosen for its ability to its inherent flatness and its ease of machinability, which was needed in order to attach add-on functionality to it such as the tool changer, vise, and 4th-axis.

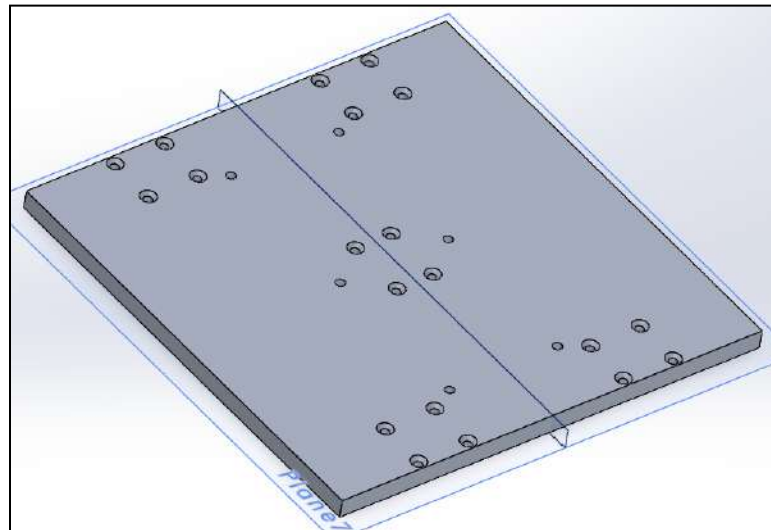
The plate, starting from the previous team's design, had holes for fastening the linear rail and ball screw mounts, as well as their vise (Figure 7.51). With the goal of implementing all functionalities into the machine's plate, spacing of the holes was important as warping and durability concerns grew with the increase in holes.

Figure 7.51: Initial Design of the Work Area Plate with Bed Leveling Helicoils



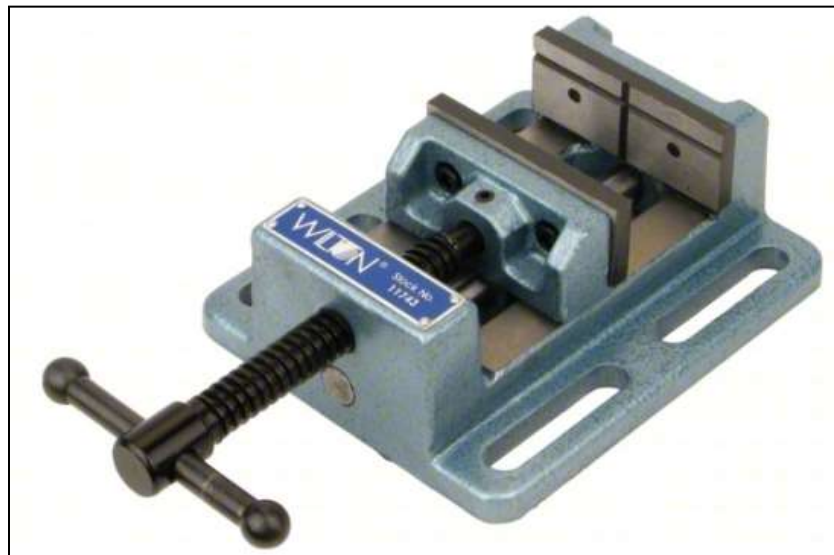
Early design of the work area plate featured holes for the 4th-axis baseplate (Figure 7.52). With the chuck and tailstock pieces being screwed right into the 4th-axis baseplate, the six mounting holes in the work area plate fastened down the 4th-axis to the bed. The holes were placed so when the 4th-axis is into the machine, it runs parallel with the x-axis.

Figure 7.52: Work Area Plate Design with Holes for Initial 4th-axis Base Plate Design



In an effort to increase the size of parts capable of being milled in the machine, a larger vise was swapped out for the 2023-2024 team's model. With a maximum jaw size of 4", the Wilton 4" machining vise was chosen (Figure 7.53).

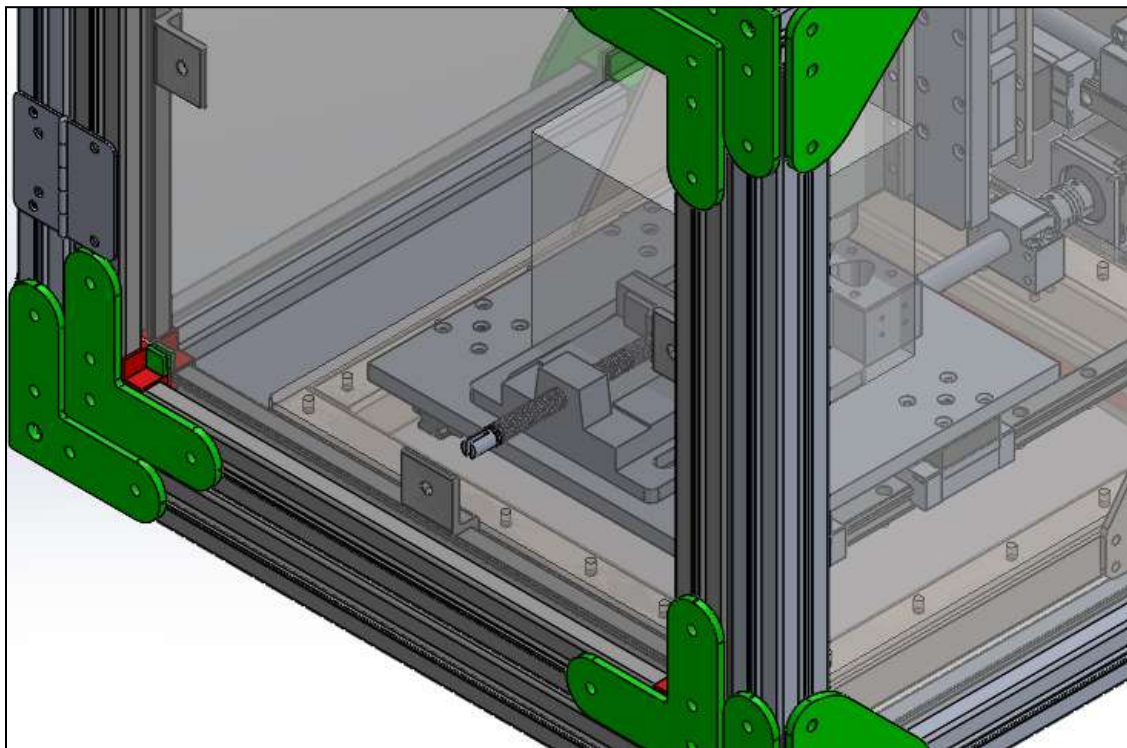
Figure 7.53: Image of Wilton 4" Machining Vise



Note. Reproduced as is from (4 in Jaw Face Wd, 4 in Max Jaw Opening, Machine Vise, n.d.).

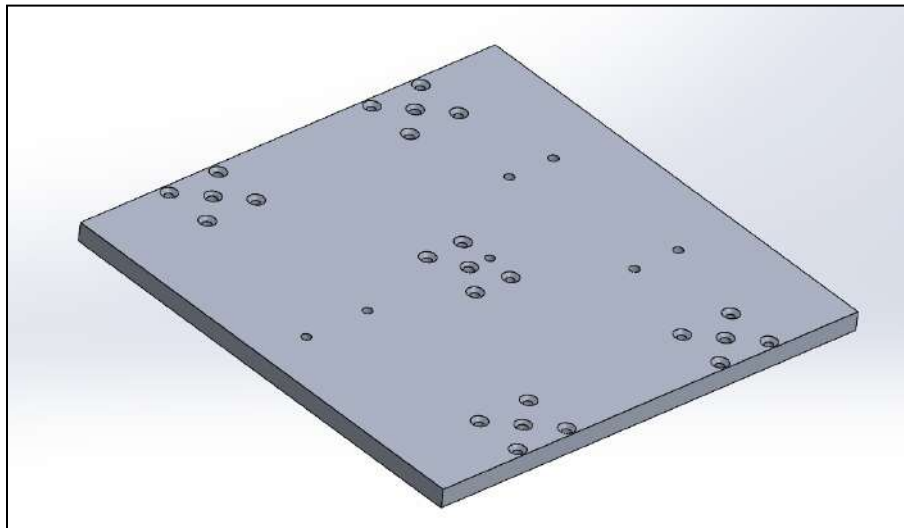
Although the vise has great clamping length, it was too long to be placed parallel to the y-axis. As seen in Figure 7.54, about two and a half inches of the vise's handle sticks out through polycarbonate on the machine's door. As a result, the vise must have been oriented 90 degrees such that the handle for adjusting the jaws was pointing towards the right side of the machine. Doing so made tightening and loosening the clamp much easier as turning the knob from the side made for an easier motion than where it would have been closest to the door.

Figure 7.54: Image Showing Contact of the 4" Wilton Vise with the Door



In an effort to reduce the modifications done on the original work area plate designed by the previous team, only holes for bed leveling, tool changer, and a router vise were placed (Figure 7.55).

Figure 7.55: Final CAD for Option 1 of the Work Area Plate



To provide options for clamping, a second work area plate was designed. With many more holes than the first option, the second plate gives users the opportunity to utilize the 4" Wilton vise, and 4th-axis functionality as represented in Figure 7.56. These additions pair with the features found in plate 1 including bed leveling and a tool changer.

Figure 7.56: Final CAD for Option 2 of the Work Area Plate

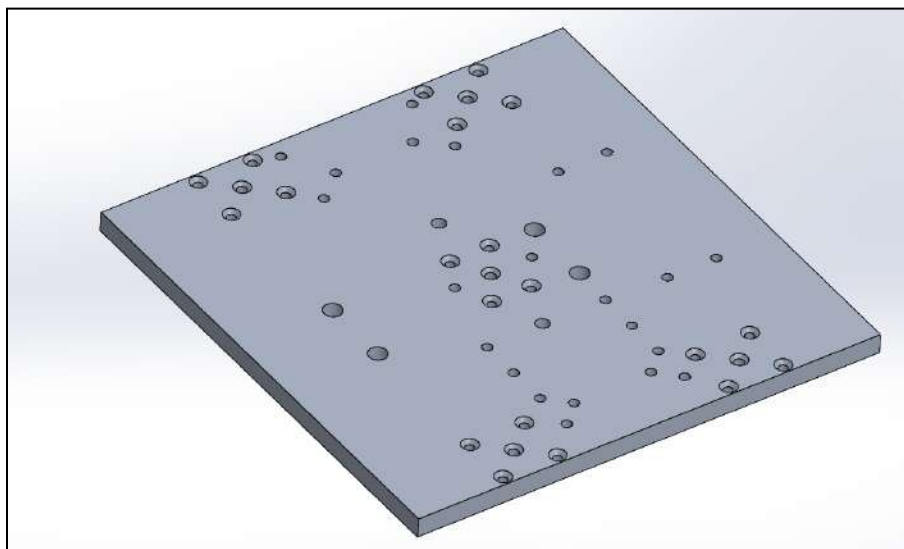


Table 7.5: Machines 1 & 2 Hole Sizes for Work Area Plates

Drilled Hole Type	Type of Hole	Screw for Hole	Machine
4th Axis Mounting	Tapped Hole	M6 - 1	Just Plate 2
Tool Changer Mounting	Tapped Hole	M6 - 1	Plates 1 and 2
Linear Rail Mounting	Clearance Hole	M5	Plates 1 and 2
Bed Leveling Helicoil	Tapped Hole	1/4" - 20	Plates 1 and 2
4" Wilton Vise	Tapped Hole	7/16" - 14	Just Plate 2
Foxalien Router Vise	Tapped Hole	M5 - 0.8	Just Plate 1

Although both work area plate designs differ in functionality, the diverse nature of the plates offers a sense of modularity to users. Depending on what a user is looking to get out of their machine, they have the option to implement functionality most relevant to them. Once the base model of the plate is formed including the holes for fastening the linear rail and ball screw mounts, any combination of additional functionality can be provided.

7.6 Enclosure Design

The following sections cover the design choices and strategies that the team used to create and manufacture the updated enclosure.

7.6.1 Enclosure Guarding

The group looked at different plastic options for the guarding, comparing polycarbonate, acrylic, PETG (polyethylene terephthalate glycol), and Tuffak. OSHA regulations 29 CFR 1910.212(a)(2), 1910.212(a)(3)(iv)(e), 29 CFR 1910.212(a)(3)(ii) require machine guarding to be placed on the machine wherever possible and at the point of operation to keep the operator from having any part of their body in the danger zone or work area. From this, the team deemed impact strength, tensile strength, and corrosive resistance

to be the most important properties to consider. Impact strength is a material's ability to resist fracture and cracking under a sudden force (McClements, 2023), this property is the most important when considering that a broken cutting tool or an incorrectly fixtured part can travel at high speeds into the guarding. Additionally, the tensile strength is a material's resistance to stretching under a load (McFadden, 2020), a high tensile strength value can ensure that the guarding does not deform significantly after enduring a large impact. Lastly, as the guarding will encounter spray from coolant while machining, the material must be resistant to corrosion as to not change in property or shape due to prolonged contact with the machining coolant.

7.6.2 Filament Selection

As the group planned to use 3D prints to outfit areas of the machine, several different plastic filaments were considered for implementation in structural and gasket applications, see Tables 7.6, 7.7, and 7.8. When considering usage for structural applications, the team decided to take into consideration the mechanical properties of ultimate tensile strength, yield strength, and Young's Modulus. The ultimate tensile strength measures the maximum stress a material can withstand when stretched or pulled before breaking (Ahmed, 2023); the external frame brackets of the enclosure will experience pulling forces if the panels or t-rails are pushed or shaken in any way. The yield strength is the stress at which a material begins to deform plastically (de Naoum, 2023). For the brackets, a relatively high yield strength would be desired as any inclination of plastic deformation would mean that the structure is no longer secure. Young's Modulus measures the stiffness of a material in response to uniaxial tensile or compressive stress (*Understanding Young's Modulus*, 2020). The brackets in the new design would need to

have a high Young's Modulus, however it should be noted that a high Young's Modulus value represents a more brittle material.

Table 7.6: Filament Material Properties

Filament	Tensile Strength (MPa)	Yield Strength (MPa)	Young's Modulus (MPa)	Cost
PLA	59	70	3500	\$13.00
PETG	50	40	2200	\$13.00
TPU	37	No yield	67	\$22.00
Polycarb	77	61	2300	\$40.00
Nylon	48	69	1100	\$30.00

Table 7.7: Filament Design Matrix (PLA & PETG)

Criteria	Weight (1-5)	PLA	PLA (Weighted)	PETG	PETG (Weighted)
Tensile Strength	4	4	16	4	16
Yield Strength	5	4	20	3	15
Young's Modulus	3	5	15	3	9
Cost	2	5	10	5	10
Total		18	61	15	50

Table 7.8: Filament Design Matrix (TPU, PC, Nylon)

Criteria	Weight (1-5)	TPU	TPU (Weighted)	PC	PC (Weighted)	Nylon	Nylon (Weighted)
Tensile Strength	4	3	12	5	20	4	16
Yield Strength	5	5	25	3	15	4	20
Young's Modulus	3	1	3	3	9	2	6
Cost	2	3	6	1	2	2	4
Total		12	46	12	46	12	46

7.6.3 New Enclosure

The new designed enclosure has an increased focus on sealing, serviceability, and security. The new design, as seen in Figure 7.57, is 23.01" in length, 26.41" in width, and 26.20" height. It utilizes 3D-printed brackets to hold together the t-rail and the panels, shown in Figures 7.58, 7.59. 3D printed materials were also utilized in the making of the gaskets, panel spacers, and t-rail slot-fillers as well.

Figure 7.57: Full Enclosure Early Design

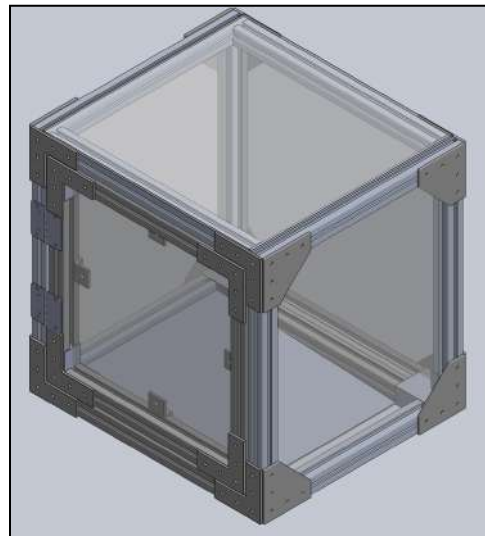


Figure 7.58: Triangle Bracket for Enclosure Frame

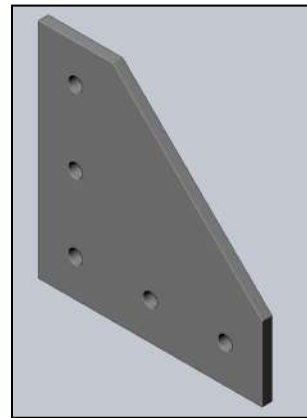
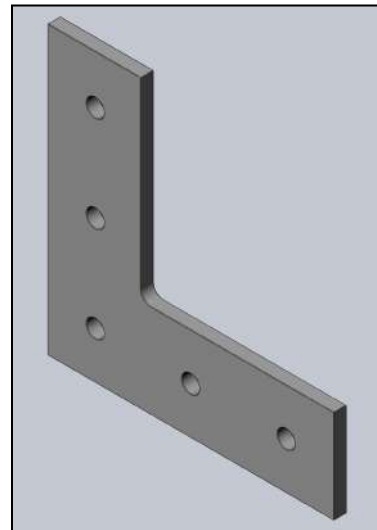


Figure 7.59: Angle Bracket for Enclosure Door Frame

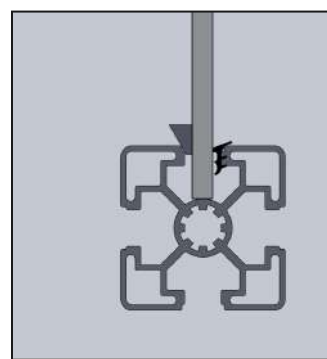


As noted previously, ensuring that there are no leakages in the machine was one of the main concerns addressed with this design. Initially, the polycarbonate panel sitting on top of the table cracked, and was the major proponent of leaking. To counteract this, the group has decided to utilize a 0.002" polypropylene film to cover the bottom of the machine. This material has good corrosion resistance, and will not crack from bolts and nuts being fastened through it due to its plasticity.

Additional components were designed to ensure that coolant does not pool up and leak from areas above the bottom of the table. T-rail corner connector gaskets were designed and printed to ensure that empty spaces would be filled if any misalignment occurred while fastening the t-rail framing the enclosure. T-rail slot-filters were printed to place in the slot of the t-rail, and they prevent coolant from pooling up; this allows for a majority of the coolant to return back to the coolant reservoir.

Mounting of the panel needed to be robust enough to ensure that coolant leaks would not occur, while also providing an easy opportunity to service the machine if necessary. The design for mounting required two additional pieces to help secure the panel in place. As seen in Figure 7.60, a 3D printed wedge-shaped spacer would be used to push the panel to the wall of the slot that is closest to the machining area. This would aid in creating a tight seal with the panel and the rubber gasket, also depicted in Figure 7.60. Since no caulk or adhesives are required to put together this design, removing a panel to work inside the machine involves removing the wedge spacer, gasket, and the upper t-rails of the enclosure.

Figure 7.60: *T-rail with Panel Cross Section*



Furthermore, a ramp has been implemented to the design to create a focal point for coolant to drain from the system, shown in Figure 7.61. The material of the ramp was

chosen to be ABS plastic, due to its high corrosion resistance and its high impact strength (*ABS Plastic Properties | Advantages Of Acrylonitrile Butadiene Styrene*, 2022). These properties were chosen to be of highest importance as the ramp would constantly be subjected to flood coolant, and will not easily crack which would introduce coolant leaks into unserviceable areas. The ramp is supported through a 3D printed ramp standoff as shown in Figure 7.62, which requires the ramp to be pushed into the slot.

Figure 7.61: Coolant Ramp

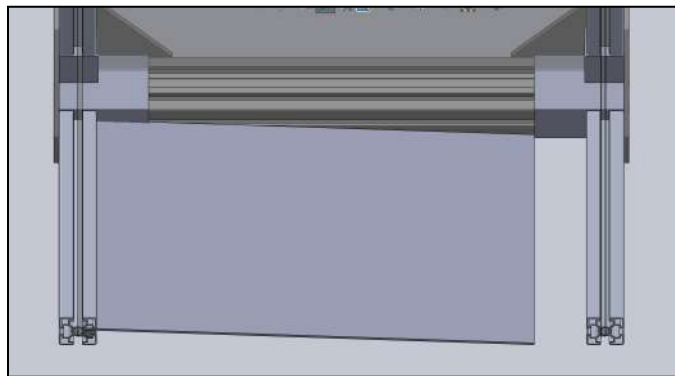
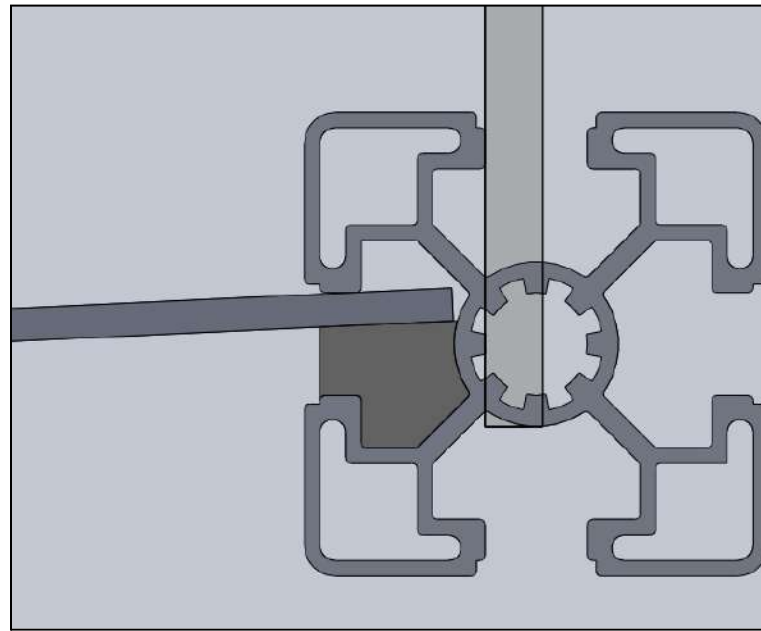


Figure 7.62: Ramp Standoff Cross Section



Additionally, the new enclosure design features a hinged door with an interlocking switch. The door's panel is configured in the same way as the other panels of the machine, with a rubber gasket and wedge spacer ensuring stability and sealing. The door is outfitted with a neoprene foam strip around its perimeter to create a seal and stop leaks when it is closed. The style foam chosen has a NEMA 4X rating, preventing liquid from leaving the enclosure (Polycase, 2021). This door design allows for easy access into the machine, and can be taken off the machine by simply unscrewing the four bolts holding the hinges to the enclosure's t-rail.

To ensure a safe operating procedure, the door is equipped with a latch and reed switch system. Per OSHA regulations, it is imperative that the door remains closed at all times during operation. The reed switch's connection is completed if the latch is in the down position; the only way to accomplish this is to have the door closed. The reed switch allows for the machine to be operational only if the door is closed, ensuring standard operating

procedures are followed. This prevents the risk of the door swinging open while the machine continues its cutting operations. All parts for the safety latch were designed to be machined and cut on the CNC mill.

7.7 Coolant Design

Machining coolant is necessary for machining metals, such as aluminum and steel, to prevent chip welding and spindle overheating. The group decided to use the same coolant delivery system (a 5-gallon bucket, water-based coolant, a submersible pump, a hose with barbed fittings, and a coolant nozzle) as the previous MQP team (Brown et al., 2024).

While flood coolant is being sprayed inside the machine, all of the coolant delivered needs to be efficiently returned to the coolant reservoir (5-gallon bucket) and all of the chips need to be flushed away with the coolant, separated from the coolant, and accumulated at a known location that can be easily accessed for regular maintenance. The group solved this design problem by implementing a ramp underneath the gantry base that directs coolant and chips that spill over the gantry to the right-hand side. On the right-hand side the coolant drains through a hole in the table fitted with a PVC pipe and the chips accumulate on top of a steel wire mesh that covers the drain hole. Finally the coolant in the PVC pipe returns to the bucket under the table ready to be pumped back onto the work area.

7.8 Lockout-Tagout

This year's machine's lockout-tagout system follows all the rules laid out by OSHA. The plugs for the VFD and the AC to DC converter are stored in a lockout box that is stored behind a key box only accessible by the team (Figure 7.63). The lockout box is clearly labeled, and will be replaced if any hinge or other component breaks. The machine cannot be powered while these plugs are isolated. Any users of the machine are instructed to

remove the two indicated plugs from their sockets and store them within the lockout box when the machine is not in use.

Figure 7.63: Lockout Box Containing Both Plugs



The new machines improve dramatically upon the mechanical design sphere from last year's project in terms of the vacuum system, tool changer, 4th-axis, bed leveling, and hardware design of the gantry and enclosure. In aspects that previously existed, the functions work better, in addition to several physical systems new to this year's project.

8.0 Electronics and Software Updates

In order to update the machine to the new control system, there were several updates that were designed. This included system analysis, circuit design, and software design. These designs improved the safety of the machine, the user interface, and added new features compared to last year's machine.

8.1 Final Control System

To decide which control system to use, which includes the control board, low level firmware/software, and user interface software, factors included what features were available, the cost, and many other aspects. To evaluate the requirements of the new CNC machine, a design matrix was created to objectively decide the best control system.

8.1.1 Control System Criteria

The user interface control software considered were Mach3, LinuxCNC, bCNC, CNCJS, and UGS. The control boards that were considered were the Keenso control board used by the original CNC mill, the 7I96S Mesa card, parallel port breakout board, PicoCNC/TeensyBoB, and AOLDHYY board. The Keenso board was only compatible with Mach3, the 7I96S Mesa card was only compatible with LinuxCNC, a parallel port breakout board (BoB) was compatible with Mach3 and LinuxCNC, the PicoCNC/TeensyBoB was compatible with grblHAL with limited functionality with grbl, and the AOLDHYY board was compatible with grbl and with limited functionality grblHAL.

Choices between the user interface control software needed to be evaluated since this directly relates to the control board that would be available to choose from. These were evaluated by operating system (OS) support, cost for the software, compatibility for

4th-axis, compatibility for tool changer, general ease of use, installation ease of use, z-probing, custom module creation, hardware resource requirements, and software bed leveling functionality (Table 8.1). Each board was evaluated with these scores, with weighted criteria to give final unweighted and weighted scores for each control software (Tables 8.3 and 8.4). Based on the evaluation criteria, the best control software in order from best to worst were UGS, bCNC, CNCJS, LinuxCNC, and Mach3.

Table 8.1: Control Software Decision Matrix Criteria

Category & Scoring	Criteria
OS Support (Cumulative)	4 points: Windows 10/11 1 point: MacOS M chips 1 point: MacOS Intel chips 2 points: Raspberry Pi Computer 4/5 1 point: Windows 9/8/7 1 point: Linux
Software Cost (Absolute)	10 points: Free 9 points: \$0-\$25 8 points: \$25-\$50 7 points: \$50-\$75 6 points: \$75-\$100 5 points: \$100-\$125 4 points: \$125-\$150 3 points: \$150-\$175 2 points: \$175-\$200 1 points: >\$200
4th Axis (Absolute)	10 points: Supports 4th axis 0 points: Does not support 4th axis
Tool Change (Cumulative)	3 points: Fully automatic 2 points: Manual touch off 2 points: Manual 3 points: Supports custom implementation
General Ease of Use (Cumulative)	1 point: Moveable modules 1 point: Hover hint boxes 1 point: Well documented online resources 1 point: Keyboard/External hardware shortcuts 1 point: GCode editor/Visualizer 1 point: Can be controlled for basic use only by mouse 1 point: Clean main interface 1 point: Clear indicators (Important statuses, colored indicators, etc.) 1 point: Pre movement toolpath/spindle simulation 1 point: 3D model navigation of tool path
Installation Ease of Use (Absolute)	10 points: Install on all existing OS's 9 points: Install on all existing OS's with small amount of work 8 points: Install on one OS

Category & Scoring	Criteria
	7 points: Install on one OS with slight setup, Install on all OS's with significant setup 6 points: Install on one OS with significant setup 5 points: Install new OS 4 points: Install new OS with small amount of setup 3 points: Install new OS with significant amount of setup 2 points: Install new OS without GUI 1 point: Install new OS without GUI with significant amount of setup
Z-probing (Absolute)	10 points: Supports Z-axis probing 0 points: Does not support Z-axis probing
Custom Modules (Cumulative)	3 points: Well documented 1 point: Not well documented 3 points: Easy for others to install 1 point: Not easy for others to install 2 points: Read data from control board 2 points: Custom graphics view (ie. drawable)
Resource Requirements (Cumulative)	4 points: 0MB-512 MB RAM 3 points: 512 MB-1 GB RAM 2 points: 1 GB-2 GB RAM 1 point: >2 GB RAM 3 points: 0 GHz-1 GHz CPU clock speed 2 points: 1 GHz-2 GHz CPU clock speed 1 point: >2 GHz CPU clock speed 3 points: Integrated GPU 1 point: Dedicated GPU
Software Bed Leveling (Absolute)	10 points: Full auto leveling of bed 5 points: Community extension for auto leveling 3 points: Use gcode ripper (or similar external program) to level bed 0 points: Not supported

Table 8.2: Control Software Decision Matrix for Mach3, LinuxCNC, and bCNC

Criteria	Weight (1-5)	Mach3	Mach3 (Weighted)	LinuxCNC	LinuxCNC (Weighted)	bCNC (Grbl & GrblHAL)	bCNC (Weighted)
OS Support	2	4	8	3	6	9	18
Cost	5	2	10	10	50	10	50
4-axis	1	10	10	10	10	8	8
Tool Change	2	10	20	10	20	5	10
Ease of Use (EOU)	5	7	35	7	35	6.5	32.5
Installation EOU	4	8	32	4	16	7	28
Z-probe	2	10	20	10	20	10	20
Custom Modules	3	10	30	8	24	8	24
Resource Requirements	3	10	30	7	21	10	30
Autolevel	2	3	6	3	6	10	20
Total		74	201	72	208	83.5	240.5

Table 8.3: Control Software Decision Matrix for CNCJS and UGS

Criteria	Weight (1-5)	CNCJS (Grbl)	CNCJS (Weighted)	Universal Gcode Sender (Grbl & GrblHAL)	UGS (Weighted)
OS Support	2	10	20	10	20
Cost	5	10	50	10	50
4-axis	1	0	0	10	10
Tool Change	2	5	10	5	10
Ease of Use (EOU)	5	6	30	8.5	42.5
Installation EOU	4	7	28	9	36
Z-probe	2	10	20	10	20
Custom Modules	3	10	30	8	24
Resource Requirements	3	10	30	8	24
Autolevel	2	5	10	10	20
Total		73	228	88.5	256.5

For the low level control board, it had to be evaluated since many features, such as 4th axis, tool changing, etc. are determined by the capabilities for the hardware and the low level software for it. The boards were evaluated based on cost, cost for using a Raspberry Pi computer (for onboard computing instead of requiring dedicated laptop/desktop), 4th-axis support, tool change support, spindle speed control support, and z-probe support (Table 8.4). Each board was evaluated using these scores, with weighted criteria to give final unweighted and weighted scores for each control board (Tables 8.5 and 8.6). Based on the evaluation of the criteria, the control boards from best to worst were PicoCNC, grblHAL-Teensy, Keenso, 7I96s, desktop parallel connection, Raspberry Pi 4 with parallel adapter, Raspberry Pi 5 with parallel adapter, and AOLDHYY.

Table 8.4: Control Board Decision Matrix Criteria

Category & Scoring	Criteria
Cost (Absolute)	10 points: Free 9 points: \$0-\$25 8 points: \$25-\$50 7 points: \$50-\$75 6 points: \$75-\$100 5 points: \$100-\$125 4 points: \$125-\$150 3 points: \$150-\$175 2 points: \$175-\$200 1 points: >\$200
Cost with Raspberry Pi Computer (Absolute)	10 points: Free 9 points: \$0-\$25 8 points: \$25-\$50 7 points: \$50-\$75 6 points: \$75-\$100 5 points: \$100-\$125 4 points: \$125-\$150 3 points: \$150-\$175 2 points: \$175-\$200 1 points: >\$200
4th Axis (Absolute)	10 points: Supports 4th axis 0 points: Does not support 4th axis
Tool Change (Cumulative)	3 points: Fully automatic 2 points: Manual touch off 2 points: Manual 3 points: Can be Coded/Added
Spindle Speed Control (Absolute)	10 points: Dedicated board terminals with speed control well documented 8 points: Well documented with adaptive IO terminals 5 points: Dedicated board terminals with speed control not well documented 3 points: Not well documented with adaptive IO terminals 0 points: Not supported
Z-probe (Absolute)	10 points: Dedicated board terminals with speed control well documented 8 points: Well documented with adaptive IO terminals 5 points: Dedicated board terminals with speed control not well documented 3 points: Not well documented with adaptive IO terminals 0 points: Not supported

Table 8.5: Control Board Decision Matrix for Boards Supporting LinuxCNC

Criteria	Weight (1-5)	7196s	7196s	Parallel BoB Adapter	Parallel BoB Adapter	Parallel BoB PCIE	Parallel BoB PCIE	Parallel BoB	Parallel BoB
Cost (Not Raspberry Pi)	3	4	12	0	0	0	0	9	27
Cost (Raspberry Pi)	5	1	5	4	20	1	5	0	0
4-axis	4	10	40	10	40	10	40	10	40
Tool Change	4	3	12	3	12	3	12	3	12
Spindle Speed Control	3	10	30	5	15	5	15	5	15
Z-probe	1	3	3	3	3	3	3	3	3
Total		31	102	25	90	22	75	30	97

Table 8.6: Control Board Decision Matrix for Boards Supporting grblHAL, grbl, and Mach3

		GrblHAL				Grbl		Mach3	
Criteria	Weight (1-5)	PicoCNC	PicoCNC	Teensy	Teensy	AOLDHYY	AOLDHYY	Keenso	Keenso
Cost (Not Raspberry Pi)	3	8	24	6	18	8	24	9	27
Cost (Raspberry Pi)	5	3	15	2	10	4	20	3	15
4-axis	4	10	40	10	40	0	0	10	40
Tool Change	4	3	12	3	12	3	12	3	12
Spindle Speed Control	3	10	30	10	30	5	15	3	9
Z-probe	1	10	10	10	10	3	3	3	3
Total		44	131	41	120	23	74	31	106

8.1.2 Final Control System Evaluation

Based on the positives and negatives of each control system and available features, a decision matrix was used to objectively determine the best system to use. For each control board type, multiple boards were selected to give a wide range of selectable options. The Keenso Mach3 board that last year's team used was also included as a comparative baseline

for the new control systems. First, the control software was evaluated to determine what would be the most user friendly, while also supporting the new desired features (Tables 8.2 and 8.3). Then, the control hardware was evaluated based on supporting new features and cost (Tables 8.5 and 8.6). Finally, combining the correlating control hardware and software, a final decision matrix was constructed to determine the final control system (Table 8.7).

Table 8.7: Final Decision Matrix for Software Control Systems

Combined	Add	Add	Multiply	Multiply	Normalized	Normalized
Mach3 Keenso	105	307	2294	21306	0.5891	0.6341
LinuxCNC 7I96s	103	310	2232	21216	0.5732	0.6314
LinuxCNC Parallel Pi4	97	298	1800	18720	0.4622	0.5571
LinuxCNC Parallel Pi5	94	283	1584	15600	0.4068	0.4643
LinuxCNC Parallel Desktop	102	305	2160	20176	0.5547	0.6004
bCNC PicoCNC	127.5	371.5	3674	31505.5	0.9435	0.9376
bCNC Teensy	124.5	360.5	3423.5	28860	0.8792	0.8589
bCNC AOLDHYY	106.5	314.5	1920.5	17797	0.4932	0.5296
CNCJS AOLDHYY	96	302	1679	16872	0.4312	0.5021
UGS PicoCNC	132.5	387.5	3894	33601.5	1.0000	1.0000
UGS Teensy	129.5	376.5	3628.5	30780	0.9318	0.9160
UGS AOLDHYY	111.5	330.5	2035.5	18981	0.5227	0.5649

Based on the results of the final decision matrix, UGS and grblHAL were chosen as the final control system. This enables development of both the user interface and control hardware based on custom specifications. Both platforms are actively being developed and also support user-installable plugins, enabling users to get the latest versions of the softwares while still supporting custom features. The grblHAL board chosen was PicoCNC. This board is officially supported and developed for the grblHAL platform, integrating four axes, dedicated spindle control, optional ethernet connectivity, sd card interface, and many

more features. The board also includes seven auxiliary outputs, I2C, SPI, and serial communication interfaces to communicate with any custom systems (Barrett, n.d.).

8.1.1 grblHAL

With the firmware being controlled through grblHAL, it is configured much differently to the previous Mach3 solution. All settings are configured and stored when the firmware is built, with only some that are able to be edited afterwards. Settings such as number of axes, number of tools, etc. cannot be changed once the firmware is loaded onto the board. To change them, the source code has to be modified, then the new firmware can be uploaded and the changes applied. Some settings that are modifiable at any time include motor step size, homing directions, speeds, etc. All of these settings are stored on the control board itself, not on the software controlling it. This means that any computer with compatible software can be used to control the machine, without the base settings being altered.

8.1.2 UGS

With the user interface being controlled through UGS, it gives a much more user friendly interface compared to the previous Mach3 solution. All colors and icons are more consistent, windows can be configured based on preference, and the interface is more consistent with modern day standards. While it does not officially have support for grblHAL systems, it does support grbl's systems. This means that some UI elements, such as GCode commands not supported on grbl but with grblHAL, will display as possibly unsupported commands when they are not. Despite this, the user interface does not have any problems running a grblHAL system even with non grbl commands. The interface also supports

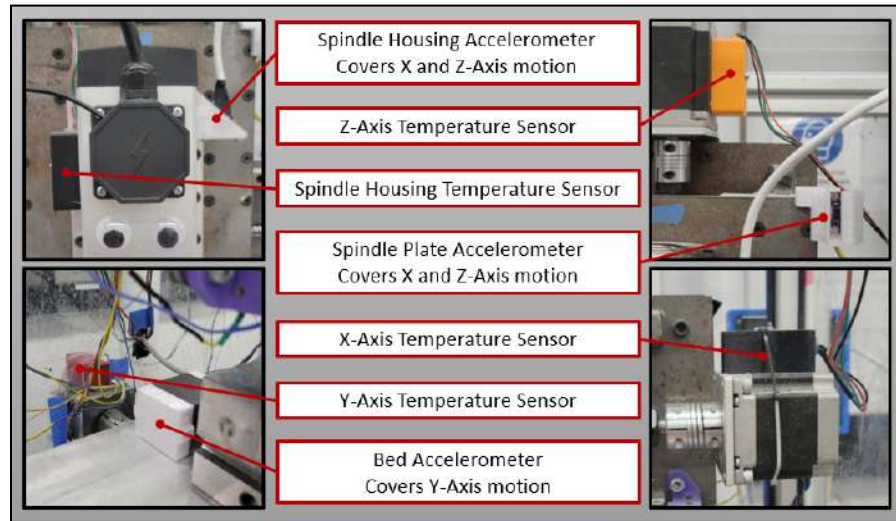
connecting to devices through ethernet and wireless connections, provided they are enabled on connected control boards. This means that while it has a friendly user interface, it also has all the capabilities necessary for basic operation and for future upgrades.

8.2 Sensor Integration

During the process of iterating on the previous CNC machine, predating any updates, the state of the original machine had to be evaluated in order to get a baseline of the original system and to verify that any changes made were not a detriment to the new machine. To do this, various sensors were attached to the machine to get readings.

There are four temperature sensor units affixed to the machine. There are three DHT11 sensors fixed to the axis motors and one DHT22 sensor fixed to the spindle motor. There are three Inertial Measurement Unit (IMU) sensors inside the machine that are used to record acceleration and gyroscope data from the milling machine. Two of these IMUs are BNO055 accelerometers, wired accelerometers located in mounts on the bed and spindle housing, then a third wired IMU, the BNO08x accelerometer, is also placed in a mount located at the top right of the spindle plate. These sensor locations are shown in Figure 8.1 below. There were two additional accelerometers, wireless WitMotion IMUs which were located outside of the machine on the enclosure and table.

Figure 8.1: Sensor Placement on the Machine



8.2.1 Inertial Measurement Units

There are five Inertial Measurement Units (IMU) sensors located in and on the milling machine. IMU sensors have different capabilities depending on the manufacturer and model but generally they are a combination device of accelerometers, gyroscopes, and magnetometers. This allows them to measure linear acceleration, angular velocity, absolute orientation, and magnetic force. For this testing the IMU sensors were used to record linear acceleration data from the milling machine and gyroscope data which was ultimately not used in data analysis. These sensors were placed at various locations in and around the mill to obtain baseline operating conditions while machining a part.

Two of the IMU sensors were BNO055 Accelerometers, wired accelerometers located on the bed and spindle housing. A third wired IMU sensor, the BNO08x Accelerometer, was located at the top right of the back plate where the spindle is mounted, referred to as the spindle plate. Wireless WitMotion IMUs were also used in this testing which run through a separate software and not the sensor board. These sensors are located

outside of the machine on the outer frame and table. On the bed, the primary direction of motion with respect to the machine's coordinates is the y-axis. On the spindle housing and spindle plate the primary directions of motion are the x-axis and z-axis. The accelerometer mounts were adhered to the machine in the desired locations and the sensors were screwed into the mounts to isolate the motion of the machine while limiting additional vibrations.

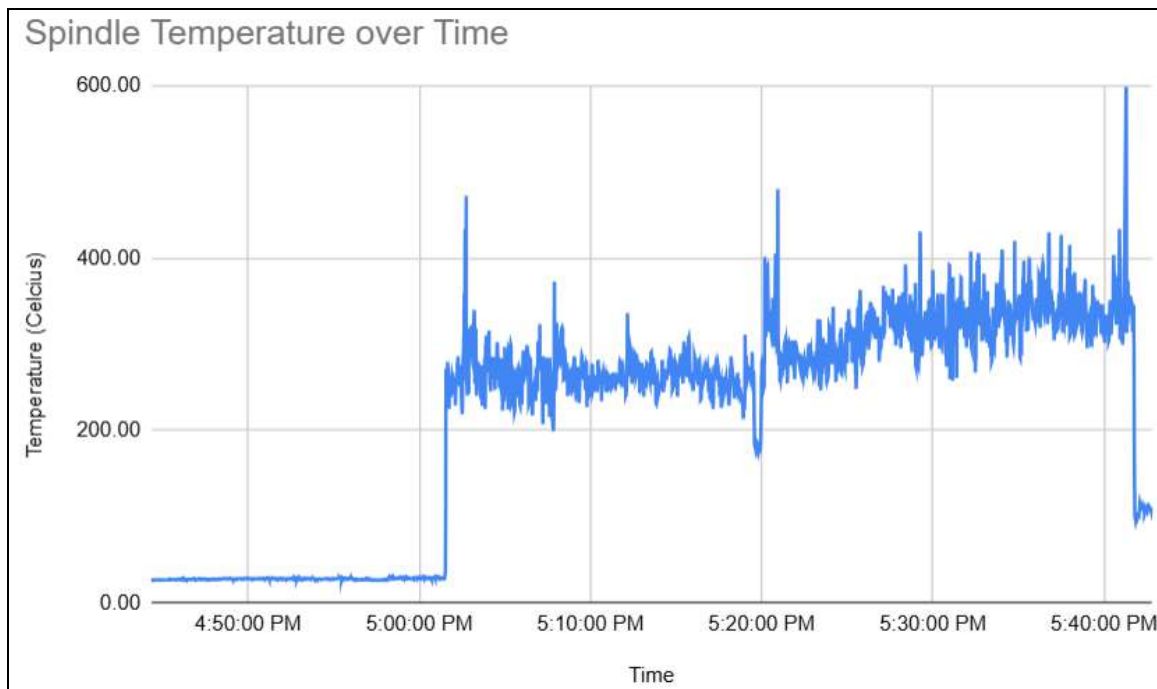
8.2.2 Temperature Sensors

There are four temperature sensor units affixed to the milling machine. There are three DHT11 temperature sensors, each fixed stepper motors controlling the motion of the x-, y-, and z-axis motors, and one DHT22 sensor fixed to the spindle motor. The DHT11 sensor has an operating range of 0°C to 50°C with an accuracy of $\pm 2^\circ\text{C}$ at 25°C (Aosong Guangzhou Electronics Co, n.d.). The DHT22 sensor is very similar to the DHT11 sensor however it has an operating range of -40°C to 80°C with an accuracy of less than +/- 0.5°C (Liu, n.d.). The sensors are mounted in a rectangular case that protects them from chips and coolant splash. The mounts are open to the face of the sensor, this side is placed against the motor so the sensor is about 1 cm away from the motor to measure the surface temperature of the motor housing. The sensor casing only covers a portion of one of the motors' sides, the remaining sides of the motor housing are not covered, the intent behind the design is to protect the sensor but not insulate the motor which would artificially raise the temperature thus skewing results.

During the process, the temperature of the spindle was also a datapoint to be recorded. In the initial attempt to measure the spindle temperature, an infrared temperature gun was used. The gun had many limitations, however. Since the machine was encased in polycarb, the gun would not work through the material, requiring a hole to be cut in order to

measure the temperature. The gun also had to be constantly held by an individual and aimed towards the spindle, causing the data that was recorded from it to fluctuate due to human error. Even accounting for these issues, it was discovered during initial testing that it would not work to record the spindle temperature since the tool is a black body surface, making IR readings absorbed by the sensor (Liu et al., 2011). The spindle temperature jumped to around 230 degrees celsius, steadily rose, then jumped down to around 100 degrees celsius when the spindle stopped spinning (Figure 8.2). This data does not correlate to what the temperature curve should be.

Figure 8.2: Erroneous Spindle Temperature Data

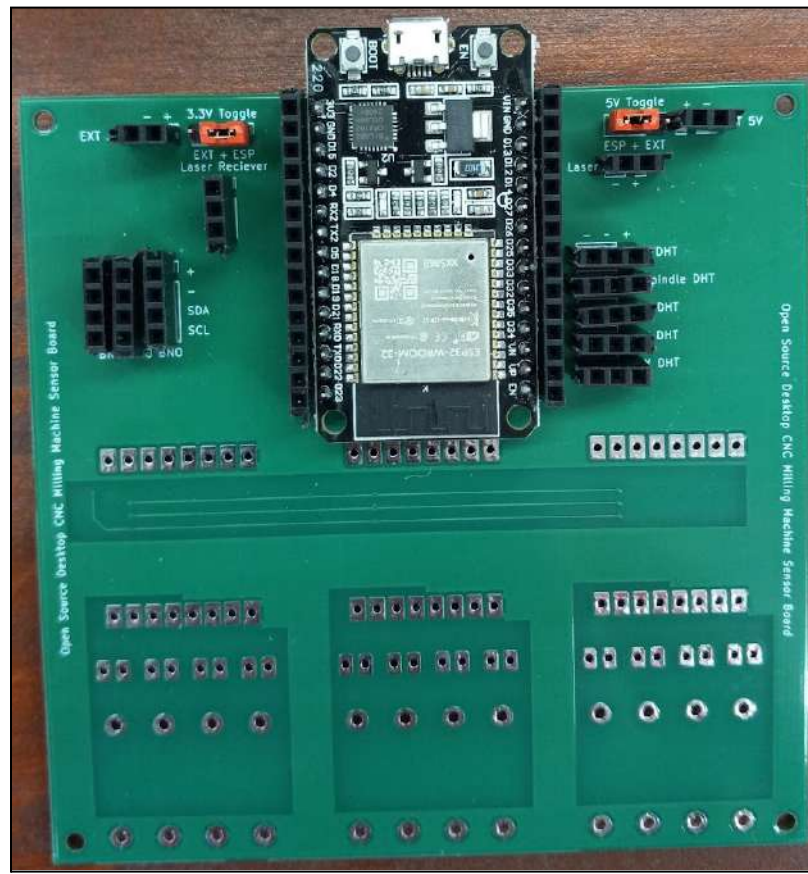


8.2.3 Sensor Data Collection

In order to collect and save data from the wired sensors on the machine, an ESP32 microcontroller was used. The ESP32 used compiled code to transmit/receive data from sensors, store the collected data, and then transmit the data for a specified polling frequency. This microcontroller was then plugged into a computer to transmit collected data in order to be saved for future use. Any data collected from the board was sent to the computer by serial communication in the form of formatted numbers. This data would then be stored in a log file by the computer, along with the real time and ESP32 on-time to correlate readings. These readings were filtered into CSV files to make analysis of the readings easier. In addition to wired sensors, there were also wireless sensors that required a dedicated desktop application in order to initialize the sensors and get readings from them. These files were subsequently stored as CSV files, requiring further filtering to separate the different sensors from each other and remove unwanted data.

To make connections to the microcontroller easier and to keep connections organized, a custom PCB was created (Figure 8.3). This custom board enables switching between internal/external power, reduces electrical noise between components, and provides connecting interfaces to sensors. The sensor interface pins then extended along long wires to then connect to the relevant pins on the connected sensors. There was also an extra set of connectors for every ESP32 pin added in case any new connections needed to be made without needing to have a new board manufactured. This board was then mounted to the frame of the machine to keep it close to sensors and be out of the way of any other components.

Figure 8.3: Custom Sensor Interface Board



8.2.4 EMI Effect on Sensors

Throughout implementing and testing different sensors on the machine, EMI came up as an issue for several sensors. With EMI creating stray voltage spikes and traveling throughout the entire metal machine, it caused issues when communicating with sensors. With specific sensors, such as strain gauges, they are very sensitive to stray voltage since their flexing corresponds to changes in the microvolt range (*Strain Gauge Measurement – A Tutorial*, n.d.). Stray EMI would cause the readings from these sensors to be wildly inaccurate and unreliable. Additionally, stray EMI also causes issues with signals that oscillate at high frequencies, since they can cause artificial spikes that affect readings. With

the constant EMI being generated in the machine while powered, it ultimately caused some sensors to not be implemented due to the time and financial constraints of the project.

8.2.4.1 Inertial Measurement Units

For the wired accelerometers, EMI caused issues with the I2C communication protocol. While moving the x-, y-, and z-axes on the machine, the sensors were able to record data without any issues. However, when the spindle motor was powered, it caused the microcontroller to constantly get I2C read errors (Figure 8.4). These errors caused the board to get the same readings for roughly a second and in the worst cases, completely reset the board. When the board was reset, it caused it to go into the calibration phase, resulting in no new data collected until the machine was stopped and the BNO sensors were calibrated. The fix for this was to make sure that the wire connections were secured. While EMI did cause issues with other sensors, it only became an issue with the BNOs when the EMI was combined with bad connections. This resulted in most sensor board data collected to have periods of bad data, affecting the averaging of IMU data. After the pin connections were fixed, there was not any issue with EMI causing I2C errors or the board getting reset.

Figure 8.4: I2C Read Error

```
17:06:14.066 > ,4848382,-0.00,0.00,-0.00,0.10,0.84,-0.02,-0.00,0.00,0.00,0.01,-0.04,0.20,-0.03,0.00,-0.00,-0.08,-0.02,-0.11,31.20,30.60,31.30,28.30,
17:06:14.165 > ,4848481,-0.00,0.00,-0.00,0.10,0.84,-0.02,-0.00,0.00,0.00,0.01,-0.04,0.20,-0.03,0.00,-0.00,-0.08,-0.02,-0.11,31.20,30.60,31.30,28.30,
17:06:14.266 > ,4848582,-0.00,0.00,-0.00,0.10,0.84,-0.02,-0.00,0.00,0.00,0.01,-0.04,0.20,-0.03,0.00,-0.00,-0.08,-0.02,-0.11,31.20,30.60,31.30,28.30,
17:06:14.365 > ,4848681,-0.00,0.00,-0.00,0.10,0.84,-0.02,-0.00,0.00,0.00,0.01,-0.04,0.20,-0.03,0.00,-0.00,-0.08,-0.02,-0.11,31.20,30.60,31.30,28.30,
17:06:14.466 > ,4848782,-0.00,0.00,-0.00,0.10,0.84,-0.02,-0.00,0.00,0.00,0.01,-0.04,0.20,-0.03,0.00,-0.00,-0.08,-0.02,-0.11,31.20,30.60,31.30,28.30,
17:06:14.565 > ,4848881,-0.00,0.00,-0.00,0.10,0.84,-0.02,-0.00,0.00,0.00,0.01,-0.04,0.20,-0.03,0.00,-0.00,-0.08,-0.02,-0.11,31.20,30.60,31.30,28.30,
17:06:14.666 > ,4848982,-0.00,0.00,-0.00,0.10,0.84,-0.02,-0.00,0.00,0.00,0.01,-0.04,0.20,-0.03,0.00,-0.00,-0.08,-0.02,-0.11,31.20,30.60,31.30,28.30,
17:06:14.765 > ,4849081,-0.00,0.00,-0.00,0.10,0.84,-0.02,-0.00,0.00,0.00,0.01,-0.04,0.20,-0.03,0.00,-0.00,-0.08,-0.02,-0.11,31.20,30.60,31.30,28.30,
17:06:14.866 > ,4849182,-0.00,0.00,-0.00,0.10,0.84,-0.02,-0.00,0.00,0.00,0.01,-0.04,0.20,-0.03,0.00,-0.00,-0.08,-0.02,-0.11,31.20,30.60,31.30,28.30,
17:06:14.965 > ,4849281,-0.00,0.00,-0.00,0.10,0.84,-0.02,-0.00,0.00,0.00,0.01,-0.04,0.20,-0.03,0.00,-0.00,-0.08,-0.02,-0.11,31.20,30.60,31.30,28.30,
17:06:14.985 > [4849302][E][Wire.cpp:513] requestFrom(): i2cRead returned Error 263
```

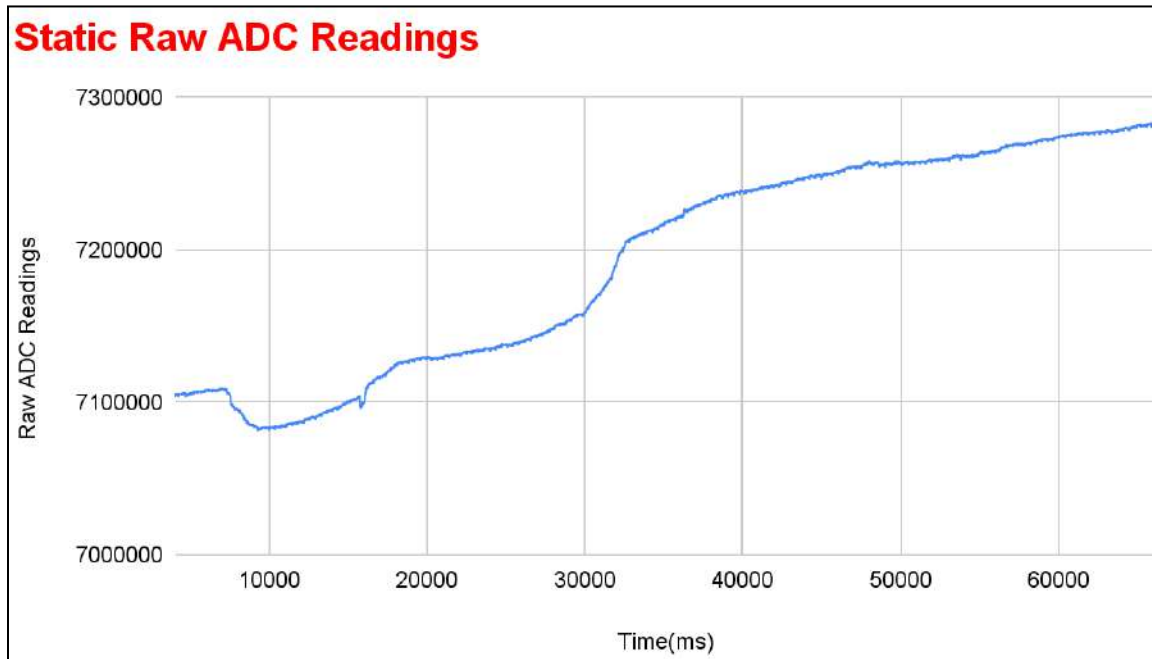
8.2.5 Strain Gauges

In order to measure stresses and strains on the machine at different points, strain gauge sensors were mounted to the machine to measure the forces. To do this, any interface with the sensors would need to collect data at a reasonable rate and accuracy. The initial plan was to use an amplifier designed specifically for measuring strain gauges and then directing the various strain gauges through a multiplexer so that only one amplifier would be needed. This was done because each amplifier would cost ~\$15 and having one for each of the 12 strain gauges would result in having \$180 worth of sensors just for measuring strain. The multiplexer would allow for a single channel to be selected (one strain gauge on each channel) to then be put through the sensor, severely reducing cost and reducing the amount of connections required to read all strain gauges. However, during testing, it was discovered that while the amplifier worked well, the multiplexer did not. The multiplexer had internal resistance and noise that made any results from the strain gauges noisy and unreadable.

After finding out the amplifier/multiplexer idea would not work, a new approach was to use multiple 24-bit ADC modules to measure the changes in voltage from the strain gauges. These modules would be sensitive enough to pick up any change in voltage and with each ADC having four channels, 12 strain gauges could be read using only three ADC modules that cost about \$20 each and still use a small amount of pins on the microcontroller. When first interfacing with the ADCs, the results from only reading one channel were very noisy and had significant drift (Figure 8.5). With the drift being roughly 300,000 units and the total data range being 8,388,608 units, this resulted in a drift of 118 mV. This is a drastic change since strain gauge voltages typically change in the microvolt range, not the millivolt range. This error was a result of not enabling external voltage references and using the

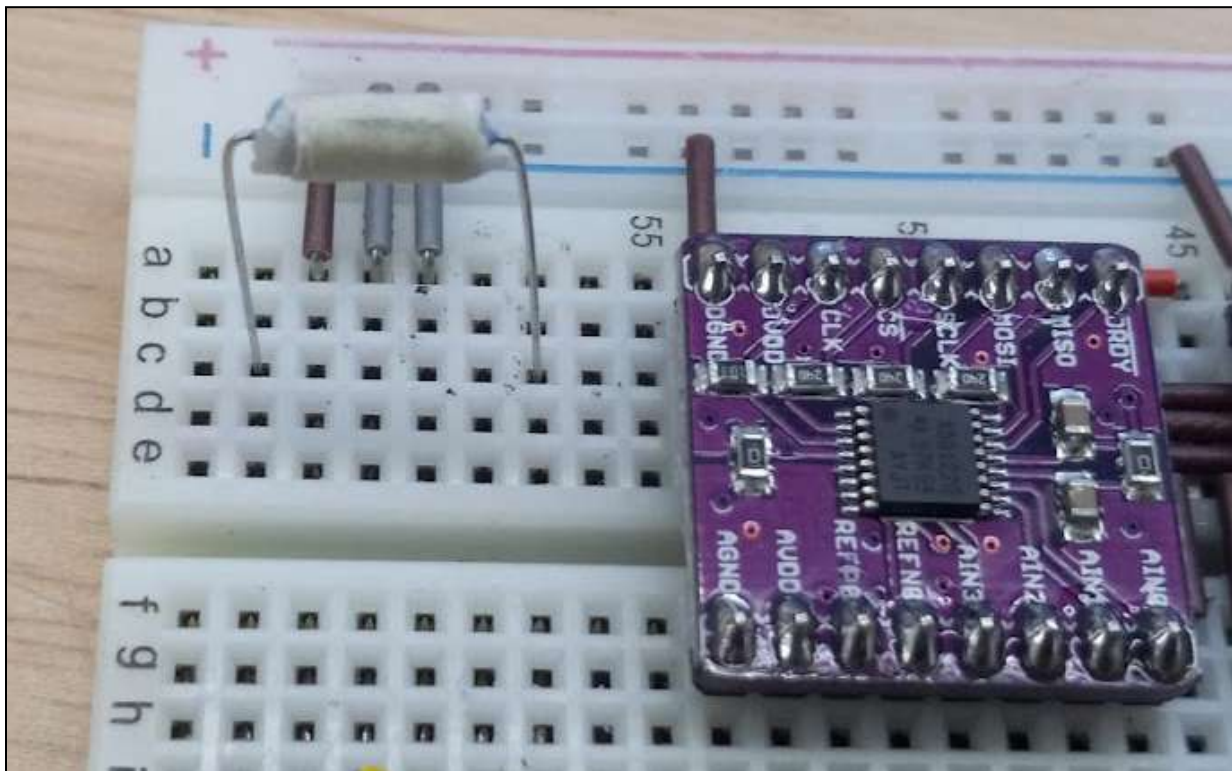
internal ~2 V reference, resulting in drift and noise since the strain gauges used a different 3.3 V voltage source.

Figure 8.5: Drift Data Collected from Reading Resistors



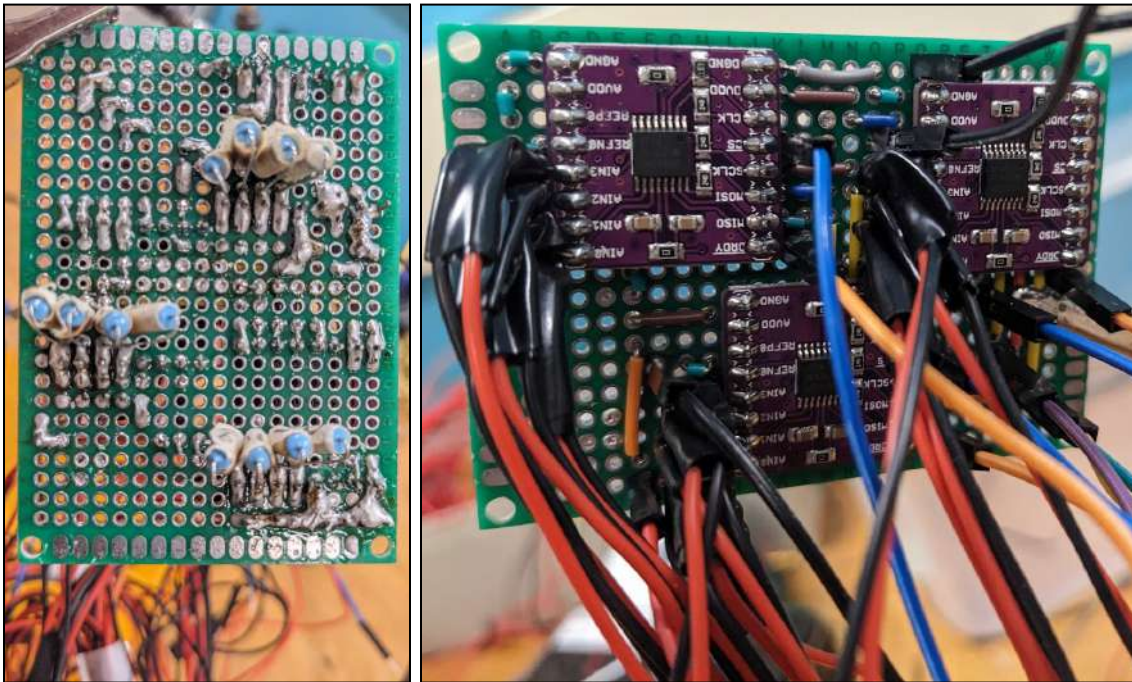
After setting the correct reference voltage to compensate for drift and noise, there was even more noise coming from the breadboard used for testing. Due to the pins from the resistors not being big enough for the breadboard, the loose fit allowed the resistors to experience too great a range of motion that readings were affected since they are read at microvolt levels (Figure 8.6). Further contributing to noise and drift in the system is that breadboard connections are not secure in the first place, resulting in compounded error. In order to fix this, a PCB was used to solder connections between the strain gauges, their resistors, and to the ADC modules. Aside from those connections, none of the other connections needed to be soldered to work but soldering the other sensors made it more reliable and would have easy to read labels for connectors.

Figure 8.6: Resistor Placed on Breadboard with Pins that are too Small to be Secured



When first trying to solder the PCB for the strain gauges, perfboard on hand was used to solder connections just for the ADC, strain gauges, and resistors. This, however, caused many problems and delays. Because of the size of the perfboard, it had to be soldered on the front and back to pack all of the connections together. This made working with the board extremely difficult and all of the connections unreliable (Figure 8.7). This resulted in the custom PCB being created in order to reduce the artificial noise from the strain gauges to read forces on the gantry.

Figure 8.7: Back and Front of Perboard that was Soldered



After the ADC modules and strain gauge wires were soldered to the custom PCB (Figure 8.8), the readings still drifted and did not read correctly. This was likely due to the wrong pins being used as reference voltages, resulting in drifting. Shortly after this, the EMI issue was discovered that led to the abandonment of these sensors. Even if the custom board could read the strain gauges accurately, the stray EMI would cause the gauges to not have reliable and accurate readings.

Figure 8.8: Original Soldered Custom PCB



8.2.6 Spindle Speed

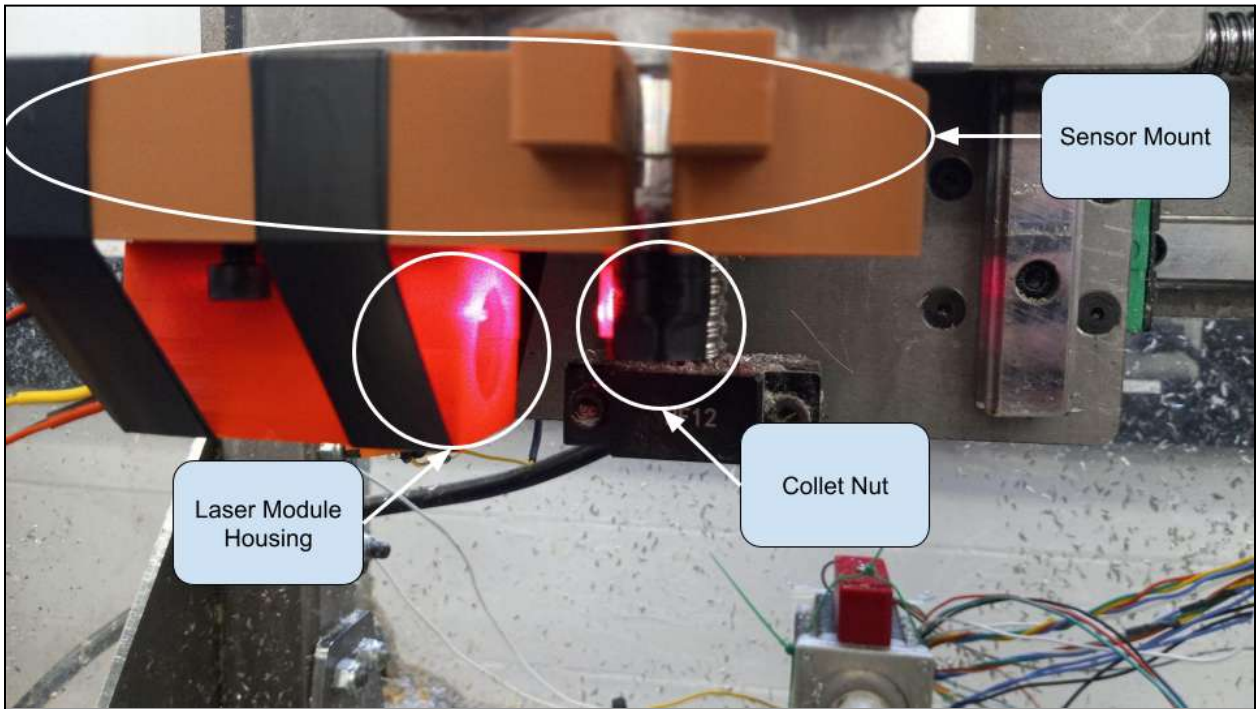
Another aspect of the physics analysis was to measure the actual speed of the spindle and not just basing it off of the software reported speed. The first idea was to use an IR transmitter and receiver to measure the speed of the spindle. The spindle would have IR reflective tape on it so that when placed far enough away, it would only read when the IR emission passed the tape. However, there were multiple problems that arose from this solution. One problem was that the IR module did not work through the polycarbonate panel. This is an issue since it would need to be close to the spindle and if any debris (coolant, chips, etc.) got on it, it would be damaged. With it not working through polycarb and likely any other transparent material, there would be no good way to protect it.

Another issue that arose was EMI generated by the spindle. When testing the sensor in environments outside the machine, it appeared to work accurately and reliably, given the

correct setup. When it got mounted in the machine, the spindle was manually spun, which worked well (since it was spun by hand, it could only go to a few hundred measured RPM). When the spindle motor was turned on, however, the readings were extremely noisy, going anywhere from a couple hundred RPM to a couple hundred thousand RPM. The module was tested by turning at different orientations to the motor and only when the bottom of the PCB was facing the motor did the module work reliably. The EMI adversely affected the IR readings since signals were sent thousands of times a second to the ESP32 and any stray voltage would severely affect those readings.

To fix the issue with the IR module, the sensor was replaced with a laser transmitter and receiver. This was used since a normal tachometer worked well outside the machine, which used a laser system, but it could not log data for analysis later. This also means that if the new laser module also experiences issues with EMI, it would be able to be mounted outside the machine and be unaffected. When testing the laser modules, it also had issues with EMI since it still had high frequency signals that were sent relatively close to the spindle (Figure 8.9). It was less susceptible to EMI affecting the sensors themselves but it still affected any wires that came close to any part of the metal gantry. Another issue that arose was that the sensors needed to be placed in exactly the correct position to get the beam to the receiver. Since the laser transmitter needed to go to the spindle and then bounce back to the receiver that was offset about half an inch, it made it very difficult to line up. Any time the case needed to be opened, the sensors would lose alignment and any attempts to realign them did not work, resulting in the sensor not being used in the end.

Figure 8.9: Laser Spindle Speed System



8.3 Control Board Circuit

When the electrical systems were designed for the new machine, it was designed to use as many components from last year's machine as possible. This included the AC to DC converter, stepper motor drivers, terminal block, E-stop, VFD, limit switches, and some stepper motors. This meant that the only substantial change to the wiring was the control board and the integration with the existing electrical components. The old Keenso control board had less connection terminals and electrical functionality compared to the new PicoCNC board. Comparatively, the new board had dedicated x-, y-, z-, and a-limit switch pins, stepper motor enable pins, safety door pin, E-stop pin, spindle pins, and more. This made connecting these features more accessible due to dedicated ports compared to reconfigured general purpose input-output ports. With the AC to DC converter outputting 25 A, it provided enough power to all electrical devices connected.

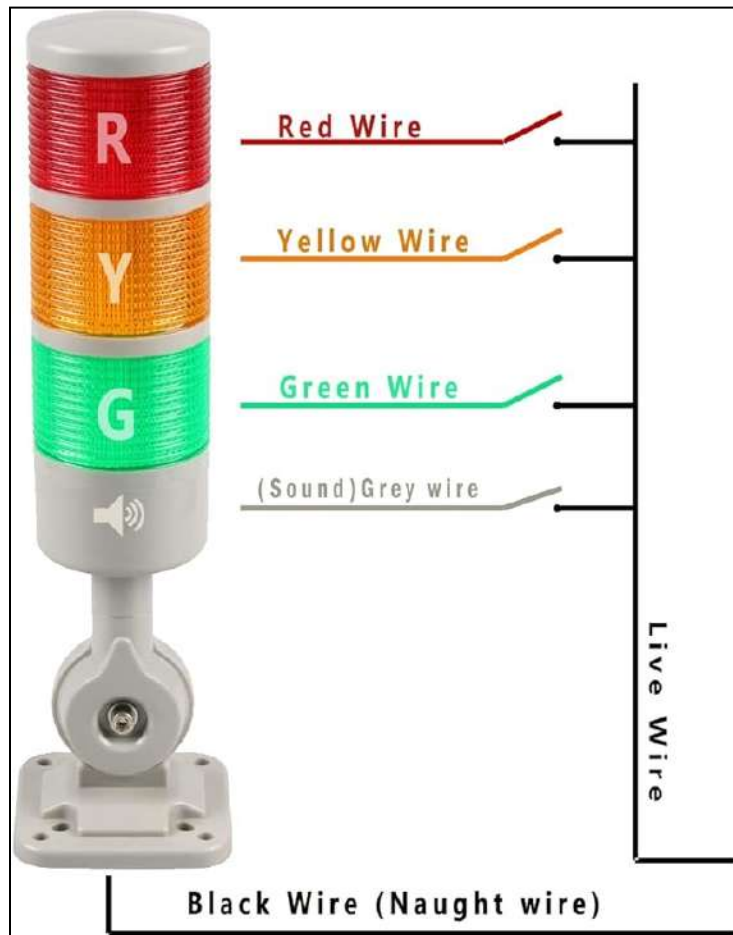
8.3.1 Door Switch

Last year, the machine had no way of knowing whether the front door was open or closed. The previous machine's vertical garage-like door was changed to a horizontal door on a set of hinges, with a latch with a normally-closed reed switch inside of it. The new door mechanism has a magnet inside that, when close to the latch's reed switch, opens the circuit, cutting the signal to the board, and puts the machine in pause mode. Both the E-stop and door switches are designed to have override buttons, intended solely for use by high-level administrators during maintenance that requires the door to remain open while the machine is running.

8.3.2 Stack Light

The stack light was a relatively late addition to the project, and is set up to indicate three different states. “Ready mode” is indicated when the machine is ready to be run, lit up green when the machine is running or ready to be run, yellow when the door is open, and red when in stop mode. “Pause mode” stops the axes and spindles from moving, but does not completely back out of the program, allowing it to be resumed after any maintenance is completed. “Emergency Stop (E-stop) mode” cuts power to the axes and spindle and also backs out of the program, which is used when a limit switch is reached or the machinist presses the E-stop button in case of an emergency.

Figure 8.10: Stack Light Wiring Diagram



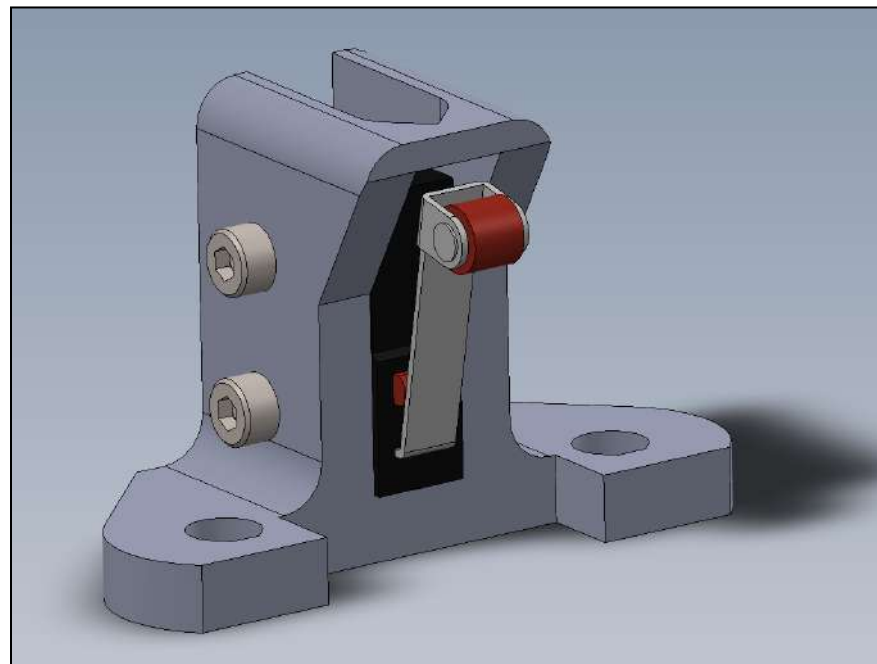
Note. Reproduced as is from (*LUBAN Led Signal Tower Stack Lights*, n.d.).

The stack lights were wired to use external relays to control the outputs. Since the PicoCNC board had open collector outputs and the stack light shared a common ground, the lights could not be directly controlled from the board's auxiliary outputs (Figure 8.10). To control them, 24 V relays were chosen. With the power supplies in the circuit, the relays could have been powered by 24, 12, 5, or 3.3 volts. 3.3 and 5 volts were not chosen since it would have placed extra strain on the PicoCNC 5 V regulator, which already ran hot. Both 12 and 24 volts would have worked for the machine, but 24 V was chosen since 24 V relays were readily available.

8.3.3 Limit Switches

The first update to the limit switches was to switch their pinout to be normally closed (NC), instead of their prior state of being normally open (NO). This means, when not pressed, an electrical signal flows through the limit switch, and when it is pressed, the signal is cut. In last year's machine, if a wire broke, a connector came loose, or something else cut the signal to the limit switches, the switches would not work as intended when coming into contact with the milling axes, risking damage to the overall machine and user. Now, if a breakage occurs, the machine will interpret this as a limit switch being triggered, and the machinist can identify and fix the problem without any risk to themselves or the machine. Additionally, a CAD design was made to house the limit switches on each side of the machine (Figure 8.11).

Figure 8.11: *Limit Switch Mount Render*



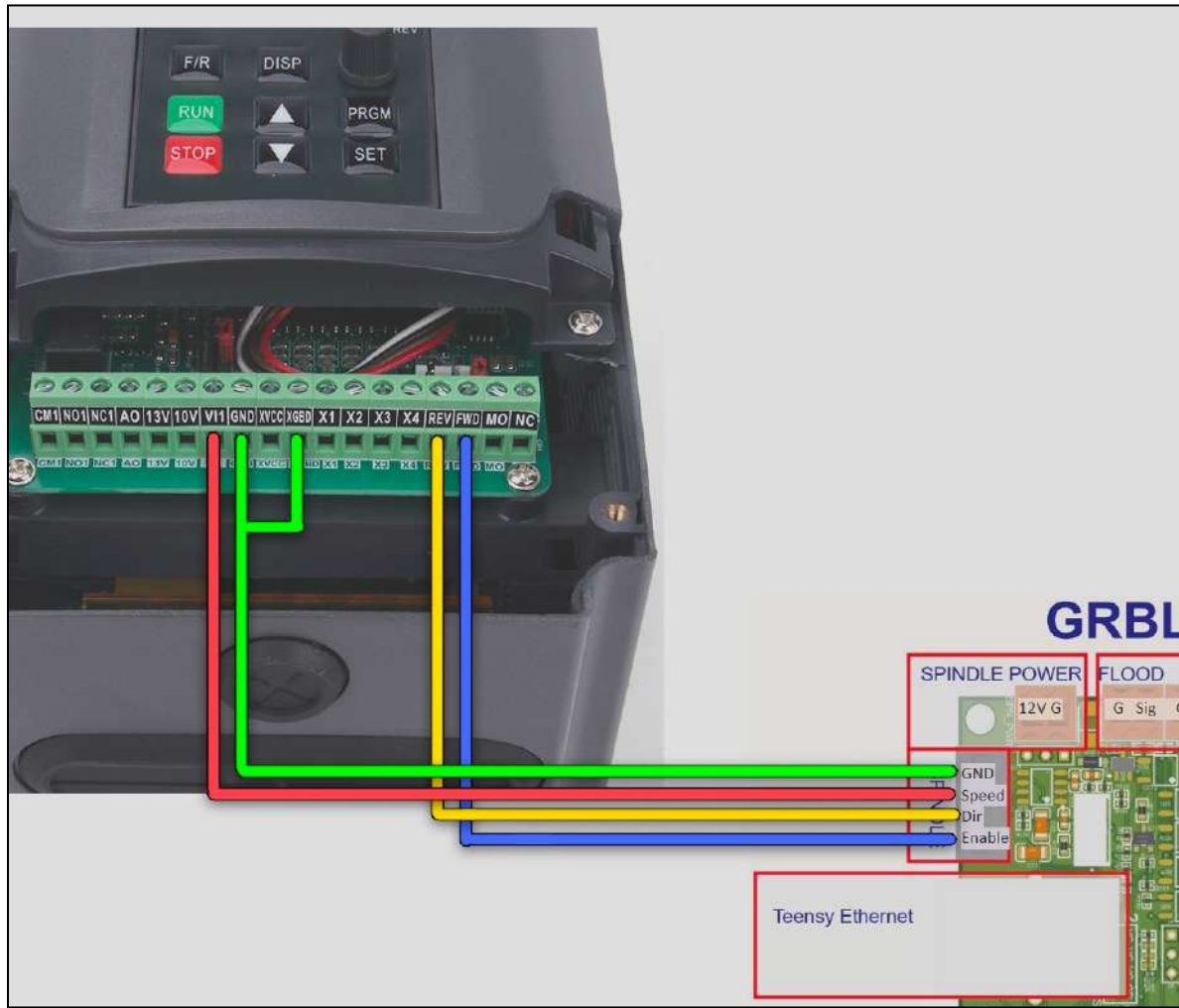
8.3.4 Spindle

In order to have tool changing functionality and spindle speed that is controllable through G-code, the spindle needed to be electrically controlled by the machine control board. In the original Mach3 machine, the spindle was not set up to be controlled by the software and had to be done manually. Initially, the plan was to set up proper spindle calibration for Mach3 to run test parts before transitioning to grblHAL. After wiring the spindle and using an Excel script to correlate spindle speed to voltages, it only produced an accurate RPM range between 7,000 RPM and 15,000 RPM. This was far from the 5,000 to 24,000 RPM range the spindle was rated to. After the calibration of the spindle effectively failed for Mach3, all initial testing manually controlled the spindle RPM. After the conversion from Mach3 to grblHAL, the spindle had to be wired and calibrated to be controlled through G-Code.

When transitioning to grblHAL, there were multiple issues relating to the spindle. First, the spindle had to be properly configured to use the grblHAL control scheme. With the Mach3 board, it only needed a power, ground, and analog signal pin. This allowed the G-code to control the speed but not the direction. With the grblHAL setup, it needed both speed and direction control for tool changing and full spindle functionality. When the new settings were applied to the VFD controller and the new wiring connections were made (Figure 8.12), the spindle did not spin. To troubleshoot this issue, the control pins were verified for voltage and a second FVD controller was tested, both still not resulting in spinning. After that configuration failed, the Three-Wire method was implemented and worked. This method also allowed for spindle speed and direction control, but would not integrate as well with the control board. The new setup required external relays to toggle the

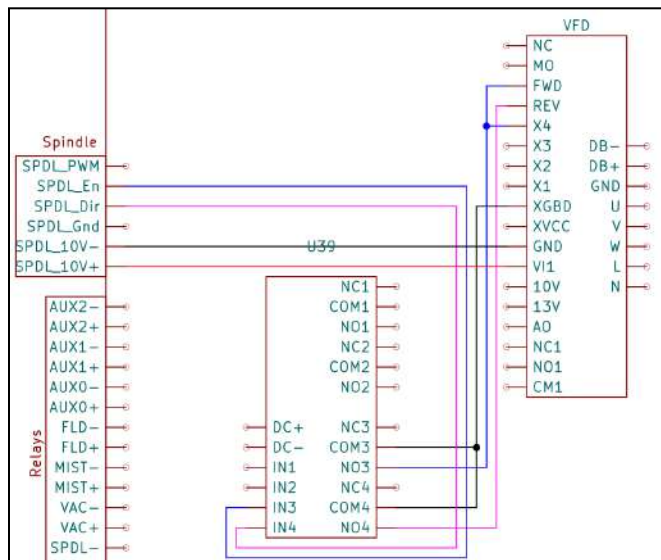
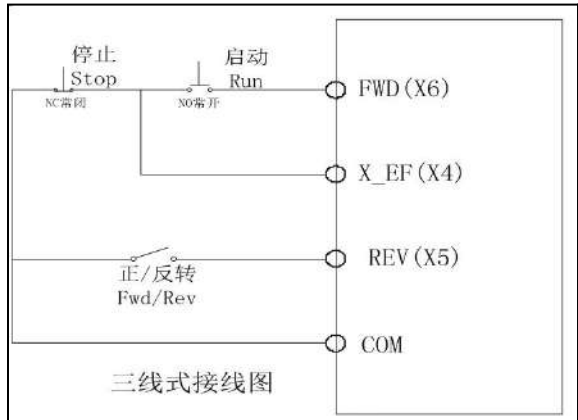
connections when the direction and reverse pins were triggered on the new control board (Figure 8.13).

Figure 8.12: Intended grblHAL Spindle Wiring



Note. Reproduced as is from (*VFD Control with GrblHAL*, n.d.).

Figure 8.13: Three-Wire and Machine Spindle Wiring



Note. Reproduced as is from (Yalang, n.d.).

In addition, the spindle was updated to now stop when either the E-stop button was pressed or the enclosure's door was opened. This ensures the safety of the user, preventing them from coming into contact with a live spindle or tool.

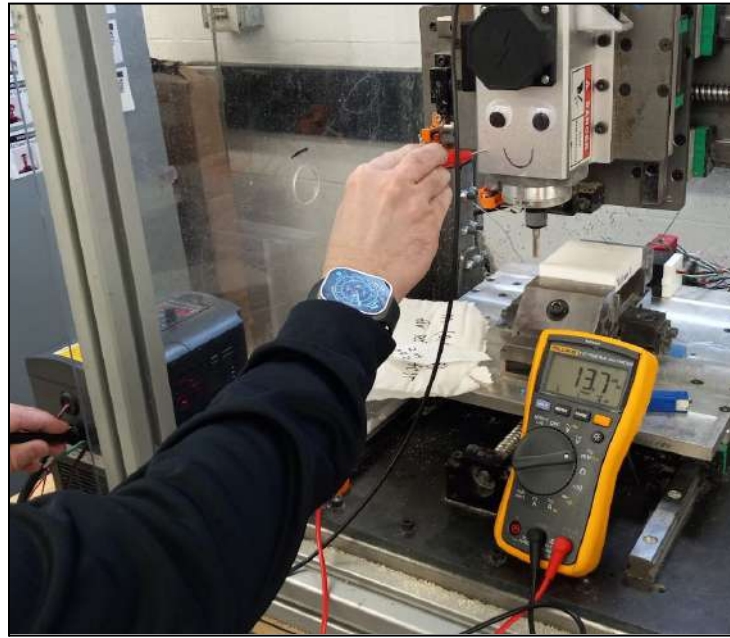
8.4 EMI Analysis

Having inadvertently discovered EMI effects on the sensors, the decision was made to test for stray voltage in the machine, after the sensors had been thoroughly inspected and the interference was still present. When placing a Fluke 117 multimeter probe against the gantry frame, there was a potential that wildly varied between a few mVAC and greater than 200 VAC.

The source of the EMI needed to be determined: it was either coming from the variable frequency drive (VFD) that powers the spindle, or from the 120 VAC to 20 VDC converter that supplies power to the other electrical components on the machine. To determine the source, the 120 VAC that powered the VFD was unplugged. The remaining components were left powered by the 120 VAC to 20 VDC converter; however, the Fluke multimeter did not detect stray AC or DC voltage. It was therefore concluded that the source of the EMI was not the 120 VAC to 20 VDC converter.

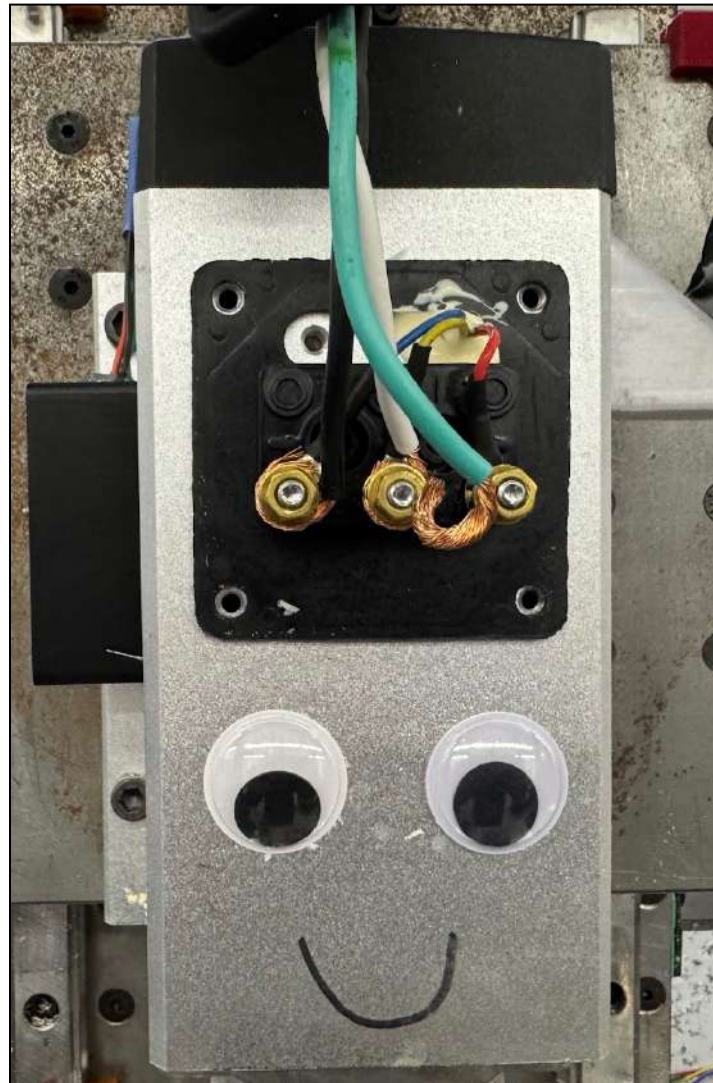
The 120 VAC to 20 VDC converter was unplugged and the 120 VAC cable was plugged back into the VFD. When placing the multimeter probe against the outside of the spindle power cable coming from the VFD, the multimeter read over 400 mVAC. The spindle power cable was then placed in such a way that the cable did not rest against any metal components on either the gantry or the enclosure. This reduced the wild fluctuations on the multimeter to a steady 13.7 mV, which was detected to be originating from spindle casing (Figure 8.14).

Figure 8.14: Image of the 13.7 mVAC Noticed on the Spindle Casing



The 120 V going to the VFD was unplugged, and the cover for the power coming from the VFD to the spindle was removed. This exposed the wiring of the spindle, showing that the ground wire was not installed (Figure 8.15).

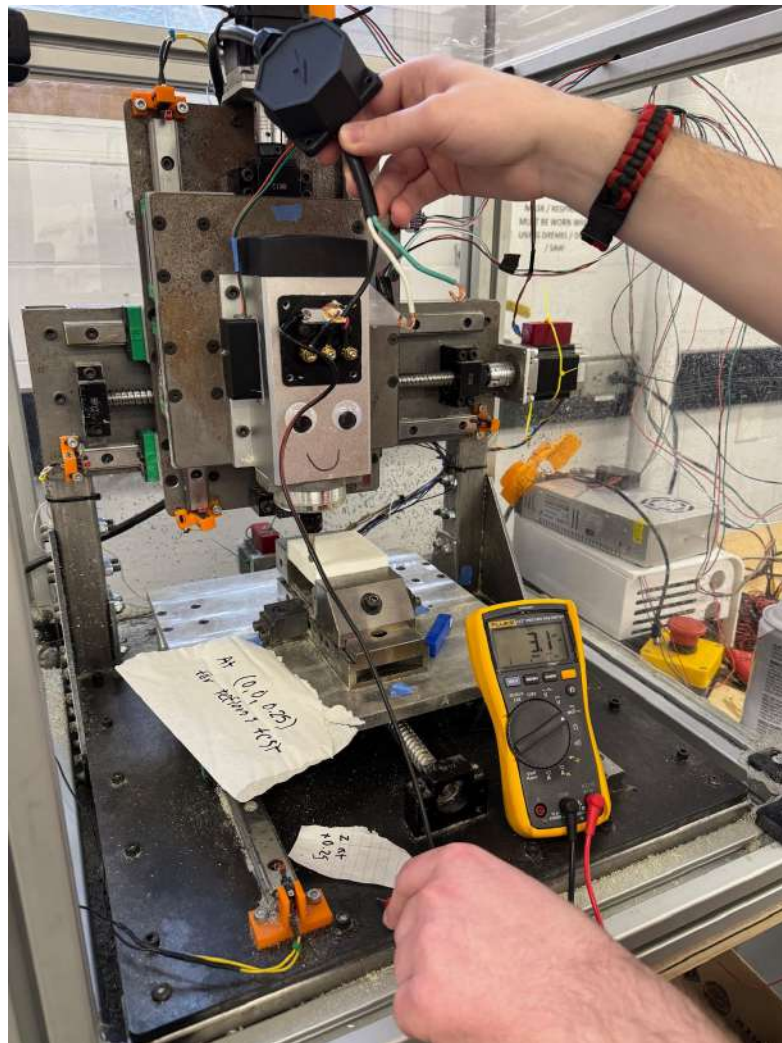
Figure 8.15: Image of the Ground Wire Installation Point



A ground wire was installed on the spindle, and connected to the ground of the VFD.

After adding the ground, the stray voltage was reduced to a steady 3.1 mVAC (Figure 8.16).

Figure 8.16: Image of the Reduction in Voltage Leakage Down to 3.1 mVAC



The 3.1 mVAC could not be eliminated any further. The reduction of stray voltage by approximately 77% was substantial, however. Keeping the VFD power cable from coming into contact with any metal components was also critical in reducing the effects of EMI.

8.5 Software Work

Before the software and firmware could be worked on for the new machine, code needed to be developed to analyze the machine through sensors. This code was developed for the ESP32 microcontroller. The ESP32 has two cores, adequate CPU speed, and

adequate memory for collecting sensor data. One core was used for strictly data collection while the other core was used to transmit the data to the host computer. The code included a calibration sequence for the BNO055 accelerometers and printed out the calibration status. While calibration was enabled for the BNO08X, the IMU did not expose the calibration status to the microcontroller, making it unclear when or if the IMU was calibrated. Once the calibration sequence was completed, the ESP32 displayed the real time, system on-time, gyro and accelerometer readings for each BNO IMU, and then the DHT temperature readings. The program also includes the ability to read the data received from the laser speed sensor and strain gauges, but were not used due to the issues mentioned with EMI. The ESP32 software also includes the ability to read values from a single strain gauge in order to use the data to calibrate them. This data was then used to get an average baseline reading for different applied strains that could be used later to calculate strain.

After the code was set up to retrieve and store sensor readings, the readings needed to be filtered. For this, two scripts were created, one for the wired sensors and one for the Witmotion IMUs. For the wired sensors, extra artifacts in the log file needed to be stripped in order to produce results in a valid CSV format. Since all of the BNO accelerometer axes did not align with the machine axis, the axes all needed to be remapped according to the machine coordinates. For the Witmotion script, it was required since the Witmotion software saved sensor readings for both sensors in the same file. The script was used to programmatically separate the sensor readings for easier analysis. It also removed unnecessary data from the dataset to include only relevant data.

8.6 grblHAL

In order to get the machine ready to use, there were many adjustments that needed to be made. The default method of installing grblHAL is to use their dedicated web builder (*GrblHAL Web Builder*, n.d.). This, however, is very limited in selectable features and does not allow for custom implementations. This required that the firmware was set up and compiled manually. Additional features that were enabled from default settings were a 4th-axis, tool table, door switch, ethernet control, spindle linearization, I2C, and jerk settings. For the 4th-axis, the number of enabled axes was changed from three to four. For the tool table, it was automatically enabled when the number of stored tools were higher than zero (default is zero). For the door switch, spindle linearization, I2C, and jerk control, these were enabled. For ethernet control, it had to be enabled and be configured to use the right ethernet chip as many were available to use.

In addition to the base functionality needing to be edited, the firmware settings also needed to be modified. This included changes such as storing homing directions, enabling hard limits for limit switches, setting the step size of motors, and more. These settings were used to make the tolerance of the parts more accurate, calibrate spindle settings, and more. When the firmware was originally stored to be used later, version 20241023 was used.

To make sure that new bugs that arised from grblHAL's development did not make it into the machine, a local copy of that version was saved. This version worked well until the team tried to move the machine in smaller increments. When moving from large distances, it was able to get within around 0.002" when it stopped after step tuning. However, when the machine tried to move just 0.01", it did not move with the default settings. This was due to the acceleration curve that grblHAL used. Since the distance was so small, the voltage

would almost immediately ramp up and then settle, not leaving enough time for the motor drivers to turn the motors. When the acceleration values were lowered, it enabled the machine to move the smaller, discrete increments, but also slowed down every movement on the machine. To adjust to this problem, the firmware was updated to 20250405, which included new jerk settings. With jerk being the derivative of acceleration and able to control the acceleration curve, it enabled small, discrete movements while keeping the speed of all other movements. However, the new version of the firmware caused an issue with the spindle being inverted. This resulted in the source code requiring edits to make the spindle work as it did in the past. This exposes a problem with grblHAL, being that they update the software every few days, without big releases every few months, causing some systems to not be fully tested when new changes are applied.

8.6.1 Custom Plugins

In addition to configuring the default functions of grblHAL, a stack light plugin and tool changer plugin were developed. The stack light plugin configured either a green, yellow, or red LED based on the machine state. In order to trigger the LED's, the PicoCNC built in auxiliary ports were used. These ports can be controlled manually through M-Codes and through the firmware. The auxiliary ports were first claimed by the firmware. This means that no other plugin or function could try to use those ports for some other function, since they are listed as unavailable. After the plugin was initialized, a function that was called whenever the machine state changed configured which LED should be active and if it should oscillate. To trigger the auxiliary ports, the realtime function was hijacked to also toggle the LEDs based on if they needed to be turned on or off. This means that the realtime functionality needed to be optimized, since the realtime function needed to be executed

quickly and without any laborious calculations to slow down processing and possibly cause unexpected results.

The grblHAL tool changer plugin involved many additions to the firmware. Firstly, custom firmware settings were included in the plugin. These settings allowed the user to set the location of pockets, the feed rates used, positioning z heights, and more. These settings were added to the core settings, which saves them on the controller and restores them after startup or reset. Additionally, custom M-Codes were added to toggle the dust cover, set status of loaded tools, and unload the current tool from the spindle. There were also custom grblHAL commands added, which were to retrieve the tool statuses and poll for any valid I2C devices.

In order to communicate with the physical tool changer module, I2C communication was used. This was chosen to not need the extra wires that SPI uses and to not interfere with any serial communication that was needed between any computer and the Raspberry Pi Pico. For communicating to the module, the control board sent commands to toggle the dust cover, which the tool changer would then parse and execute. For communicating to the control board, the module sent whether the laser was blocked or not, which the control board then parsed. If the control board was not able to communicate with the module and I2C communication was enabled, the tool change command was stopped. Having the laser connectivity was essential in order to set the tool offset and to check for any mechanical errors while exchanging.

After creating the settings and ability to communicate with the tool changer module, the motion paths had to be planned. For loading and unloading the tool from a pocket, the machine moved to a safe z height, moved to the pocket x and y coordinate, executed the

change, then moved back to the original x and y coordinate before the exchange, and finally, back to the starting z height. For unloading the tool, the spindle would start to spin at the designated unload RPM counter-clockwise, then go down into the pocket. Once the bottom position was reached, the spindle stayed for a set period of time, then returned back to the safe z height. For loading the tool, it would start the spindle clockwise, move to the bottom of the pocket, stop the spindle, move up, and repeat again. Then, if enabled, it would move over to the laser probe to set the tool height offset. The spindle would move down fairly quickly until it hit the laser, move up 1 cm, then move back down much slower until it hit the laser again, setting the offset. During the operations of loading and unloading, the control board would check if the laser beam was blocked or not, to make sure the collet was or was not engaged when it was supposed to be the opposite.

8.7 UGS

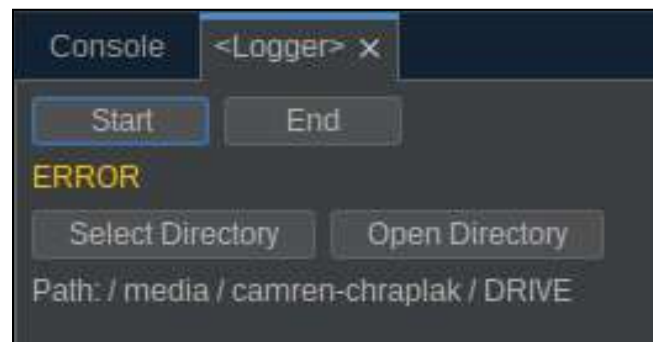
Configuring UGS to work with grblHAL was straightforward. The only change that was required was changing the communication method from USB to Ethernet. Aside from that, the machine could be used to its full function after the firmware was installed on the machine. To expand on the existing features of UGS, a custom logging plugin and tool changer plugin were created. The logging plugin used the verbose output of grblHAL, usually hidden. This output displays the machine coordinates, feeds, spindle speed, work coordinate offsets, and more. The plugin scanned for this data to log in CSV format. The plugin created two log files, one for any G-Codes commands sent and one for the status of the machine. For both files, the timestamp for when the commands were sent to the machine were logged for reference. For the command CSV, the timestamp did not always correspond to when the command was executed, just sent. This is due to grblHAL storing a buffer of

commands to execute and when it gets too low, requests more. This makes grblHAL not pause and wait for individual commands and instead, executes them when they are ready.

The second CSV file logs the machine state and the G-Code line it executed. When line numbers were inserted into the program file, grblHAL listed those numbers when it was executed. If no line numbers were inserted or a user manually typed in commands, there would be no line number printed.

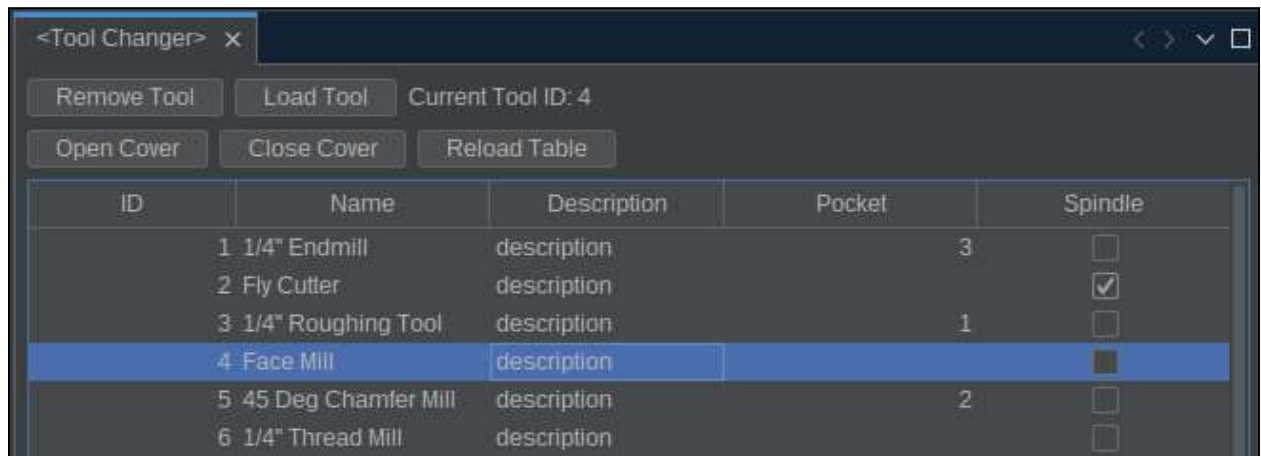
The plugin interface allowed the user to start recording, stop recording, select storage directory, and open storage directory. It also displayed color coded text to show the status of data storage. The “start” button only worked when any board was connected and a valid output directory was selected. If there was not a board connected, it simply did not start. If the directory was not a valid path, then the program displayed an error to alert the user (Figure 8.17). Once logging was started, it continued saving the data to the files until either the “end” button was pressed, or the window was closed. The plugin also allowed the user to select the directory to store the files using the Java file selector interface. Once a valid directory was selected, a user could open the directory using the operating system’s built in file explorer.

Figure 8.17: Error with UGS Logger Plugin



For the UGS tool changer plugin, it expanded on the functionality of the grblHAL tool changer plugin. It provided a user interface to toggle the dust cover, load and unload tools, and view tool positions. The buttons “Open Cover” and “Close Cover” toggled the dust cover once they were pressed by sending I2C commands to the tool changer module. The button “Remove Tool” unloaded the tool in the spindle if there was one loaded. Tools are selected by clicking on the row of the tool to load. “Current ToolID” displayed the tool ID to the user that was about to be loaded. Once a tool was selected, the “Load Tool” button was pressed to load that tool into the spindle, if it was not already there. The “Reload Table” button refreshed the table manually if the user noticed that there was an issue or discrepancy between the UI and the actual machine state (Figure 8.18).

Figure 8.18: *UGS Tool Changer Plugin*



The screenshot shows a software window titled "<Tool Changer>". At the top, there are four buttons: "Remove Tool", "Load Tool", "Current Tool ID: 4", and three others labeled "Open Cover", "Close Cover", and "Reload Table". Below these buttons is a table with six rows. The columns are labeled "ID", "Name", "Description", "Pocket", and "Spindle". The data in the table is as follows:

ID	Name	Description	Pocket	Spindle
1	1/4" Endmill	description	3	<input type="checkbox"/>
2	Fly Cutter	description		<input checked="" type="checkbox"/>
3	1/4" Roughing Tool	description	1	<input type="checkbox"/>
4	Face Mill	description		<input checked="" type="checkbox"/>
5	45 Deg Chamfer Mill	description	2	<input type="checkbox"/>
6	1/4" Thread Mill	description		<input type="checkbox"/>

The pocket and spindle states were set in the plugin to tell the control board where tools were without requiring tool changes to swap their positions. The table display was loaded when a valid control board was connected and when the plugin was displayed. The plugin monitored the verbose output in the same way that the logger plugin did. It instead looked for status updates that were sent when the board first connected to the control

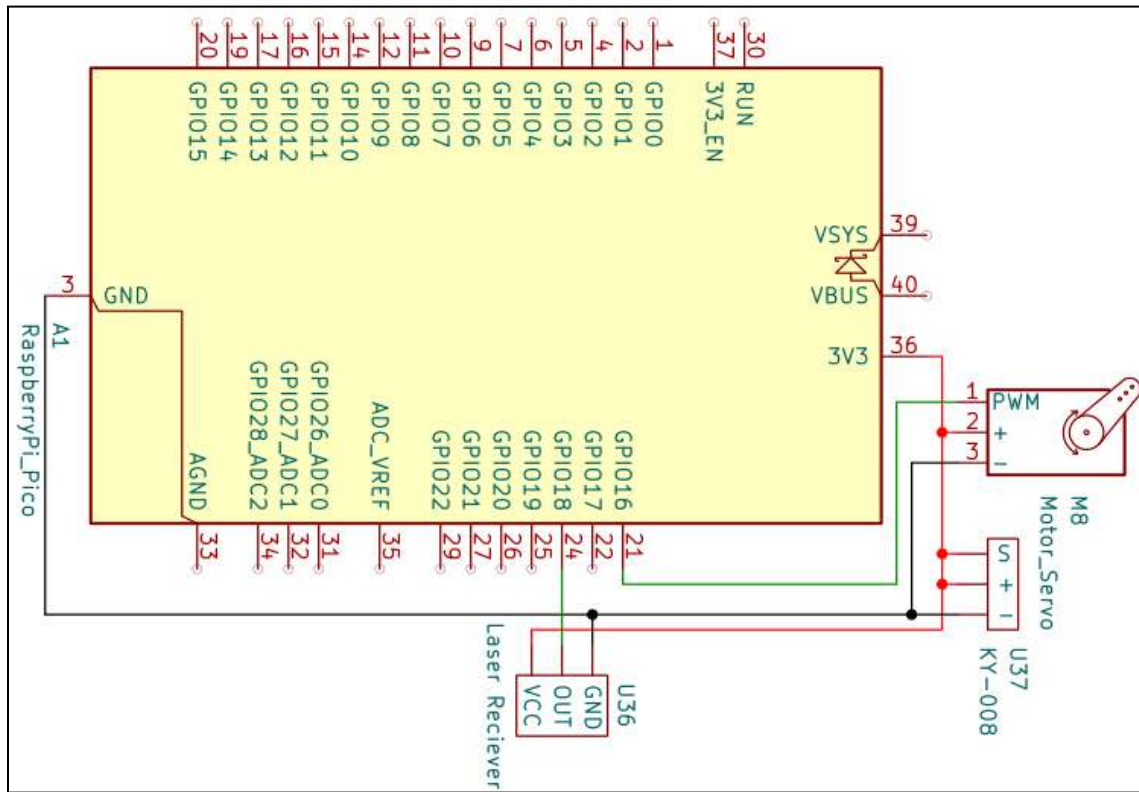
software. When the plugin then received the signal to update the tool table, it sent G-Code commands to get the number of tools enabled in grblHAL, then the status of the tool locations.

8.8 Tool Changer Module

For ATC in a CNC machine, it required a physical module that exchanges the tools loaded in the spindle. With the design constraints of the machine, a new tool changer needed to be designed. The tool changer was designed from the basic concepts from the RapidChange ATC. The new ATC module required custom wiring and software to operate the module.

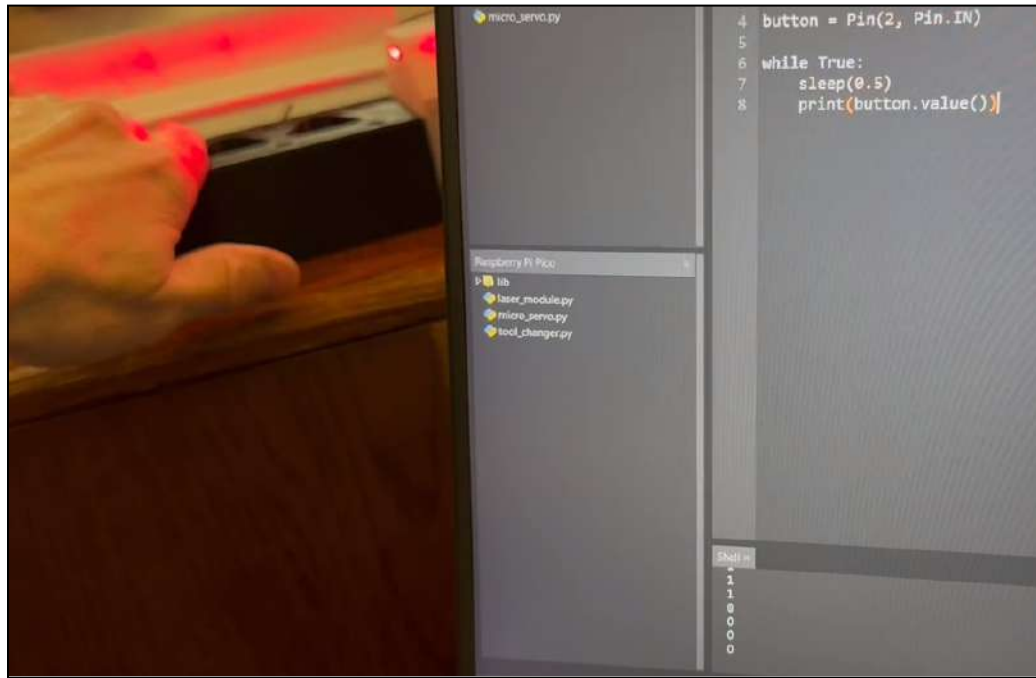
The wiring of the module consisted of a laser transmitter, laser receiver, and servo motors (Figure 8.19). The servo motor was used to actuate the dust cover, turning the specified amount in the code. The laser system consisted of a transmitter and receiver. When the receiver did not detect any signal, the signal line read as 0 V. When the receiver detected a laser signal, the signal read as the supply voltage, which was 3.3 V. The sensors were connected to the pico that was in the casing for the tool changer. The pico would then be wired through the I2C communication protocol to the PicoCNC. The module would then receive signals to move the servos to either the open or close position. The module would also send a signal indicating if the laser beam was connected or not.

Figure 8.19: Tool Changer Module Wiring Diagram



For the software, a prototype was coded in micropython. The prototype would then display to the screen when the laser beam was broken or clear (Figure 8.20). It also actuated the servo between the open and closed position to demonstrate that it was able to toggle correctly. I2C communication was not able to be implemented into the module, meaning that it was not able to communicate with the control board.

Figure 8.20: Tool Changer Module Implementation

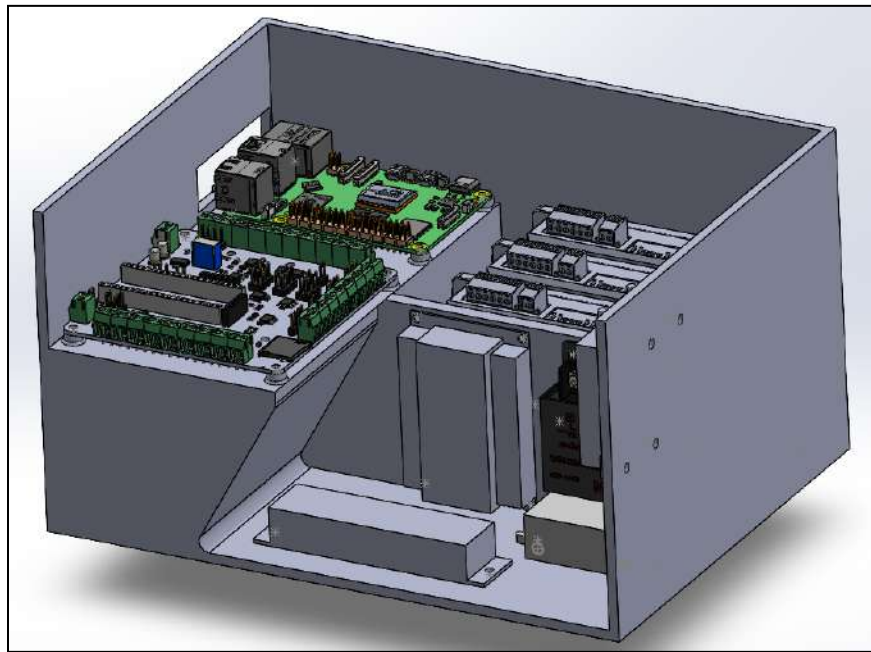


8.9 Electrical Box

The box containing the electrical components of the milling machine was completely overhauled from the previous box. Due to the addition of another motor driver, a Raspberry Pi, several new connections, and the unorganized state of the previous electrical box, a new box was needed for the new machine.

The new electrical box, shown in Figure 8.21, was made larger to fit more components, given specific mounting holes to keep things in place, and printed thicker to provide a more structurally stable container, as the previous electrical box had broken in multiple places from normal handling. Some components were mounted on the sides to save space, and the placement of components was decided based on what things connected to each other, to decrease the amount of loose wires inside the box. Overall, the new electrical box was more accommodating to all the components necessary.

Figure 8.21: Electrical Box Render



With the completion of the control system and sensor integration, the milling machine was ready to be tested. The sensors were able to record the status of the machine while the mechanism was able to be actuated for mechanical testing.

9.0 Testing of Mechanical Improvements

This chapter outlines the verification testing of all mechanical improvements made by the 2024-2025 team. This includes durability testing and coolant-retention testing of the enclosure. In addition, this chapter highlights the testing conducted of various add-on features to evaluate success of their implementation, such as the vacuum, 4th-axis, tool changer, manual bed-leveling, and the lockout-tagout system.

9.1 Enclosure Testing

The following sections lay out the processes used to test the effectiveness of the enclosure. This relates to the enclosure's safety and durability, as well as its ability to properly contain coolant and mitigate leakages.

9.1.1 Enclosure Durability Testing

To ensure the design of the enclosure was rigid and secure, the team subjected the enclosure to durability testing. As shown in Figure 9.1 below, the group assembled the entire enclosure of the machine without placing the panels in. This setup required all necessary 3D-printed brackets with the proper hardware, two C-clamps, a force gauge, and a dial indicator. Two C-clamps were used to hold down one end of the base to the table. This experiment would provide quantitative data showing the relation between force exerted on the system and the overall deflection it caused.

Figure 9.1: *Experiment Setup*



To obtain accurate measured readings, a dial indicator was used. The dial indicator was set up on the corner of the upper corner of the panel and the same side as the C-clamps holding down the base, shown in Figure 9.2. The indicator was moved into the part so that an initial reading was obtained and allowed for the tool to be zeroed.

Figure 9.2: Setup of Dial Indicator



After zeroing out the dial indicator, measurements could start to be recorded. In the upper portion of the t-rail where the dial indicator is placed, the hook of the force gauge was placed into the hollowed out portion of the t-rail, shown in Figure 9.3. Ensuring to zero the force gauge in its configuration force each test, the team varied the pulling forces and noted the corresponding displacement.

Figure 9.3: Testing of Forces Pulling on the Enclosure



The force gauge was then flipped 180 degrees, to do a “push” test, pushing it away from the dial indicator. It was the same configuration as shown in the figure above, however the dial indicator was pushed far into the enclosure as the pushing during the zeroing process, as this test will move the enclosure away from the indicator. See results for this test in Section 12.2.1.

9.1.2 Enclosure Coolant Testing

To verify the enclosure’s ability to maintain coolant, testing was carried out in two separate stages. The first stage was a heavily controlled testing of the sealability of the base of the machine. The second stage involved the practical application of coolant during a machining operation.

9.1.2.1 Base Leak Test

After completing the construction of the enclosure's base, the team wished to verify that there were no major gaps or leakage points with the current assembly. For this, 2000mL of water was poured down the ABS ramp, and then drained through the mesh covered drainage hole (Figure 9.4). The team then timed the drainage rate, and also visually certified that no leakages had occurred; the results of which can be seen in Section 12.2.2.

Figure 9.4: Initial Coolant Ramp Testing



9.1.2.2 Entire Enclosure Leak Test

Upon determining that the base of the enclosure posed no leakage issues, the team conducted the second stage of testing. This required using coolant during the entirety of a two hour long aluminum machining operation. As the previous test only tested the base, the splashing and flow produced from the coolant nozzle would allow for a full assessment of the entire enclosure. The team used this operation to not only validate the enclosure's design,

but to also address any leakage points that may have arisen. The results and discussion for the conducted stages of testing can be found in Section 12.2.3.

9.1.3 Vacuum Test

Testing was carried out to verify the success of the vacuum system's ability to efficiently remove chips from the work area. A wood workpiece was used as it would be a sufficient test because the size of the wood chips are larger than those of teflon. It was not possible to test the vacuum system with aluminum because coolant was needed for cutting aluminum and without coolant, the end mill could overheat and cause chip welding.

During testing, ear plugs were worn and the shop-vac was turned on and off periodically when there were chips building up on the workpiece. The shop-vac could have been running for the entire testing duration, but the team did not deem it necessary to have the vacuum on for the entirety of the operation. The results and discussion for the testing can be found in Section 12.3.

9.2 4th-Axis

In an effort to verify accurate rotation of the 4th-axis chuck motor, testing was done on a rounded piece of wooden stock. After fastening the piece into the clamp, starting with the stock farthest from the chuck, the spindle was jogged in the x-direction. Upon removing stock, the end mill was backed off and the 4th-axis was rotated 90 degrees in the clockwise direction. The process then was repeated until two perpendicular flat faces were milled into the part. The angle of the corner was then measured to check for accuracy.

9.3 Tool Changer

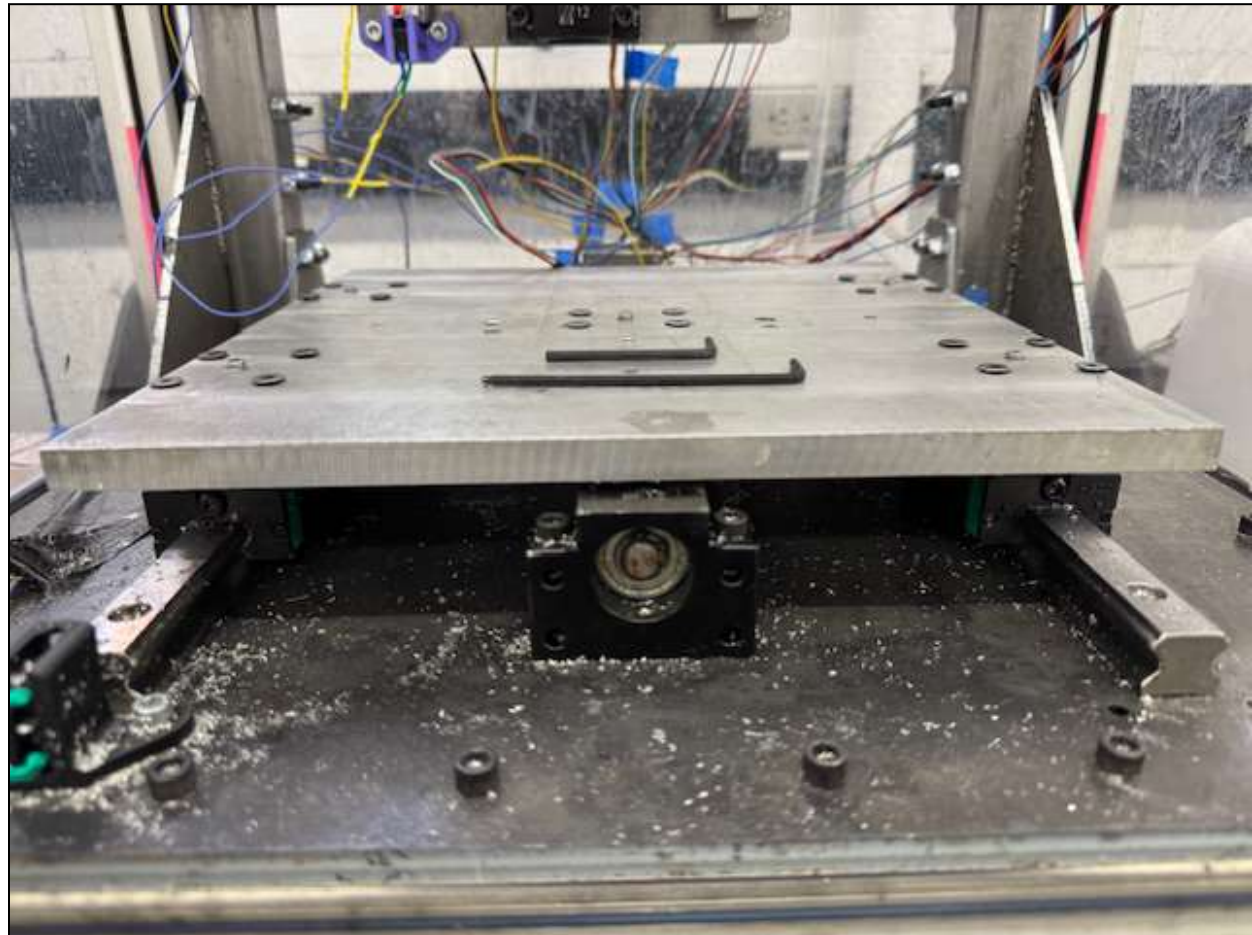
In order to see if the design and software for the tool changer worked, a test was run with 3D printed end mills on the machine. A $\frac{1}{4}$ " diameter end mill and $\frac{1}{8}$ " end mill diameter were created and placed into brand new collets to run the test. In these tests, an unloading of the tool into the tool changer and loading of a tool in the tool changer were run. When unloading a tool, the spindle ran at 3,000 RPM and was successful. As for loading a tool, the spindle spun at 3,500 RPM and began to thread onto the spindle but was unsuccessful.

When it came to the development of the dust cover and laser sensor, the micro servos were able to lift the dust cover over the tool changer and laser sensor was able to register if an object blocked it's path. However, implementation into grblHAL was unsuccessful as the software was not developed in time leading to it not being able to work.

9.4 Bed leveling

To test the effectiveness of the bed leveling design, a dial indicator was used to measure the difference in z-height from limit switch to limit switch in both the x- and y-axes. To begin, the flat-head screws for mounting the bed were loosened (Figure 9.5). The z-axis was lowered such that the dial indicator was brought down to the surface of the bed in the (0, 0, 0) coordinate position. The z-axis was brought down further such that the indicator dial began to turn. The set screw in that corner was turned down to lift that side of the plate up. Whether the set screw could adjust the corner of the plate to within 0.0025" was then determined.

Figure 9.5: Image of the Starting Point of the Flat-Head Screws and Set Screws for Bed Leveling



As can be seen in Figure 9.6, the initial position of the plate was off from the dial's zero position by 0.022". As the set screw was tightened, the dial smoothly turned until it was within a fraction of 0.0005" from the dial's zero position (Figure 9.7).

Figure 9.6: Bed Leveling Testing



Note. The Dial Indicator was brought down until the dial was off from 0.000" by 0.022" in the clockwise direction, which is the direction it will turn when the set screw is turned clockwise.

Figure 9.7: Bed Leveling Adjustment



Note. The set screw was tightened until the dial was within <0.0005" from 0.0000".

The next step was to determine whether the plate could maintain the adjustments when leveling out the opposing sides. The process above was repeated while keeping the z-axis at a constant height, until each of the four corners were adjusted. The final results of bed-leveling testing are given in Section 12.13.

9.5 Lockout-Tagout

The lockout-tagout system is physically composed of a plastic case that locks and holds two plugs in place. At first, the box that was purchased was too large for the intended cables, so a new, smaller box was subsequently bought. The plugs fit snugly in this box, and there was no way to get them out without unlocking the lock or breaking the box or lock.

This chapter examines the testing of various physical components of the machine, including the enclosure, vacuum, coolant, 4th-axis, tool changer, bed leveling, and lockout-tagout. Many tests centered around the machine's operation, with most proving successful, while a few were unsuccessful but nearly functional.

10.0 Testing of Electronics and Software

The software and hardware of the CNC milling machine's electronics went through thorough testing before the end of the project. This chapter details what these tests entailed.

10.1 Safety Systems

The robustness and consistency of the machine's safety systems was of the utmost importance. The team made sure that every component of the machine's safety systems was integrated correctly and worked properly.

10.1.1 E-stop

On the previous year's machine, when the E-stop was pressed, only the motors cut out. With the new control system, it required that the E-stop stopped the spindle to ensure that the machine would not damage itself or harm users. The buttons were used consistently throughout the year, and there was never any kind of mechanical failure within the E-stop mechanism. The button was temporarily wired backwards at one point in the construction process to test limit switches, but this was quickly reversed. The machine's E-stop system is robust and functions as intended. Due to being normally closed (NC), if any wires between the E-stop button and the terminals on the control board were to fail, the system would detect it and act like the button was pressed. The only way that the E-stop could fail is due to mechanical problems in the button itself.

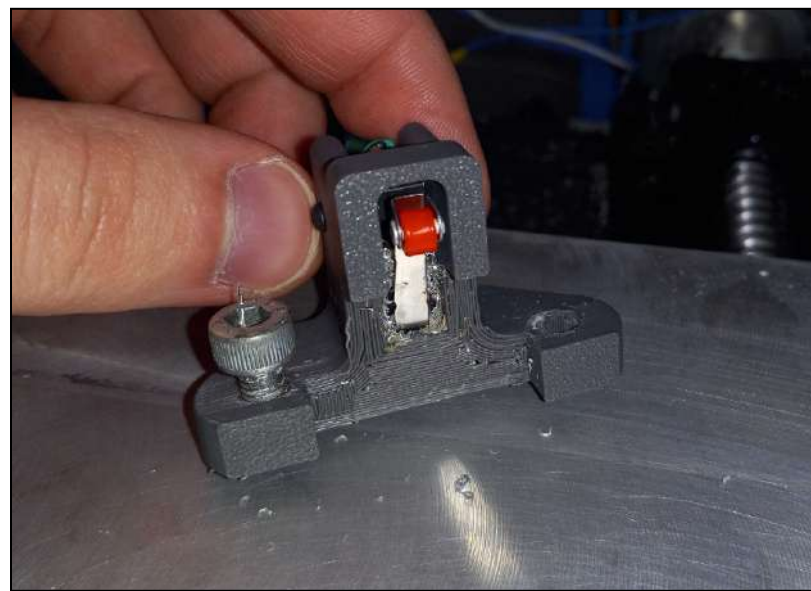
10.1.2 Limit Switches

The limit switches were tested to ensure they worked properly and were resilient. When the machine was first built, the limit switches were pressed to verify that the machine

would go into an alarm state. While the machine recognized the switch as pressed, it did not alarm the machine. This required a grblHAL setting to be enabled to cause it to alarm. An issue that appeared with the limit switches was electrical corrosion. When coolant was run in the machine, despite the heat shrink on the wires, some electrical connections degraded within a day, preventing the machine from being used. After the connections were resoldered on the switches, they started to work properly. It was then concluded that the heat shrink should better cover the contacts, and it was proposed that additional electrical tape be applied to the contacts to protect against any coolant.

Chips from machined parts also began to collect inside the mechanism of the limit switches (Figure 10.1), the underside of which was facing the work area. These limit switches needed to be reoriented so that this would not occur.

Figure 10.1: *Chips Stuck in Limit Switch*



10.1.3 Stack light

The stack light was a component that did not need in-depth testing. There was some confusion about how the relays that power it would be hooked up, but as soon as it was programmed correctly, the stack light lit up either red, yellow, or green corresponding to the state of the machine.

10.1.4 Door Switch

On the previous machine, there were no checks that the door was open. This meant that the machine could still operate with the door open and a user could get severely hurt. With the included door switch functionality built into grblHAL, it was enabled and implemented into the machine. The functionality was tested by flipping the switch while the machine was moving. This immediately stopped the machine from moving, stopped the spindle from spinning, and displayed a door alarm on UGS. When the door was closed and the program resumed, the machine started the spindle again and redid some of the passes on the part before continuing. It was discovered during testing that if the switch was flipped while jogging the machine, the machine would hang and would need to be power cycled. Included with the door was a button override. This was used when setting work offsets, which require the door to be open. Once the button was released, the machine went into the door alarm state.

10.2 Control Board

The control board was tested to ensure that each of the connected systems worked as intended.

10.2.1 Motors

The motors were connected to the control board through the stepper drivers. After the drivers were set to the proper settings, the motors were tested to move the machine. When the machine was set to move a set distance in G-code, it did not line up with the distance set. This was due to the step size not being calibrated for the machine. The steps were calibrated by moving the machine a set distance in G-code. Then, the actual distance measured was used to update the existing step size using the equation:

$$s_{new} = d_{real} * s_{old} / d_{sim}$$

With all three x-, y-, and z-motors have the same step angle, they all used the same final step size: 40.17076 steps per mm. This resulted in an accuracy of around 0.15% of the programmed distance.

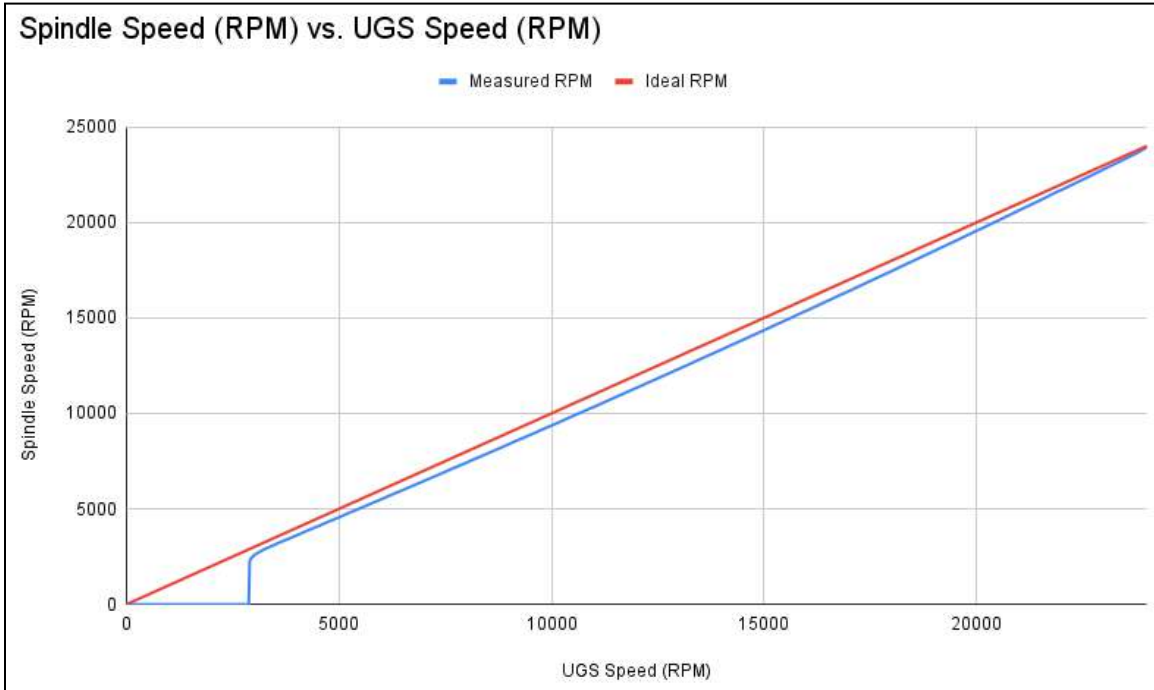
With the default acceleration settings, the machine encountered problems moving in small increments. It had no problem moving distances larger than 0.1" but any lower, and the steps would not be accurate. This was due to the acceleration curve of grblHAL. The initial version of the firmware used an on/off acceleration curve. This meant that if the distance to go was too small, the motors would not be powered on enough in order to go to the next step in the motors. When the acceleration was decreased, the motors were able to move smaller distances, but the overall speed of the machine was severely lowered. After a newer version of grblHAL was installed, jerk settings (the derivative of acceleration) were available to alter the acceleration curve. With jerk settings applied, the machine was able to move small distances while maintaining a respectable speed. The final acceleration values were 50 mm/s² and the final jerk values were 100 mm/s².

For the 4th-axis motor, it was wired and configured in the same way as the other three motors. However, since the motor uses a pulley ratio to affect the turning action, the motor speed and rotation do not correlate well to the intended actuation. After the step size was altered to turn the motor the correct amount, it did not turn as fast as it would have. This meant that the feed rate for the motor had to be increased to move at a similar speed to the other three motors. This also meant that without manual edits to the G-code, the machine would not be able to make accurate parts that required milling while turning. The final step size of the 4th-axis motor was set to 2.25 steps per mm. This value was not properly calibrated but was close for basic testing.

10.2.2 Spindle

Once the issues were resolved with the spindle wiring, a new issue that came up was calibrating the spindle speed. grblHAL has a built-in method that uses up to four lines to compensate for any mismatch between the spindle RPM and the control board analog speed voltage (Figure 10.2). In order to set the calibration lines, grblHAL uses four lines with slope, offset, and range parameters to compensate for speed drift. grbl has a script available that allows users to calibrate the spindle speed based on the programmed speed and the actual speed (“Spindle Linearization Script”). Even when getting the results back from the script, the spindle speed still did not line up. In the end, it required that the slope and offset values be manually adjusted in order to get them into an acceptable range.

Figure 10.2: Default Measured Motor Curve without Linearization Compensation



10.3 Software

For the custom plugins that were implemented in both grblHAL and UGS, they were first tested on a standalone Pico, then on the actual machine.

10.3.1 grblHAL plugins

The stack light plugin was tested first in simulation by having the LED status printed to the console. This showed what LED was active, and whether it was on or off. Initially, the code used delays to trigger the LED update functionality. This was done to verify that the status changes would only update as needed and not called enough to block machine operation. This method, however, did not work. This caused the machine to hang after operating for a few minutes. This was likely due to the grblHAL delay function scheduler. It likely interfered with another function that was called with delay, causing the firmware to

hang. The only way to get the machine working again was to power cycle the board. Afterwards, the code was changed to use the real time function that was called. This prevented any issues with scheduling and stopped the machine from hanging. In the real time function, the time since the last update was checked and if 250ms passed, only then did the function toggle the LED. This prevented the logic from constantly taking up system resources from other systems.

For the tool changer plugin, it was tested using UGS. For the I2C poll function, a spare BNO055 was connected to the standalone Pico I2C pins. When the function was called, it successfully recognized the address of the device and printed it to the user. For the sequence of motions required for loading and unloading tools, the UGS visualizer was inspected to verify it moved correctly. The custom settings that were added to grblHAL were also tested to ensure that each setting was properly parsed and that it updated the settings that were intended. For the tool probe functionality, it was not able to be tested. Due to the motions required to calibrate the tool offset, it needed the laser sensor feedback in order to properly test it. This meant that it could not be tested in simulation and was not able to be physically tested due to time constraints. Additionally, the custom M-codes were tested to verify that they performed properly and parsed command arguments correctly.

10.3.2 UGS Plugins

For the machine logger plugin, it was verified that it stored data properly and that the files could be located. When the plugin was resized, the plugin would not allow it to go past the width of the file path due to the nature of the string. This was fixed by adding spaces and converting the text to HTML text, which allowed the plugin to be resized smaller and for the overflow to wrap to the next page. After the plugin was verified in simulation, it was tested

on the machine. It was discovered that depending on the features enabled on the machine, that the commands would not parse correctly. This was fixed to account for any information collected.

For the tool table plugin, it was tested rigorously in simulation. It was verified to read the console correctly, that commands were not sent redundantly, and that it followed the restrictions based on the firmware, not the plugin. During extensive testing, it was discovered that both the grblHAL and UGS plugin had a bug regarding a tool appearing in two places. For an unknown reason, a tool would appear as loaded in a pocket and in the spindle. This made grblHAL confused when performing tool changes as it did not know how to operate. This also caused a bug in UGS as it displayed the altered state and did not update when the locations on grblHAL were reset.

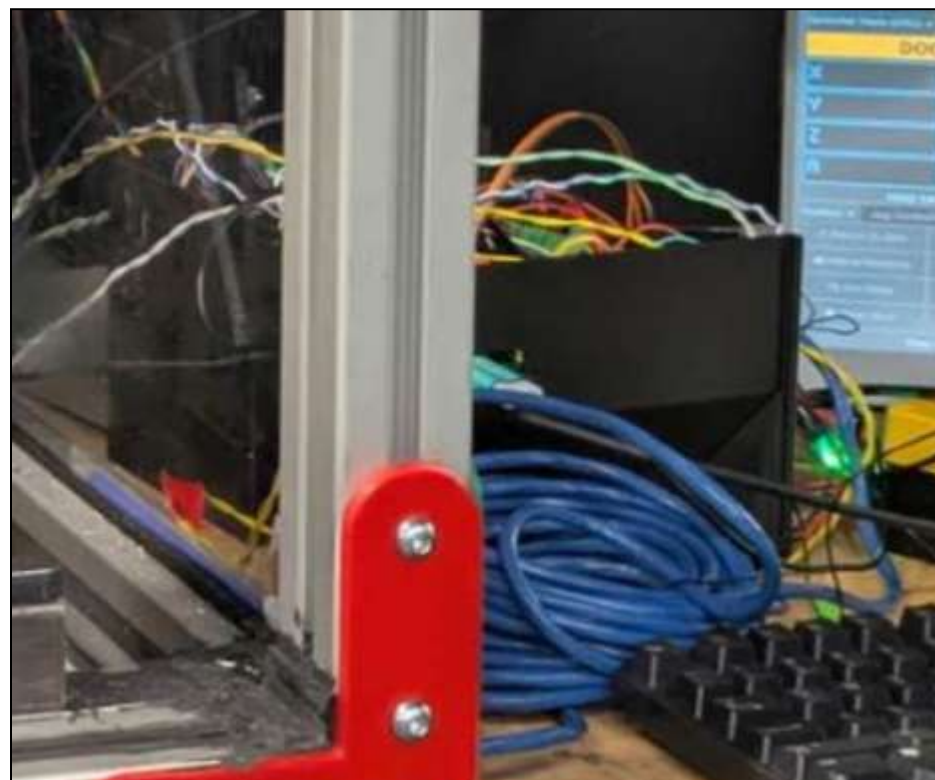
10.4 Sensors

When the sensors were implemented in the machine, they were tested and verified to ensure they worked as intended. For the DHT temperature sensors, a sensor was used to read the ambient temperature. After reading for a few seconds, a lighter was placed near the sensor to verify that sensor value rised to reasonable values. For the IMUs, they were tested to ensure that their values updated properly when the sensors were moved and rotated. There was not any proper procedure applied to verify that the readings were accurate nor to see if the built in calibration sequence was accurate. The laser tachometer system, when it worked, was tested on the spindle in the machine. After the spindle went to the speed set, the laser readings were compared to readings taken by the tachometer. The difference between the readings never got to more than 10 RPM in difference.

10.5 Electrical Box

The electrical box was implemented into the second machine as shown in Figure 10.3, and does a far better job at containing everything than the original model. There were some issues with there not being enough holes in the sides to cover all the wires that needed exits, and some components being hard to reach, but overall, the parts all fit inside the box.

Figure 10.3: *Printed Electrical Box*



Based on the testing done on the safety systems of the machine, the machine can be stopped in emergencies, prevents users from injuring themselves on the machine, and alerts others in the room to the status of the machine. Additionally, the control systems were tested to ensure that it functioned as expected and that the new features were able to be integrated with the mechanical systems. In the next chapter, the physical implementation is discussed as a result of the hardware, software, and electrical work done on the machine.

11.0 Physical Implementation

This chapter covers the combination of the planned physical components into one working milling machine. The chapter goes over the 3D printing of parts, the construction of the overall system, and the process of leveling the workbed of the machine.

11.1 3D Printing Information

Many of the structural components of the enclosure and the sensor mounts on the gantry were made using FDM 3D printing (Fused Deposition Modeling). Components such as the external frame brackets needed to be 3D-printed because the brackets available for purchase online were too expensive. Additionally, components like the limit switch mounts were 3D-printed because they needed to be customized to fit to the gantry.

PETG and PLA were the two types of filaments used to create all the parts needed for the assembly. PLA is the most common printing filament, it is cost-effective, prints fast, and is rigid. However, PLA is also brittle, has poor layer adhesion, starts to warp at 50 degrees Celsius, and it is not resistant to corrosion. PETG is also cost-effective, less brittle than PLA, more heat resistant than PLA, corrosion resistant, and it has better layer adhesion. However, PETG prints slower, it is more difficult to print with, and it is slightly less rigid than PLA.

Due to PETG's corrosion resistant property, all 3D-printed components contained inside the enclosure that are exposed to the flood coolant during operation were printed in PETG so that they would not corrode over time. All of the remaining 3D-printed components were printed in PLA due to its accessibility and fast printing times. PLA was also used to make early prototypes of the components that had finally been made of PETG.

11.2 Overall System Construction

The construction of the mini-mill was a long and arduous process and each step needed to be executed in a specific manner and order. The order of assembly is best explained by breaking down each step into subassemblies that can be executed individually before moving on to the next subassembly.

The first subassembly to be constructed was the “base” of the enclosure frame. This needed to be built first because the gantry will later be fastened on top of this base and it cannot be easily serviced after that. The first subassembly’s construction consisted of preparing the table with holes and film, attaching the t-rail extrusions together with the corner connectors and silicone, fastening that base to the table, sealing the seams of the base with silicone, attaching 3D-printed slot-filters and ramp supports, and inserting the ramp into position and sealing all remaining seams with silicone.

The second subassembly to construct was the gantry’s frame. This refers to just the beams, brackets, and plates that all other linear axes are attached to. The frame was constructed from the bottom up and the holes drilled into the steel square tubing were marked using the holes in the custom ordered plasma-cut steel plates as a reference.

The third, fourth, and fifth subassemblies to construct were the three linear axes, y, x, and z respectively. Each subassembly consisted of two linear rails, a ball screw, a steel mounting plate, aluminum spacer blocks, and fasteners. The y-axis was attached to the base plate of the gantry. The x-axis was attached to the upper plate of the gantry. The z-axis was attached to the plate on the x-axis. At this point the majority of the gantry assembly was complete and ready to be fastened to the base of the enclosure frame with bolts and hammer nuts.

The sixth subassembly to construct was the remaining upper portion of the enclosure. The vertical t-rails were attached to the four corner connector from the base. 3D-printed triangle brackets were fastened to the bottom corners on all sides of the frame with bolts and hammer nuts. The left, right, and rear panel were cut to size using a dremel tool and placed into their respective slotted t-rail. The upper t-rails were fastened to the vertical t-rails with the 3D-printed brackets, bolts, and hammer nuts and the top panel was fastened to the top of those t-rails. Finally, a rubber gasket strip was inserted into the slot of each interior edge of the left, right, and rear panels.

The seventh, and final, subassembly to construct was the hinged door of the enclosure. A polycarbonate panel for the door was cut to size in the same manner as before and slotted between four t-rail extrusions. These four t-rails were attached to each other by corner connectors with silicone and fastened together with the same 3D-printed triangle brackets as before. An adhesive strip of neoprene foam was then attached to the external perimeter of the door. A rubber gasket strip was inserted into the slot of each interior edge of the door panel in the same manner as previous panels. Finally two standard door hinges with custom holes were fastened to the left t-rail of the door and also fastened to the corresponding left t-rail of the enclosure's door frame.

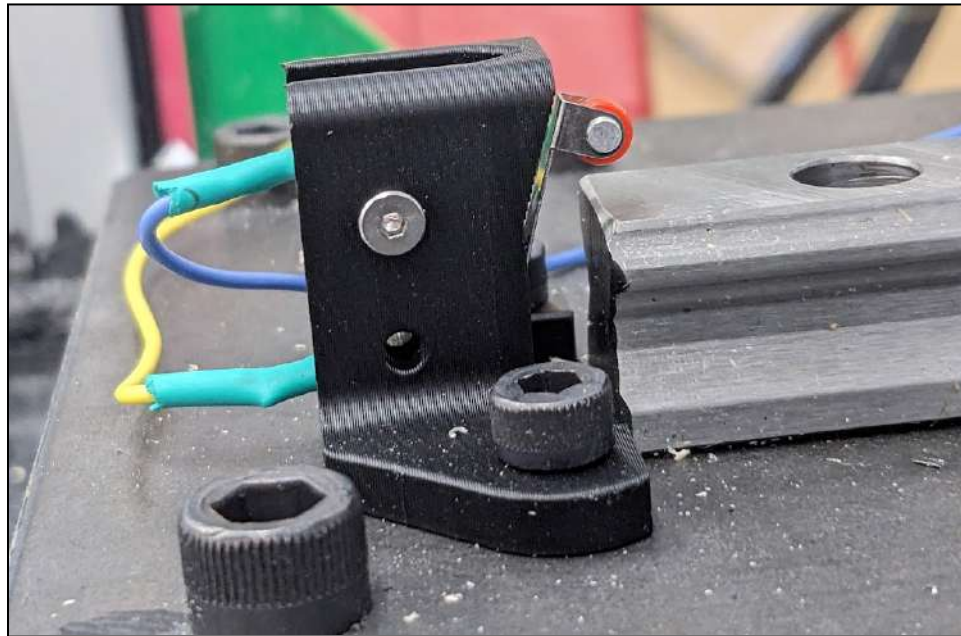
11.2.1 Electrical Connections

The system's wires connect to three main things: the electrical box, the sensor board, and to components within the machine.

The limit switches used in the machine contain two terminals, so that either the NO or NC terminal is connected to the common terminal at any given point in time. In a practical sense, this update entailed switching the wiring to the normally open terminal to

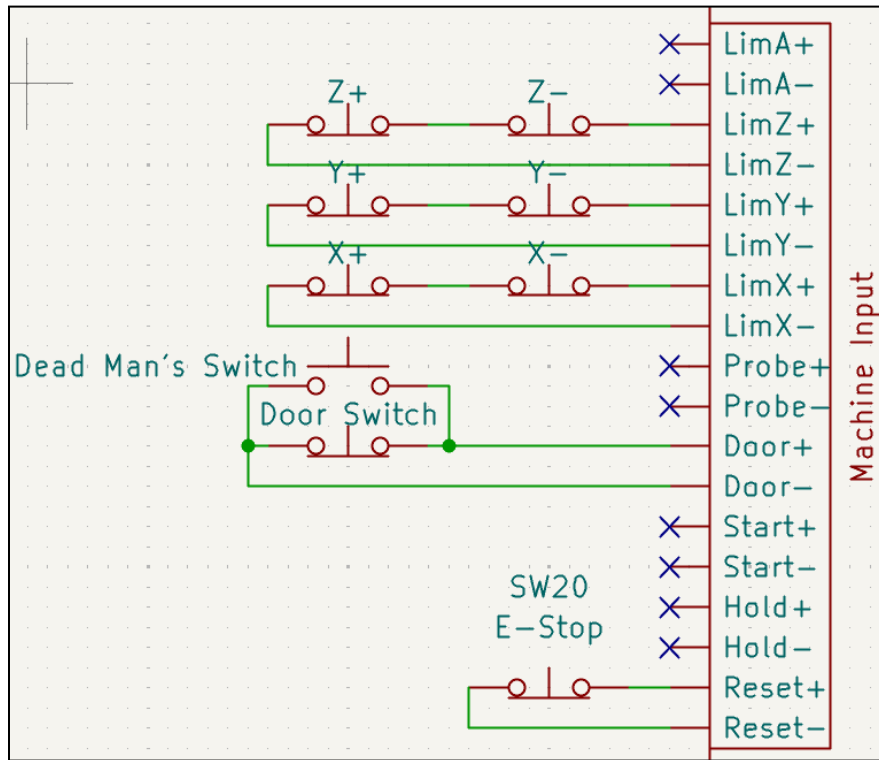
the normally closed one on each of the six limit switches in the first machine, and mirroring this change in the second machine.

Figure 11.1: Limit Switch Implementation



Each pair of axis limit switches were wired in series for their corresponding axes (Figure 11.1). After some initial testing, it was found that if the homing sequence was triggered while a non homing side limit switch was pressed, that the gantry would ram into itself. This caused a temporary fix that made all non homing side limit switches wired in series with the E-stop button, which stopped the machine from ramming into itself. It was later discovered that by default, grblHAL assumes that the limit switch connectors only have one switch attached. The settings that two were in series were set and the limit switches were put back in series with each other. This state is the current state of the machine showcased in Figure 11.2, and operates correctly.

Figure 11.2: Limit Switch Schematic



Several sensors are also placed inside the machine enclosure. Several IMU (acceleration) and DHT (temperature and humidity) sensors were mounted throughout the machine's interior, and are wired to the sensor board mounted on the back of the enclosure. Figure 11.3 is an example of the casing mounts used for this purpose, in this case to hold a DHT sensor.

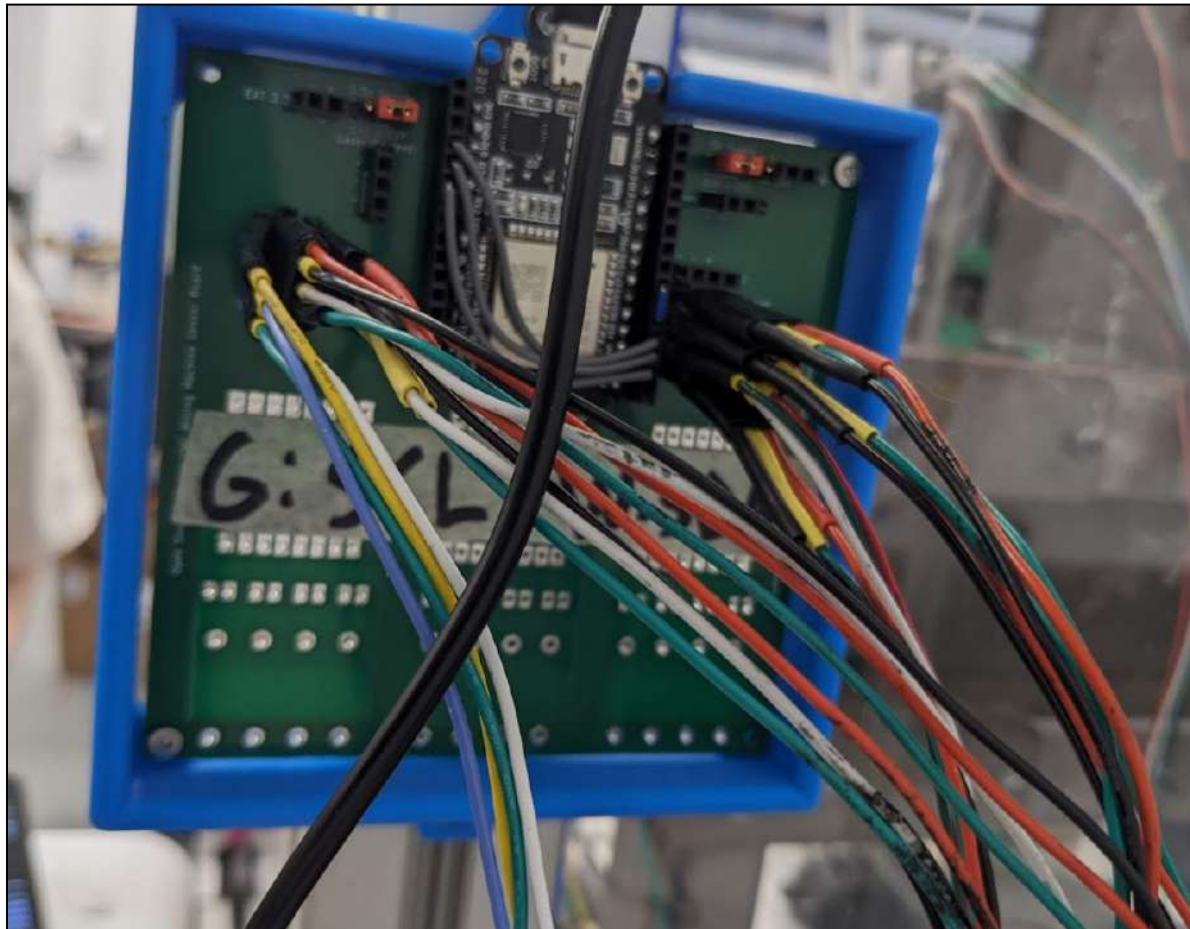
Figure 11.3: DHT Sensor Mount



The sensor board was mounted on the back of the enclosure (Figure 11.4), and acted as a connection between the computer and the components within the machine enclosure.

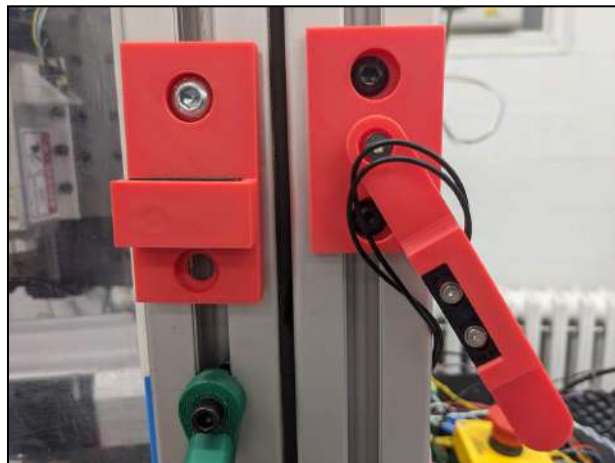
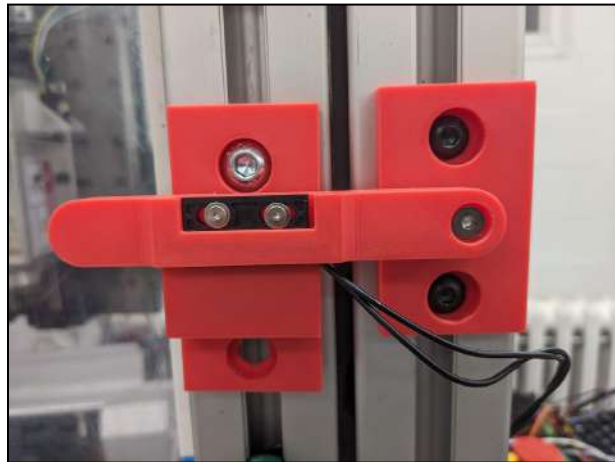
It enabled continuous monitoring of the machine and contained plugs that sensors were able to connect to easily. Additionally, it kept the sensor board away from the coolant and chips that got out of the machine.

Figure 11.4: Mounted Sensor Board



The door switch was mounted on a handle on the non-hinge side of the enclosure's door (Figure 11.5). After some slight issues with tightening the switch's handle too much, it functions exactly as intended. The magnet must be within about half a centimeter to activate the reed switch, which is plenty to shut off the machine when the door is opened, but not so close that it is difficult to get out of "pause mode".

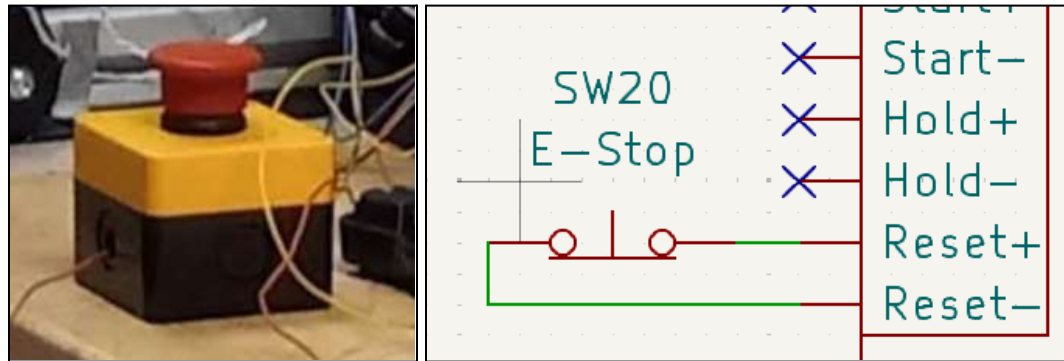
Figure 11.5: Implemented Door Switch



The lockout-tagout system worked as intended, and keeps unauthorized people from using the machine. It did end up being a little cumbersome to unlock and relock each time the machine was used, but that was unavoidable.

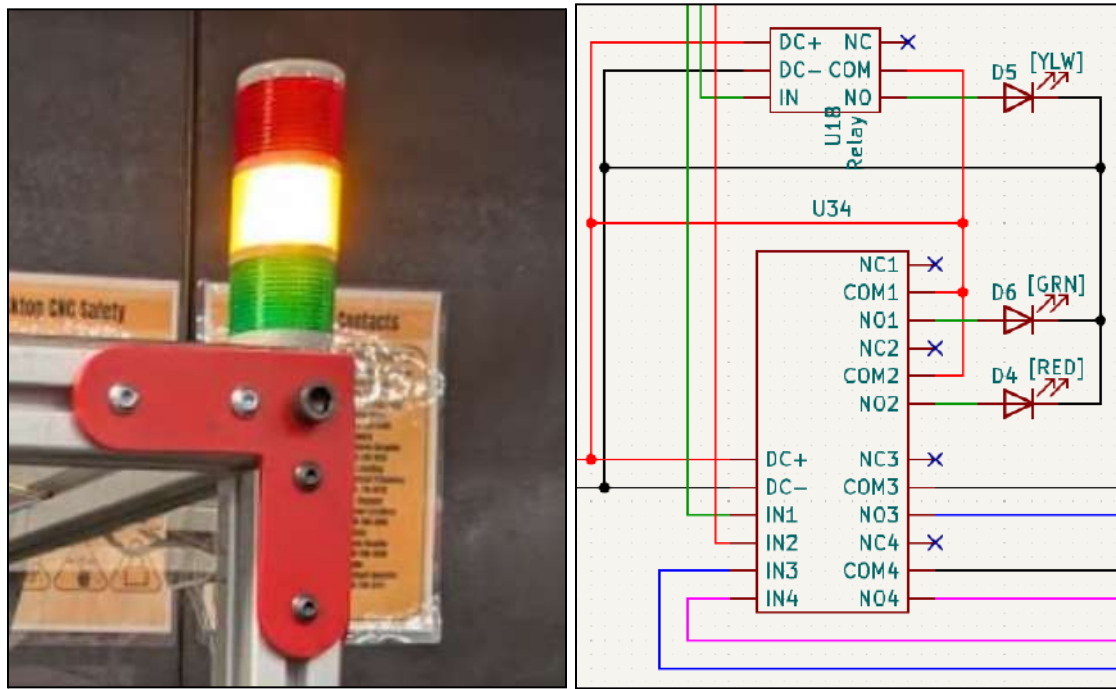
The E-stop also worked as intended, backing out of the program, cutting power to the spindle and motor axes, and setting the stack light to red when triggered (Figure 11.6). The E-stop is directly wired up to the reset pin of the PicoCNC board.

Figure 11.6: Physical E-stop and Schematic



The stack lights were also implemented and worked as intended. The stack light required relays to provide the lights with enough power to turn on, as detailed in the below schematic (Figure 11.7).

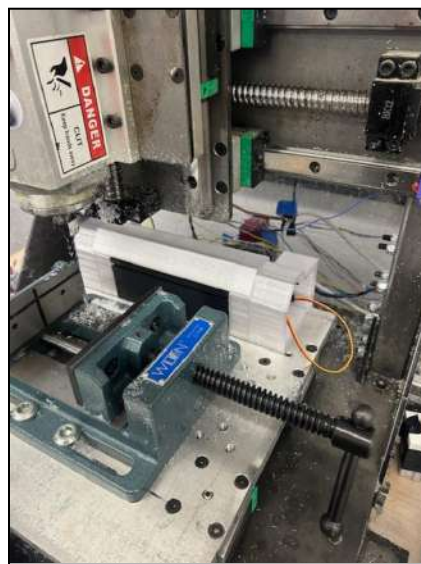
Figure 11.7: Physical Stack Light and Schematic



11.2.2 Tool Changer

When building the actual model of the tool changer (Figure 11.8), the entire structure was 3D printed using PETG and Nylon.

Figure 11.8: Completed Tool Changer in the Machine



The only parts that were printed in Nylon were the clips (Figure 11.9), those were printed with the following settings:

- Layer Thickness: .039"
- Wall Loops: 6
- Infill Density: 60%

Figure 11.9: Nylon Clip with Ball Bearings Inside



The clips were printed at these values because of the amount of stress the clips would be under with the spindle. Nylon is also a stronger material than PETG which would help with dealing with the stress (Filamatrix, n.d.). When putting the clip into the tool changer, a 1.18" spring (Figure 11.10) is placed underneath to bring the clip back up to the top after a tool change.

Figure 11.10: 1.18" Spring Placed Underneath the Clip



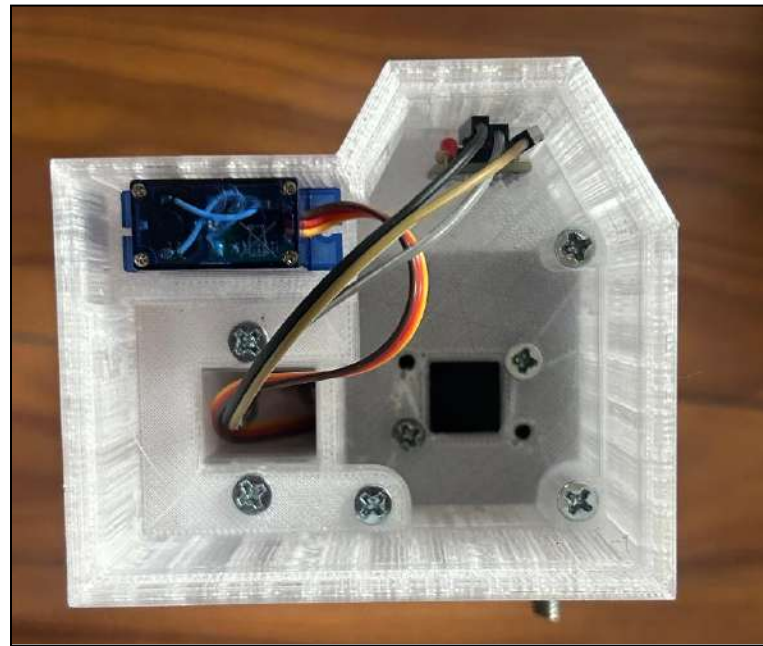
All other parts were made with PETG and were printed with the following settings:

- Layer Thickness: .006"
- Wall Loops: .8
- Infill Density 20%

The rest of the components do not need a high infill as many of them are not going through a lot of stress. However, the base has held up in testing at those values which is why it has not been adjusted.

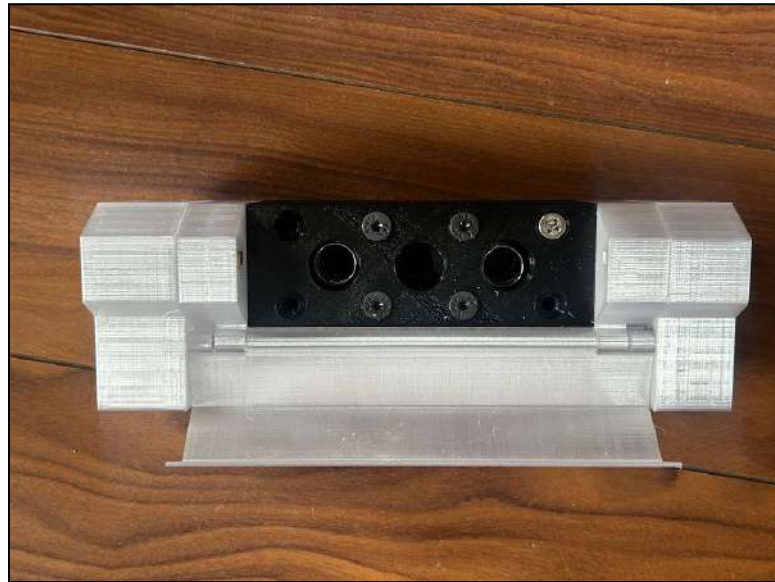
As for assembly, the entire system uses #6 .75" zinc flat head screws to attach each part together (Figure 11.11) besides the top layer and the base.

Figure 11.11: Side Part with all Components Attached to each other using #6 Zinc Screws



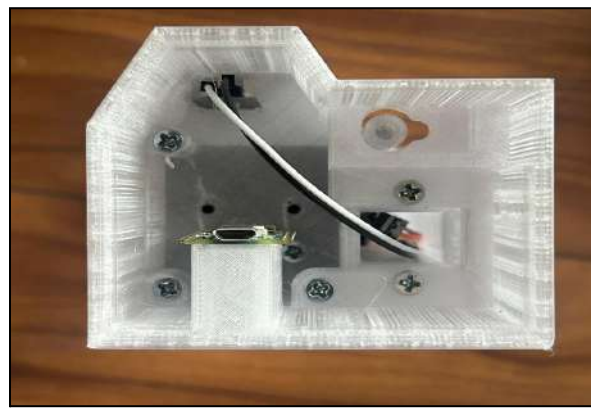
In order to attach the top layer and base, a M6 .787" countersunk screw must be screwed into the top layer to connect the base and the top layer. In order to connect the tool changer to the bed a M6 2.56" countersunk screw must go in the top layer and threaded onto the bed of the machine to attach (Figure 11.12).

Figure 11.12: Top view of Tool Changer with M6 .787" Black Screws and the M6 2.56" Grey Screws



When adding the laser sensor system, the receiver goes in the slot on the right side, and the sensor goes in the slot on the left side. Finally, add in the Pico Raspberry Pi board into the slot on the left side and screw in a M2 screw in the hole of the Pico assuming it is lined up with the hole in the servo cover (Figure 11.13).

Figure 11.13: Left Side part with Pico Board, and Laser Sensor Inside Mounts



11.3 Tests Carried Out

During the course of this project, many tests were carried out including mechanical, electrical, and machining. Appropriate measurement methods were used depending on what was needed in the test. As discussed in Section 8.2 sensors were integrated inside and outside of the machine to monitor operational parameters and verify that no changes made over the course of this year were a detriment to the machine's functionality.

11.3.1 Physics Analysis of the Initial Machine

During the process of iterating on the previous CNC machine, predating any updates, the state of the original machine needed to be measured in order to get a baseline of the original system. To do this, various sensors to the machine to get readings. For the physics analysis, there were two main parameters measured: the temperature of the stepper motors and spindle, the acceleration of the machine, enclosure, and table at various points, and the speed of the spindle.

Testing was completed by machining a simple test part which can be seen in Figure 2.13, the concept of the test part was passed down from the previous MQP team. When the part was machined, it only covered facing the stock and creating the circular and rhombus detail on the top of the part. The stock itself was not machined to a specified overall dimension, original length and width were kept the same. There were four tests completed, two using softwood and two using teflon. The tests were named Softwood_1, Softwood_2, Teflon_1, and Teflon_2 respectively; they are discussed further in Section 12.5.

These four tests that were done as part of the experimental testing used a $\frac{1}{4}$ " flat end mill that had 4 flutes. The initial goal was to run the same NC code for each part however after running the first test part, it was discovered that there was an error when setting the top

height in the CAM software leading to an extended program run time. Softwood_1 ran a slightly different NC Code than Softwood_2, Teflon_1, and Teflon_2, as the CAM was adjusted to fix the error, the three tests used the same process adjusted for the stock dimensions and material. The values for testing can be seen in Table 11.1 below, the feeds and speeds used were approximate values for machining the given material with the ¼" end mill determined based on general machining parameters.

Table 11.1: *Machining Parameters Used for Initial Machine Testing*

Test	Parameter	Target Value	Measured
SoftWood_1	Speed (RPM)	11460	11459
	Feed (IPM)	458.4	458.4
	Depth (IN)	0.01	0.01
	Surface Speed	750.055	750.055
SoftWood_2	Speed (RPM)	11460	11459
	Feed (IPM)	412.56	458.4
	Depth (IN)	0.01	0.01
	Surface Speed	750.055	750.055
Teflon_1	Speed (RPM)	7640	7633
	Feed (IPM)	192.528	192.528
	Depth (IN)	0.01	0.01
	Surface Speed	500.037	500.037
Teflon_2	Speed (RPM)	7640	7634
	Feed (IPM)	213.92	192.528
	Depth (IN)	0.01	0.01
	Surface Speed	500.037	500.037

At the time of initial machine testing, the speed, which refers to the revolutions per minute of the spindle, could not be controlled by the NC controller and had to be adjusted manually. Due to the limited precision of manually adjusting the spindle speed, it was not possible to achieve the goal speed for each test.

The WitMotion accelerometers on enclosure and table are used to take vibration data from surfaces outside of the machine. These sensors are located on fixed items that do not experience motion but motion can be transferred through these rigid structures as there is no designated damping method. The data from outside the machine was processed as if it were data from inside of the machine. Since the machine locations are not actually moving, the wireless sensors' purpose is to detect vibrations and rocking motions created by momentum transfer as the linear motion changes.

11.3.2 Additional Physics Testing

Following the same general process described in Section 11.3.1 additional testing was done while machining the test part at varying points in the process of updating the machine. The first set of testing was completed after the x- and y-axis motor were replaced, Mach3 control board and software replaced with the grblHAL board and UGS software. This testing was completed with softwood and machining parameters shown in Table 11.2.

Table 11.2: *Machining Parameters Used for Testing Softwood_FEB26 After Electrical and Software Updates*

Parameter	Target	Measured
Speed (RPM)	11460	11457
Feed (IPM)	458.4	412.56
Depth (IN)	0.01	0.01
Surface Speed	750.055	750.055

More testing followed the completion of updates made to the CNC machine. The testing that followed was again completed using the same test part and included softwood, teflon, and aluminum. The cutting parameters were updated from the approximate values

used for initial testing to specific values verified as being optimal for machine performance.

The values used for testing can be seen per material in the Table 11.3 below.

Table 11.3: Machining Parameters Verified for Optimal Machine Performance

Material	Spindle Speed (RPM)	Feed (IPM)	Depth of Cut (in)
Softwood	12223	244.46	0.010
Teflon	9167	110	0.010
Aluminum	611	49	0.010

One round of softwood testing involved implementing parameters that limited Mach3 into the UGS software. The parameters limited the feedrate and the acceleration to a maximum of 120 in/min and 4 in/s² respectively. This testing was intended to be used as a comparison to the Softwood_2 testing completed on the initial machine to observe how the updated enclosure, control board, and software affected the performance.

11.4 Bed Leveling

To implement bed leveling, the design that was first created in SOLIDWORKS CAD needed to be used to generate tool paths for drilling the holes for the helicoil threading. These tool paths were created using Mastercam, then the plate was drilled at Washburn shops.

After the holes were drilled, they were tapped by hand for inserting the helicoil. This process was tedious, but it ensured that the tap would not break and thereby the plate would not have to be scrapped. Using oil on the tap, along with proper technique, ensured that the tapping process was successful. The helicoils were then installed, and the set screws were placed within them (Figure 11.14).

Figure 11.14: *Image of the Bed with the Helicoils and Set Screws Installed, in the Center of Each of the Five Mounting Points*



A single solid length of stainless steel was purchased to make the set-screw plates. This material was cut to size using a saw designed to cut metal. The CAD was then used to locate the dimensions of each hole, and the holes were then drilled out by hand. The burr that resulted from drilling was removed with a tool, using the drill press. These stainless-steel plates were then inserted in their respective positions, between the bed and the mounting plates (Figure 11.15). The flat-head screws were installed, but not tightened, as shown in Figure 11.16. Leveling of the bed was then performed, and this process can be found in Section 9.4.

Figure 11.15: Image of the Set Screw Plates Installed Between the Bed and the Aluminum Mount Blocks for the Bed

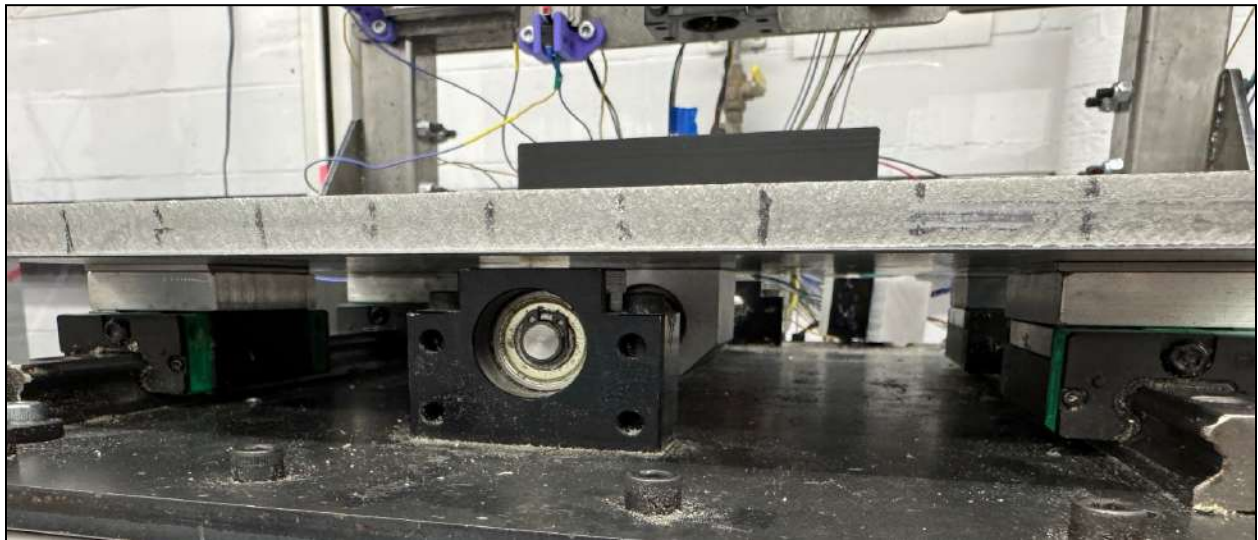
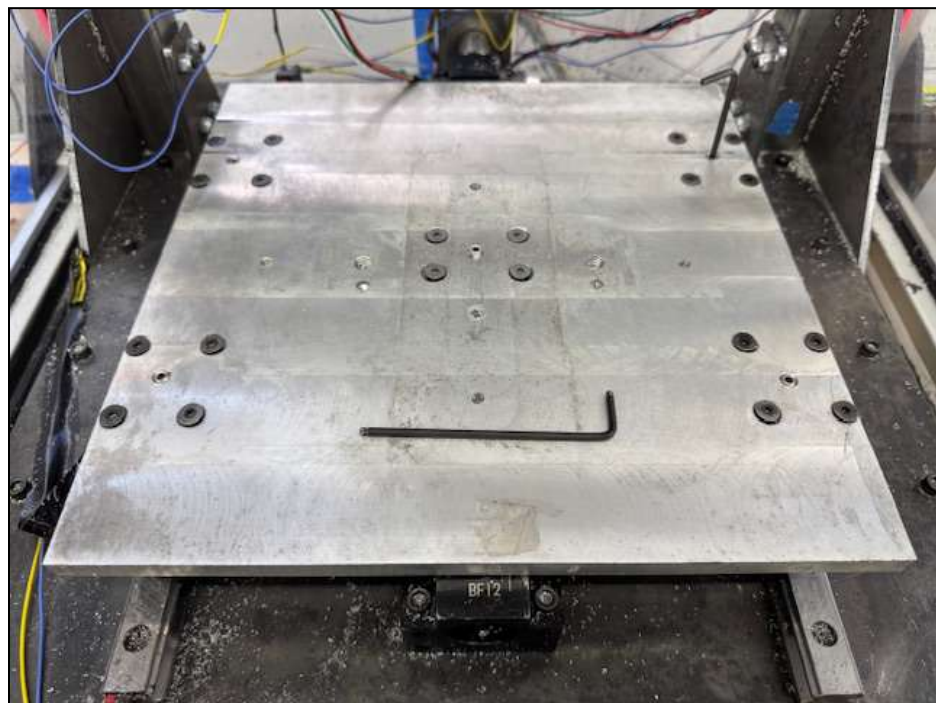


Figure 11.16: Image of Adjusting the Set Screw while the Flat-Head Screws are Loose



11.5 4th-Axis

After the final CAD model of the 4th-axis baseplate was sent to SendCutSend, the design was waterjet cut and sent back over as a manufactured part (Figure 11.17). With all holes within tolerance and aligned, the last thing needed to complete the 4th-axis was to redrill the holes for the chuck piece to ensure it could clamp onto the work area plate properly.

Figure 11.17: 4th-axis Baseplate From SendCutSend

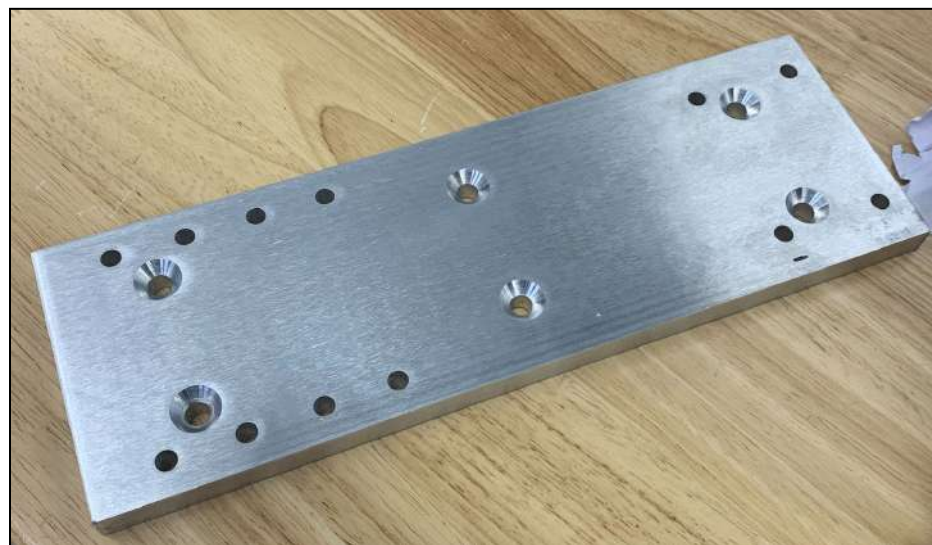
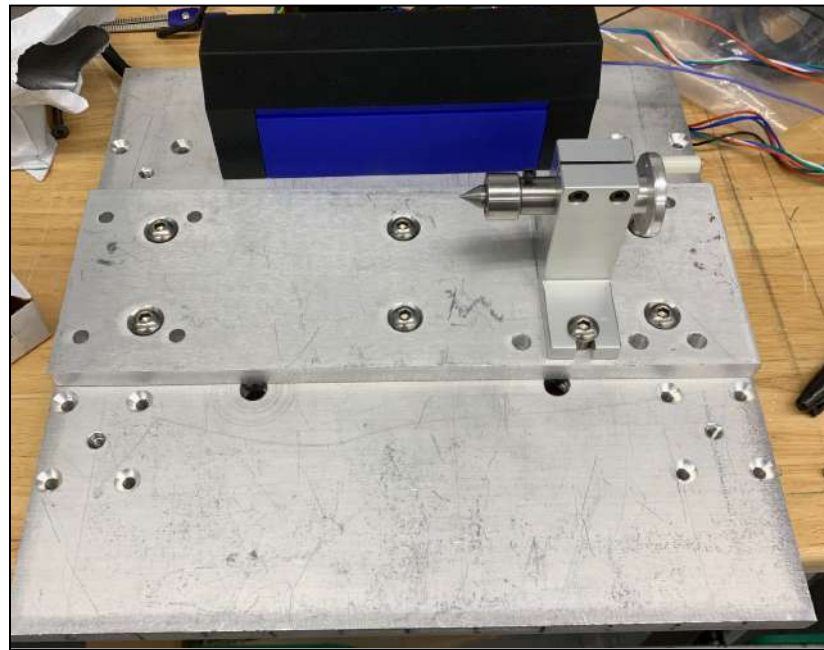


Figure 11.18: 4th-axis Base Plate Mounted to Work Area Plate



Using a drill press, each of the four holes were remeasured to be 0.385" away from the edge of the baseplate, where they were then drilled with a U drill bit on the drill press. After the operation (Figure 11.19), the 4th-axis baseplate was complete and ready to be assembled within the machine.

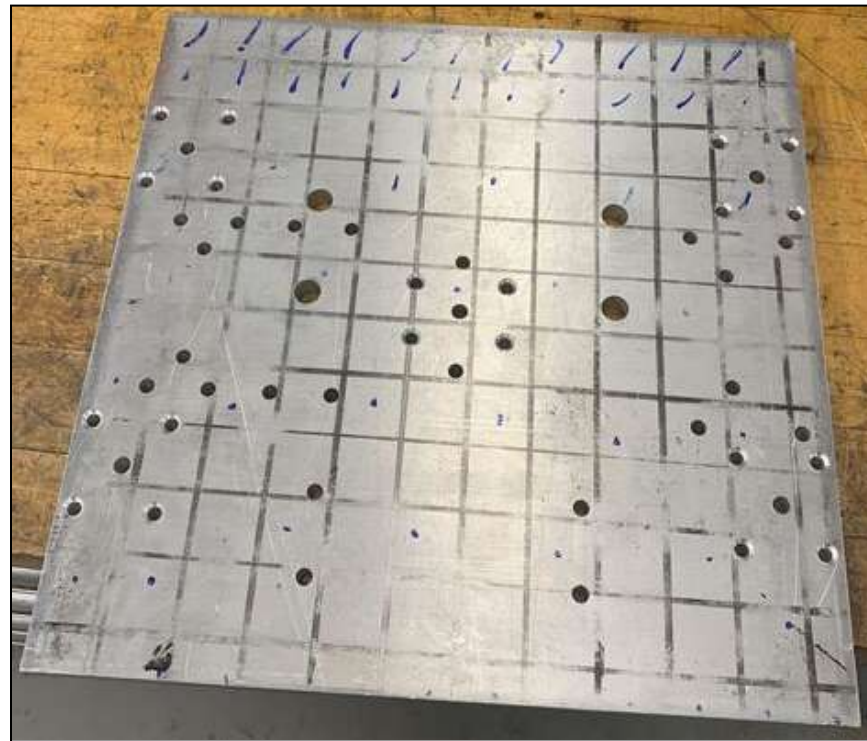
Figure 11.19: 4th-axis Assembly in Current Machine



11.6 Work Area Plates

Once the CAM was complete for the second work area plate, the 12" x 12" x 0.5" plate of 6061 aluminum was taken to the Washburn manufacturing lab at WPI where it was fixed into a Haas Mill. Starting with a spot drill, each pilot hole was drilled using the appropriate drill. As observed in Figure 11.20, work area plate 2 was milled with holes for mounting onto the linear rails and ball screw mount, tool changer, 4th-axis, bed leveling, and the Wilton 4" Vise.

Figure 11.20: Milled Work Area Plate Design 2



In order to mount the functionality onto the plate, the holes needed to be tapped with their respective tap sizes. In doing so, this allowed everything to fasten right to the plate.

- **Bed Leveling:** 1/4" - 20 Helicoil Tap
- **4" Wilton Vise:** 5/16" - 18 Tap
- **4th-axis:** M6 - 1.0 Tap
- **Toolchanger:** M6 - 1.0 Tap

Figure 11.21: Work Area Plate 1 in Current Machine

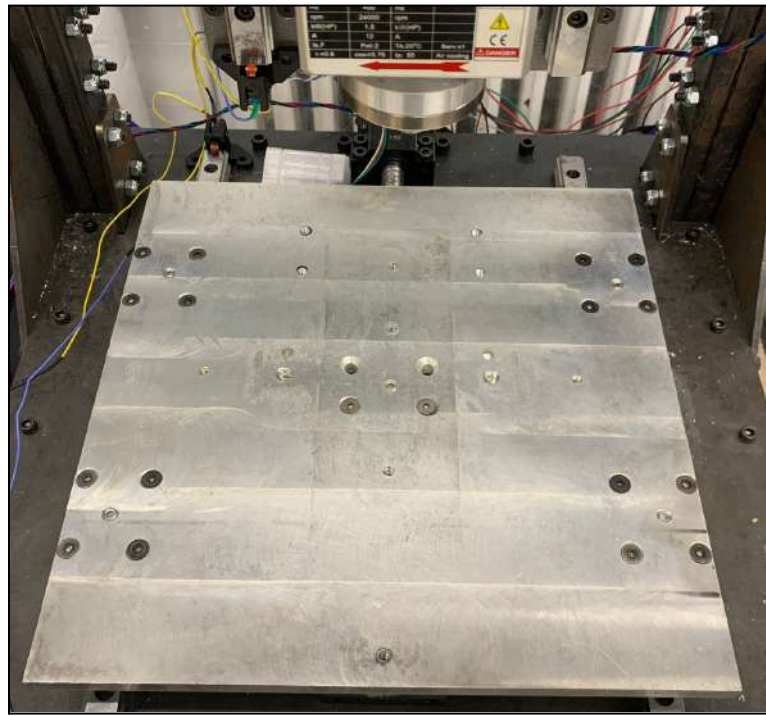
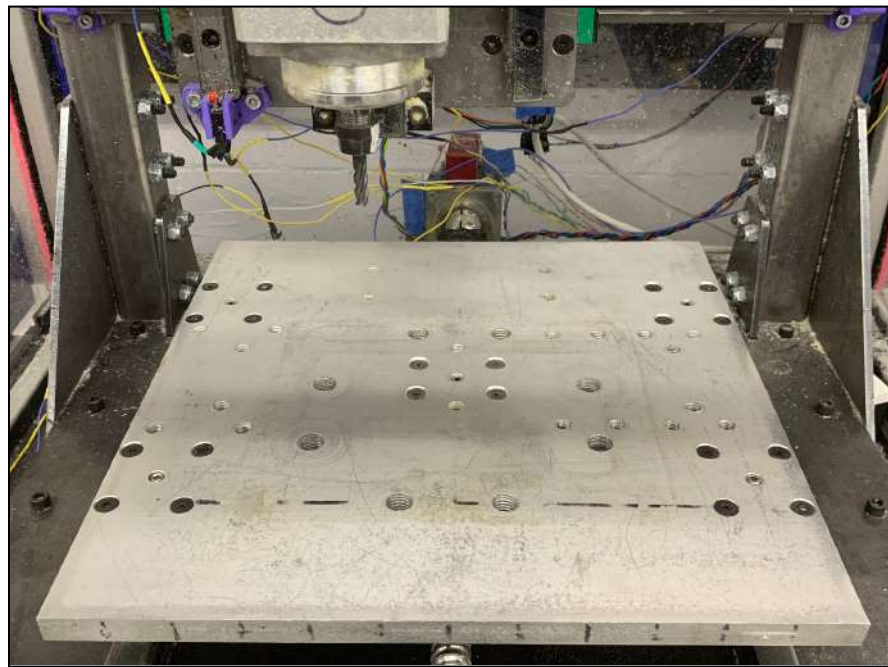


Figure 11.22: Work Area Plate 2 in Current Machine



With tapped holes in each plate for all additional functionality, adding and removing components is very user friendly. Especially with all screws and bolts being standardized, a standard metric and SAE set of allen keys is all a user needs to install their equipment onto the work area plate.

Throughout the chapter, numerous physical implementations were successfully integrated into the machine. Although some faced challenges, the implementations—including the 4th-axis, bed leveling, and tool changer—were tested to obtain results for each. Furthermore, all electrical connections were established, enhancing the overall safety of the machine.

12.0 Results

This section reviews the machining results following the team's modifications, which included the tolerancing of various materials like softwood, aluminum, and Teflon. It also presents the outcomes related to the enclosure, bed leveling, and vacuum, along with tests on physics vibrations and motor temperatures.

12.1 Machining Tolerances Verification

To effectively test the accuracy of the 2024-2025 team's machine in comparison to the 2023-2024 machine, the test part previously discussed in Section 2.8.2 (Figure 2.13) was machined using the updated changes. Utilizing similar toolpaths and modified feeds and speeds, a clear difference in the parts geometric tolerancing could be assessed. The first material machine on the 2023-2024 machine conducted by the current team was soft wood. With a spindle speed of approximately 11460 RPM, feed rate of 458.4 IPM, and a depth of cut of 0.010", this part failed to maintain within the allotted +/- 0.005" tolerance set. As seen in Table 12.1 below, the machine struggled with interpolated geometries, as noted by the failed dimension of A, the OD of the extruded circle. However, when machined on the updated mini-mill with modified feeds and speeds, the tolerancing of all dimensions was within the +/- 0.005" threshold and significantly better at interpolating the circle's OD.

Table 12.1: Wood Test Part Tolerance Verification

Material	Machine	Spindle Speed (RPM)	Feed (IPM)	Depth Of Cut	A Tolerance	B Tolerance	C Tolerance	D Tolerance	E Tolerance
Wood	OLD	11460	458.4	.010"	-0.013"	0.005"	-0.005"	0.000"	-0.003"
Wood	NEW	12223	244.46	.010"	-0.001"	0.001"	0.003"	-0.003"	-0.002"

In addition to machining soft wood, teflon (PTFE) was utilized as another material to gauge the accuracies of the two machines. Initially, teflon was milled using a spindle speed of 7640 RPM, a feed rate of 192.528 IPM, and a depth of cut of 0.010". As with the previously mentioned wood test part, the 2023-2024 machine encountered difficulties with accurately producing circular geometries. For this test, dimensions A (extruded circle OD) and B (extruded circle ID) failed to remain within the +/- 0.005" tolerance as seen in Table 12.2.

When machining the teflon test part in the updated mini-mill, the speeds and feeds were adjusted to assist in creating a better finish with limited burrs. Additionally, this test part also reflected similar findings as the wood test part. For the updated machine, the interpolated toolpaths were within the +/- 0.005" tolerance and created a cleaner finish with less vectorized motions on the extruded circle's OD.

Table 12.2: Teflon (PTFE) Test Part Tolerance Verification

Material	Machine	Spindle Speed (RPM)	Feed (IPM)	Depth Of Cut	A Tolerance	B Tolerance	C Tolerance	D Tolerance	E Tolerance
Teflon	OLD	7640	192.528	0.010"	-0.017"	0.010"	-0.005"	-0.001"	-0.003"
Teflon	NEW	9167	110	0.010"	-0.001"	0.002"	-0.003"	-0.001"	-0.005"

Lastly, aluminum 6061 was the final material to machine tested by both the old and new machines. Aluminum presented various challenges, such as being difficult to machine without the presence of coolant. Due to the old machine lacking proper sealant precautions to maintain machining with coolant, coolant had to be turned on and off intermittently. As a result, a poor surface finish was created and a depth of cut greater than 0.005" was unachievable.

However, as a result of the updated machine possessing the capability to retain coolant and continuously filter and cycle, the aluminum part tested on the new machine produced a significantly better finish. This tolerancing testing also supports the observations made in regards to the wood and teflon parts machined previously. A lack of accurate interpolated geometries was subsequently reproduced when machining on the 2023-2024 machine. Yet, the change in surface finish is not a direct result of the updated machine having a better machining capability. As shown in Table 12.3, the speeds and feeds were inaccurate for machined aluminum when conducted on the old machine.

Table 12.3: Aluminum Test Part Tolerance Verification

Material	Machine	Spindle Speed (RPM)	Feed (IPM)	Depth Of Cut	A Tolerance	B Tolerance	C Tolerance	D Tolerance	E Tolerance
AL 6061	OLD	17572	351	0.005"	-0.015"	0.000"	-0.006"	-0.001"	-0.001"
AL 6061	NEW	6111	49	0.010"	-0.002"	0.003"	0.001"	0.000"	0.000"

While the cutting parameters changed from machine to machine, this testing did provide the team with conclusive data on the inaccurate interpolation of the 2023-2024 machine. Based on the significant undersize of the extruded circle's OD in all three instances, in addition to the vectorized finish shown in Figure 12.1, it was evident that the old machine was not as efficient in creating these toolpaths.

Figure 12.1: Vectorized Aluminum Part Machined on 2023-2024 Mini-Mill



12.2 Enclosure Verification

Sections 12.2.1 and 12.2.2 discuss the testing conducted on the updated enclosure design to validate its coolant retention rate. Within these sections, it lays out the results from the respective testings as well as the challenges and areas for improvement of this design.

12.2.1 Enclosure Durability Testing Results

Based on the data collected from Figures 12.1 and 12.2, a minimal and steady increase in displacement was shown when increasing the force for both pushing and pulling respectively. At a force of 10 lbs, the enclosure only moved at a maximum of 0.04" for pushing and 0.07" for pulling, shown in Figures 12.2 and 12.3 respectively. This follows the trend of the elastic deformation portion of a stress vs. strain curve, where in the elastic region there is a linear relationship before an exponential function takes over when plastic deformation occurs. It is vital to have elastic deformation so the enclosure, if impacted by an

internal or external force, can relocate itself back to the “zero” reference. Plastic deformation is not wanted as it will cause for the enclosure to lose its structural integrity and misalign key functions, such as the door or coolant leakage system. As such, this test proves the enclosure’s ability to withstand forces without compromising its integrity.

Figure 12.2: Force vs. Displacement for Enclosure Pushing Test

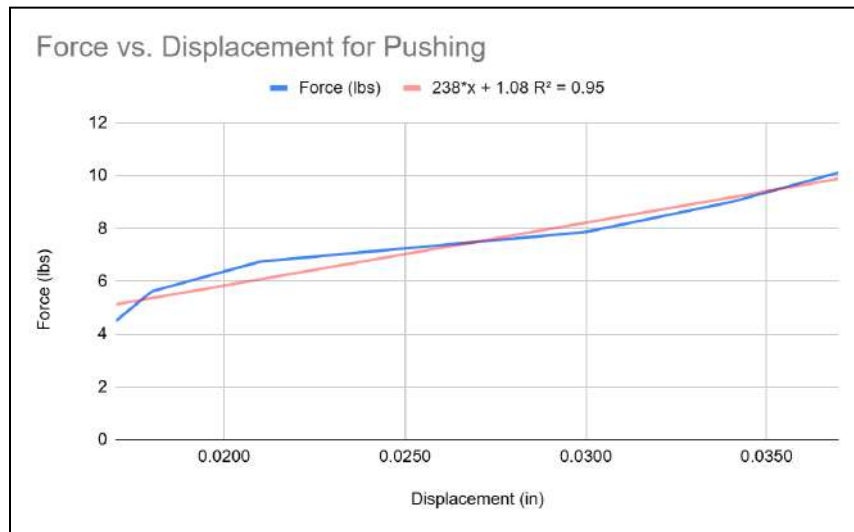
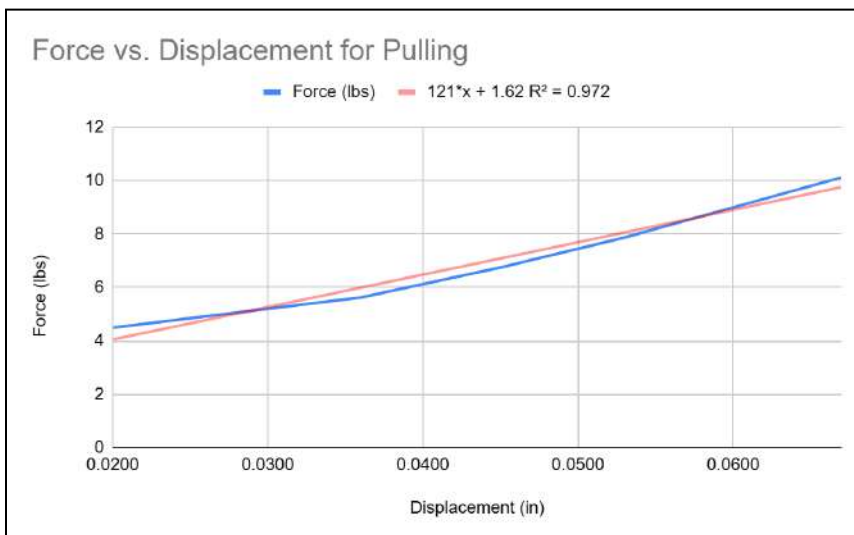


Figure 12.3: Force vs. Displacement for Enclosure Pulling Test



12.2.2 Base Leak Test Results

To verify the sealability of the enclosure's base a controlled test was conducted, as described in Section 9.2.1. All 2000 mL of water had been successfully drained from the enclosure through the mesh drainage hole after 1 minute and 30 seconds. No water was found to have penetrated any of the caulk sealing the t-rail and the polypropylene sheet, nor the areas covered by the 3D printed t-slot fillers. After confirming that no excess water had found its way to the outside of the machine or in any unwanted areas, the team determined this test as a success. It had effectively proven the enclosure base's ability to withhold liquids while properly and efficiently draining them.

12.2.3 Fully Assembled Enclosure Leak Test Results

This section describes the results of the two separate enclosure leak tests conducted during the machining of an aluminum test part.

12.2.3.1 Fully Assembled Enclosure Leak Test 1 Results

To validate the entire enclosure's sealability, it was determined to test a practical application of coolant with the machining of an aluminum part, as described in Section 9.1.2. During the entirety of the two hour long machining operation, the enclosure endured a fair amount of leakage. Many of the leakages propagated due to the baseplate-door interface. As the coolant flowed off the bed and onto the baseplate, any gaps from the foam to the bottom of the t-rail became leakage points. This allowed for coolant to pool up in the slots of the double slotted t-rail, and make its way through the 3D printed corner gaskets. As such, coolant began leaking out of the areas where the corner brackets were located (Figure 12.4).

Figure 12.4: Front Face of T-Rails where the Coolant is Leaking From



Additional leakages from the corner gaskets were noted to be caused from the pooling of coolant at the upper faces of the base t-rail. Despite applying heavy layers of caulk in this area to both the t-rail and the corner gasket, the amount of coolant this area experienced was fairly significant. Furthermore, the enclosure utilized a two-part design for the corner gaskets. At the location where the two pieces met, there were gaps that allowed coolant to seep through. The team addressed this and designed a part corner bracket to remedy this issue.

Another area that possessed high amounts of leaking was the back panel's motor mount cutout. Since the team had used hand-tools to cut this portion, there were gaps between the motor and the motor. Coolant that had been sprayed or splashed far enough to reach the back panel was able to escape through this cutout.

Smaller leakages came through the holes in the table where the t-rails were secured with bolts and hammer nuts. The team had not anticipated coolant to access any of the areas beneath the t-rails, including the bolt holes, and did not caulk those areas. However, due to leakages through the corner gaskets, coolant was able to build up in these areas and escape. This was found in both the front and the back of the machine.

Furthermore, the enclosure possessed some issues regarding coolant drainage and recycling. Through the initial first quarter of the machining process, the coolant successfully made its way through the drainage hole, and was cycled back through the system. However, after significant chip removal due to the time of operation, the drainage hole consistently became clogged. This was due to only having one drainage hole, and a mesh covering that was too fine. The chips would cover the hole and not allow coolant to drain, often pooling up high enough to nearly reach the upper face of the t-rail. Thus, a recurring stoppage of the program was required to remove the chips and allow the coolant to cycle back through the system.

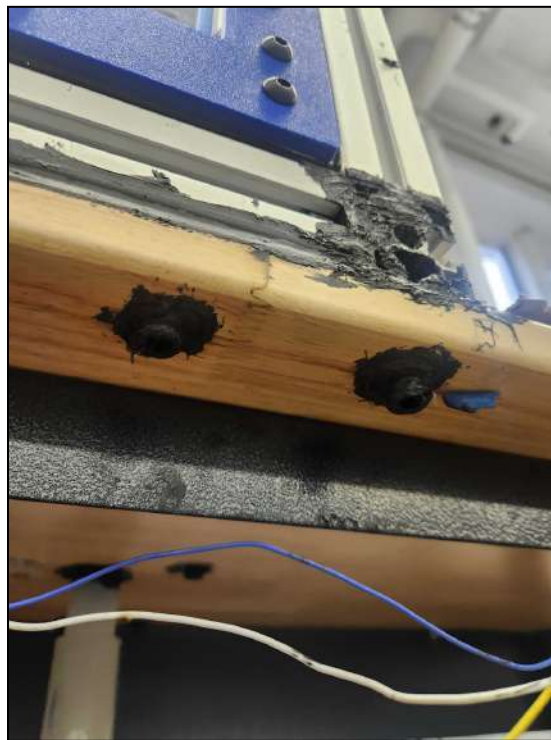
Despite the large amount of leakages in the system, the gasket and panel interface appeared to work as intended. With a majority of the coolant splashing on the side panels, no leakages of any kind were found to be due to the gasket and panel interface. This comes as a result of the panel spacers pushing the panel into the gasket creating an extremely tight seal. It should be noted however that a small amount of coolant did pool up at the bottom of the t-rails, which was deemed to have been attributed to the leakages from the corner gasket.

12.2.3.2 Fully Assembled Enclosure Leak Test 2 Results

After analyzing the shortcomings and potential problem areas in the design, the team decided to apply a significant amount of caulk to the corner gasket areas as well as the bolt

holes. In doing so, the second iteration of this test posed slightly better results, albeit still having some areas of leakages. During the second testing there were still leaks stemming from sealing issues with the corner gasket, as a small amount of coolant was to be pooled up in the t-rails and leaking from the door foam. Nevertheless, the second applied layer of caulk did help in some areas as there were noticeably less leaks from the front and back face of the t-railss, as well as the bolt holes (Figure 12.5).

Figure 12.5: Bolt Holes



Note. After caulking.

12.3 Vacuum Test Results

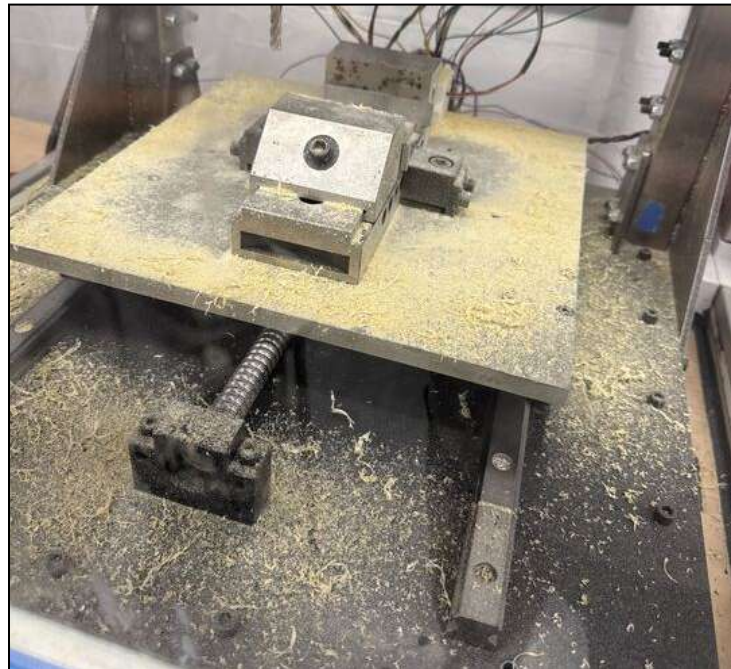
To validate the vacuum system's capability, testing was done on wood. The machining operation took less than 1 hour. The vacuum was turned on periodically throughout the test when chips started building up on the vise and wood part as mentioned

in Section 9.1.3. The figures below showed the work area plate after milling wood with and without the vacuum system.

Figure 12.6: *The Work Area After Milling Wood with Vacuum System*



Figure 12.7: The Work Area After Milling Wood without Vacuum System



The difference between the two above figures showed that there was a significant improvement to the work area with the vacuum system. There were still chips on the sides, under the bed plate, and the back of the machine with the vacuum system. Although the vacuum system was moderately loud, it was able to remove a significant amount of wood chips from the work area. Even though the vacuum system proved to be extremely effective, there are improvements that could be added to the system (reference Section 14.1.1.1).

12.4 Physics Initial Testing Results

This section will go into detail the results achieved when completing physics testing on the initial machine as described in section 11.3.

12.4.1 Motor Temperatures

The axis motors have an ambient temperature operating range between -10°C to +50°C and a temperature rise of 80°C (STEPPERONLINE, 2025). By referencing the instruction manual that came with the spindle motor, it was also found to be operating within safe temperatures. It has an ambient temperature range of -5°C to 40°C but is meant to operate at a temperature of 20°C. The motor is rated as having class F Insulation, meaning it can operate at temperatures up to 155°C. There is built-in error detection for the spindle along with the VFD where if the inverter temperature exceeds 65°C an error will be reported on the VFD screen (Yalang, n.d.).

Figures 12.8 - 12.11 show the temperatures recorded during the four different machining processes. An observation that can be noted about the temperature data is that for all four tests, the spindle motor always had the lowest temperature. The x- and z-axis experienced similar temperature curves to each other while the temperature of the y-axis stayed above the spindle temperature but below the x- and z-axis motor temperature. This pattern makes sense as the machining process for the test part makes long passes in the x- and y-directions while the positions in the z-direction are not experiencing continuous motion. Additionally, the y-axis motor is exposed to air when the x-axis isn't, causing it to be cooled.

Figure 12.8: Softwood_1 Motor Temperatures

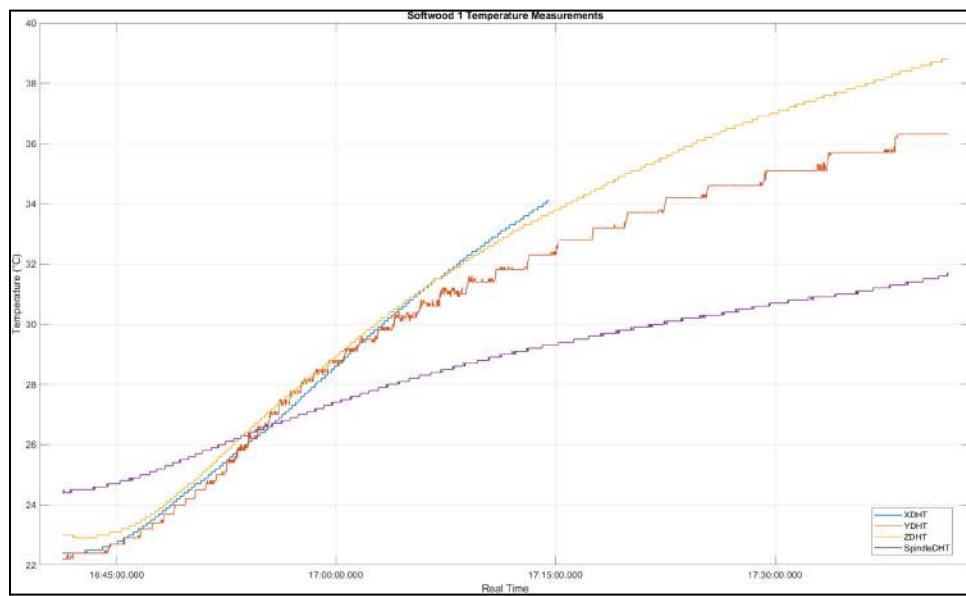


Figure 12.9: Softwood_2 Motor Temperatures

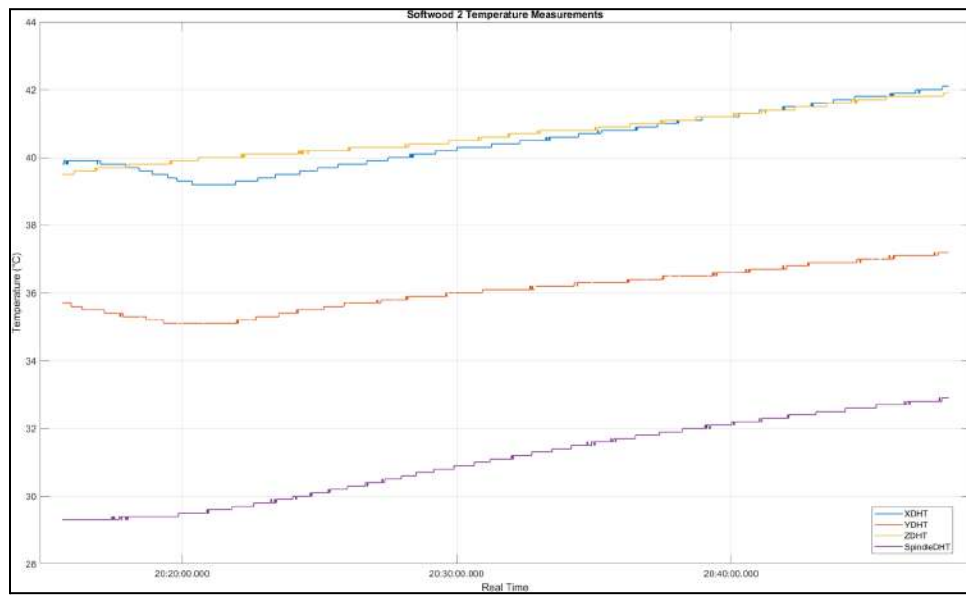


Figure 12.10: Teflon_1 Motor Temperatures

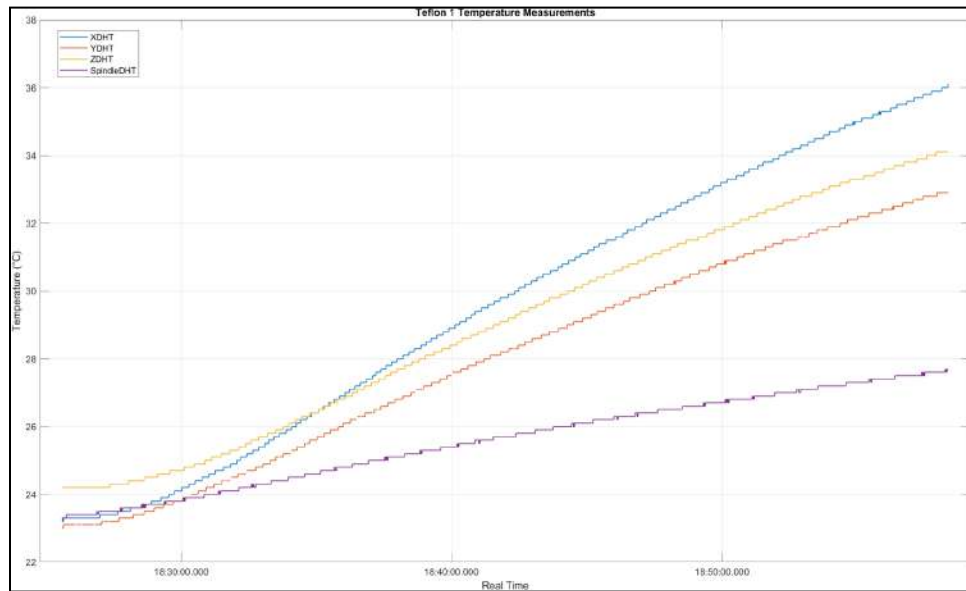
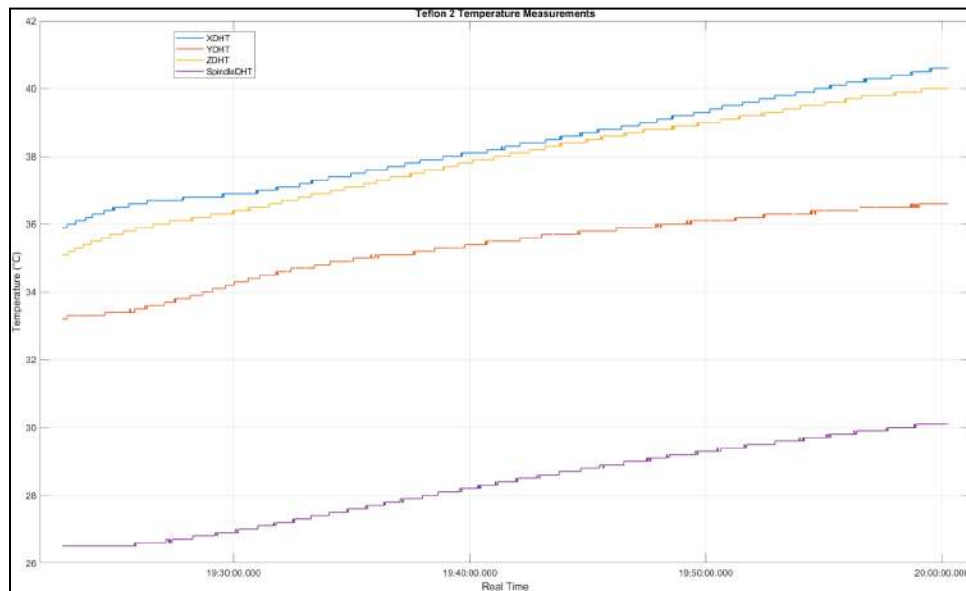


Figure 12.11: Teflon_2 Motor Temperatures



The temperature data was analyzed and graphed using MATLAB; the graphs were plotted with minimal filtering only included to classify any temperature values below 20°C or any values outside of four standard deviations as a non-number. Noise and outliers were

uncommon in this data set, therefore, most raw data did not contain any values that required filtering.

The axis motors were found to be operating at safe temperatures, during this testing the maximum they reached was 42.1°C which is well within their operating temperature. The spindle also experienced a maximum temperature recorded on the spindle was 32.9°C which is well within the operating range. The testing does not follow a consistent path during the machining process despite running practically identical CAM. The final conclusion of this testing is the temperatures of the motors increase over time but remain well within safe operational limits.

12.4.2 Acceleration Data

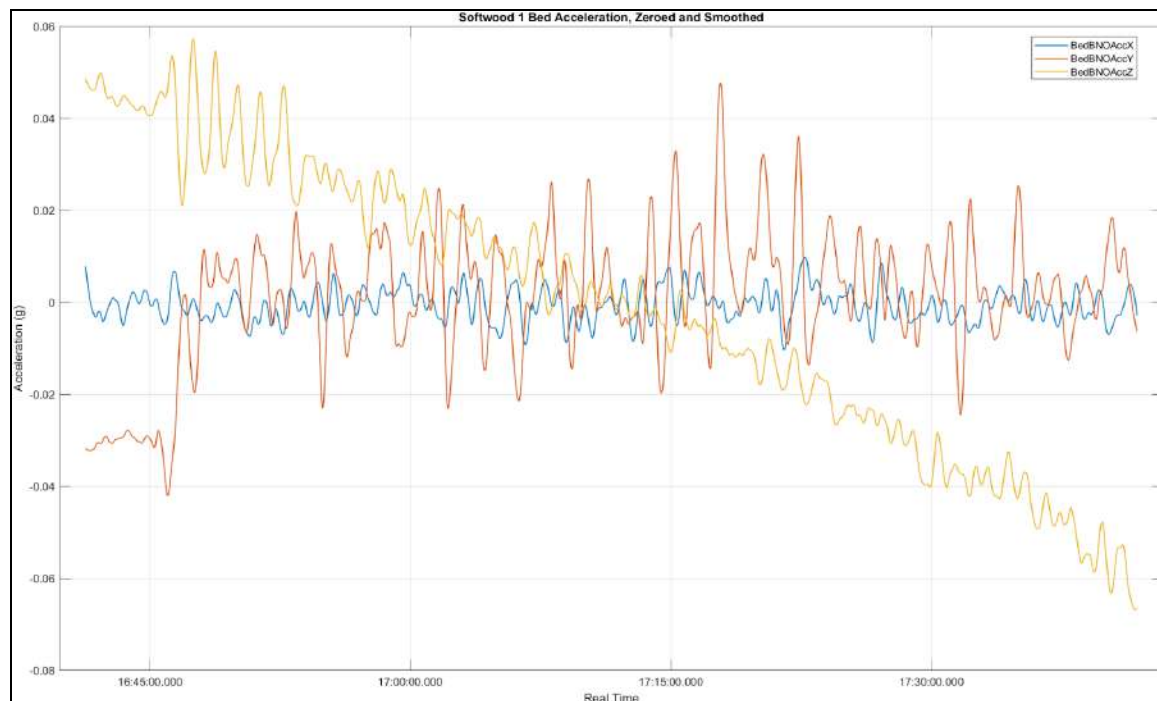
Unlike the temperature data, the acceleration data contained a significant amount of noise and experienced drift during some of the testing. Much troubleshooting was done with the MATLAB code to effectively zero the data and smooth it to remove any outliers. Additionally, there were issues in consistently obtaining reading from the accelerometers as they would regularly report I2C errors which contributed to inconsistent data. Most data obtained only serves the purpose of comparing to other testing results taken from the machine. The data from accelerometers was collected at a rate of 10 points a second and recorded up to two decimal places.

An important note for this section is any graphs that are referred to as the “frame” are discussing the structure of enclosure that surrounds the machine gantry.

12.4.2.1 Softwood Testing

This testing was the first use of the custom sensor system to obtain data during machining. The bed accelerometer data from the Softwood_1 can be seen in Figure 12.12 and experienced the greatest amplitudes of data in the y-direction. This finding makes sense as the y-direction is the only direction that experienced axis motion on the bed. Any data in the x- and z-directions on the bed is indicative of vibrations propagating through the machine.

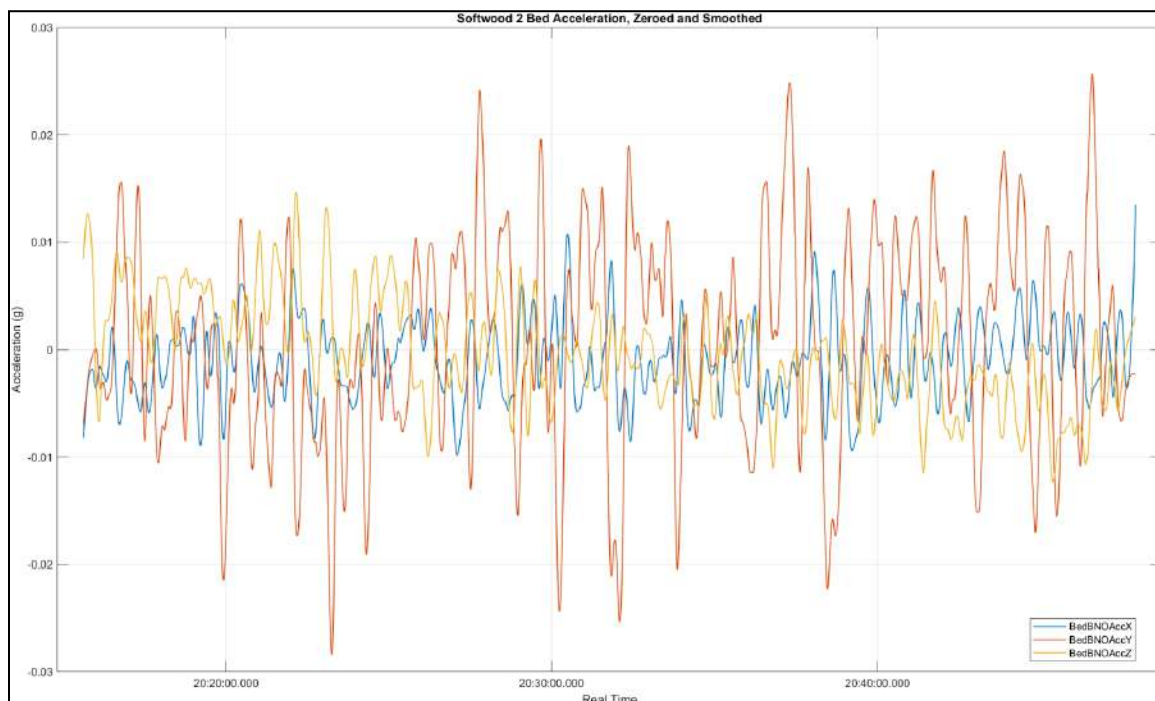
Figure 12.12: Zeroed and Smoothed Acceleration Data from the Bed of Softwood_1



The Softwood_2 testing used a slightly different CAM process than Softwood_1 however the intent of the testing was the same. The data collected from the bed accelerometer during Softwood_2 can be seen in Figure 12.13, as with Softwood_1, the Softwood_2 bed acceleration was the greatest along the y-axis During the Softwood_2 the

sensors experienced less drift than the first softwood test providing better precision. The x- and z-axes experienced accelerations mainly between 0.01 g while the y-axis acceleration had an amplitude of 0.025 g. Although the amplitude is less for the Softwood_2 than Softwood_1, there were no changes to the machining process that could explain this apparent decrease.

Figure 12.13: Zeroed and Smoothed Acceleration Data from the Bed of Softwood_2



The smoothed and zeroed data from the spindle plate and spindle housing of Softwood_1 can be seen in Figures 12.14 and 12.15. The spindle plate and spindle housing both cover the motion of the x- and z-axes, and are rigidly constrained to each other meaning that theoretically, they should experience the same motion front the the axis motion. When looking at the graphs, since they cover the same motion, one would expect the two graphs to display the same patterns and spikes in data at the same time. Briefly studying the graphs it is obvious that the two graphs do not display the same motions which

is most likely due to the sensors being two different BNO models with capabilities that differ slightly. Despite the sensor data being smoothed and zeroed using the same code, the spindle plate displays a larger acceleration range than the spindle housing accelerometer. Both sensors do display the largest amplitudes in the x-direction compared to the other axes as that is the primary axis of motion for the test part machining process. Motion that occurs in the z-axis is much smaller and less frequent, therefore the amplitude of approximately 0.015 g makes sense.

Figure 12.14: Zeroed and Smoothed Acceleration on the Spindle Housing during *Softwood_1 Testing*

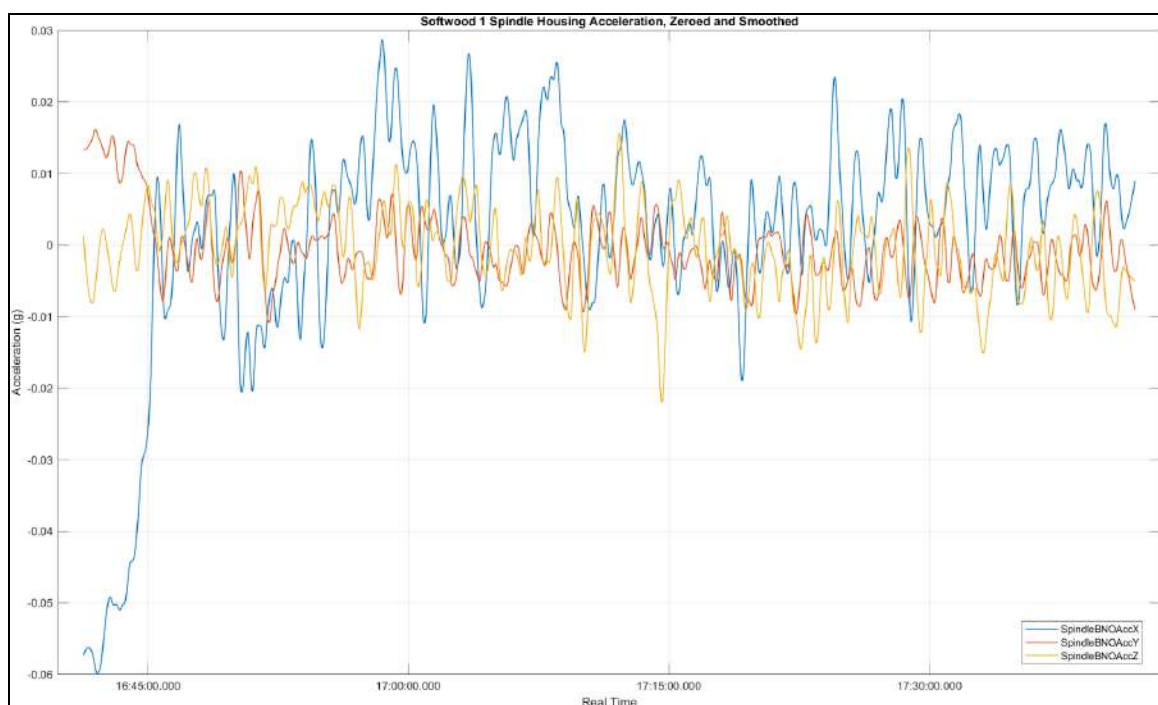
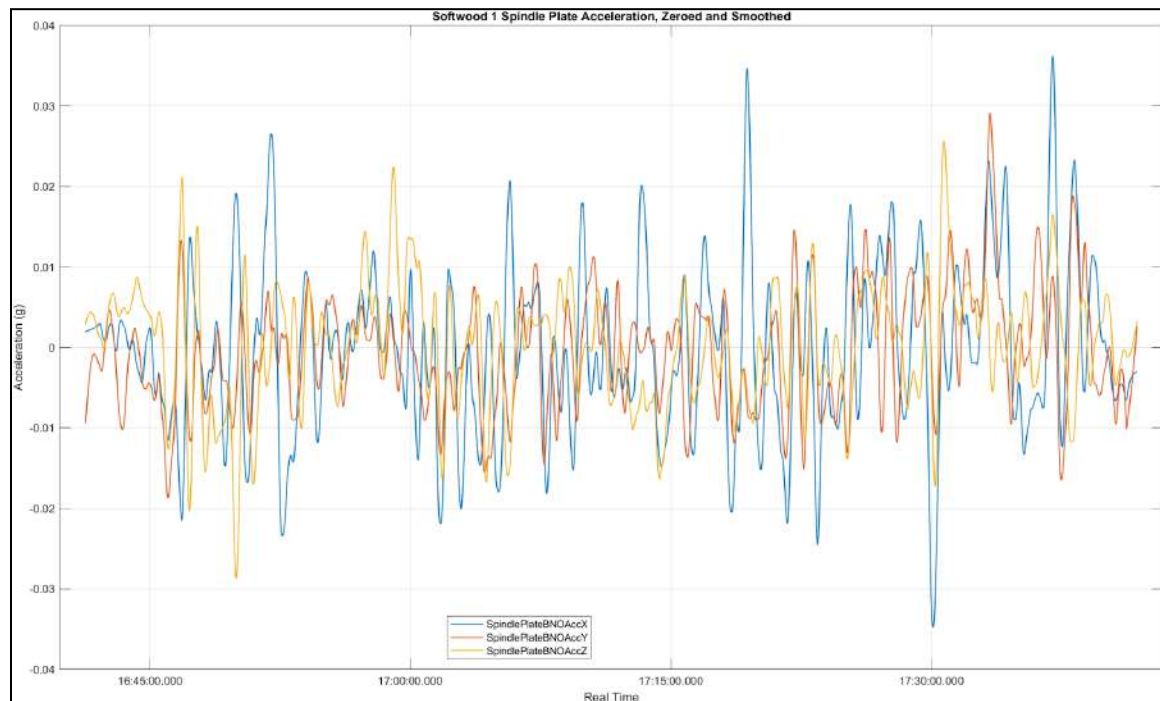


Figure 12.15: Zeroed and Smoothed Acceleration on the Spindle Plate during Softwood_1 Testing



The spindle housing and spindle plate acceleration from Softwood_2 can be viewed in Figures 12.16 and 12.17 respectively. The spindle housing data between Softwood_1 and Softwood_2 is similar and they both experience a rapid increase in x-axis acceleration at the start of the data collection period. The y-axis is fixed at the spindle housing; it experiences a greater acceleration amplitude at the start and end of the data window for unknown reasons but otherwise the vibration amplitude is primarily between 0.01 g. Compared to spindle housing of Softwood_1, the y-axis acceleration is slightly higher as the amplitude for y-axis acceleration of Softwood_1 had an amplitude below 0.01g for the duration of the test. As stated above, the x-axis experiences the greatest acceleration amplitude at this sensor location. Motion is also experienced along the z-axis during the machining process but it is

smaller increments and less frequent. Finally the y-axis does not move at this sensor location.

The spindle plate of Softwood_2 recorded greater spikes in acceleration and did not maintain the same range as for the spindle housing; this could have been introduced by a difference in fixturing between the two sensors. The y-axis acceleration during both Softwood_1 and Softwood_2 experienced acceleration spikes up to 0.035 g which was also not present in the spindle housing acceleration.

Figure 12.16: Zeroed and Smoothed Acceleration on the Spindle Housing during Softwood_2 Testing

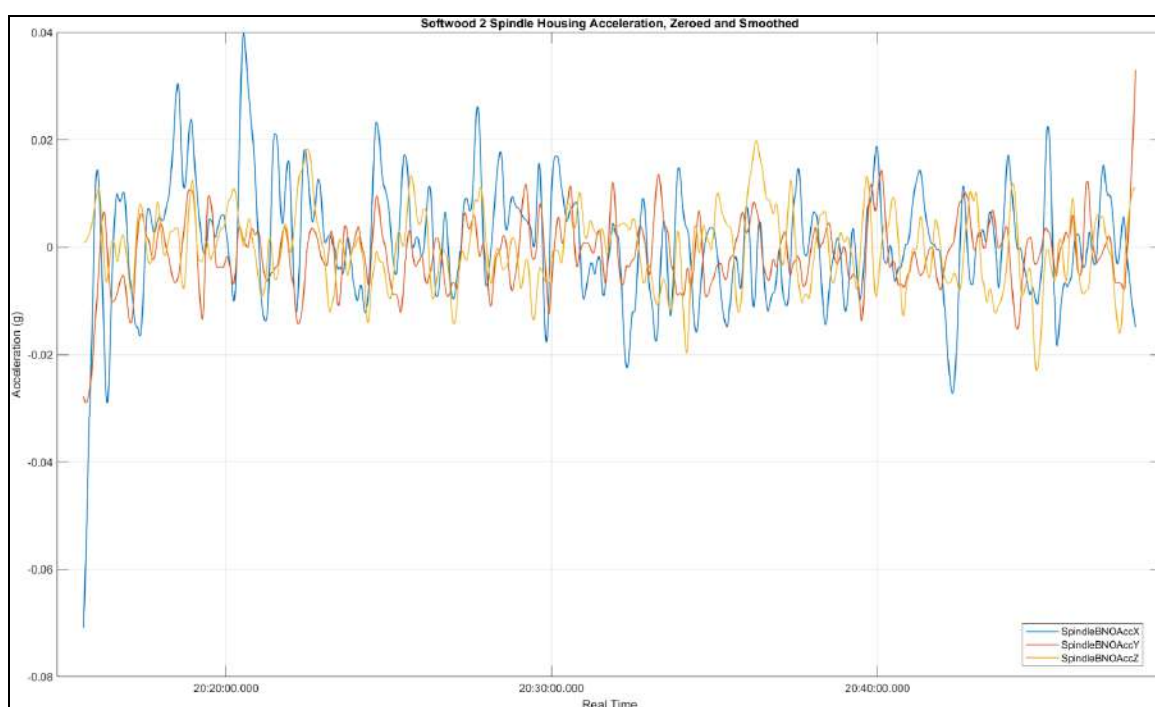
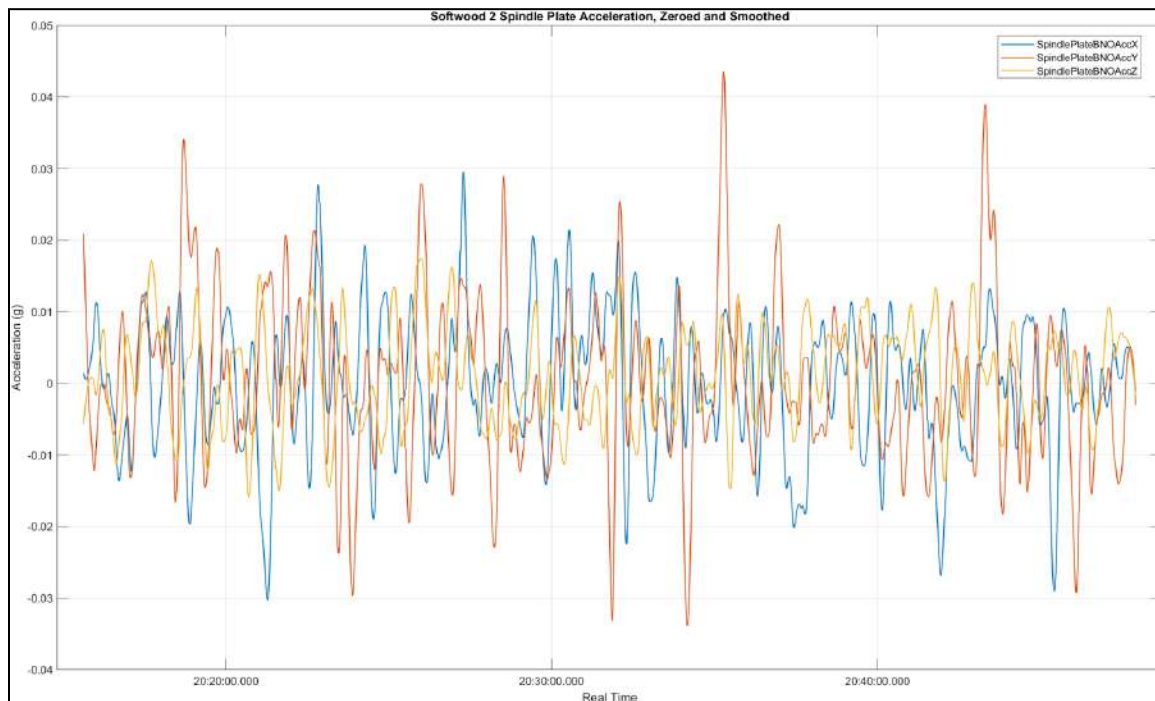


Figure 12.17: Zeroed and Smoothed Acceleration on the Spindle Plate during Softwood_2

Testing



Once smoothed and zeroed the vibrations outside of the machine for both tests are almost negligible with amplitudes of $\pm 0.4 \times 10^{-4}$ g. The acceleration data from Softwood_1 for the enclosure and table can be seen in Figures 12.18 and 12.19. For Softwood_1 the sensors did experience drift over time especially for the enclosure acceleration. The two sensors do not demonstrate the same behavior as the enclosure did not experience any acceleration in the z-direction however the table did. The drift and discrepancies between the two sensor readings indicates that the data is not suitable for thorough analysis but can be used to identify a pattern in the discrepancies.

Figure 12.18: Zeroed and Smoothed Enclosure Acceleration for Softwood_1

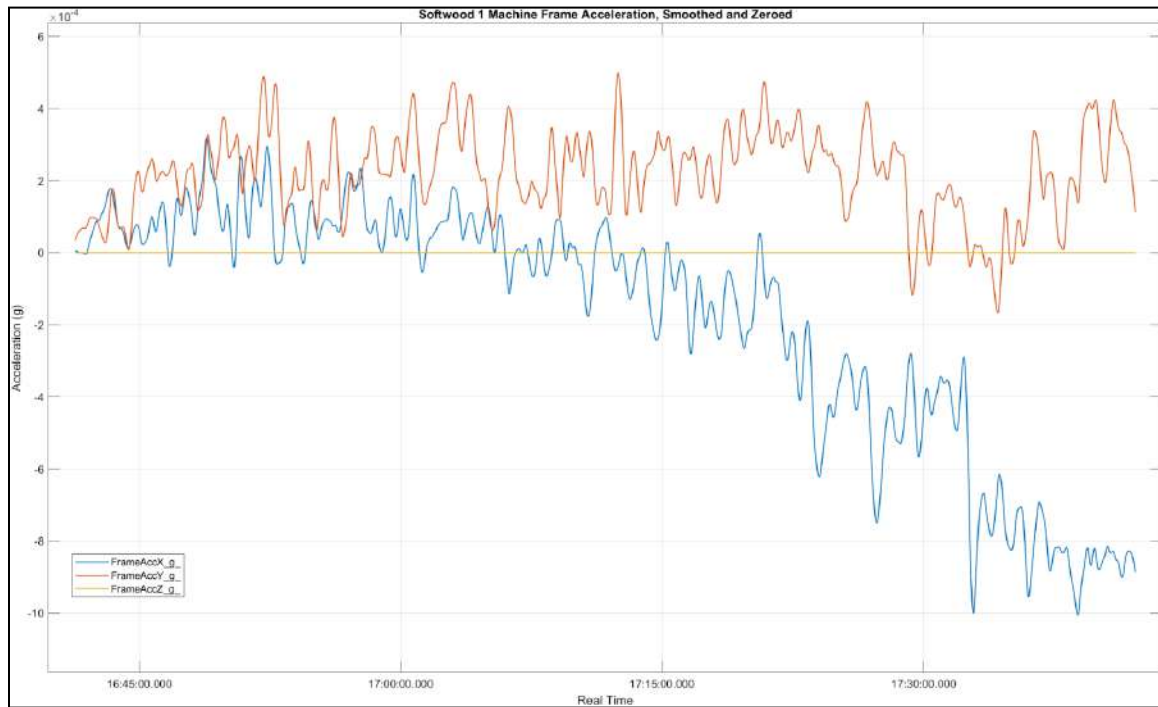
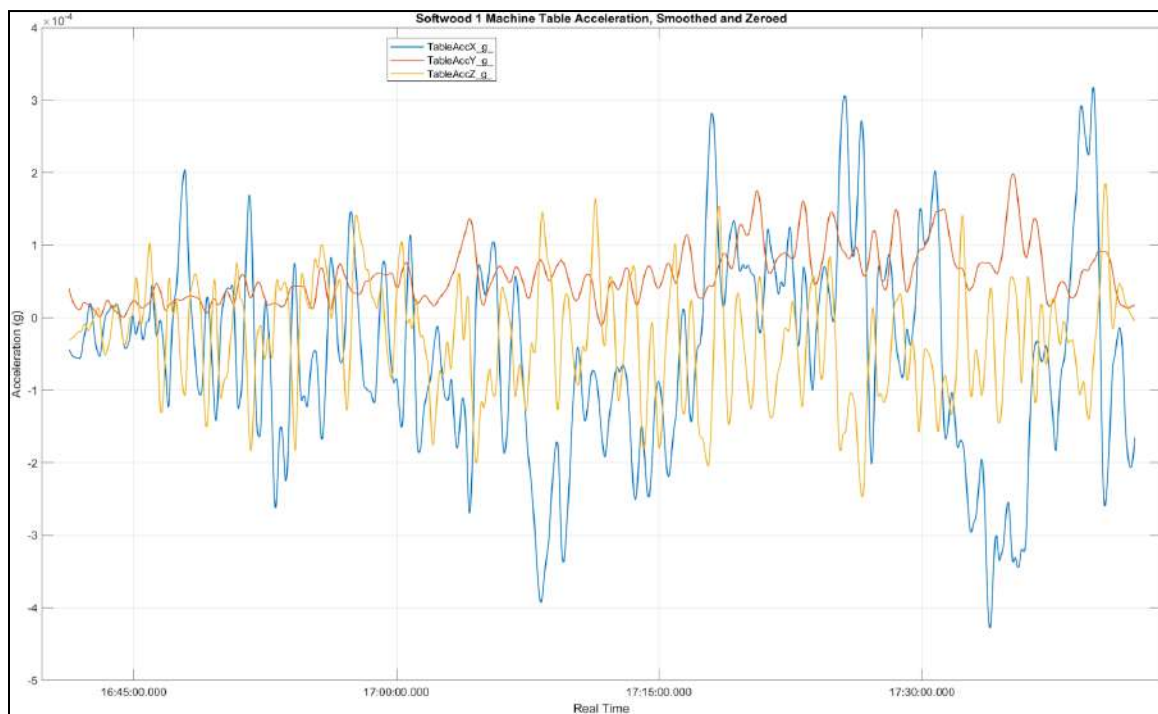


Figure 12.19: Zeroed and Smoothed Table Acceleration for Softwood_1



The acceleration data from Softwood_2 for the enclosure and table can be seen in Figures 12.20 and 12.21. During the Softwood_2 testing the sensors located outside of the machine experienced z-axis acceleration with the data smoothed and zeroed which was not present during Softwood_1 testing. The acceleration experienced in Softwood_2 closely matches Softwood_1 testing in the x- and y-axes, however the appearance of z-axis acceleration in Softwood_2 cannot be explained between the two tests.

Figure 12.20: Zeroed and Smoothed Enclosure Acceleration for Softwood_2

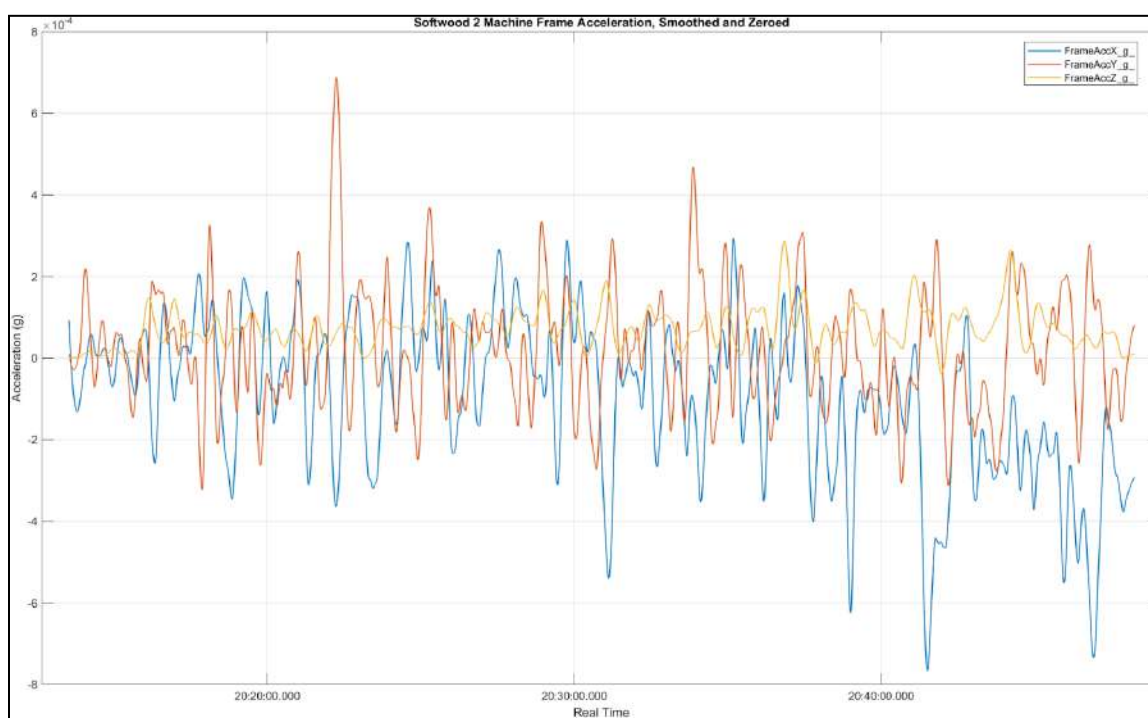
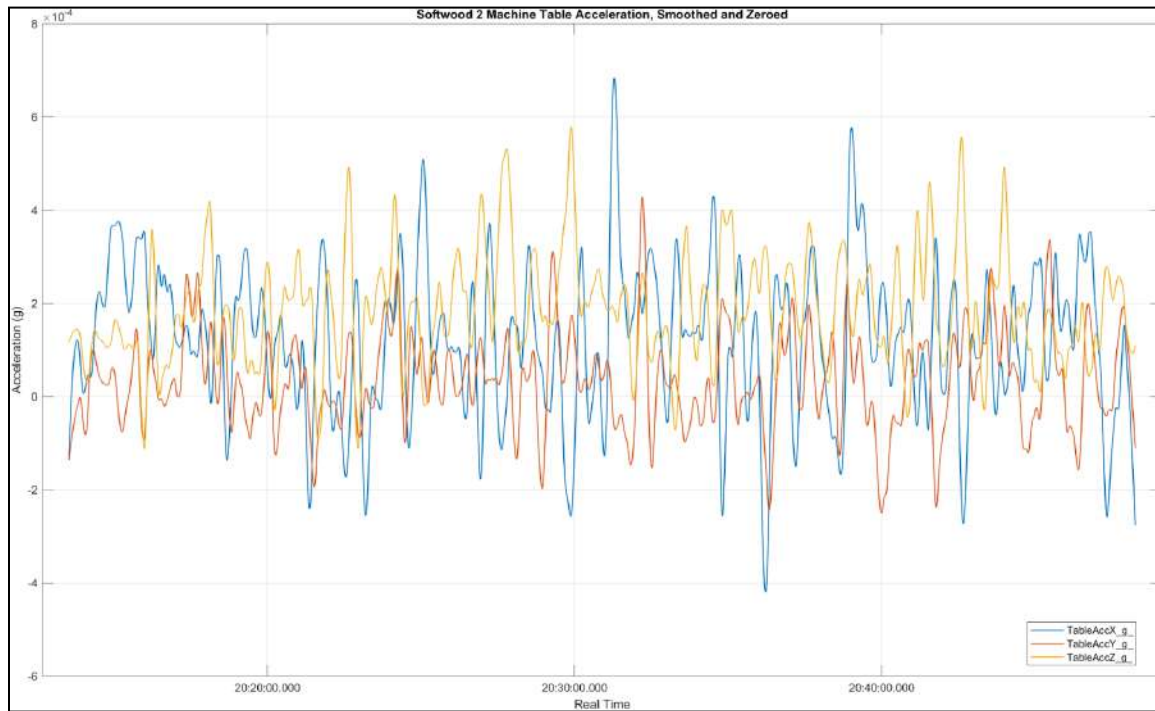


Figure 12.21: Zeroed and Smoothed Table Acceleration for Softwood_2



12.4.2.2 Teflon Tests

The teflon bed acceleration for both tests experienced the same pattern seen during the softwood testing where the greatest acceleration experienced was in the y-direction. This acceleration had a maximum amplitude of approximately 0.02 g. The x- and z-axis accelerations experienced were solely vibrations and they were within the range of +/- 0.01 g. The amplitude of the Teflon_2 bed acceleration was slightly less than the Teflon_1 bed acceleration, this observation cannot be explained as the CAM process was nearly identical. It could have emerged due to I2C errors skewing the data once smoothed. The graphs of bed acceleration for Teflon_1 and Teflon_2 can be seen in Figures 12.22 and 12.23 respectively.

Figure 12.22: *Teflon_1* Bed Acceleration Zeroed and Smoothed

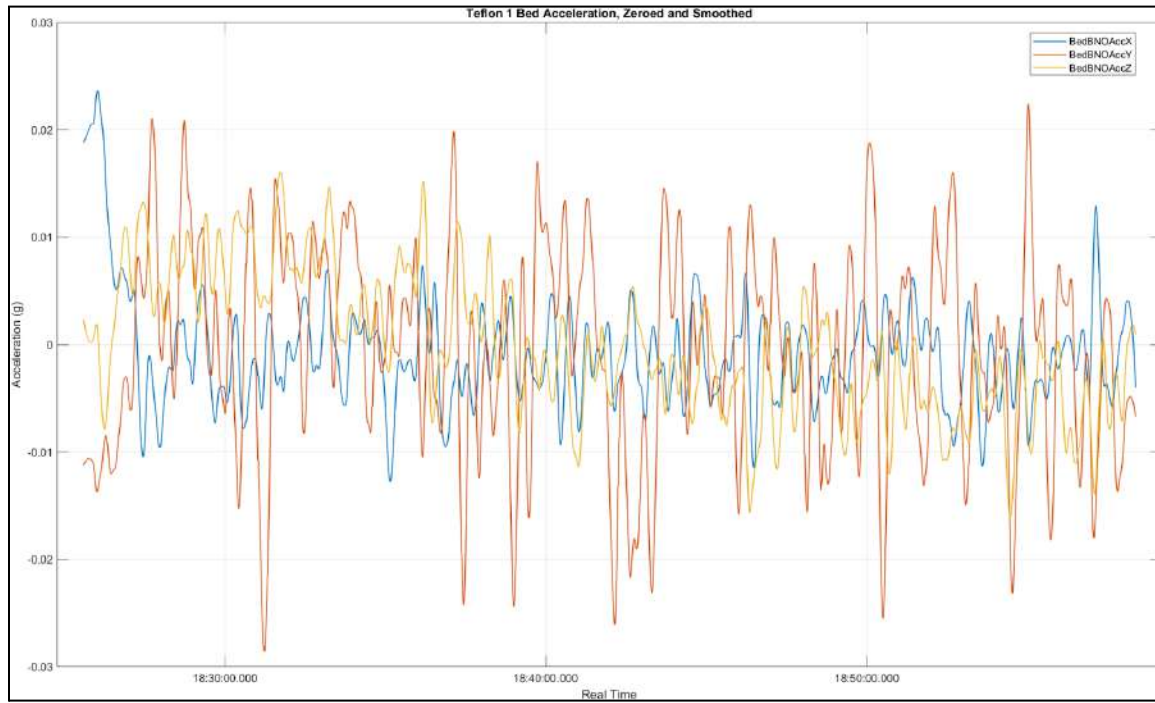
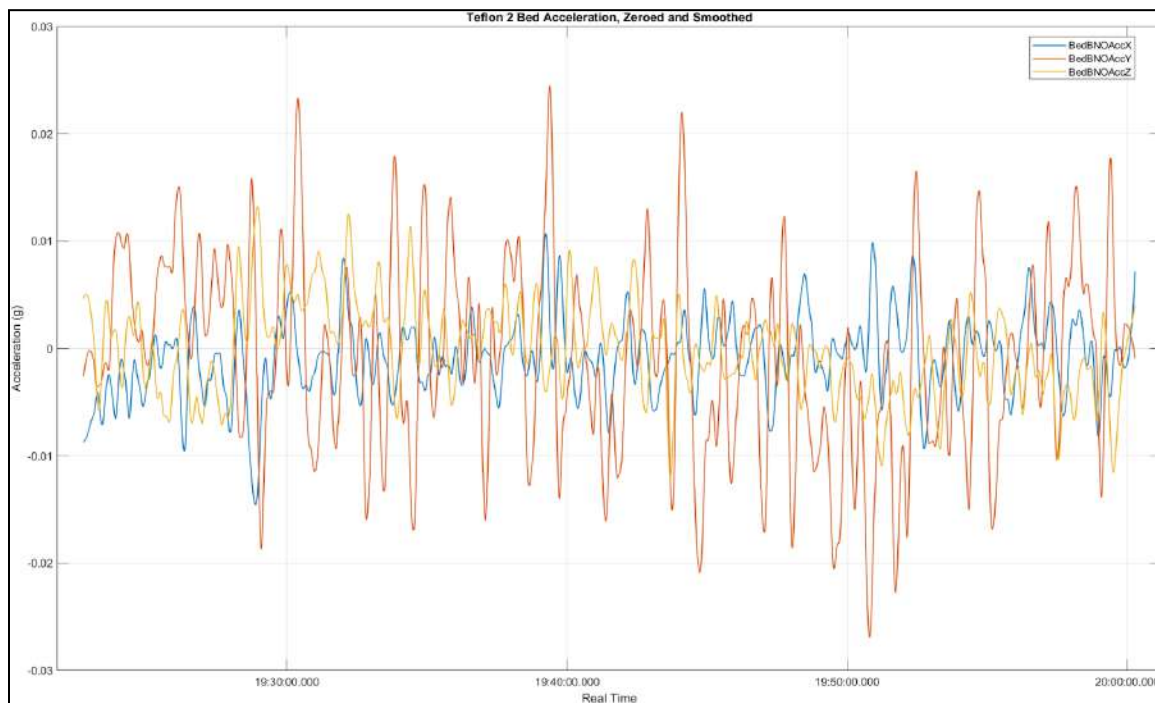


Figure 12.23: *Teflon_2* Bed Acceleration Zeroed and Smoothed



The teflon spindle housing acceleration between Teflon_1 and Teflon_2 can be seen in Figures 12.24 and 12.25. Just as with the teflon testing bed acceleration, the amplitude of the accelerations is slightly less from Teflon_1 to Teflon_2, the amplitude for Teflon_1 in the x-direction is about 0.02 g while the x-direction of Teflon_2 is slightly below 0.02 g. As expected for the spindle housing acceleration, the y- and z-axes experience lower acceleration values than the x-axis. This agrees with findings from the Softwood_1 and Softwood_2 testing. For both tests the x-axis experiences the greatest acceleration, although in Teflon_1 testing the z-axis acceleration starts at a value of about 0.11 g. This large acceleration does not show in the data from Teflon_1 spindle place acceleration, seen in Figure 12.26. This indicates the probability of noise being read and functionally freezing for approximately 2 minutes, or the sensor did not calibrate properly causing the error to persist.

Figure 12.24: Teflon_1 Spindle Housing Acceleration Zeroed and Smoothed

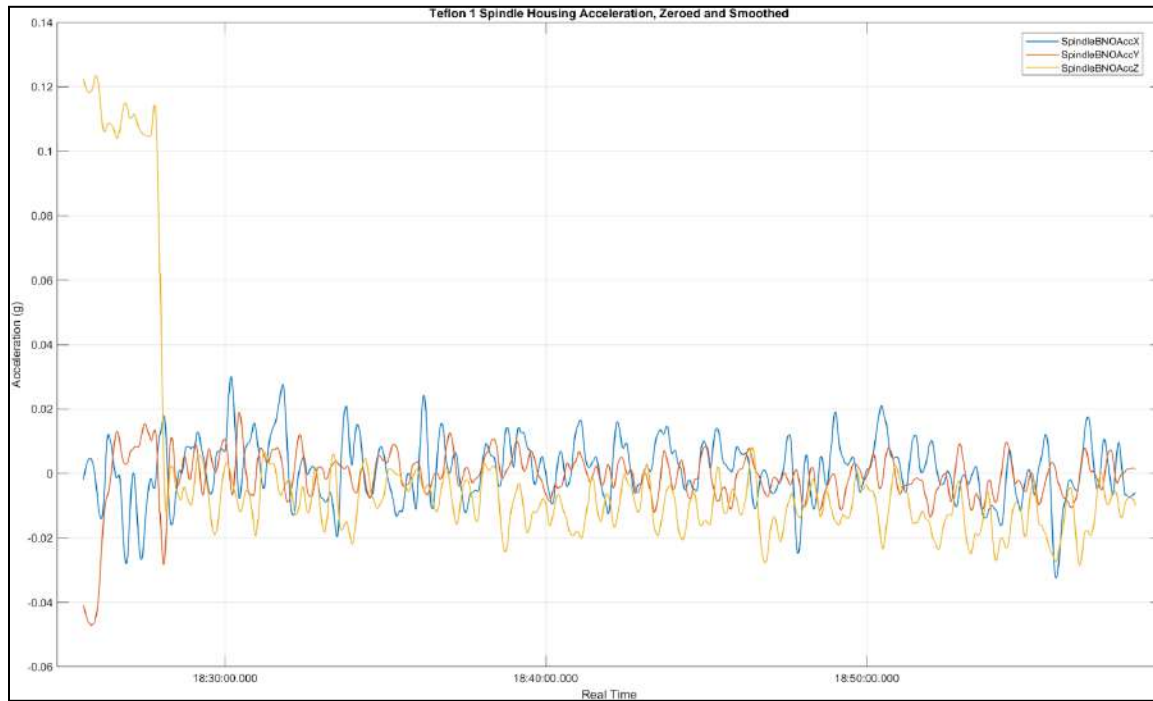
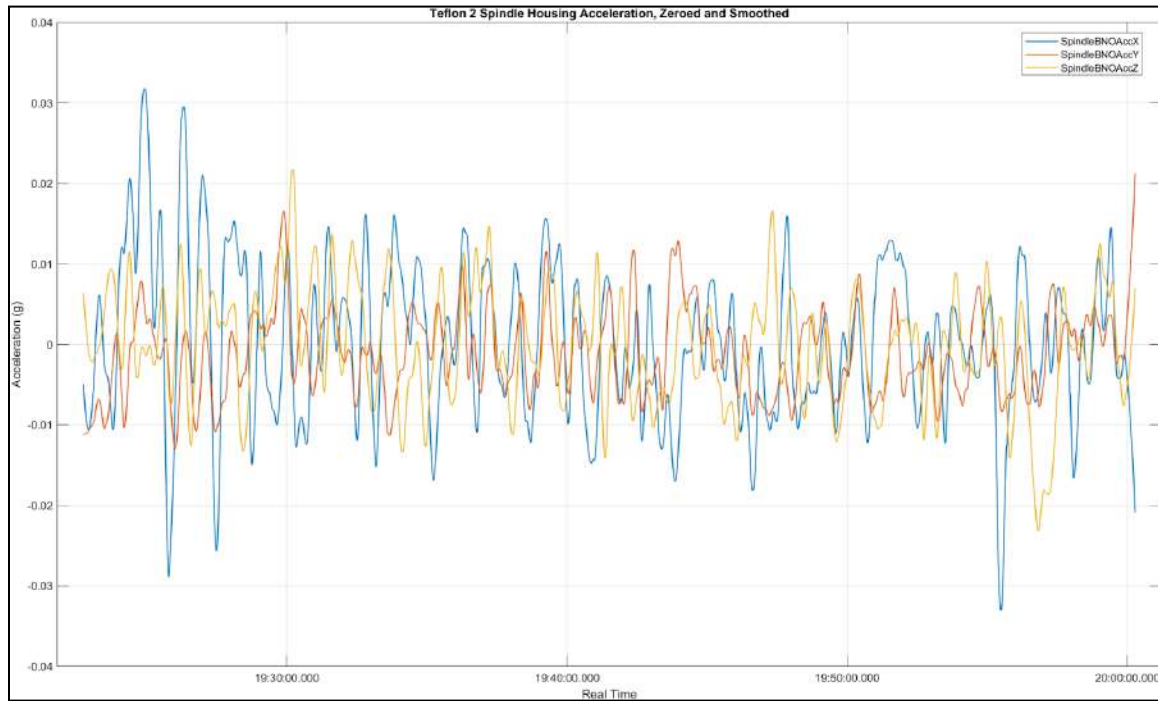


Figure 12.25: Teflon_2 Spindle Housing Acceleration Zeroed and Smoothed



Acceleration data for Tefon_2 spindle plate acceleration can be seen in Figure 12.27.

For Teflon_1 and Teflon_2 spindle plate acceleration there was less noise and erroneous data spikes than seemingly recorded by the spindle housing accelerometers. The data from the spindle plate does have a greater amplitude than the spindle housing, which as explained when discussing the results of softwood testing, could be from the sensors being different BNO models and fixtured with a different number of points of contact. Similarly to the spindle housing acceleration, the majority of the spindle plate acceleration was within the range of +/- 0.02 g which is to be expected as they experience the same motions.

Figure 12.26: Teflon_1 Spindle Plate Acceleration Zeroed and Smoothed

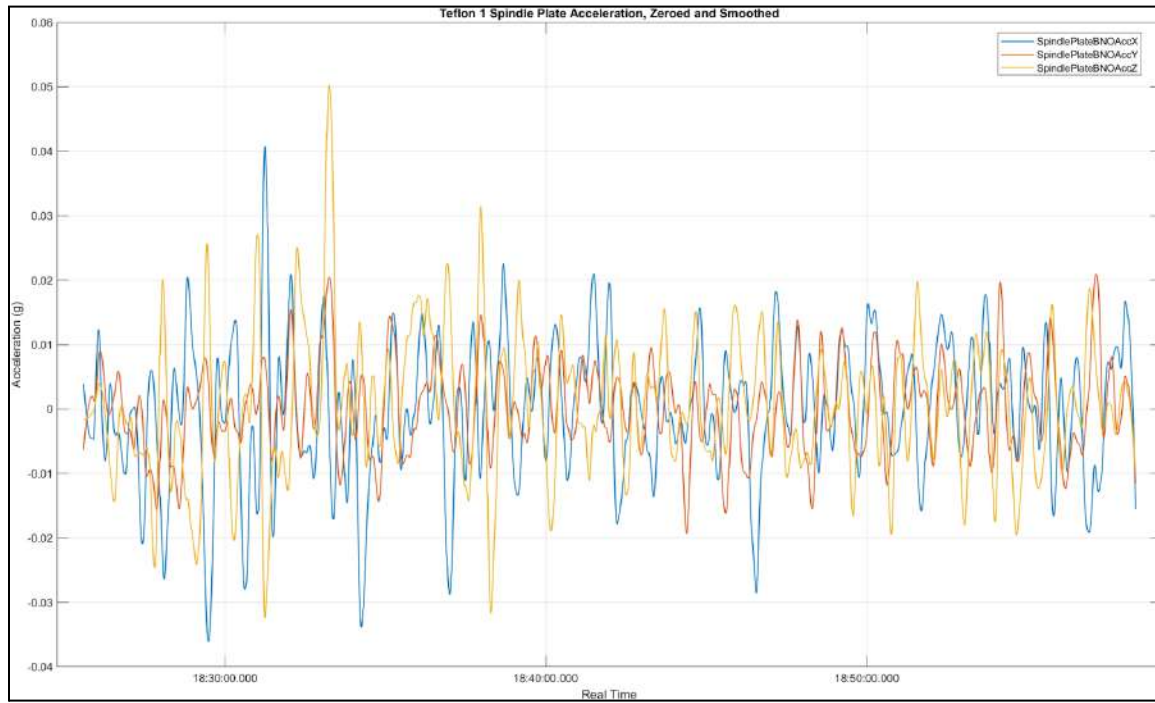
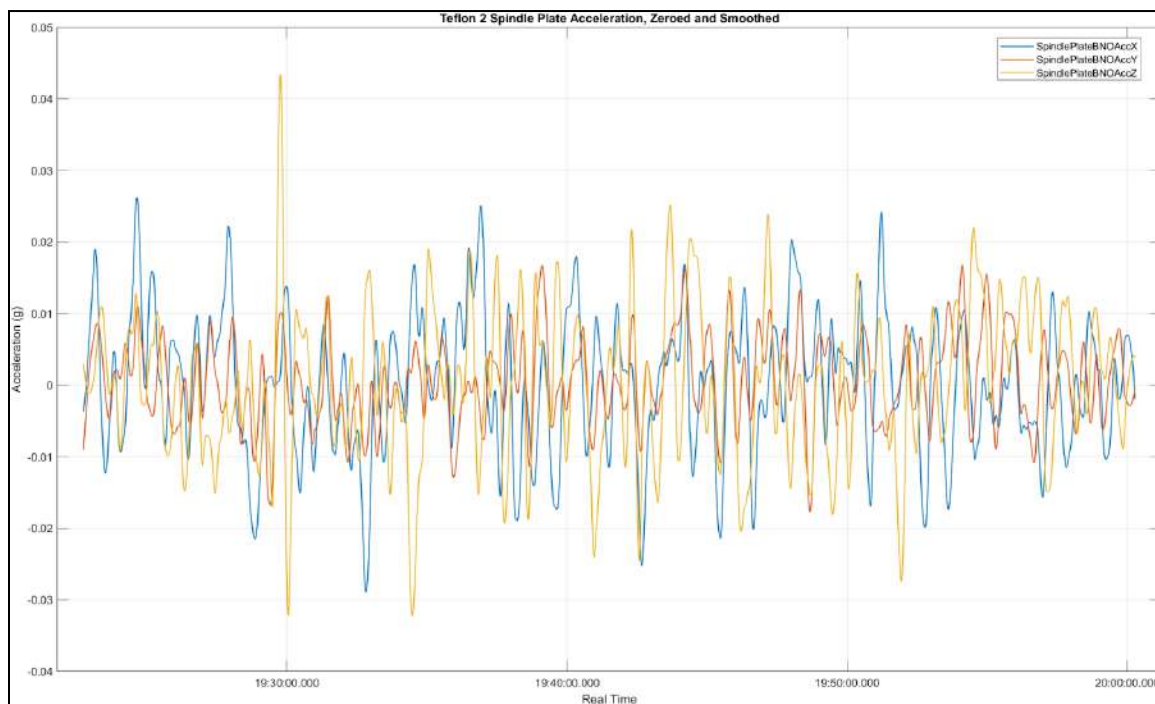


Figure 12.27: Teflon_2 Spindle Plate Acceleration Zeroed and Smoothed



As seen with the softwood testing, the teflon testing experienced small amplitudes of acceleration on the machine enclosure and table. Data for acceleration of Teflon_1 enclosure, Teflon_2 enclosure, Teflon_1 table, and Teflon_2 table can be viewed in Figures 12.28, 12.29, 12.30, and 12.31 respectively. All experienced greater acceleration amplitudes for the x- and y-axes as the z-axis should be relatively stable with its placement on the floor thus it experiences less acceleration. The acceleration amplitude for both tests is approximately 4×10^{-4} g overall which has been seen with the softwood acceleration outside the machine as well.

Figure 12.28: Teflon_1 Enclosure Acceleration Zeroed and Smoothed

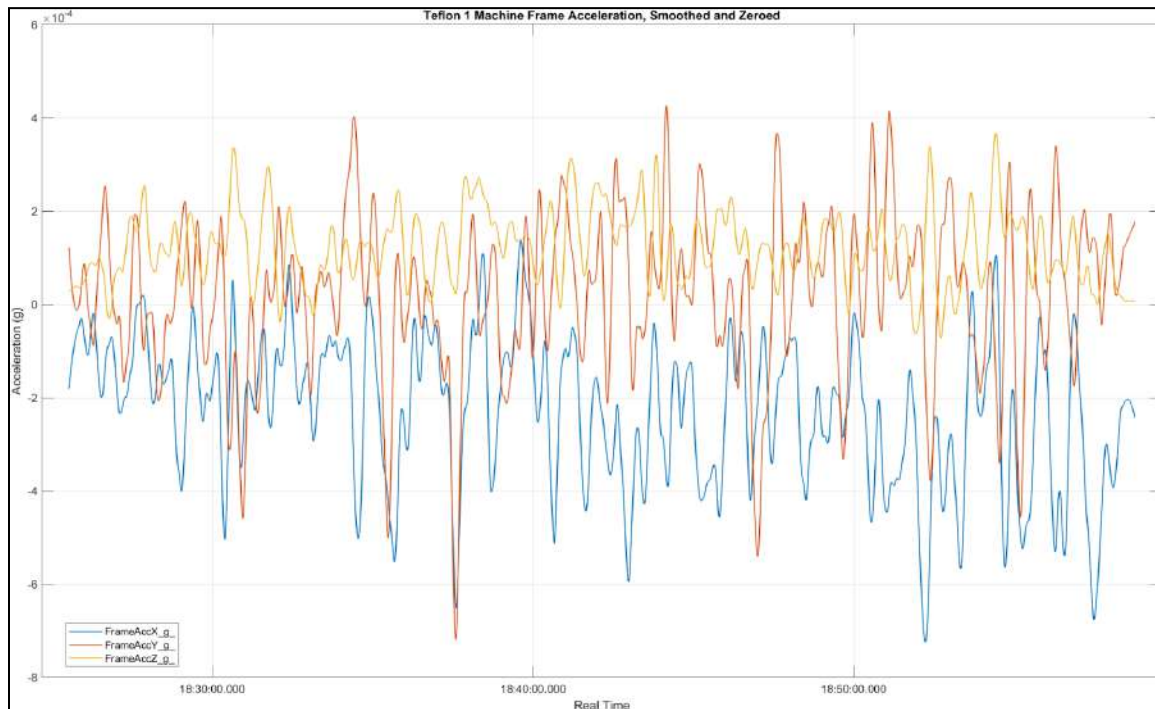


Figure 12.29: Teflon_2 Enclosure Acceleration Zeroed and Smoothed

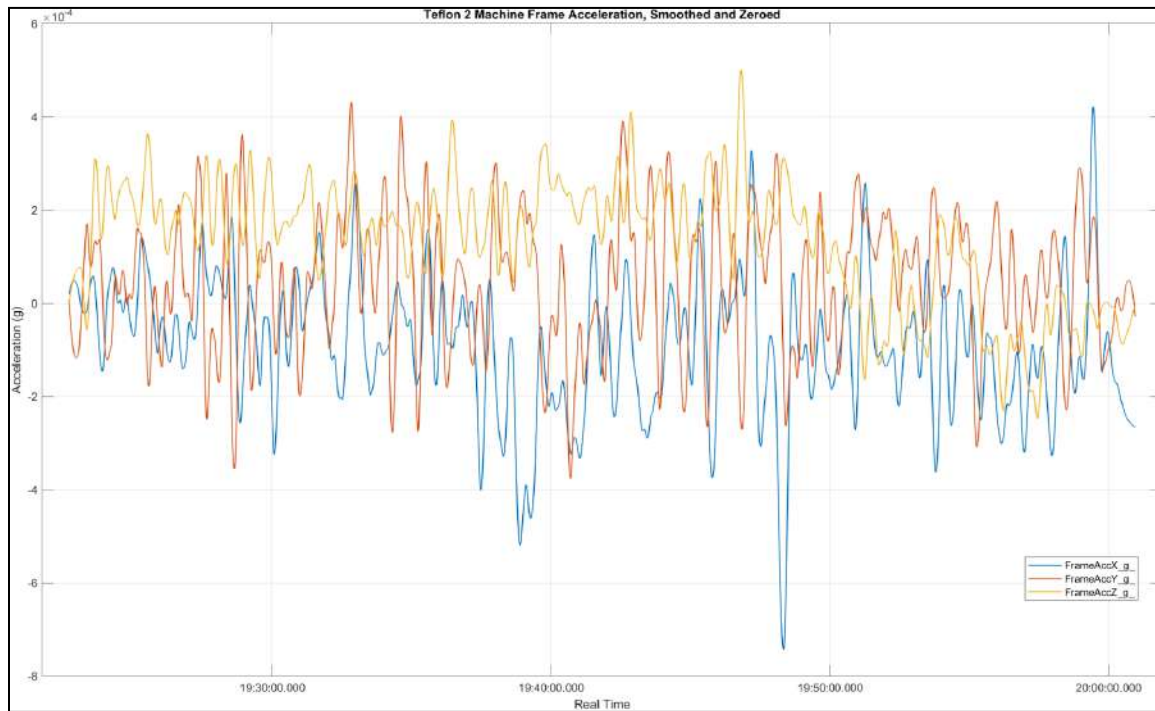


Figure 12.30: Teflon_1 Table Acceleration Zeroed and Smoothed

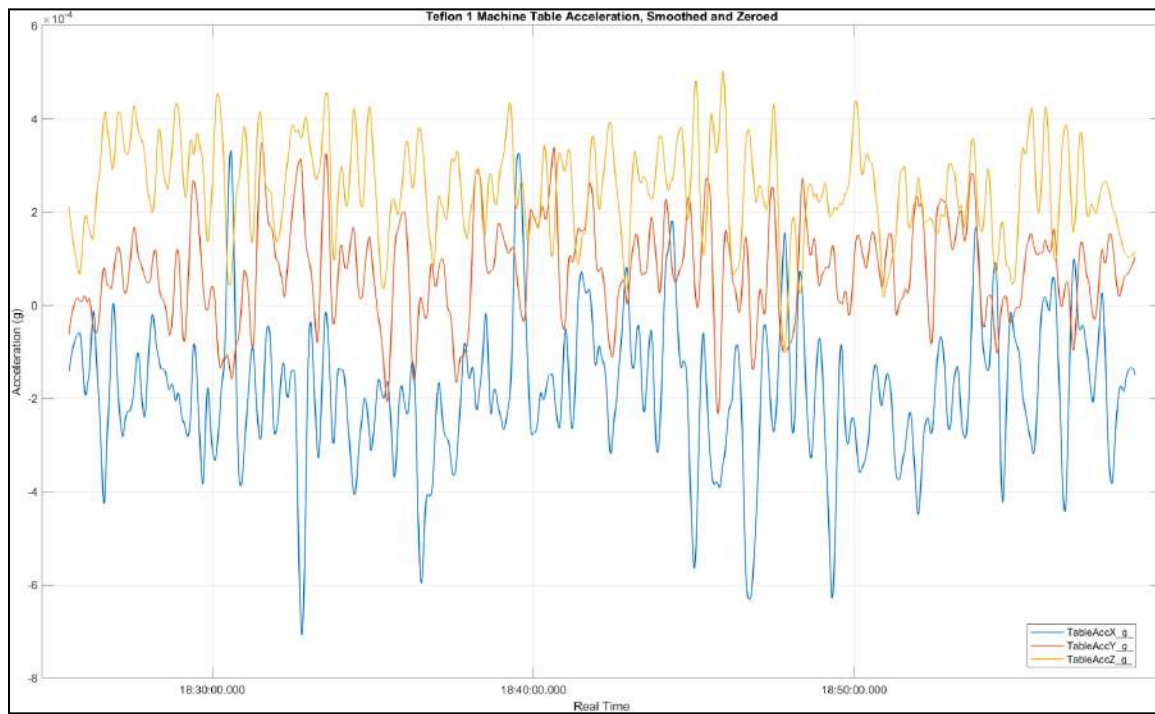
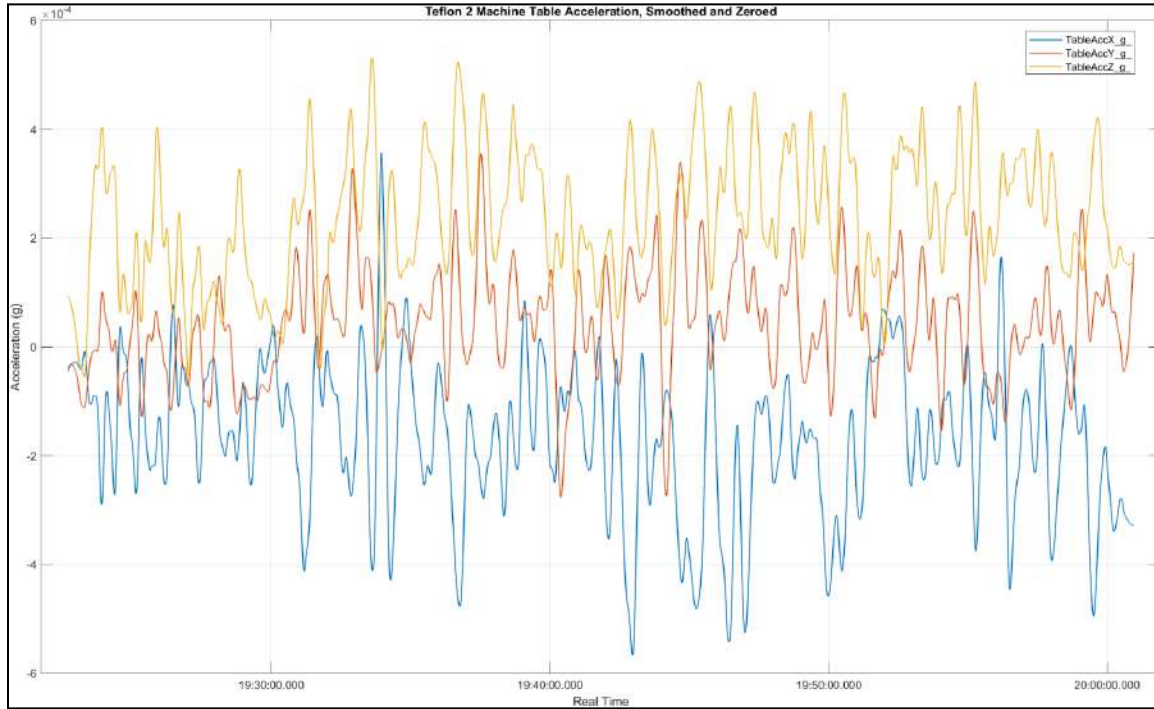


Figure 12.31: Teflon_2 Table Acceleration Zeroed and Smoothed



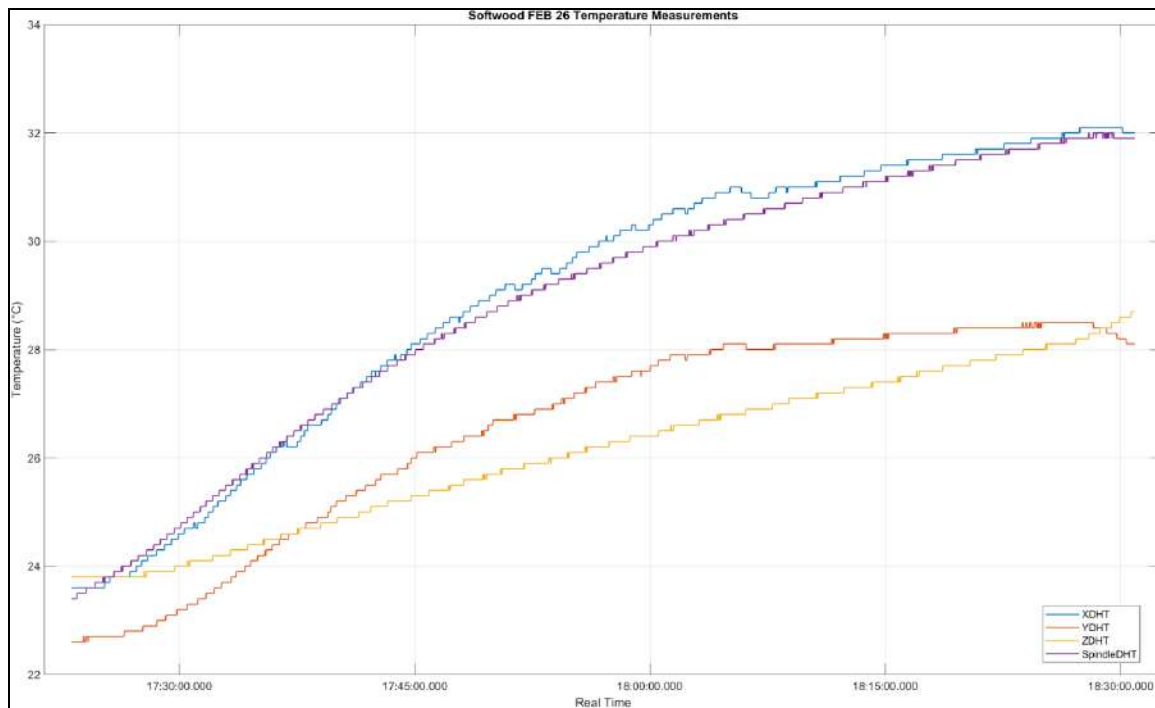
12.5 Physics Testing After Controller Updates

The standard test part was used in an attempt to machine softwood with the original gantry, new motors, and grblHAL controller. The machining process was run for an hour before being stopped as it was going to take four times the amount of time it was initially expected to. Sensor failure was experienced at a greater number than previous testing of the initial machine. The spindle housing accelerometer did not collect any data and the bed accelerometer stopped working early in the machining process.

The temperature data was collected without failure for the duration of this test and can be seen in Figure 12.32. Unlike the initial softwood testing, the spindle experienced greater temperature compared to the other motors. With the initial testing the spindle temperature was the lowest of all the motors, although the maximum temperature

experienced by the spindle motor during the initial testing was 32.9°C while this testing reached a peak of only 32.0°C. The x- and y- axis motors were replaced during the updates predating this testing, which could explain the drop in temperature readings for those motors compared to initial measurements but would not explain the low z-axis temperature readings. The change in the controller board and software might have contributed to the lower temperatures as well. If the trend continues in further testing, that is a clear indication of the controller allowing the motors to function more efficiently. The low temperatures are ultimately a good sign that the machine is operating safely.

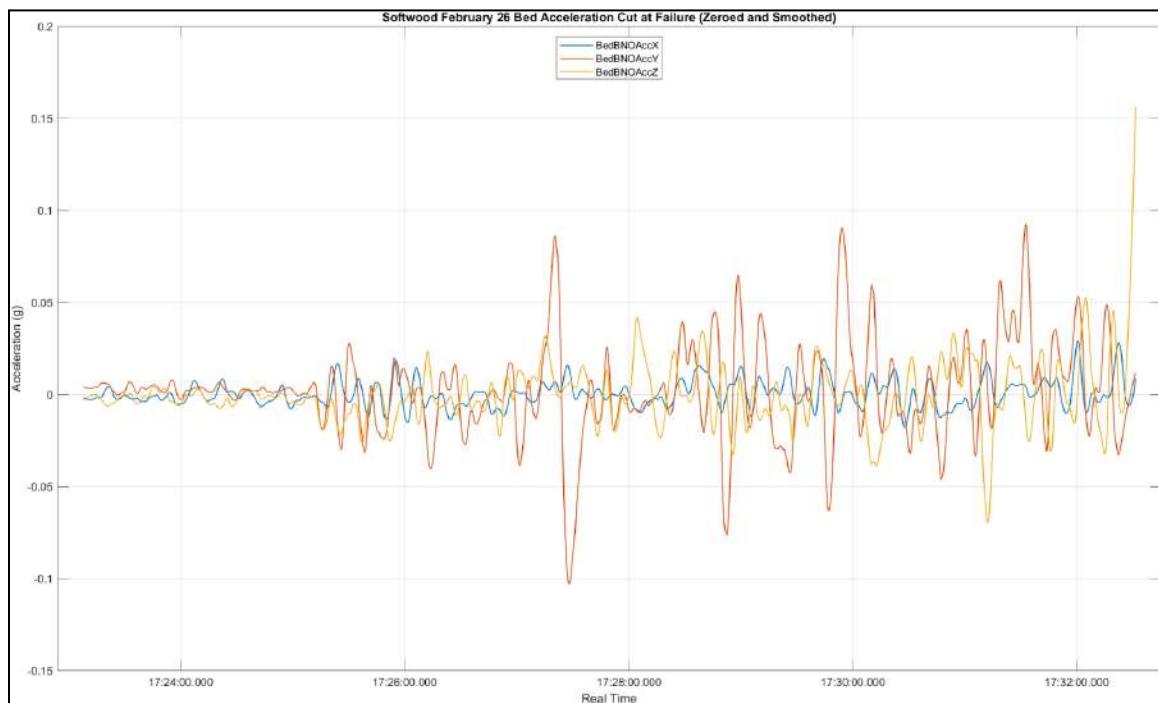
Figure 12.32: Softwood Temperature After February Updates



Data was only collected by the bed accelerometer for the first 9 minutes of the machining process due to an unknown error that caused the sensor to fail, this data can be seen in Figure 12.33. The y-axis experienced the greatest acceleration amplitude of

approximately 0.09 g when zeroed and smoothed. The x-axis acceleration has the smallest amplitude of approximately 0.02 g which is slightly higher than the amplitude of the readings before the machining process began. This indicates that the x-axis acceleration can be attributed to low vibrations introduced by the machining process. The z-axis acceleration has an amplitude of approximately 0.04 g which can also be identified as an increase from before the machining process began.

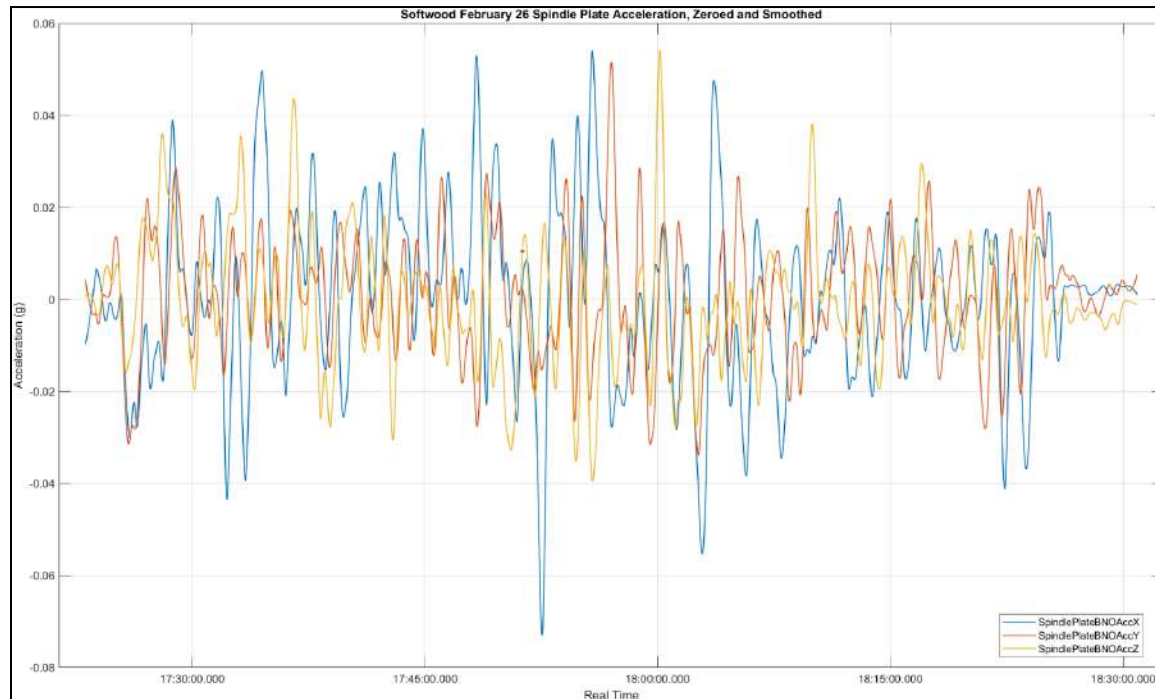
Figure 12.33: Softwood Bed Acceleration After February Updates Before Sensor Failure, Zeroed and Smoothed



The spindle plate acceleration from this round of testing can be seen in Figure 12.34. As expected from previous testing, the spindle plate experiences the greatest amplitude of acceleration in the x-direction, with an amplitude of approximately 0.05 g. The y-axis acceleration and z-axis acceleration amplitudes were approximately 0.04 g which makes

sense as the acceleration value trend has been the values experienced by the spindle plate are slightly elevated when compared to other recorded accelerations.

Figure 12.34: Softwood Spindle Plate Acceleration After February Updates Zeroed and Smoothed



For this round of testing, the machine table acceleration became zero in all three directions when smoothed. The machine enclosure also had zero acceleration when smoothed except in the y-direction and the amplitude was comparable to all other enclosure acceleration ranges. Therefore the graphs are not included here.

12.6 Comparison Test of Softwood

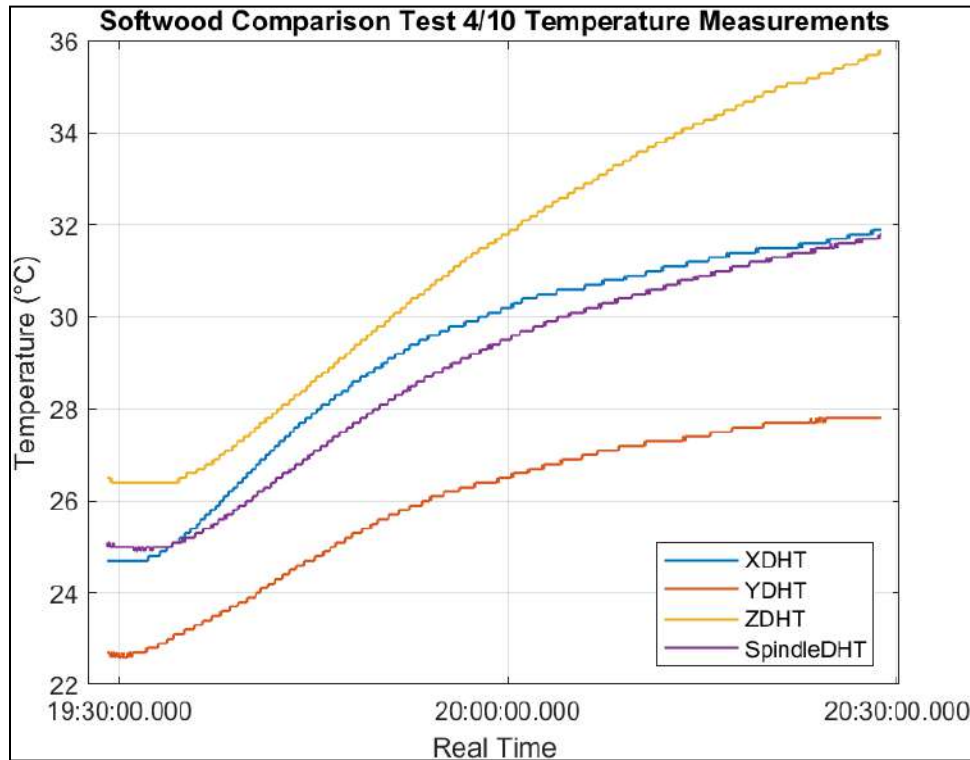
The Softwood_2 G-code was run on the machine following all major updates made by the 2024-2025 MQP Team. The limits present in Mach3 were implemented into UGS

with a maximum feed rate of 120 in/min and acceleration of 4 in/s². This was done in an attempt to replicate the conditions and parameters of Softwood_2 testing.

The temperature data for the softwood comparison test can be viewed in Figure 12.35. The overall temperature range is lower than both initial softwood testing. As seen in the initial softwood testing, the z-axis motor experiences the highest temperature. The x-axis temperature is sitting lower where in the initial testing the x- and z-axis motor temperatures practically overlapped as the highest motor temperatures of the tests. The spindle motor does not follow the same curve as Softwood_2 testing, however it does closely match the temperature curve from Softwood_1.

The x-axis motor temperature almost exactly follows the curve expressed during the softwood testing following the controller updates in February. It is likely due to the fact the x-axis motor was replaced with a smaller motor. The y-axis motor experiences very little growth over the machining process with a temperature change of only about 5°C and the curve roughly follows the same pattern of the controller updates in February. As with the x-axis motor, the reduced temperature of the y-axis motor is related to the new motor and in conjunction with the new controller.

Figure 12.35: Softwood Comparison Test Temperature Data

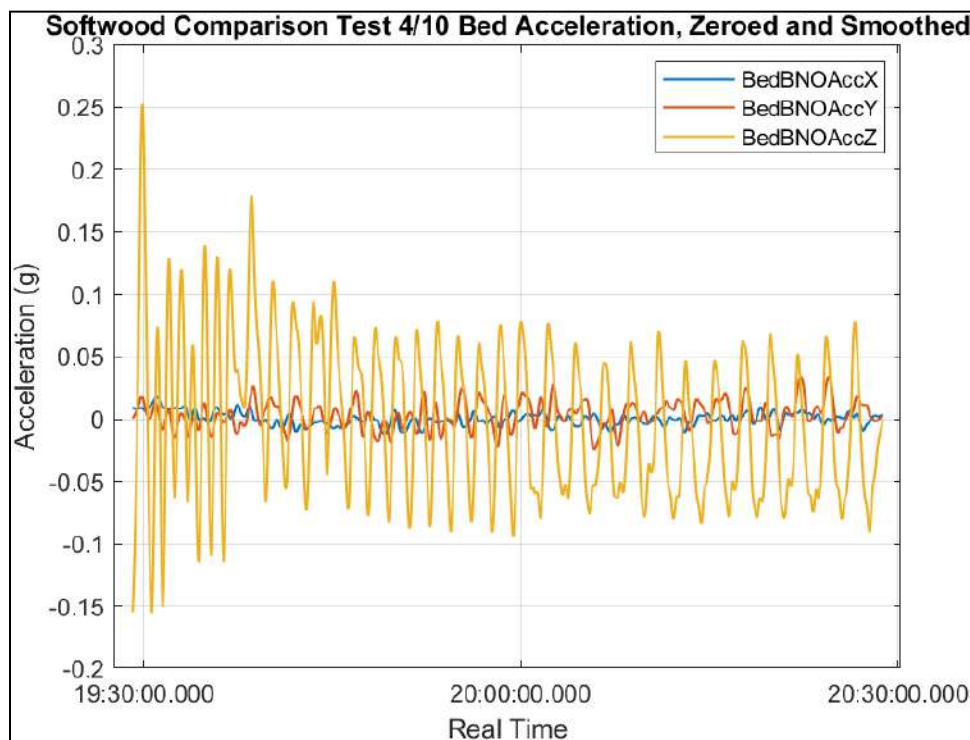


The machine bed acceleration data can be viewed in Figure 12.36. The collected data displays low acceleration amplitudes in the x- and y-directions with an amplitude of approximately 0.025 g. The z-axis acceleration is much greater than any values previously collected and must not be used for any significant analysis. As the bed experienced motion along the y-axis, the y-direction should have displayed the largest acceleration amplitudes of the three axes.

The actual source of the error with the z-axis readings is unknown however there are some theories. The first theory is that the accelerometer came loose in its mount which freed it from the constraints that would usually prevent it from experiencing any vertical motion not transferred directly from the bed. If the sensor came loose in the mounts and was then free to move in the z-direction, the design of the mount would have still prevented most

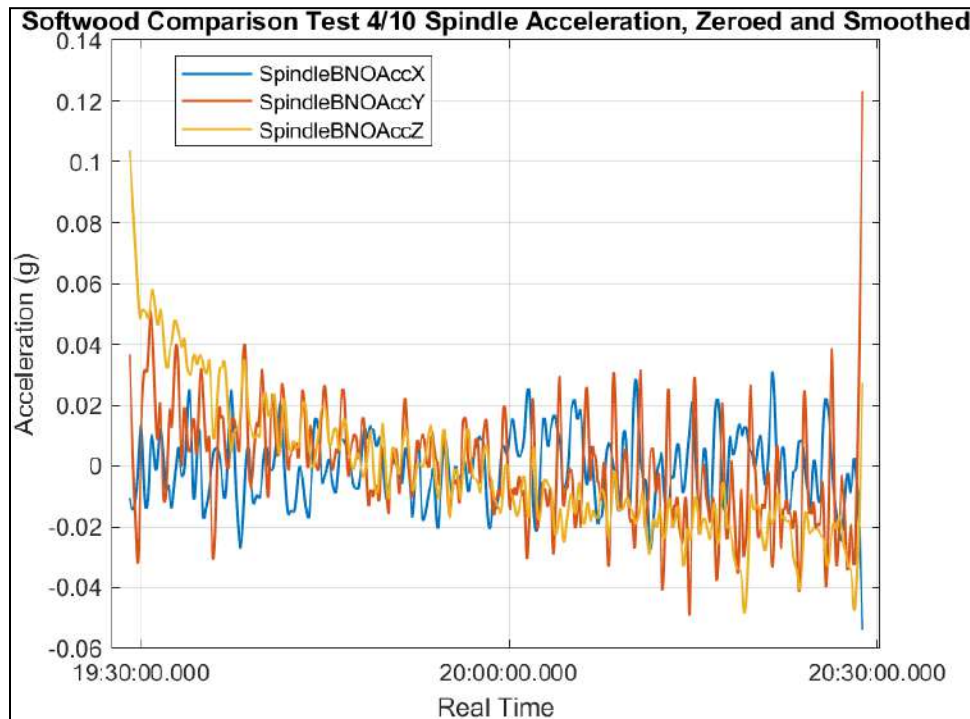
horizontal motion thus explaining the readings. The second theory of what caused the error is that the bed was not properly mounted to the linear rails and ball screw resulting in the bed not being fully constrained in the z-direction. This could have caused the error seen but is less likely to be the case as it would less easily go unnoticed.

Figure 12.36: Softwood Comparison Test Bed Acceleration Data Zeroed and Smoothed



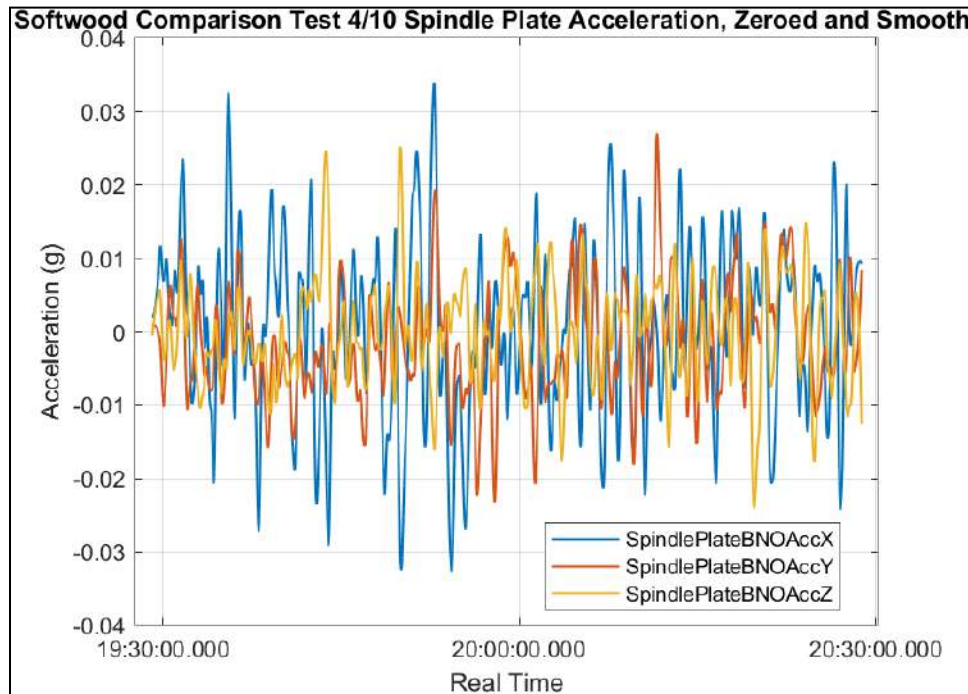
The spindle housing acceleration, which can be seen in Figure 12.37, experienced some drift in the z-axis over the test duration. Compared to the overall spindle housing acceleration of Softwood_2 in Figure 12.16, the acceleration amplitude of the spindle housing was about double the amplitude. During the comparison testing, the acceleration amplitude was the greatest in the y-axis with an amplitude of 0.04 g. The x- and z-axis acceleration more closely matches the values of Softwood_2 as the amplitude was closer to 0.015 g during both sets of testing.

Figure 12.37: Softwood Comparison Test Spindle Housing Acceleration Zeroed and Smoothed



The spindle plate acceleration data from the comparison testing most closely matches the results from Softwood_2. The acceleration amplitudes are mainly within 0.02 g. The main difference is during Softwood_2 the y-axis experienced the largest spikes whereas during the softwood comparison testing the x-axis is experiencing spikes. The spikes of both rounds of testing are occurring at amplitudes of 0.03 g. The comparison testing data for the spindle plate accelerometer can be seen below in Figure 12.38.

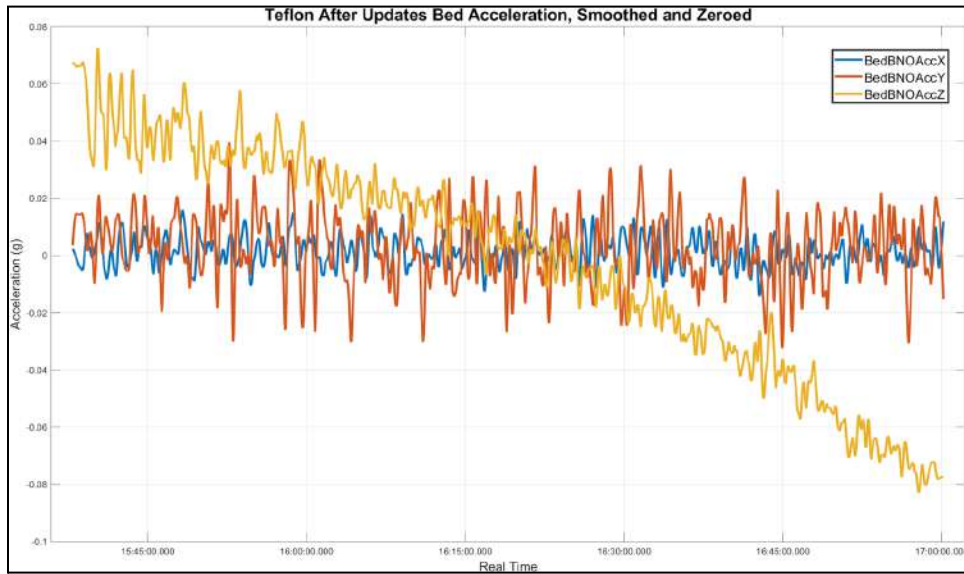
Figure 12.38: Softwood Comparison Test Spindle Plate Acceleration Zeroed and Smoothed



12.7 Teflon Testing Following All Updates

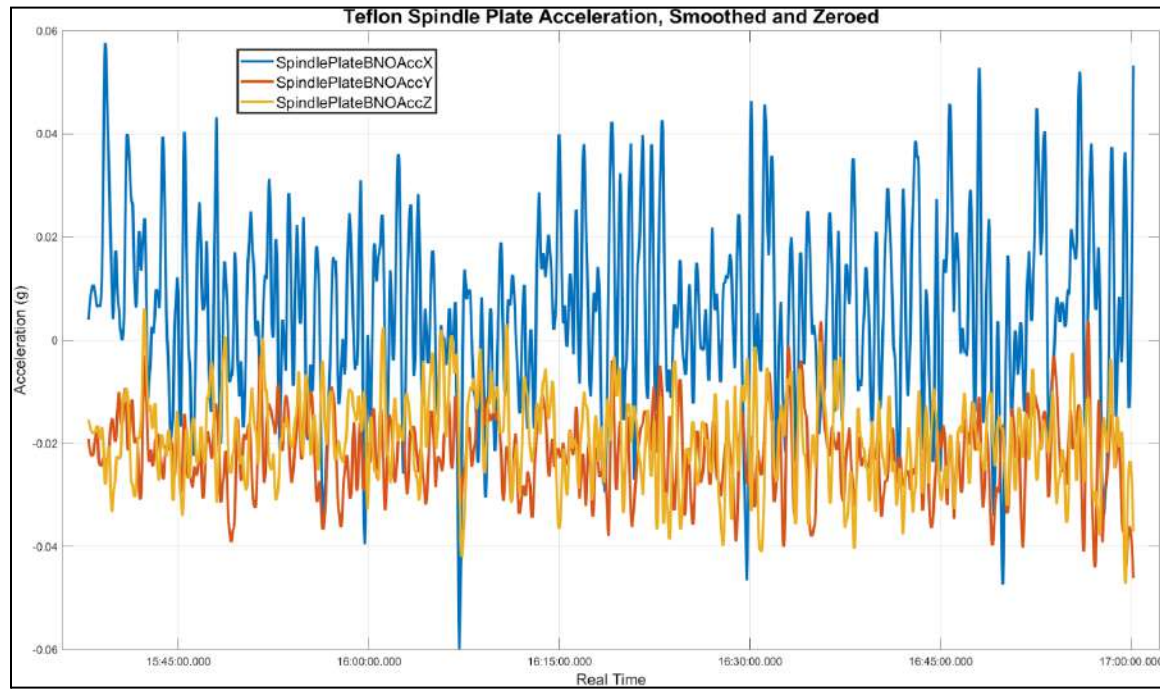
The bed acceleration experienced during a final round of teflon testing can be seen in Figure 12.39. Although the CAM was different from the CAM used for initial testing, the teflon tests are still able to be compared. The y-axis amplitude from this round of testing was greater than the initial testing but had an amplitude of 0.03 g, so only slightly greater. This increase could be explained by the difference in jerk settings between Mach3 and UGS. With the new software, the machine appeared to experience more sudden changes in acceleration that were not observed on the initial machine. The x- and z-directions which do not experience motion directly from the bed align with the findings of an acceleration amplitude of approximately 0.01 g.

Figure 12.39: Teflon Bed Acceleration After All Updates, Zeroed and Smoothed



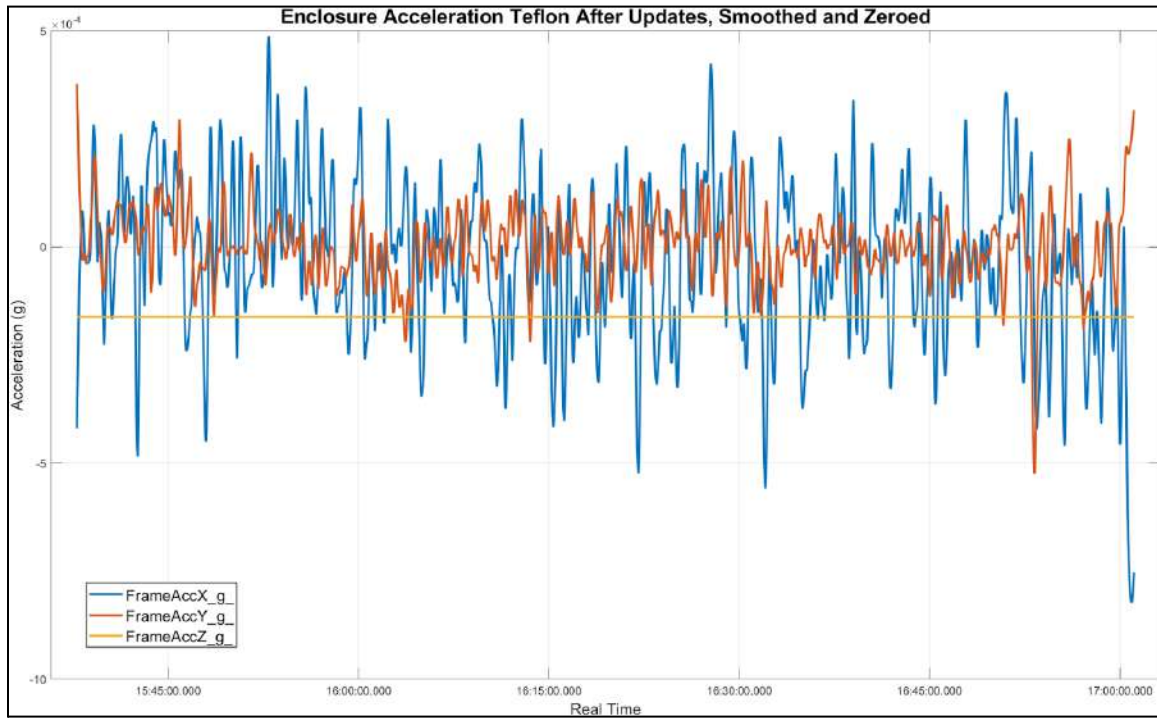
The spindle plate acceleration can be seen in Figure 12.40 and despite the code including zeroing, there is a somewhat significant offset with the acceleration datasets. The x-axis notably also experienced a slight increase in the acceleration amplitude and is approximately 0.03 g. As with the bed y-axis acceleration, this increase is also most likely due to the different jerk settings between Mach3 and UGS, more abrupt acceleration was also observed in this case. The y- and z-axis acceleration has an amplitude of 0.01 g and 0.02 g respectively which agrees with data collected during initial teflon testing. No data was able to be collected from the spindle housing accelerometer as the sensor failed during this round of testing.

Figure 12.40: Teflon Spindle Plate Acceleration After All Updates, Zeroed and Smoothed



As seen from other sensors during this round of testing, the acceleration of the enclosure has also increased in the x-direction. This can be used to confirm the jerk settings between Mach3 and UGS impacted the acceleration experienced. The test part experienced the most motion along the x-axis during the machining process. As the machining process was executed, changes in the motion of the x-axis could be seen as visually rocking the table. This data can be seen in Figure 12.41 and the values are still small with an amplitude of about 5×10^{-4} g. The z-axis acceleration when smoothed and zeroed is zero and the y-axis acceleration amplitude is less than initial testing with an amplitude of approximately 2×10^{-4} g.

Figure 12.41: Teflon Enclosure Acceleration After All Updates, Zeroed and Smoothed



12.8 First Aluminum Testing

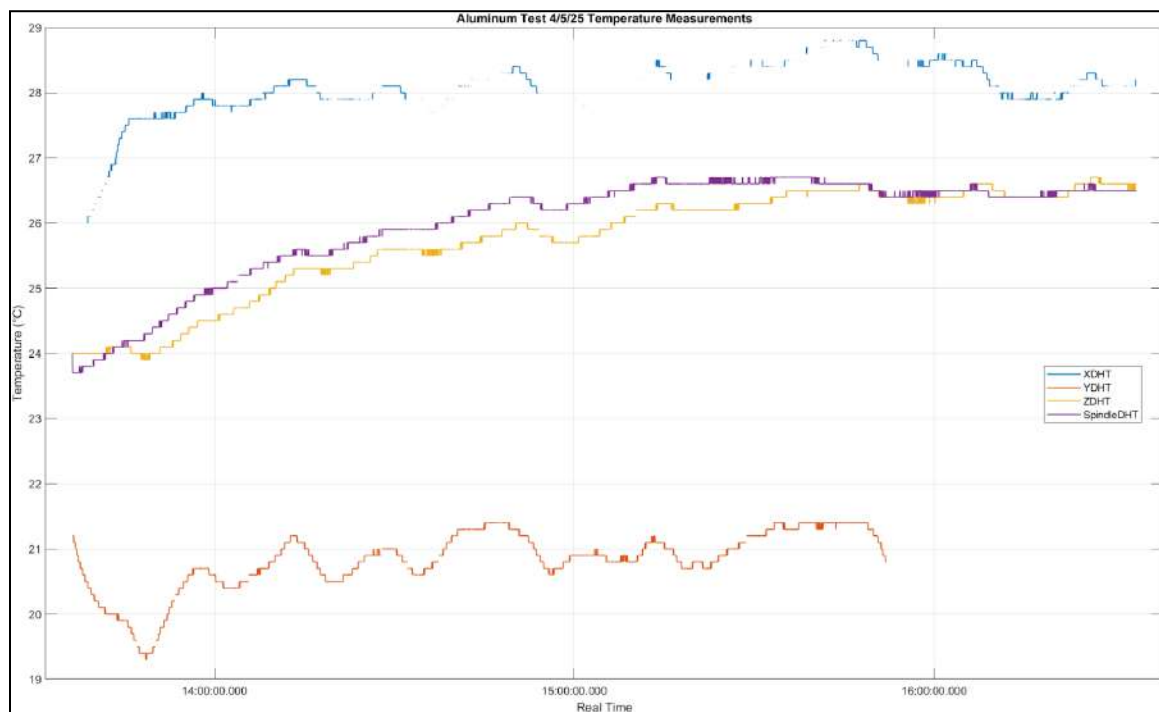
Aluminum was first machined while collecting sensor data with the new machine.

Due to the coolant, aluminum was unable to be machined with the Physics Initial Testing as the enclosure experienced too much leakage. Unfortunately during this testing accelerometer data from inside the machine was unable to be collected as the coolant caused the sensors to fail. Temperature data was able to be collected although the data collection was spotty and the y-axis temperature failed before testing could be completed, this data can be seen in Figure 12.42. Unlike all previous temperature data, not all axes experienced a relatively logarithmic growth in temperature. The spindle motor temperature and z-axis motor temperature most closely resembled any other temperature data collected. The y-axis motor temperature was being hit directly with coolant during the machining process which is what caused the sensor to fail. During the testing process, the temperature fluctuated between

about 19.3°C and 21.2°C and ceased functioning with about 40 minutes of the machining process remaining.

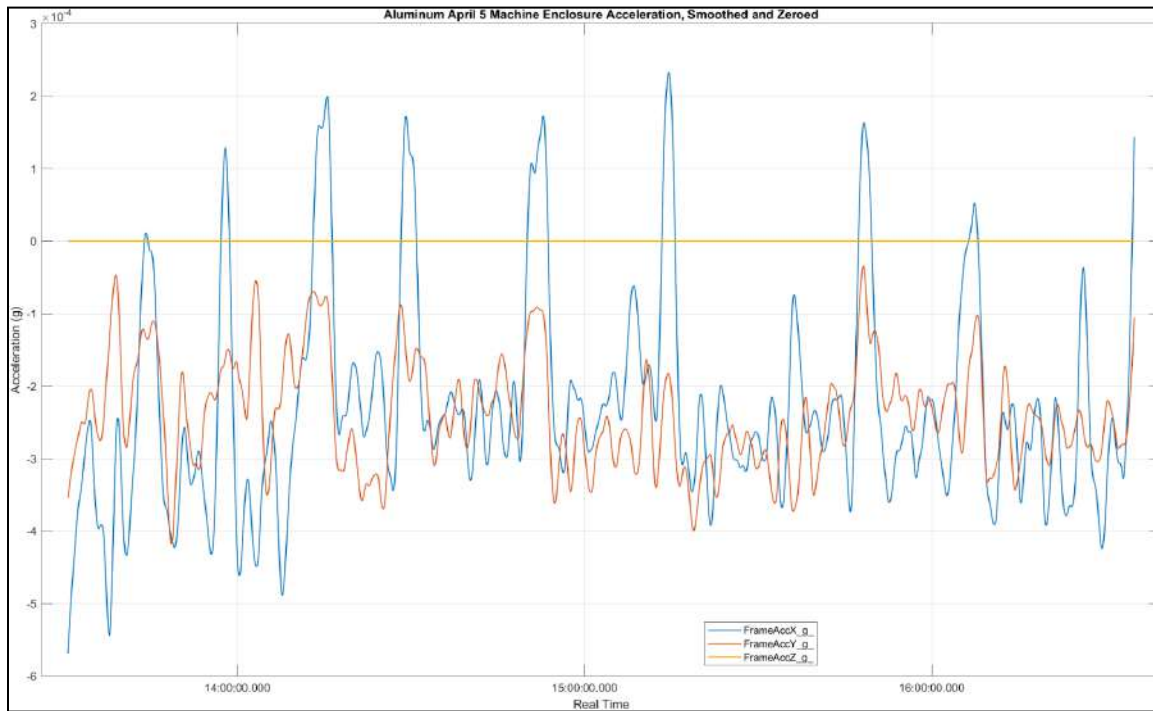
The x-axis motor data was the greatest but remained well within the safe operating parameters. This sensor cut in and out the most frequently and also experienced some fluctuation primarily between 27°C and 29°C.

Figure 12.42: Aluminum Test Temperature Data



Acceleration data was able to be collected outside of the machine and the enclosure acceleration can be viewed in Figure 12.43. In the y-direction the acceleration amplitude was 1.5×10^{-4} g and in the x-direction an amplitude of approximately 3×10^{-4} g. When smoothed and zeroed, the z-axis acceleration is zeroed and all acceleration for the table is zero. This machining process took about 3 hours and thus ran slower which would reduce the acceleration experienced.

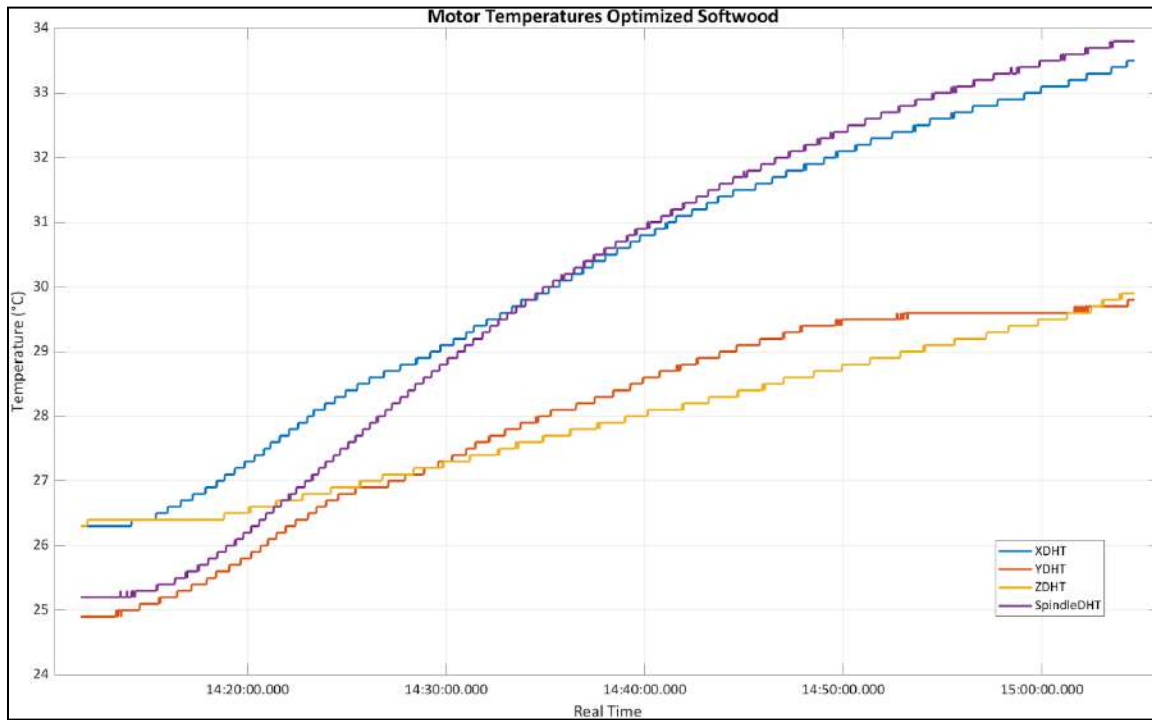
Figure 12.43: Aluminum Enclosure Acceleration Zeroed and Smoothed



12.9 Optimized Softwood Testing

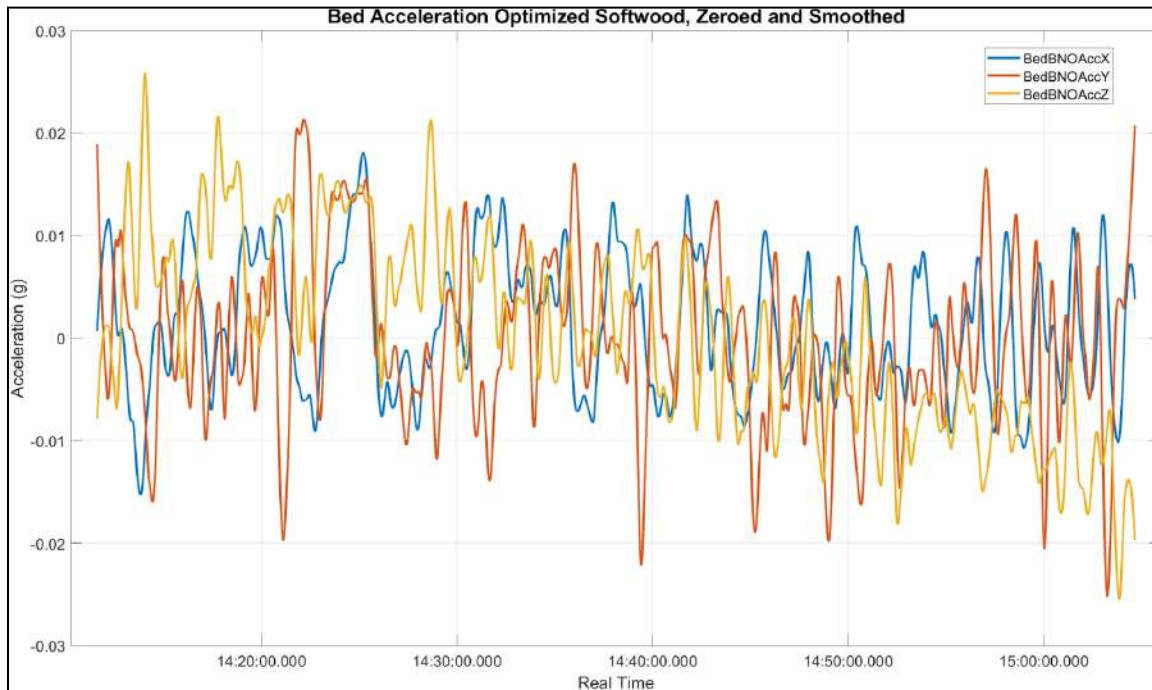
Softwood, machined after all machine updates, using a CAM process optimized for part geometry, and using verified feed and speed for softwood. The temperature data can be seen in Figure 12.44, all data stayed in a similar range and demonstrated an almost identical pattern to the temperature data displayed in Figure 12.32 but only about 2°C higher. The consistency in temperature data between these two sets of tests is a good indicator of expected temperature values going forward.

Figure 12.44: Motor Temperatures for Optimized Softwood Process



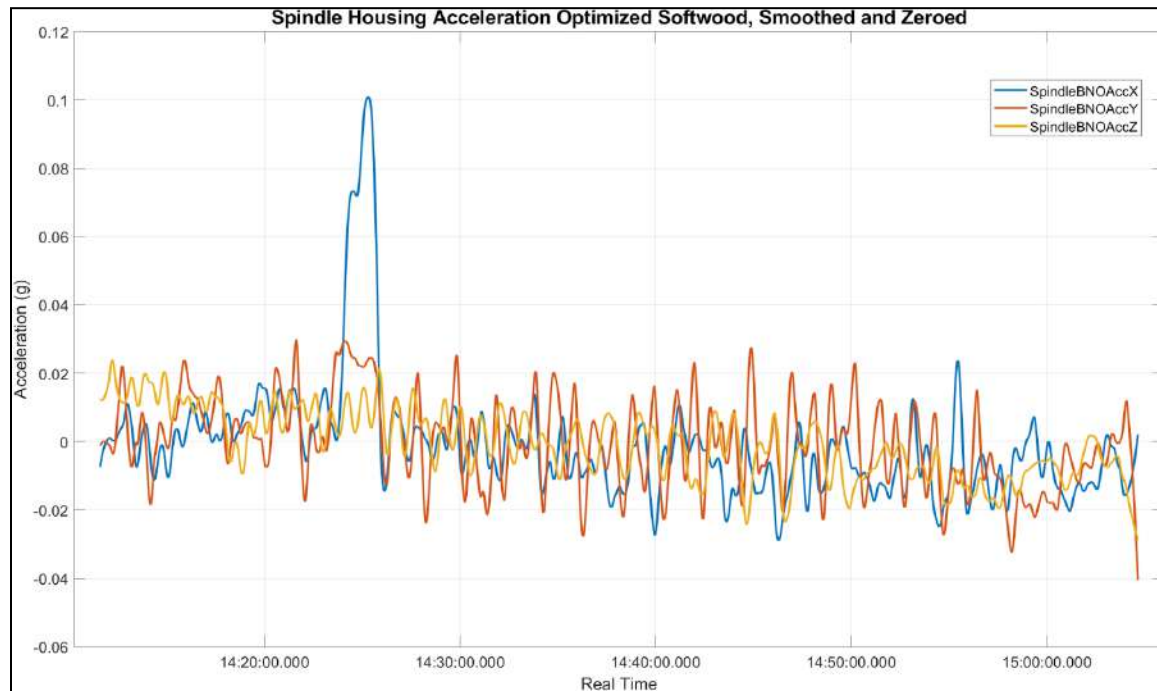
The bed acceleration during this testing can be seen in Figure 12.45 and remains with an amplitude of approximately 0.015 g for all axes. This aligns with other data collected and is reasonable.

Figure 12.45: Bed Acceleration for Optimized Softwood Process Zeroed and Smoothed



The spindle housing acceleration has a y-axis amplitude of approximately 0.025 g which goes beyond the expected range, especially since the spindle housing does not experience y-axis motion. Despite some spikes, the x- and z-acceleration the acceleration amplitude remains around 0.015 g which is greater than in the initial testing. This data can be seen in Figure 12.46 below.

Figure 12.46: Spindle Housing Acceleration for Optimized Softwood Process Zeroed and Smoothed



The acceleration outside of the machine can be seen in Figures 12.47 and 12.48 with the first being the table acceleration and the second being the enclosure acceleration. Although the z-axis acceleration outside of the machine is zero in both locations, the acceleration amplitude in the x- and y-directions is greater than the initial testing values. The amplitude is mainly between 3×10^{-4} g for the table acceleration and about 4×10^{-4} g for the enclosure acceleration.

Figure 12.47: Table Acceleration for Optimized Softwood Process Zeroed and Smoothed

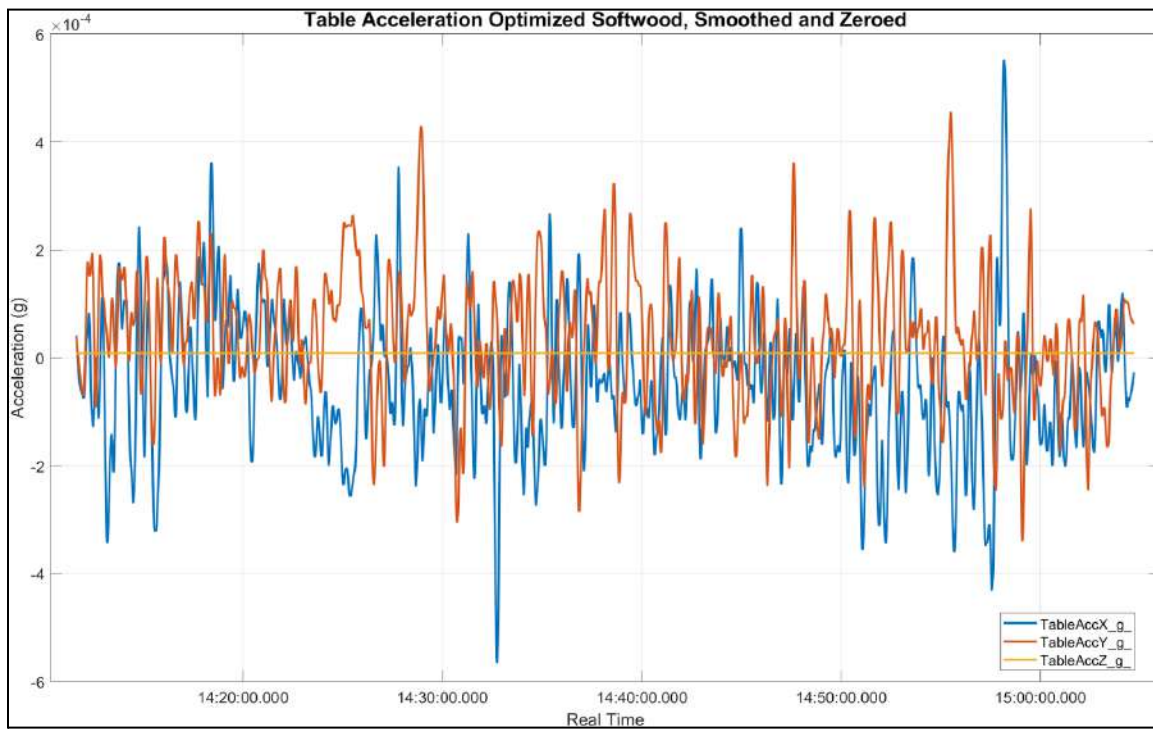
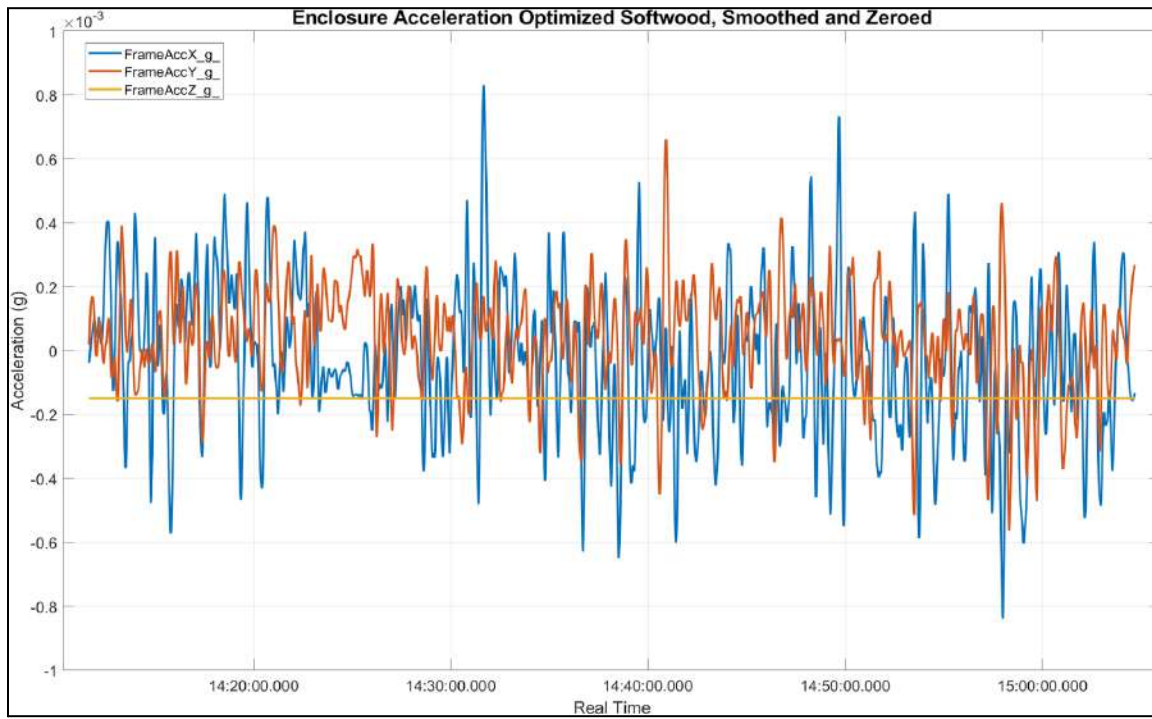


Figure 12.48: Enclosure Acceleration for Optimized Softwood Process Zeroed and Smoothed



12.10 Overall Results of Physics Testing

The acceleration inside the machine generally stayed within $-0.04g$ and $+0.04g$.

Acceleration of the machine enclosure and the table on which the machine is installed, generally stayed within a range of $\pm 5 \times 10^{-4} g$. These results are solely the product of monitoring machine operations and cannot be used to show any sort of decrease in vibration. The temperature data following machine updates suggests that normal operation is well within safe limits for the motor and should be expected to be below 38°C for most operations. As seen by the results, the dimensions of machined parts was within the $\pm 0.005"$ tolerance of all three materials. The enclosure went through a series of results such as leak and durability testing.

12.11 Bed Leveling Results

Testing confirmed that the set-screw design did indeed deliver the level of accuracy desired, as it was five times more accurate than what was required. The bed was easily adjusted to within 0.0005", and the aim was to be within 0.0025".

$$\frac{0.0025"}{0.0005"} = 5$$

Moreover, when adjusting the subsequent corners, the bed maintained its position within 0.002". Therefore, from one limit switch to the other on each axis, the plate was able to be leveled to within 0.004", which is 1.25 times more accurate than the target of 0.005".

$$\frac{0.005"}{0.004"} = 1.25$$

In conclusion, the bed leveling functionality was successful. The design of using a set screw allows for accuracy with variance less than 0.0005" on each corner. The tolerance was maintained from one limit switch to the other in the x- and y-axes, to within 0.004". These values are within the target goal of the bed achieving leveling within 0.005" on the x- and y-axes.

This chapter provided quantitative data pertaining to each of the implemented components and their respective verification tests. The following chapter uses this information to provide an analysis and discussion for the overall success of the subsystems.

13.0 Discussion

The following section discussed what was achieved and what difficulties were faced at the end of the project based on the goals set in Section 4.0 by the 2024-2025 MQP team.

13.1 Affordability

Although the initial goal aimed to have a price point of the base model under \$2,500, the finalized base model pricing for the machine was calculated to be \$2,681.99, as shown in Table 13.1. The discrepancy of roughly \$200 can be attributed to the outsourcing of several work area components and the enclosure pricing. The work area pricing, totaling over 50% of the base model's price, incurred the most cost through the outsourcing of gantry components for precision machining. The sizing and overall quantity of t-rails purchased additionally significantly increased the incurred cost due for the machine's enclosure, totaling nearly \$550. A similar price point can be seen with the electrical aspect of the machine, as the overall cost of the stepper motors and their respective drivers contributed a large amount to this number.

Table 13.1: Price Breakdown of Base Model

Base Model Breakdown	Price	Percentage of Total Base Model Price
Total Enclosure Price	\$544.61	20.31%
Total Tooling Cost	\$120.15	4.48%
Total Electrical Price	\$486.75	18.14%
Total Work area Price	\$1,409.90	52.57%
Total Software/Control Price	\$55.98	2.09%
Total Hand Tools Price	\$64.61	2.41%
Total Price	\$2,681.99	100.00%

Although the base model's pricing was slightly more than expected, the add-on functionality's \$9,66.04 price point resulted in a total cost of less than \$4,500, shown in Table 13.2. The 4th axis kit and its corresponding base plate resulted in the highest cost for add-on functionality at \$350. Additional high price points can be seen with electrical components pertaining to vibration analysis and add-on control, each aspect totaling \$185. All other components' low price points aided in the overall achievement of creating a fully operational machine with add-on functionality at a total price of \$3,648.03.

Table 13.2: Price Breakdown of Add-on Features

Add-on Price Breakdown	Price	Percentage of Total Add-on Price
Total Coolant Price	\$144.01	14.91%
Total Vacuum Price	\$59.88	6.20%
Total Vibration Price	\$183.72	19.02%
Total Tool Changer Price	\$41.95	4.34%
Total Control Addon Price	\$185.74	19.23%
Total 4th Axis Price	\$350.74	36.31%
Total Price	\$966.04	100.00%

13.2 Accuracy

As noted in Section 3.9 of this report, the measurable goal of accuracy was to maintain a machine tolerance +/- 0.005" for plastic parts and +/- 0.010" for metals. Showcased in Section 12.1, this goal was achieved by the machines created by the 2024-2025 MQP team. According to Table 12.2, the maximum tolerance variance of a plastic part was 0.005". Furthermore, Table 12.3 shows that the maximum tolerance variance of a metal part was 0.003". The variance in tolerance between the same materials was a result of an error in the toolpaths. Initially, the CAM for the test part used a 2D Adaptive Clear to not only clear the excess material to make the design, but also provide the finishing pass. After consideration, the toolpath had been updated to include a 2D Contour toolpath after setting the stock-to-leave of the 2D Adaptive Clear to 0.020". With this modification, the geometric tolerance increased as well as the surface finish of the design.

13.3 4th Axis

According to Section 3.9, the goal of 4th-axis implementation was the ability to machine more complex and rounded parts. The 4th-axis kit, as detailed in Section 6.6, offered a user-friendly wiring and chuck setup which implemented easily in the machine's UGS software. At approximately \$250 in price, the full 4th-axis design can be made using explicitly a drill press to drill the holes in the 4th axis baseplate, and taps to thread the holes in the work area plate.

With that being said, the goal of implementing a 4th-axis rotary kit was a great success. The ability for users to easily implement the system in their machine will provide both novice and advanced machinists the ability to expand the type of part they can mill. However, there is certainly room for improvement when it comes to the complexity of parts

that can be milled using the system. Without the ability to produce milled turns, users are limited to the parts that can be made.

13.4 Chip Evacuation

At the beginning of the year, the goal for the chip evacuation system was to “Reduce chip buildup in the work area and cutting tool path”, refer to Section 3.9. In Section 12.2.2 and 12.3, results of the coolant and vacuum system were discussed. Although there were leakages outside of the enclosure from the coolant system, the continuous flow of the coolant throughout the machining process for aluminum was able to push away chip buildup from the tool and the work area. The vacuum system was able to remove a significant amount of chips when machining wood, with the main drawback being the noise of the “shop-vac”. Overall, the goals of removing chips from the work area and cutting tool path was achieved, although improvements to both systems can be still integrated in the future. The recommendation for improvements can be found in Sections 14.1.1.1 and 14.1.2.1 of this report.

13.5 Tool Changer

The development of a tool changer was one of the goals for this project. Adding a tool changer would allow for an increased tool library while running a part and reduce the time needed to change a tool from removing the tool with a wrench. Chapter 7 explains the entire process of creating the tool changer while chapter 11 explains how the tool changer is assembled. While the tool changer was able to be unloaded, loading the tool was unsuccessful. Additionally, the implementation of the laser sensor and dust cover into GrblHAL was unsuccessful. The design for the tool changer does work but software for the

mechanism still needs to be tested as well as testing with a part that uses multiple tools should be done.

13.6 Bed Leveling

The bed leveling turned out to be successful. The bed was able to be leveled out within 0.004", which is within the target range of <0.005". The method allows the user to simply loosen the bed's mounting screws and make fine-tune adjustments to the set screws on the fly. In comparison to what was discovered in the industry during research, which were methods that primarily consisted of designs requiring disassembly of numerous parts of the machine, the design used in this machine enables leveling that is quicker and easier to perform.

13.7 Enclosure

The enclosure of the mini-mill received many major design changes to improve its liquid sealing, rigidity, serviceability, user safety, chip management, and coolant drainage. A ramp was implemented underneath the suspended gantry of the mill to direct coolant and chips to the mesh drain hole. Polycarbonate panels were slotted within the grooves of the t-rail frame and sealed with rubber gasket strips which prevents coolant leaks and also allows the panels to be easily removed for future maintenance. A rigidly attached hinged door lined with neoprene foam strips was made to replace the old loosely attached sliding door with no safety precautions. 3D printed t-rail corner connectors, designed to function as a gasket with silicone, reduce the risk of leaks by fitting perfectly to the profile of the t-rail.

While many of the leak tests during assembly had promising results, the final machine had a handful of leak points which is likely a result of incorrect or insufficient

application of silicone. The hinged door also tends to leak residual coolant when it is opened due to the raised gantry frame being too close to the front lip of the door.

13.8 Safety

The safety of the machine has been massively overhauled and improved from the state it was in after last year's project. There are multiple redundancies in place to ensure that the end user of the new CNC milling machine remains safe and unharmed. As discussed, the E-stop, door switch, LOTO systems, limit switches, and stack light all work as intended.

It may behoove any future milling machine team to add some kind of locking mechanism to the electronics box to secure that as well from any unauthorized access, but this is more of a security risk than a safety one, as the machine cannot be actuated with the plugs locked away.

13.9 Ease of Manufacturing

A goal of this project was to be able to assemble a desktop CNC machine with only simple tools and parts. This is because it would allow those with novice machine skills and lack of access to advanced machines to be able to quickly and cheaply produce their own desktop CNC machine. Chapter 11 goes in depth on how the machine was assembled; however, the takeaway is that a majority of the parts were able to be procured and assembled with only using simple tools such as 3D printers, drill presses, bandsaws and hand tools. Parts were also ordered using SendCutSend and Amazon with no major modifications needed for them to be assembled on the machine. One aspect where this did fail was the work area plates. A CNC was used to drill the holes needed for the tool changer, vise, and 4th axis in the work area plate. This went against the intention of having all parts

be able to be produced without the use of advanced machines, and was done so out of time constraints and a need for precision and accuracy in the plates.

13.10 Control System

For the new control system implemented into the machine, satisfactory progress was made towards the established goals. The software completely supports a 4th-axis, all common computer operating systems, and is completely free and open-source. For the automatic tool changer, the control software supports the implementation aside from setting the Z offset and correctly accounting for the laser sensor signals. For the tool changer module itself, it did not support I2C communication nor external commands. With some small modifications to the grblHAL firmware and tool changer module firmware, the machine could be updated to include full automatic tool changing functionality. For the control board, it integrated with no problems from last year's electronic systems, with some necessary rewiring.

13.11 Vibration

The previous MQP team handled vibration damping under the constraints and goals of the project well. The use of steel for the machine structure which increased the weight, bolted joints in the gantry construction, and spacers to create rigid connections from the spindle to the linear rails. All of these implements were kept on the 2024-2025 project as they were beneficial to vibration reduction of the machine. Cavity filling was not feasible to increase the weight of the machine further as the design intent of the machines was for them to be somewhat portable. Mass dampers and active damping additionally were not feasible for this project due to the price point. The tolerances and acceleration values achieved by the final iteration of this projects' machine were appropriate for a small-scale open source CNC

mill available to undergraduate students and hobbyists. The vibration measurements are considered low and did not appear to have an effect on the machine to produce accurately toleranced parts.

13.12 Broader Impacts

This project will have a lasting impact on undergraduate students at WPI, specifically Mechanical Engineering students. Students will be able to use the milling machines as part of coursework to gain experience with CAD, CAM, G-code, and CNC machine operation. For students already familiar with CNC machining, they will gain experience using different softwares and interfaces. The location of the machines in the teaching lab will be more accessible to students than the machine shop in Washburn. The small scale of the machine will allow for smaller projects to be completed.

With current federal work study students from the MME Teaching Lab trained on how to operate the desktop mill, the extent of machinable parts for students has become evermore expansive. Additionally, these machines offer an opportunity for students to further engage in machining as well as assist in manufacturing machined parts for classes, personal use, or MQP. Furthermore, with interest from Professor Daniello of Washburn Labs at WPI, this machine has the potential to be implemented into manufacturing courses offered at WPI. With the aim to showcase ME 1800 students how G and M code operates, how a CNC mill works, and testing students' toolpaths, the desktop mini-mill has the potential to boost student interaction with the manufacturing department. Overall, the desktop CNC mini-mill offers students at WPI an avenue for pursuing their interests in CNC machining in a user-friendly manner.

14.0 Conclusion

Quality open-source desktop CNC milling machines are a rarity to find, and commercially available ready built machines are simply too expensive, decreasing the machinings outreach to students and hobbyists interested in milling their own parts. This year's MQP team successfully developed and improved upon a previous iteration of a desktop CNC mini-mill. This resulted in a low-cost and open-sourced desktop machine that met the majority of the goals outlined at the start of the project. New features such as the 4th-axis, automatic tool changer, bed leveling system, and the newly designed enclosure improved not only the ease of use of this year's machine, but also increased its capabilities over previous iterations of the machine. Safety features such as a door switch, emergency stop button, and a lock-out-tag-out system were implemented to comply with industry best practices with hopes that these machines can be used in WPI curriculum, exposing more novice students to CNC machines and how they function. This culminated in a final design and two ready-built machines that will enable students and hobbyists to engage in machining with minimal entry barriers.

While the project was an overall success, the team noticed several issues that should be addressed in future iterations. Notable issues included: coolant leaking through the enclosure with extended use, heat generation when machining aluminum resulted in tool degradation, significantly increased noise level when shop vac was in use for chip evacuation, and sensor accuracy was prone to interference. Furthermore, a less complex and more organized wire management system would greatly improve electrical troubleshooting and decrease the risk of accidental contact with exposed wire.

14.1 Recommendations for Future Work

Over the course of the year, the team's goals shifted and changed as everyone became more familiar with the machine and its construction. There were several future changes that the group learned over the course of working on the CNC milling machine that could be implemented by a future MQP group.

14.1.1 Minor Recommendations

This subsection highlights future recommendations that future teams can take into consideration, but are not to take precedence over the major recommendations (Section 14.1.2).

14.1.1.1 Vacuum System Recommendation

Although the vacuum system was able to remove most of the dust and chips with little to no issues, there are still some improvements that can be added to the system.

Subteam 1 recommends:

- Design and 3D print a cover for the vacuum hole on the top panel
- Purchasing a diffuser for the “shop-vac”
- Build a sound-dampening box for the “shop-vac”

As of the conclusion of this project, there is no cover for the vacuum hole on the top panel for both enclosures. This is not an issue if the vacuum system is being utilized, but if it is not, there is a vacant hole on the top panel. The team did not run into any issues with the hole while the coolant system was operating (i.e. coolant splashing from the hole), however, it would still be beneficial for the machine to have a cover in case the end mill breaks.

As mentioned in Section 9.1.3, the “shop-vac” was incredibly loud. There are two methods to reduce the noise of the shop vac. The first method is to purchase a diffuser for

the “shop-vac”. This method is not super effective because the diffuser is mainly used to reduce dust blowback from the exhaust port, and while this does muffle some of the noise, the reduction is insignificant. The second method is to build a sound-dampening box. This method would require more research, but the Youtuber “Samcraft” was able to build a “shop-vac” damping box that reduced the noise level to 40 dBA compared to the regular average of noise 80+ dBA (Samcraft, 2020).

The CAD for the “dust-boot” and “dust-skirt” are on Github, so if there need be changes to some of the dimensions, future teams can freely download and edit them.

14.1.1.2 4th-axis Recommendation

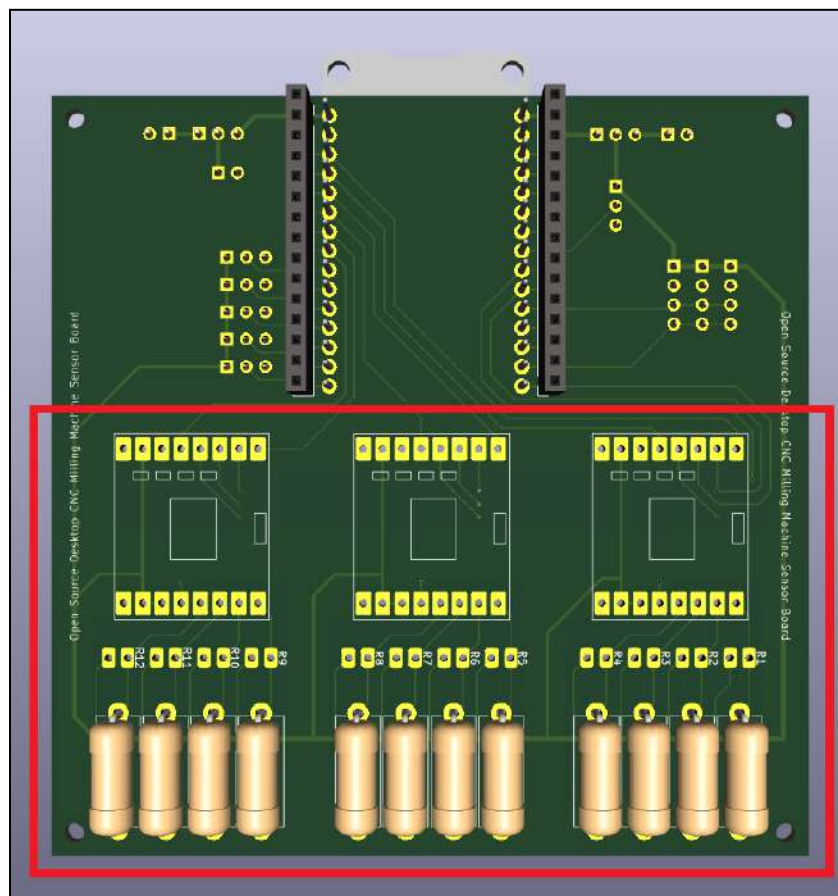
Like a traditional lathe operation, many large-scale enc machines are capable of milled turning. This means while the spindle is milling a part in either of the other axes, the 4th axis can also rotate. As a result of the lack of torque present in the 4th axis NEMA 17 stepper motor, a milled turn is not capable in the current 4th axis design. What this means is more complex rounded pockets cannot be milled. At the moment, the step angle of the motor is 1.8 degrees with a reduction ratio of 4:1. If the motor were to take two steps too much, the part would see close to 1 degree of error in rotation. With that being said, a substitution for a motor with higher torque or a better resolution should be sufficient enough to withstand a milled turn.

14.1.1.3 Strain Gauge Recommendation

Our team made efforts to implement arrays of strain gauges on our machine in an attempt to measure the strain on various places of the gantry. However, problems arose with planning, wiring, and gathering data. The plan was to have three sets of four strain gauges in Wheatstone Bridge formation, but even then, twelve sets of wires added a large amount of

bulk to the already overcrowded wiring system. In the end, our strain gauges did not end up gathering any useful data, and it was decided to scrap the strain gauge implementation in favor of spending time on other aspects of the machine. Remnants of the strain gauge's implementation can be found in the KiCad and on our sensor board. It should be noted for any future teams that the footprint of the ADC on this board is slightly too wide for the component's pins to fit within the guided holes (Figure 14.1).

Figure 14.1: Custom PCB Render, with Strain Gauge Section Highlighted



14.1.1.4 Wire Management Recommendation

Last year's project had room for improvement when it came to the management of the wires connecting the machine, control board, and other devices. With the introduction of

several new sets of sensors and a new motor driver for the 4th axis, wire management was a higher priority than ever. The dedicated sensor PCB being mounted on the back of the machine instead of inside the electrical box saved space, a new electrical box was designed to fit all the needed parts in designated places, and the wiring was generally tidied up from last year, but there is still room for improvement in the next year.

One proposal that the team did not end up having time to implement was the addition of a parallel port. Several sensors and motors shared common power and ground wires, so a parallel port would cut down on the amount of wires in the back of the machine. It would also keep the wires bundled together and not splayed out like in both last year's machine and this year's machine. The addition of a parallel port, likely installed somewhere on the back panel, would also make it easier to disconnect the electrical box for maintenance.

14.1.1.5 Automatic Bed Leveling and Tool Probing Functionality

After considerable time spent on this process, it is recommended that the bed leveling remains mechanical. The reason for this is that the bed does not need to be leveled frequently. Moreover, the loss of space, risk of damage to the components required for automatic bed leveling, and the additional financial cost of those components is not worth it given the infrequent need to perform bed leveling.

Tool probing is also partially implemented in the machine. It is recommended that the next team finishes this task. The starter code for the laser that can be used as a tool probe can be found in Appendix A. The tool changer may also need to be sealed properly, such that coolant doesn't get onto the electronics.

14.1.1.6 Sensor Recommendation

Due to issues brought up during EMI, most sensors were not implemented. If the EMI issues were resolved, each unimplemented sensor would still have issues. For the laser sensor, even when the values read were good, the laser transmitter and receiver required precise positioning, otherwise, the readings would not register. A future recommendation would be to design a mount that holds the sensors securely while still being able to properly read the spindle speed. For the strain gauges, they still need refinement in their electrical connections to get consistent readings. This would involve rigorous testing of the connections and methods to mitigate the EMI transmitted through the gantry. Additionally, sensors should be implemented that measure the temperature of the spindle as its machining, to see the effects of cutting material and coolant on the spindle.

14.1.2 Major Recommendations

This subsection lists recommendations for future teams that should be prioritized at the onset of the project.

14.1.2.1 Coolant System Recommendation

As discussed briefly in Section 12.1, coolant plays a pivotal role in expanding the machinable materials for this mini-mill. However, this coolant also impacts electrical systems within the machine, leading to corroded wires and broken connections (Section 10.1.2). In order to solve these issues and allow for coolant to be used in the machine, it is recommended to wrap the sensor and limit switch wiring in conduit to prevent potential damage from coolant.

Furthermore, the enclosure also needs improvements to better contain coolant and prevent damage to outside components. Subteam 1 recommends:

- Using the redesigned 3D printed corner gaskets for the first machine
- Drill multiple drain holes into the table for the coolant to exit
- Use a new drain mesh that is less fine than the current one
- Purchase more caulk and coolant

Changing the redesigned 3D printed corner gasket on the first machine will require a complete disassembly of the machine's enclosure. Although this will be a tedious process, it is an important step to prevent future leakages. To remove the caulk, Subteam 1 recommends using a sharp blade to scrape off all the caulk.

Drilling multiple holes into the table will prevent the coolant from pooling up inside the machine. Using a new, less fine drain mesh will prevent the chips from clogging. The team ran very low on coolant and completely ran out of caulk towards the middle of D-term. As a result, the team was unable to do further testing with the coolant system. Furthermore, because there was no more caulk, there are still gaps within the second machine that still needed to be sealed.

14.1.2.2 Tool Changer Code

For the tool changer implementation, there is still some work that needs to be done to get it to work. The code for the dedicated module needs to be implemented to include I2C communication to the control board. Once the functionality is implemented, the tool changer firmware controls need to be tested with the physical module to verify that it works as intended. The firmware and likely module code would need to be updated based on the results that were expected from the machine versus the actual results from the machine.

14.1.2.3 Expanded Specialized Tool Library

As of the completion of this project, the tool library created by Andrew P. includes wood, teflon, 6061 aluminum, and delrin. While these are commonly machined materials for individual projects or MQPs, it is limited to the tool size and cutting parameters for each material. The basis of each material's cutting parameters was gathered from the data collected from running the test parts for each material. This included using a single 0.250", four flute flat end mill to create all the contours. The tool library, using the Apps Script provided by Google Sheets, then calculates the cutting parameters for different end mills based off of the parameters measured for the 0.250" flat end mill. For example, if a user enters a tool diameter of 0.125", the speeds, feeds, and depth of cut will all change in proportion to the base parameters measured from the 0.250" end mill. To counteract this lack of tool information, a future team can run the test parts with different sized and style end mills to expand on the parameters of these existing materials, but also branch out to other machinable plastics and metals.

14.1.2.4 IRB and Student Testing

Due to the result of a restricted timeline and unforeseen machine issues towards the end of academic year, student testing of the desktop mini-mill was unable to be achieved. With the current number of students testing the machine limited to the number of federal work study students in the MME Teaching Lab department, a wide variety of data was not attained. In order to continue increasing the user-friendly nature and encourage students to explore manufacturing engineering, it is required that more data be collected from novice and first-time users to collect their input on how this machine operates. Having received approval from WPI's IRB (Institutional Review Board) to conduct student testing on the

machine, a future MQP team should utilize the resources created by the 2024-2025 team to carry out this aspect of the project. These resources are located in Appendix H, and walk the user through creating a part in Solidworks, creating the toolpaths in Fusion360, uploading the post-processed file to Universal G-Code Sender, and setting the part up in the machine to be machined.

Looking long term, an expectation would be to have a certain number of FWS students as experts of the desktop cnc machines. In doing so, these students would be responsible for administering the educational material to interested students, overseeing the user-testing process, as well as assisting students with their own personal projects on the mills. To ensure an adequate user experience, a similar process to the one initially planned to collect data for this year's user testing, with feedback being implemented as seen fit.

14.1.2.5 EMI

It is recommended that next year's team replaces the cable, which delivers power from the VFD to the spindle, with a shielded cable. There was substantial EMI detected on this cable, and it is not the proper electrical cable for using such a device, as it is not designed to be used in combination with a variable frequency driver in a system that is highly-susceptible to electromagnetic interference. It is also highly recommended that the proper gauge wiring is determined through rigorous research, to ensure the safety of users of the mill.

14.1.3 Testing and Data Analysis Recommendations

Further data analysis should include accelerometer sensor verification of reading known acceleration for linear motion of a known distance to determine how the sensors

collect the data. Another method of data collection would be by conducting a stability lobes experiment and fitting data with a Fast Fourier Transform to determine what the vibration waves consist of. The stability lobes experiment would also refine machining capabilities if completed once there will no longer be any structural machine updates.

14.2 Personal Reflections

Echo:

I came into this project as a Mechanical Engineering Major with some CNC milling experience. This project allowed me to do a lot of hands-on work but also much research about CNC machines. I was also able to gain a lot of valuable experience with running experiments using sensors to collect data and how to analyze that data. I was able to grow my skills of working with a group while also learning more about completing primarily self directed research. This was an excellent experience and I hope to use the knowledge and skills I have gained over the past year in my engineering career.

Rafael:

I had no prior experience in CNC Mills before this project, so being a part of this project showed me a different side of engineering. The project allowed me to expand my knowledge not only on CNC mills but also further my understanding of Solidworks as that was my main role in this group. I've learned new techniques when it came to creations of CADs and additionally understanding 3D printing filaments. While working in an 11 person team was challenging with communication, I found it to be an experience that truly taught me what it was like to work in an engineering team. I had an amazing experience and feel fortunate to be a part of the project.

James:

I enjoyed working on this project because it allowed me to gain more experience with the design process and rapid prototyping. My experience operating CNC mills in the past came to my advantage during this project because I was already familiar with computer aided manufacturing, g-code, and how 3-axis were supposed to work in general. Working with a large team of students each with diverse skill sets was also very beneficial because I was able to learn so much from each of my teammates when I would collaborate with them.

Camren:

Throughout the course of this project, I thoroughly enjoyed working on it. I got to work with almost every aspect of the machine, from the electronics, to software, and to mechanical building and design. I also enjoyed working with an interdisciplinary team, with different strengths, and managing those within our group. From the project, I learned a great deal about CNC mills, which I had little experience with before working on the project. After this project, I feel confident in my ability to learn CNC mills and to apply my knowledge to improving them.

Michael D.:

This MQP project has been an enjoyable experience. Meeting and working with other majors outside of mechanical engineering has taught more important lessons when working with people with different backgrounds. This has taught me to work with those who, because of their academic disciplines, have different approaches to solving problems,

and it is important to be open minded to their solutions. Furthermore, working with a large team has taught me the importance of communication and accountability when it comes to assigning and completing tasks. The project also taught me significantly more about CNC machines, which I have had few experiences with.

Perrin:

I enjoyed working as a part of an interdisciplinary team, as I felt I learned more about working on real-world projects than I would have as a part of a solely ECE-oriented team. Working with such a large team was a new experience for me, and it was fun communicating with the rest of the team and applying the skills I've learned at WPI to finish my own goals as well as helping others with theirs. I have only worked with CNC machines before a little in high school, so that was a huge learning experience for me as well.

Andrew:

This project allowed me to explore my interest in CNC machining. With a background as a CNC operator and toolmaker, this project allowed me to incorporate everything I learned at WPI in addition to my background knowledge. I enjoyed building and operating a CNC machine freely, allowing me to expand my understanding and experience with CNC machining. Working within an 11 person team was a first for me, and I thought it would be challenging. It forced me to further my communication skills and get out of my comfort zone. This MQP was a great reflection on my time at WPI and allowed me to complete my four years here in a project I loved.

Daniel:

My prior experience with CNC machining prompted me to pursue this project. I thoroughly enjoyed the ability to freely access the mini-mill, creating the G and M-code, as well as conducting part and tool setup. Operating within an 11 person team was something that I had never worked with before, and it pushed me to ensure my communication skills were up to the task. Overall, I had a great time working on this project and was extremely proud of the fact that the team was able to successfully construct a machine to be utilized by both WPI students and hobbyists alike.

Michael P:

Being older than the traditional student, I took on substantial risk when I left my job at a robotics company to return to college. I also own a machine shop, which I had shut down because I wanted to transition from providing CNC machining services, to developing autonomous machinery to sell directly to customers. I had tried to make an autonomous product, but I got stuck when working on the controller. I realized then that I had to learn more, so I applied at the robotics company with the intent of landing a job where I'd get paid to learn. I did well there, and they offered to pay my tuition for me to return to college. I applied to WPI's robotics program, and got in. Because of scheduling, I was faced with a choice: either return to college, or play the safe route and stay put at a well-paying job. And here I am. As things played out, this MQP project came to my attention, and I jumped at the opportunity to get hands-on experience working on the exact problem I had originally encountered during my first attempt at developing a robotic product and company. After taking part on this project, I've proven to myself that I now have those skills I previously

lacked and desperately needed. In addition, this project has proven to me that I made the correct decision when I decided to take the risk associated with going back to college.

JR:

The only experience I had with CNC machining before this project was ME 1800. This project not only expanded my knowledge on CNC machining, but also allowed me to use skills that I've learned at WPI. Working with this team has been one of the best experiences I've had with a group project. Communication was never a problem, and we were able to work together very efficiently. Although we were behind schedule on things, I'm still extremely proud at what our team had accomplished over the past year. I'm overall extremely happy that I decided to work on this MQP.

Dante:

As an individual with very little machine experience prior to joining the project, I can confidently say that this project sparked my enthusiasm towards manufacturing. Before this project, much of my experience came from design, especially with mechanical systems. From developing the designs for the machine's parts, to building and implementing them into the machine, I have learned tremendously about the manufacturing industry, as well as common practice exercises in machining. The project was a great combination of challenging and enjoyable, a great mix that pushed me to grow as an engineer. I am very appreciative to be able to learn so much from the project, and look forward to expanding my machining knowledge as I move forward from the desktop cnc milling machine project.

References

1910.212—General requirements for all machines. | Occupational Safety and Health Administration. (n.d.). Occupational Safety and Health Administration. Retrieved May 6, 2025, from

<https://www.osha.gov/laws-regulations/regulations/standardnumber/1910/1910.212>

8020 Aluminum Extrusions—Buy 80/20 Aluminum at Zetwerk. (n.d.). Retrieved May 5, 2025, from

[https://www.zetwerk.com/resources/knowledge-base/aluminum-extrusions/80-20-a
luminum-framing-extrusion/](https://www.zetwerk.com/resources/knowledge-base/aluminum-extrusions/80-20-aluminum-framing-extrusion/)

23517973 | Detroit Diesel Series 50/Series 60 Impeller. (n.d.). Highway and Heavy Parts | Diesel Engine Parts. Retrieved May 6, 2025, from

[https://highwayandheavyparts.com/product/23517973-detroit-diesel-series-50-serie
s-60-impeller/](https://highwayandheavyparts.com/product/23517973-detroit-diesel-series-50-series-60-impeller/)

ABS Plastic Properties | Advantages Of Acrylonitrile Butadiene Styrene. (2022).

Adreco Plastics. <https://adrecoplastics.co.uk/abs-plastic-properties/>

Advantages of T Slot Aluminum Extrusions. (n.d.). Retrieved May 3, 2025, from

<https://hvhindustrial.com/blog/t-slot-aluminum-extrusions>

Ahmed, R. (2023, July 27). What is Ultimate Tensile Strength? Metal Supermarkets.

<https://www.metalsupermarkets.com/what-is-ultimate-tensile-strength/>

Amazon.com: LUBAN Led Signal Tower Stack Lights, Industrial Signal Warning Lights, Column Tower Lamp Andon Lights with Rotatable Base, Steady/Flashing Light Switchable, 12V 24V DC(3-Layer, with Buzzer): Industrial & Scientific. (n.d.). Retrieved May 7, 2025, from

https://www.amazon.com/LUBAN-Industrial-Rotatable-Flashing-Switchable/dp/B086ZJNLBX?crid=3CE6STO5JB1YP&dib=eyJ2IjoiMSJ9._0Mh0dpddEUpAY675JsA2QbBmb96PB1sl6WxJPkQuelzHfMhVcnwgq4315Vc69X8fLdDbvr1i-EbeqsIujhOQOFj0ZoLEIIP5B5UoONOfV_9GJTU0seEkSqB9xASDhR-llUa2r6N80iCpZqlpitUP-aoXEnhrQIYsRuLjmOIhcjIF9sEBThMV_DKkwmApvvyWa2Zgfaq-JmRqTjzaNmPy2QbJH-hwwoxF-aoJ3fXTws.6lwo7fS7BimRjk602QJAjYLdjKrWs1KRM2C-pbfpWsM&dib_tag=se&keywords=stack%2Blight&qid=1738697625&sprifix=stack%2Blight%2Caps%2C140&sr=8-3&th=1

Amazon.com: STEPPERONLINE Short Body Nema 17 Bipolar Stepper Motor 1A 22.6oz.in/16Ncm DIY CNC Extruder: Electronics. (n.d.). Retrieved May 6, 2025, from

https://www.amazon.com/STEPPERONLINE-Bipolar-Stepper-22-6oz-Extruder/dp/B00PNEQ79Q/ref=sr_1_4?dib=eyJ2IjoiMSJ9.yoLUw6KcUVLROmV-vpmMWR-qr6PV6BbnB2R3tryjUjsq-C92CrRrx54K51Q759GKDUu7mklE2V71WvWWj7TpXoFpOpP-I5V9Op051gn-414hJxfkCJC0mVOjCuI5OnA6ZMGKvy8kEdnSgQvpwzk4CQK7l2L2JG6QS-5DA3-Y1NX6m_gdSvZqrvc3HyMC5xEVimB5Lzgr-wCLTK2mDAF4u4RpFYc8bwaLWp47JHVuQfM.1fnV_a_c0dTng4l29DNx682y8o05wRgrw6RIk6OxGno&dib_tag=se&hvadid=241911860858&hvdev=c&hvexpln=0&hvlocphy=9001847&hvnetw=g&hvocjjid=1159797718649055017--&hvqmt=e&hvrand=1159797718649055017&hvtargid=kwd-1834377567&hydadcr=24633_10399728&keywords=nema+17+stepper+motor&mcid=e24515616fdf3992bad8f5be82f07f4&qid=1746554591&sr=8-4

Aosong Guangzhou Electronics Co. (n.d.). *Temperature and Humidity Module DHT11*

Product Manual. Aosong Guangzhou Electronics Co.

Astro Machine Works. (2021, May 22). What Is CNC Machining? | A Comprehensive Guide. *Astro Machine Works.*

<https://astromachineworks.com/what-is-cnc-machining/>

Automatic tool changer mechanism | Sacher CNC. (n.d.). Retrieved April 3, 2025, from <https://sacher-cnc.com/en/blog/automatic-tool-changer-mechanism/>

Bacidore, M. (n.d.). *How to get the most from stacklights.* Controldesign. Retrieved May 6, 2025, from

<https://www.controldesign.com/displays/stack-lights/article/55140700/how-to-get-the-most-from-stacklights>

Bantam Tools Desktop CNC Milling Machine. (n.d.). Bantam Tools. Retrieved May 6, 2025, from

<https://bantamtools.com/products/bantam-tools-desktop-cnc-milling-machine>

Bantam Tools Explorer™ CNC Milling Machine. (n.d.). Retrieved September 29, 2024, from

<https://store.bantamtools.com/products/bantam-tools-explorer-cnc-milling-machine>

Barrett, P. (n.d.). *PicoCNC/PicoCNC User Manual.pdf at main · phil-barrett/PicoCNC.* GitHub. Retrieved April 30, 2025, from

<https://github.com/phil-barrett/PicoCNC/blob/main/PicoCNC%20User%20Manual.pdf>

- Bartnik, N. (Director). (2019, April 19). *3D Printed Vacuum Cleaner For CNC Machine* [Video recording].
https://www.youtube.com/watch?v=RtGDuiBodaQ&ab_channel=NikodemBartnik
- Benedicto, E., Carou, D., & Rubio, E. M. (2017). *Technical, Economic and Environmental Review of the Lubrication/Cooling Systems Used in Machining Processes*. (pp. 99–116). Procedia Engineering.
- British Plastics Federation. (n.d.). *Polycarbonate (PC)*. British Plastics Federation. Retrieved May 6, 2025, from
<https://www.bpf.co.uk/plastipedia/polymers/Polycarbonate.aspx>
- Brown, A., Brown, G., English, B., Hodges, A., Hoy, L., & Schools, J. (2023). *Open Source Desktop CNC Mill* (p. 164) [Major Qualifying Project]. Worcester Polytechnic Institute. <https://digital.wpi.edu/show/x920g2113>
- Carbide 3D. (n.d.). *Nomad 3—Desktop CNC Mill*. Carbide 3D. Retrieved September 29, 2024, from <https://shop.carbide3d.com/products/nomad-3>
- Carvera. (n.d.). *Carvera 4th Axis Module (Harmonic Drive Version)*. Makera. Retrieved May 6, 2025, from <https://www.makera.com/products/carvera-4th-axis-module>
- Carvera 4th Axis Module (Harmonic Drive Version). (n.d.). Makera. Retrieved May 6, 2025, from <https://www.makera.com/products/carvera-4th-axis-module>
- Castro, M. (2024, April 23). *Tackling the Worker Shortage in CNC Machining: Strategies for 2024*.
<https://www.linkedin.com/pulse/tackling-worker-shortage-cnc-machining-strategies-2024-gotomorris-l2tze>

CMU TechSpark (Director). (2021, October 26). *Machine Vise Setup | Tramming your Vice in a Manual Mill* [Video recording].

<https://www.youtube.com/watch?v=7b3p7kg9Ozs>

CNC Milling Machine Rotational Axis CNC Router Rotary Table Rotary a axis 4th Axis 65mm 3 Jaw Chuck Dividing Head w/ Nema17 stepper motor w/ 54mm Tailstock Reducing ratio 4:1 for CNC Engraving Machine—Amazon.com. (n.d.). Amazon.

Retrieved May 6, 2025, from

https://www.amazon.com/Milling-Rotational-Dividing-Tailstock-Reducing/dp/B07MDJNDNJ/?_encoding=UTF8&pd_rd_w=qHxBR&content-id=amzn1.sym.255b3518-6e7f-495c-8611-30a58648072e%3Aamzn1.symc.a68f4ca3-28dc-4388-a2cf-24672c480d8f&pf_rd_p=255b3518-6e7f-495c-8611-30a58648072e&pf_rd_r=KZ7HX96Q1ZCH24BBTXGQ&pd_rd_wg=pYkEA&pd_rd_r=231028aa-9afc-4715-ab1e-045be6b8e0ed&ref_=pd_hp_d_atf_ci_mcx_mr_ca_hp_atf_d&th=1

Control of Hazardous Energy (Lockout/Tagout). (2025). Occupational Safety and Health Administration. <https://www.osha.gov/control-hazardous-energy>

de Naoum, K. (2023, March 30). *Learn All About Yield Strength.* Xometry.

<https://www.xometry.com/resources/3d-printing/yield-strength/>

Deans, M. (2021, March 17). *What is CAM (Computer-Aided Manufacturing)?* Fusion Blog.

<https://www.autodesk.com/products/fusion-360/blog/computer-aided-manufacturing-beginners/>

Design and Fabrication of 3-Axes Mini CNC Milling Machine. (n.d.).

<https://iopscience.iop.org/article/10.1088/1757-899X/1094/1/012005/meta>

ER11-6 Premium – RapidChange ATC. (n.d.). Retrieved May 6, 2025, from

<https://rapidchangeatc.com/shop/magazines/er11-6s/>

Filamatrix. (n.d.). *PETG Vs Nylon: Which Is Better for Your 3D Prints?* Filamatrix.

Retrieved May 6, 2025, from

<http://filamatrix.com/blogs/blogs/petg-vs-nylon-which-is-better-for-your-3d-prints>

Fowle, H. (2024, October 24). *The benefits of opting for a desktop CNC machine.*

<https://www.electronicsspecifier.com/news/blog/the-benefits-of-opting-for-a-desktop-cnc-machine>

Free, M. (2023, May 19). Yes, There is a Shortage of Skilled Machinists. *CNC Machining Capacity vs. Demand in the United.*

<https://www.zyci.com/yes-there-is-a-shortage-of-skilled-machinists>

Genmitsu 4th Axis Rotary Module for 4040 and 3030 Series CNC Machines with Planetary Geared Stepper Motor, 4 Jaw Chuck, Clamped Range 10-200mm—Amazon.com. (n.d.). Amazon. Retrieved May 6, 2025, from

https://www.amazon.com/Genmitsu-4th-Axis-3030-PROVer-Planetary/dp/B0C581H2B3?source=ps-sl-shoppingads-lpcontext&ref_=fplfs&psc=1&smid=A1CJB5SYI9X4XC

González, D. M. O., & Ferreira, J. C. E. (2016). MEMS accelerometer-based system for inexpensive online CNC milling process chatter detection. *2016 IEEE International Conference on Automation Science and Engineering (CASE),* 978–983. <https://doi.org/10.1109/COASE.2016.7743510>

Goodwin University. (2024, July 9). *What is CNC Machining?* Goodwin University.

<https://www.goodwin.edu/eneews/what-is-cnc/>

Grbl Home. (n.d.). GitHub. Retrieved May 4, 2025, from

<https://github.com/gnea/grbl/wiki/Home>

Grbl Home. (2023, November 14). GitHub. <https://github.com/gnea/grbl/wiki/Home>

Grbl/doc/script/fit_nonlinear_spindle.py at master · gnea/grbl. (n.d.). GitHub.

Retrieved May 1, 2025, from

https://github.com/gnea/grbl/blob/master/doc/script/fit_nonlinear_spindle.py

grblHAL Home. (2021, May 9). GitHub. <https://github.com/grblHAL/core/wiki/Home>

grblHAL Manual, semi automatic and automatic tool change. (2024, September 24).

GitHub.

<https://github.com/grblHAL/core/wiki/Manual,-semi-automatic-and-automatic-tool-change>

grblHAL Web Builder. (n.d.). Retrieved May 2, 2025, from

<https://svn.io-engineering.com:8443/>

Groll, Y. (2018, July 5). *Cutting Tool Vibration Control Technology Boosts Machining Productivity*. Modern Machine Shop.

<https://www.mmsonline.com/articles/cutting-tool-vibration-control-technology-boots-machining-productivity>

IMI Bimba (Director). (2019, November 13). *TECH TALK: Norgren's NVP Series*

Venturi Vacuum Pumps and Generators [Video recording].

<https://www.youtube.com/watch?v=cwRdFQktDv0>

Irani, R. A., Bauer, R. J., & Warkentin, A. (2005). A review of cutting fluid application in the grinding process. *International Journal of Machine Tools and Manufacture*, 45(15), 1696–1705. <https://doi.org/10.1016/j.ijmachtools.2005.03.006>

Kasprowiak, M., Parus, A., & Hoffmann, M. (2022). Vibration Suppression with Use of Input Shaping Control in Machining. *Sensors (Basel, Switzerland)*, 22(6), 2186.

<https://doi.org/10.3390/s22062186>

Limit Switches. (n.d.). Sienci Labs.

<https://resources.sienci.com/view/lmk2-limit-switches/>

LinuxCNC. (n.d.). Retrieved May 4, 2025, from <https://www.linuxcnc.org/>

LinuxCNC Hardware Interface. (2024, September 20).

<https://www.linuxcnc.org/docs/html/getting-started/hardware-interface.html>

LinuxCNC Hardware Requirements. (2019, January 29).

https://wiki.linuxcnc.org/cgi-bin/wiki.pl?Hardware_Requirements

LinuxCNC System Requirements. (2024, September 20).

<https://www.linuxcnc.org/docs/html/getting-started/system-requirements.html>

Liu, T. (n.d.). *Digital-output relative humidity & temperature sensor/module DHT22*

(*DHT22 also named as AM2302*). Aosong Electronics Co.,Ltd.

Liu, X., Tyler, T., Starr, T., Starr, A. F., Jokerst, N. M., & Padilla, W. J. (2011). Taming the Blackbody with Infrared Metamaterials as Selective Thermal Emitters.

Physical Review Letters, 107(4), 045901.

<https://doi.org/10.1103/PhysRevLett.107.045901>

logan2225. (2025, March 2). PrintNC V4. *PrintNC Wiki*.

<https://wiki.printnc.info/en/home>

MacFab. (2024, May 28). Addressing the Skills Gap in CNC Machining. *MacFab*.

<https://macfab.ca/blog/bridging-skills-gap-cnc-machining/>

Mach About Us. (n.d.). Retrieved May 4, 2025, from

<https://www.machsupport.com/about-us/>

Mach Mach3. (n.d.). Retrieved May 4, 2025, from

<https://www.machsupport.com/software/mach3/>

Mach3 CNC Controller Software Installation and Configuration (3rd ed.). (2008).

https://www.machsupport.com/wp-content/uploads/2013/02/Mach3Mill_Install_Config.pdf

Managing thermal loads in milling processes | Secotools.com. (n.d.). Retrieved May 6, 2025, from <https://www.secotools.com/article/21483>

McClements, D. (2023, March 9). *Impact Strength: Definitions, Importance, and How It Is Measured.* Xometry.

<https://www.xometry.com/resources/3d-printing/impact-strength/>

McFadden, C. (2020, December 9). *Understanding Tensile Strength, Its Importance in Engineering.* Interesting Engineering.

<https://interestingengineering.com/innovation/understanding-tensile-strength-its-importance-in-engineering>

McMaster-Carr. (n.d.). Retrieved September 29, 2024, from

<https://www.mcmaster.com/47065T808>

Metalworking Fluids—Metalworking Fluids: Safety and Health Best Practices Manual | Occupational Safety and Health Administration. (n.d.). Occupational Safety and Health Administration. Retrieved May 6, 2025, from

<https://www.osha.gov/metalworking-fluids/manual>

Newfangled Solutions Mach3. (2024). <https://www.machsupport.com/software/mach3/>

Obreja, C., Stan, G., Andrioaia, D., & Funaru, M. (2013). Design of an Automatic Tool Changer System for Milling Machining Centers. *Applied Mechanics and Materials*, 371, 69–73. <https://doi.org/10.4028/www.scientific.net/AMM.371.69>

Occupational Noise Exposure—Overview | Occupational Safety and Health Administration. (n.d.). Occupational Safety and Health Administration. Retrieved May 6, 2025, from <https://www.osha.gov/noise>

Perens, B. (2008). *The Open Source Definition*.

https://d1wqxts1xzle7.cloudfront.net/31165688/2_semester_projects_glossary_0708_glossary_2sem_0708_aia4_srokamichal_osdtext-libre.pdf?1392239056=&response-content-disposition=inline%3B+filename%3DThe_open_source_definition.pdf&Expires=1729187859&Signature=OPJTqsoL-NxGTCK2H6af2KvL4Ac4X83TLsh66l27ytMN3cdZuAMT7JvwLU~-P-nZp3OTT3Uk5gjdA9ca7uKLFnTYgJpyr0B2p76Gpf8pAcRF3ACQv5e9efDycojnv48sEFk1FMT0E~Y7~wueBHtG8Iqf-MC4UtYMVtvFiU2THkn4NNtOoDt35y3X~slUKX3qLD5dEMMRXK-0Hau3muck~BojhdtU3glpY8EtpItvBMKENpgwz0g0eZ9vnBe9utP8A5z4HDP077oMKQEMUs tHI3~bbVG~Aa2cBovMvbPQVbE3CuEpbN~YMYUzmBFEVtcwUvLtRafC1Zx rsTFuUENBQ_&Key-Pair-Id=APKAJLOHF5GGSLRBV4ZA

Pickens Technical College. (2024, March 5). *The Significance of CNC Machining in Manufacturing*. Pickens Technical College.

<https://www.pickenstech.org/blog/what-is-cnc-manufacturing/>

Polycase. (2021, February 11). *What is NEMA 4X? Understanding the NEMA 4X Rating and Enclosures*. TechTalk Blog.

<https://www.polycase.com/techtalk/nema-rated-enclosures/nema-4x-defintion.html>

RapidChange ATC. (n.d.). Retrieved May 6, 2025, from

<https://docs.masso.com.au/wiring-and-setup/tool-changers/mill-tool-changers/rapid-change-atc>

RapidChange ATC – Rapidly Changing the CNC Industry. (n.d.). Retrieved April 3, 2025, from <https://rapidchangeatc.com/>

Rastvorova, I. I., & Klyucherev, N. A. (2021). *Design and modelling of a universal CNC machine*. Journal of Physics.

<https://doi.org/10.1088/1742-6596/1753/1/012040>

rctestflight (Director). (2021, December 4). *3D Printed Cyclone Air/Dust Separator* [Video recording]. <https://www.youtube.com/watch?v=50UtHTSGE24>

Reddy, A. C. S., Paleshwar, D. V., Murthy, K. L. N., & Sandeep, B. (2020). A Review on Coolant Feeding System of CNC Machining Process. In A. Praveen Kumar, T. Dirgantara, & P. V. Krishna (Eds.), *Advances in Lightweight Materials and Structures* (pp. 441–449). Springer. https://doi.org/10.1007/978-981-15-7827-4_44

Samcraft (Director). (2020, December 1). *AMAZINGLY QUIET 40 dB SHOP VAC Cyclone & DIY Enclosure* [Video recording].

<https://www.youtube.com/watch?v=z0dzuZWAFbc>

ShopSabre. (2021, July 14). *Benefits of an automatic tool changer and how it works*. ShopSabre CNC.

[https://www.shopsabre.com/benefits-of-an-automatic-tool-changer-and-how-it-wor ks/](https://www.shopsabre.com/benefits-of-an-automatic-tool-changer-and-how-it-works/)

Speeds and Feeds – RapidChange ATC. (n.d.). Retrieved May 6, 2025, from <https://rapidchangeatc.com/docs/installation/speeds-and-feeds/>

Spindle CNC USB Mach 3—YouTube. (n.d.). Youtube. Retrieved May 1, 2025, from

<https://www.youtube.com/watch?feature=shared&t=156&v=W1B9VC-6WL0>

Strain Gauge Measurement – A Tutorial. (n.d.).

http://elektron.pol.lublin.pl/elekp/ap_notes/ni_an078_strain_gauge_meas.pdf

Thomas, J. (2022, April 7). What Is A CNC Machinist? And How to Become One [Full Guide]. *Advanced Structural Technologies*.

<https://astforgetech.com/what-is-a-cnc-machinist-and-how-to-become-one-full-guide/>

Top-Down Design—2021—SOLIDWORKS Help. (2021). SOLIDWORKS Help.

https://help.solidworks.com/2021/english/SolidWorks/sldworks/c_Top-Down_Design_Overview.htm

T-Slotted Framing, Single 4-Slot Rail, Silver, 45 mm Square, Hollow | McMaster-Carr. (n.d.). Retrieved September 29, 2024, from <https://www.mcmaster.com/5537T915/>

Understanding Young's Modulus. (2020, November 19). The Efficient Engineer.

<https://efficientengineer.com/youngs-modulus/>

Universal Technical Institute. (2020, December 18). What Is CNC Machining and What Does CNC Mean? *UTI Corporate*.

<https://www.uti.edu/blog/cnc/what-is-cnc-machining>

Valle, A. (2022, August 9). A Fond Farewell to GrabCAD Workbench. *GrabCAD Blog*.

<https://blog.grabcad.com/blog/2022/08/09/a-fond-farewell-to-grabcad-workbench/>

Venturi Pump. (n.d.). Retrieved May 3, 2025, from

<https://www.schmalz.com/en-us/glossary/venturi-pump/>

VFD Control with grblHAL. (n.d.). PrintNC Wiki. Retrieved May 1, 2025, from

<https://wiki.printnc.info/en/grbl/vfd-control>

Wayken Rapid Manufacturing. (2021, May 17). *Choosing The Right CNC Coolant For Aluminum Milling.* Rapid Prototype Manufacturing in China - WayKen.

<https://waykenrm.com/blogs/which-cnc-coolant-should-you-pick-when-milling-aluminum/>

Wayken Rapid Manufacturing. (2023, August 11). *What is Slot Milling: Techniques, Tips, and Practices - WayKen.* Rapid Prototype Manufacturing in China - WayKen.

<https://waykenrm.com/blogs/what-is-slot-milling/>

Wei, Q. (2013). *Design and analysis of a small-scale cost-effective CNC milling machine* [University of Illinois at Urbana-Champaign].

<https://hdl.handle.net/2142/44140>

What Is An Automatic Tool Changer And The 4 Common Types—TAICNC. (2023, April 5).

<https://www.lvcnc.com/what-is-an-automatic-tool-changer-and-the-4-common-types.html>

Yalang. (n.d.). *Manual for Yalang High Performance Universal Frequency Converter.*

<https://wiki.printnc.info/y1620manual.pdf>

Ye, R. (2024a, April 23). *Applications of CNC Machining in the Automotive Industry.*

Rapid Prototyping & Low Volume Production.

<https://www.3erp.com/blog/applications-cnc-machining-automotive-industry/>

Ye, R. (2024b, November 26). *CNC Machining Wall Thickness: Definition, Importance and Optimization*. Rapid Prototyping & Low Volume Production.

<https://www.3erp.com/blog/cnc-machining-wall-thickness/>

Appendices

Appendix A: Github Links

Machine CAD: https://github.com/Desktop-CNC/New_CAD

PicoCNC Firmware: <https://github.com/Desktop-CNC/PicoCNCFirmware>

Sensor Code and Data: <https://github.com/Desktop-CNC/VibrationExperiment>

Data Analysis: <https://github.com/Desktop-CNC/CodeForSensorDataAnalysis>

Electrical Diagram: <https://github.com/Desktop-CNC/Schematic>

Tool Changer Module Code:

<https://github.com/Desktop-CNC/Tool-Changer-and-Laser-Tool-Probe>

UGS Tool Changer Plugin:

<https://github.com/Desktop-CNC/ugs-platform-plugin-toolchanger>

UGS Logger PLugin: <https://github.com/Desktop-CNC/ugs-platform-plugin-logger>

Bed Torque Script: <https://github.com/Desktop-CNC/TorqueScript>

Electrical Box CAD: <https://github.com/Desktop-CNC/electronics-box-CAD>

Appendix B: Assembly document for Electrical

 Appendix B Electrical Assembly

Appendix C: Assembly document for Machine Assembly

The documents below are detailed guides on how to assemble the enclosure:

 Base Assembly

 Door Assembly

 Table Fabrication

Appendix D: Software Installation

 Appendix D Software Installation

Appendix E: Assembly Document for Bed Leveling

 Appendix E Assembly Document for Bed Leveling

Appendix F: Software Testing

 Appendix F Software Testing

Appendix G: Other relevant info

Universal G-Code Sender Guide: [Usage · winder/Universal-G-Code-Sender Wiki](#)

grblHAL User Guide: [grblHAL Wiki](#)

PicoCNC User Manual: [PicoCNC User Manual](#)

GitHub User Guide: [☰ Github User Guide](#)

Filament Decision Matrix: [✚ Filament Decision Matrix](#)

Student Testing Guides and Surveys: [☒ IRB \(guides & surveys\)](#)

Standard Operating Procedure for Sensors [☰ Standard Operating Procedure for Testing](#)

WitMotion Instructions for Testing [☰ WitMotion Instructions](#)

Contact Info

For any questions or feedback to the team, reach out at the following:

Echo Baumer (ME, PH): esbaumer@gmail.com

Rafael Caballero (ME): jacobcaballero295@yahoo.com

James Carroll (ME): jhcarroll17@gmail.com

Camren Chaplak (CS, RBE): ch.camren@gmail.com

Michael Doucette (ME): michaeldoucettejr@gmail.com

Perrin Kristoff (ECE): perrin@hyliston.net

Andrew Petro (ME): andrewmpetro@gmail.com

Daniel Petro (ME): danielmpetro14@gmail.com

Michael Primavera (RBE): mr.michaelprimavera@gmail.com

JR Thaiprayoon (ME): cthaiprayoon@gmail.com

Dante Uccello (ME): danteucc127@gmail.com